1-29-2013

Handel's Maser-Soliton Theory of Ball Lightning: The Creation of Stable Three-Dimensional Cavitons by an Atmospheric Maser within an Open Resonator

Glenn Andrew Carlson
University of Missouri-St. Louis, g.crlsn@gmail.com

HANDEL'S MASER-SOLITON THEORY OF BALL LIGHTNING: THE CREATION OF STABLE THREE-DIMENSIONAL CAVITONS BY AN ATMOSPHERIC MASER WITHIN AN OPEN RESONATOR

by

GLENN ANDREW CARLSON

A DISSERTATION

Presented to the Faculty of the Graduate School of the

MISSOURI UNIVERSITY OF SCIENCE AND TECHNOLOGY

and

UNIVERSITY OF MISSOURI – SAINT LOUIS

In Partial Fulfillment of the Requirements for the Degree

DOCTOR OF PHILOSOPHY

in

PHYSICS

2012

Approved by

Peter H. Handel, Advisor
Jerry L. Peacher
Bruce A. Wilking
Barbara N. Hale
Harold H. Harris

To Mary Jo

ABSTRACT

This dissertation develops details of Handel's Maser-Soliton Theory of ball lightning. The atmosphere between a thundercloud and the Earth's surface is modeled as an idealized stable open resonator with water vapor as the active medium and the thundercloud and Earth's surface as reflecting surfaces. The stable resonator generates a maser beam that narrows to the beam waist at the Earth's surface, which is assumed to be planar. Two candidate rotational transitions are identified within the $\nu_1\nu_2\nu_3 = 010$ vibrational band of water having wavelengths of 13.9 cm and 1.12 cm, and relevant spectroscopic parameters are retrieved from the HITRAN 2008 molecular spectroscopic database. The maser is modeled as a continuously pumped four-level maser that includes the effects of nonradiative relaxation due to molecular collisions and of microwave absorption in atmospheric oxygen. Since maser spiking is highly unlikely to occur due to the high rate of collisional relaxation at normal atmospheric pressure, the electrical breakdown of air must be achieved by the steady state output of the atmospheric maser. A parametric analysis is performed to relate the size of the atmospheric maser to the pumping rate needed to create a steady state population inversion sufficient to generate maser radiation intense enough at the beam waist to result in the electrical breakdown of air. The analysis suggests that electric field intensities at the beam waist sufficient to cause electrical breakdown of air could only be created through huge pumping rates ($\sim 10^5$ to 10^7 times the critical pumping rate) and only for the most highly curved clouds ($g \approx 0$) that give the narrowest beam waists.

ACKNOWLEDGEMENT

I express my deep gratitude to Dr. Peter H. Handel, my advisor for this dissertation, for his support, patience, and friendship. I thank him for his living example that science is not just an exercise of the intellect, but of the imagination, and for his frequent reminders that, while a scientist needs a creative mind (beyond the cliché of "thinking outside the box"), a theory "should not be confused with proven factual knowledge and should be subjected to careful experimental verification."

My special thanks to Mary Zettwoch, Erica Marks, and the Interlibrary Loan staff of the UMSL Thomas Jefferson Library. Their diligence in filling my many hundreds of document requests, many for rare or hard-to-find items, has been invaluable. The references cited in this dissertation are but a small fraction of the number of documents they have obtained for me.

I thank the faculty and staff of the UMSL Physics and Astronomy Department, the MST Physics Department, and the UMSL and MST Graduate Colleges for their support through my graduate career in the UMSL/MST coop program.

I thank all the members of my committee for their support.

Most of all, I thank my dearest wife, Mary Jo, my son, Alex, and my daughter, Hannah, for their love and support.

TABLE OF CONTENTS

Page

ABSTRACT iv

ACKNOWLEDGEMENT v

LIST OF ILLUSTRATIONS ix

LIST OF TABLES x

SECTION

1. INTRODUCTION 1

2. CHARACTERISTICS AND THEORIES OF BALL LIGHTNING 3

2.1. CHARACTERISTICS OF BALL LIGHTNING 3

2.2. THEORIES OF BALL LIGHTNING 9

2.2.1. Phenomena That May be Mistaken for Ball Lightning. 9

2.2.2. Exotic States of Matter. 13

2.2.3. Electrochemical and Combustion Theories. 14

2.2.4. Plasma Dynamic and Electrodynamic Theories. 15

2.2.5. High-Frequency Electromagnetic Wave Interference (Kapitsa Models). 17

3. HANDEL'S MASER-SOLITON THEORY 25

3.1. MASER ACTION IN MOIST AIR INITIATED BY LIGHTNING 25

3.1.1. Water Vapor Lasers. 28

3.1.2. Atmospheric Masers. 29

3.2. MASER-CAVITON BALL LIGHTNING ENERGY SPIKES 31

3.2.1. Spiking of an Atmospheric Maser. 32

3.2.2. Low-Temperature Ball Lightning Discharge. 37

3.2.3. Humming Sounds from Ball Lightning. 38

3.3. PERCEIVED ENERGY OF BALL LIGHTNING 40
3.4. PHASE SHIFTS AND THE MOTION OF BALL LIGHTNING 43
3.5. BALL LIGHTNING IS A PLASMA SOLITON 44
4. AN ATMOSPHERIC MASER IN THE AIR-EARTH SYSTEM 46
4.1. THE ATMOSPHERIC POTENTIAL GRADIENT 46
4.2. INTERACTION OF MICROWAVES WITH THE ATMOSPHERE 51
4.2.1. Absorption of Microwaves by Oxygen. 51
4.2.2. Absorption of Microwaves by Water Vapor. 53
4.2.3. The Microwave Breakdown of Air. 55
4.3. MICROWAVE SPECTROSCOPY OF WATER VAPOR 67
4.3.1. Collisional Broadening of Spectral Lines 67
4.3.2. Nonradiative Vibrational and Rotational Relaxation 75
4.4. ATMOSPHERIC MASER DYNAMICS 80
4.4.1. “Optical” Pumping by the Electric Field Pulse of a Lightning Strike.... 81
4.4.2. Laser Rate Equations. 84
4.4.3. Einstein B Coefficient for Stimulated Emission..... 91
4.4.4. Fluorescence Lifetime. 93
4.4.5. Cavity Lifetime τ_c and Quality Factor Q. 95
4.4.6. Cavity Lifetime τ_c for Open Resonant Cavities..... 98
4.4.7. Progagation of Maser Radiation: The Beam Waist. 100
4.4.8. Maser Spiking..... 104
4.5. PUMPING RATE TO ACHIEVE BREAKDOWN OF AIR 107
5. CONCLUSIONS AND RECOMMENDATIONS FOR FUTURE WORK 112

APPENDICES

APPENDIX A: Water Lines Data from HITRAN Molecular Spectroscopic Database. 115

APPENDIX B: Spectroscopic Data for the $4_{2,2} \rightarrow 5_{1,5}$ and $5_{3,2} \rightarrow 4_{4,1}$ Transitions 133

APPENDIX C: Mathematica® Notebooks for $4_{2,2} \rightarrow 5_{1,5}$ and $5_{3,2} \rightarrow 4_{4,1}$ Cases..... 149

BIBLIOGRAPHY 178

VITA 192

LIST OF ILLUSTRATIONS

Page

Figure 4-1: Prototypical Atmospheric Maser 47

Figure 4-2: Power Absorption Coefficient for Oxygen at 1 atm, 300 K 53

Figure 4-3: Power Absorption Coefficient for Water Vapor at 1 atm 55

Figure 4-4: Limits of Diffusion Theory for Hydrogen Gas 59

Figure 4-5: Electric Field Strength for Microwave Breakdown of Air at 1 Atm 67

Figure 4-6: H_2O Energy Levels and an Idealized Four-Level System 87

Figure 4-7: H_2O Energy Levels and an Idealized Four-Level System 88

Figure 4-8: Open Resonator Stability Diagram 99

Figure 4-9: Beam Waist at $t/L = 1$ 105

Figure 4-10: Beam Waist at $t/L = 0.7$ 105

Figure 4-11: Beam Waist at $t/L = 0.9$ 105

Figure 4-12: Beam Waist at $t/L = 0.5$ 105

Figure 4-13: Spiking of Photon Number Calculated from Rate Equations 106

Figure 4-14: Pumping Ratio to Achieve Electrical Breakdown of Air
($5_{32} \rightarrow 4_{41}$, $L = 1000$ m, $\rho_{cloud} = 0.86$) 110

Figure 4-15: Pumping Ratio to Achieve Electrical Breakdown of Air
($4_{22} \rightarrow 5_{15}$, $L = 1000$ m, $\rho_{cloud} = 0.86$) 111

LIST OF TABLES

Page

Table 4-1: Einstein *B* coefficient for stimulated emission.....93

Table 4-2: Radiative and Nonradiative Lifetimes.....95

Table 4-3 : Cavity Lifetimes and Quality Factors 97

Table 4-4: Confocal Parameter and Beam Waist Location 103

1. INTRODUCTION

"Anything will lase if you hit it hard enough."

Schawlow's Law (perhaps apocryphal)
paraphrased by A. E. Siegman[1]

Handel's Maser-Soliton Theory describes ball lightning as a plasma soliton fed by a large atmospheric maser. The atmospheric maser is driven by the strong electric field pulse coincident with a lightning strike or polarization catastrophe process that creates a population inversion in closely spaced rotational-vibrational energy levels of water molecules. Constructive interference of the maser radiation creates an isolated region of intense, high-frequency electric field resulting in electric breakdown of the air and creation of a plasma discharge. Nonlinear effects within the plasma discharge create a solitary plasma wave, a soliton, which is perceived as ball lightning.

Handel's Maser-Soliton Theory accurately accounts for many of the characteristics and behaviors reported for ball lightning. However, it has yet to be shown in detail how the maser energy is concentrated into a single isolated region within the active volume resulting in electric breakdown of the air and creation of a plasma discharge.

This dissertation models the atmosphere between a thundercloud and the Earth's surface as an idealized stable open resonator with water vapor as the active medium and the thundercloud and Earth's surface as reflecting surfaces. The stable resonator

---

[1] A. E. Siegman, *Lasers*, Sausalito: University Science, 1986, p. 70.

generates a maser beam that narrows to the beam waist at the Earth's surface, which is assumed to be planar. Two candidate rotational transitions are identified within the $v_1v_2v_3 = 010$ vibrational band of water having wavelengths of 13.9 cm and 1.12 cm, and relevant spectroscopic parameters are retrieved from the HITRAN 2008 molecular spectroscopic database. The maser is modeled as a continuously pumped four-level maser that includes the effects of nonradiative relaxation due to molecular collisions and of microwave absorption in atmospheric oxygen. A parametric analysis is performed to relate the size of the atmospheric maser to the pumping rate needed to create a population inversion sufficient to generate maser radiation intense enough at the beam waist to result in the electrical breakdown of air.

2. CHARACTERISTICS AND THEORIES OF BALL LIGHTNING

This section summarizes the current state of knowledge of ball lightning, its phenomenology, a sampling of some of the many theories of ball lightning, and Handel's Maser-Soliton theory of ball lightning. I also summarize the current state of knowledge of the theories and modeling of open resonators, masers and lasers, and plasma solitons.

2.1. CHARACTERISTICS OF BALL LIGHTNING

Ball lightning researchers are in complete agreement on, perhaps, only two things: ball lightning is a mobile, luminous, globular phenomenon associated with thunderstorms[2], and ball lightning research is controversial[3].

We adopt here the following as prototypical characteristics of ball lightning:

1. Ball lightning is an electrical phenomenon closely associated in time and place to conventional lightning strikes. Ball lightning is most often observed during thunderstorms[4]. Ball lightning has been reported to have appeared simultaneously with, immediately following, and just before a conventional lightning strike[5]. Often ball lightning originates at the place

---

[2] J. Alan Chalmers, Atmospheric Electricity (Pergamon Press, New York, 1967, p. 390; M. A. Uman, *The Lightning Discharge*, Orlando: Academic Press, 1987, p. 23; Stanley Singer, *The Nature of Ball Lightning*, New York: Plenum Press, 1971, p. 2; J. D. Barry, *Ball Lightning and Bead Lightning: Extreme Forms of Atmospheric Electricity*, New York: Plenum Press, 1980, p. 39; Mark Stenhoff, *Ball Lightning: An Unsolved Problem in Atmospheric Physics*, New York: Kluwer Academic, 1999, p. 20.

[3] Singer, *The Nature of Ball Lightning*, p. 33; Uman, *The Lightning Discharge*, p. 23.

[4] M. A. Uman, *Lightning*, New York: McGraw-Hill, 1969, p. 244; Barry, *Ball Lightning and Bead Lightning: Extreme Forms of Atmospheric Electricity*, p. 39; Mark Stenhoff, *Ball Lightning: An Unsolved Problem in Atmospheric Physics*, p. 20.

[5] Singer, *The Nature of Ball Lightning*, p. 23; Barry, *Ball Lightning and Bead Lightning: Extreme Forms of Atmospheric Electricity*, p. 40; Mark Stenhoff, *Ball Lightning: An Unsolved Problem in Atmospheric Physics*, p. 20.

of the lightning strike or close by[6] within a few meters of the discharge[7]. However, ball lightning has been reported to appear in the absence of a lightning discharge[8].

2. Ball lightning is a luminous, globular phenomenon with a diameter on the order of tens of centimeters. Ball lightning is generally spherical[9]. Oval, teardrop, and rod shapes have also been reported[10]. Glowing or "hollow" balls with dark borders have been reported; boundaries may be vague or sharp[11]. Ball lightning is reported with various colors from red to blinding white[12]. Red to yellow are most commonly reported[13]. In Rayle's sample[14], the "favored colors were orange and yellow, often in combination with others." The diameter of ball lightning is usually on the order of tens of centimeters ("usually 10 to 20 cm"[15]; "usually… 10-20 cm"[16]; "most common diameter reported is 10-40 cm"[17]; "a modal

---

[6] Singer, *The Nature of Ball Lightning*, p. 63.

[7] Chalmers, *Atmospheric Electricity*, p. 391.

[8] Uman, *Lightning*, p. 244.

[9] *Ibid*; Barry, *Ball Lightning and Bead Lightning: Extreme Forms of Atmospheric Electricity*, p. 35.

[10] *Ibid.*

[11] Singer, *The Nature of Ball Lightning*, p. 63.

[12] *Ibid*., pp. 62-63.

[13] Uman, *Lightning*, p. 244; Barry, *Ball Lightning and Bead Lightning: Extreme Forms of Atmospheric Electricity*, p. 35

[14] Warren D. Rayle, Ball Lightning Characteristics, NASA Technical Note D-3188, Washington, D.C.: National Aeronautics and Space Administration, 1966.

[15] Uman, *Lightning*, p. 244.

[16] Singer, *The Nature of Ball Lightning*, 63.

[17] Barry, *Ball Lightning and Bead Lightning: Extreme Forms of Atmospheric Electricity*, p. 35.

diameter of 20-50 cm".[18] Rayle's sample[19] has a median diameter of 14 inches [35.6 cm] with "84 percent of the estimates … below a diameter 2.5 times the median." The size and brightness are usually constant[20] with a "fairly constant" luminosity[21]. According to Rayle[22], "[m]ost reports described the ball as round (87 percent) and uniformly bright (76 percent)," and "[a] substantial majority of the reports (over 85 percent…) concurred that the size and brightness of the ball remained about the same during the observation and that the appearance did not change noticeably even immediately prior to its disappearance."

3. Ball lightning has a lifetime of one to several seconds. Uman[23] states the lifetime of ball lightning is generally "less than 5 sec." According to Singer[24], ball lightning "most often lasts 3-5 seconds," while, according to Barry[25], "the lifetime of ball lightning is most often reported to be only 1-2 seconds." Ball lightning lifetimes of over a minute[26] to several minutes[27] have been reported. The results of Rayle's survey[28] show a

---

[18] Stenhoff, *Ball Lightning: An Unsolved Problem in Atmospheric Physics*, p. 181.

[19] Rayle, *Ball Lightning Characteristics*.

[20] Uman, *Lightning*, p. 244.

[21] Stenhoff, *Ball Lightning: An Unsolved Problem in Atmospheric Physics*, p. 20.

[22] Rayle, *Ball Lightning Characteristics*.

[23] Uman, *Lightning*, p. 244.

[24] Singer, *The Nature of Ball Lightning*, p. 63.

[25] Barry, *Ball Lightning and Bead Lightning: Extreme Forms of Atmospheric Electricity*, p. 39.

[26] Uman, *Lightning*, 244.

[27] Singer, *The Nature of Ball Lightning*, p. 63; Barry, *Ball Lightning and Bead Lightning: Extreme Forms of Atmospheric Electricity*, p. 39.

"most probable duration in the 4 to 5 second region" with "a substantial fraction, 8 to 12 percent [of reported durations], described as lasting over 30 seconds."

4. Ball lightning is free floating, remaining motionless or moving horizontally several meters above the ground. Ball lightning usually moves in a random manner[29] or horizontally a few meters above the ground[30]. Rayle's data[31] showed a "marked preference for mostly horizontal motion (54 percent) rather than mostly vertical (19 percent)." Ball lightning may hover motionless[32] or may fall from the bottom of a cloud[33]. Rayle's sample[34] generally describes ball lightning as slow moving. Of the estimated minimum velocities, 86% were below 15 miles per hour [6.7 m/s], and 54% were below 5 miles per hour. Of the estimated maximum velocities, 70% were below 20 miles per hour [8.9 m/s] and 17% above 60 miles per hour [26.8 m/s]. Ball lightning may rise[35], but not often[36]. While ball lightning is reported

---

[28] Rayle, *Ball Lightning Characteristics*.

[29] Barry, *Ball Lightning and Bead Lightning: Extreme Forms of Atmospheric Electricity*, p. 36.

[30] *Ibid*.; Stenhoff, *Ball Lightning: An Unsolved Problem in Atmospheric Physics*, p. 20.

[31] Rayle, *Ball Lightning Characteristics*.

[32] Uman, *Lightning*, p. 244; Barry, *Ball Lightning and Bead Lightning: Extreme Forms of Atmospheric Electricity* p. 36.

[33] Singer, *The Nature of Ball Lightning*, p. 63; Barry, *Ball Lightning and Bead Lightning: Extreme Forms of Atmospheric Electricity*, p. 36.

[34] Rayle, *Ball Lightning Characteristics*.

[35] Barry, *Ball Lightning and Bead Lightning: Extreme Forms of Atmospheric Electricity*, p. 36.

[36] Uman, *Lightning*, p. 244.

to move against[37] or unaffected by wind[38], "[i]t is, rarely, said to move against the wind"[39], and, "if wind-related motion is mentioned in a report, the ball lightning is most often observed to move along with the wind rather than against it"[40]. Ball lightning is usually observed close to the ground, but this may be because most observers are on the ground[41]. Ball lightning is reported to bounce off solid objects, including the ground[42]. Ball lightning is sometimes reported to spin or rotate[43].

5. Ball lightning may exist within enclosed spaces. Ball lightning has been reported to enter closed rooms through screens and glass windowpanes[44] and through chimneys[45]. Ball lightning has also been reported within all-metal aircraft[46].

6. Ball lightning disappears or decays silently or explosively. Ball lightning "can dissipate noiselessly, with a soft bang or with a dazzling

---

[37] Barry, *Ball Lightning and Bead Lightning: Extreme Forms of Atmospheric Electricity*, p. 37.

[38] Singer, *The Nature of Ball Lightning*, p. 63.

[39] Stenhoff, *Ball Lightning: An Unsolved Problem in Atmospheric Physics*, p. 21.

[40] Barry, *Ball Lightning and Bead Lightning: Extreme Forms of Atmospheric Electricity*, p. 37.

[41] *Ibid*., p. 43.

[42] Uman, *Lightning*, p. 245.

[43] *Ibid*.; Rayle, *Ball Lightning Characteristics*.

[44] Uman, *Lightning*, p. 245.

[45] *Ibid*.; Singer, *The Nature of Ball Lightning*, p. 63; Barry, *Ball Lightning and Bead Lightning: Extreme Forms of Atmospheric Electricity*, p. 42.

[46] R. C. Jennison, "Ball lightning," *Nature* **224**, 895 (1969); Barry, *Ball Lightning and Bead Lightning: Extreme Forms of Atmospheric Electricity*, p. 43.

explosion"[47]. It can disappear quietly with a decrease in brightness and diameter[48] occurring rapidly or slowly[49]. Explosive decay occurs rapidly and with a loud sound[50]. Rayle[51] reported that of the 78 respondents who reported seeing the end of the ball lightning, 54 reported it ended quietly, and 24 reported it ended explosively. Some compilers of ball lightning reports claim that "enclosed ball lightning decays by the explosive mode"[52] and "explosions or damage are evidently more likely in these cases[53]. However, conspicuously lacking in one eyewitness account[54] of an incident on an aircraft in flight is any mention of the violent disappearance of the "glowing sphere."

7. Ball lightning may radiate no heat. There are reports of damage to objects (trees, buildings, aircraft) that have come into contact with ball lightning, and serious injuries, burns, and deaths of people and animals have been reported[55]. However, these reports of damage and injury are contrasted

---

[47] Walther Brand, *Der Kugelblitz* (Henri Grand, Hamburg, 1923) (in German). (An English translation exists at Walther Brand, *Ball Lightning*, NASA Technical Translation, No. NASA-TT-F-13228 (National Aeronautics and Space Administration, Washington, DC, February 1971).).

[48] Barry, *Ball Lightning and Bead Lightning: Extreme Forms of Atmospheric Electricity*, p. 39.

[49] Uman, *Lightning*, p. 245.

[50] *Ibid*.; Singer, *The Nature of Ball Lightning*, p. 72; Barry, *Ball Lightning and Bead Lightning: Extreme Forms of Atmospheric Electricity*.

[51] Rayle, *Ball Lightning Characteristics*.

[52] Singer, *The Nature of Ball Lightning*.

[53] *Ibid*.

[54] R. C. Jennison, "Ball Lightning," *Nature* **224**, 895 (1969).

[55] Barry, *Ball Lightning and Bead Lightning: Extreme Forms of Atmospheric Electricity*, p. 38; Stenhoff, *Ball Lightning: An Unsolved Problem in Atmospheric Physics*, Chapter 5.

with many other reports of ball lightning where even close observers detected no heat[56].

2.2. THEORIES OF BALL LIGHTNING

There are many theories of ball lightning. Garfield[57] provides an interesting (and at times amusing) history of ball lightning theory and research from the perspective of an information scientist.

2.2.1. Phenomena That May be Mistaken for Ball Lightning. Many have expressed skepticism of the existence of ball lightning as a real, physical phenomenon. These skeptics usually suggest that reported observations of ball lightning, even when not the product of outright fraud or deliberate hoax, arise from mistaken identity or have psychological (e.g., fright, shock, or hysteria) or physiological (e.g., optical illusion or afterimage) causes.

Stenhoff[58] discusses several "phenomena that may be mistaken for ball lightning" including St. Elmo's Fire, streetlights, swarms of luminescent insects, blimps, weather balloons, hoaxes, and hallucinations. He asserts that the nonexistence of ball lightning "is supported by the large number of already well-understood phenomena that resemble

---

[56] Uman, *Lightning*, p. 245; Singer, *The Nature of Ball Lightning*, p. 67; Barry, *Ball Lightning and Bead Lightning: Extreme Forms of Atmospheric Electricity*, p. 38; R. C. Jennison, "Ball Lightning," *Nature* **224**, 895 (1969).

[57] Eugene Garfield, "When citation analysis strikes ball lightning," *Essays of an Information Scientist* **2**, 479 (1976).

[58] Stenhoff, *Ball Lightning: An Unsolved Problem in Atmospheric Physics*, Chapter 3.

its reported characteristics" and the "unreliability of eyewitnesses" and "[t]he persistent difficulty of scientists in evolving a model of ball lightning."

Michael Faraday[59] was skeptical of the existence of ball lightning as an electrical phenomenon:

> Electric discharges in the atmosphere in the form of balls of fire have occasionally been described. Such phenomena appear to me to be incompatible with all that we know of electricity and its modes of discharge. … That phenomena of balls of fire may appear in the atmosphere, I do not mean to deny; but that they have anything to do with the discharge of ordinary electricity, or are at all related to lightning or atmospheric electricity, is much more than doubtful.

William Thomson[60] (Lord Kelvin) dismissed ball lightning as an optical illusion created by an afterimage caused by the bright flash of ordinary lightning. Thomson recounted the following description of ball lightning from a meeting of the Royal Society, "which described a ball of lightning as coming in at the window, running about amongst the people, and brushing up against their legs as if a kitten was about, and after that going out up the chimney". Though he noted, "This slow discharge by ball lightning had been described by many people," he dismissed the matter as an "altogether physiological affair":

> They had been looking in some direction or other when the flash came; at the instant that the flash came there was an intense action on the centre of the retina, especially if they chanced to see the flash in the sky; naturally after such a startling incident the eyes are moved and the person after seeing the flash looks about to see what has happened – looks on the floor, looks along the wall, looks up at the window, and a spot of light follows,

---

[59] Michael Faraday, *Experimental Researches in Electricity*, Volume 1, §19, ¶1641, (Dover, Mineola, New York, 2004) (Previously published by J.M. Dent & Sons, London, 1914.).

[60] W. Thomson, "Discussion on Lightning Conductors," *British Association for the Advancement of Science* **58**, 604 (1888).

> so that he believed this marvellous ball of lightning could be seen by every person present going out of any window that he happened to look out of.

Argyle[61] also attributed ball lightning to "visual afterimages." He cited the compilation by Rayle[62] of ball lightning reports which showed that "the number of persons reporting ball lightning observations is 44% of the number reporting observation of ordinary lightning impact points" and asserted, "about half of all strokes to ground generate a high luminosity ball [i.e., a flash] at the impact point." He continued to argue how afterimages could also explain other similarities in ball lightning reports: angular size, color, shape, brightness, passage through windows and screens without damaging them, and duration. He even suggested that similar "psychological principles" could explain reports of sounds and odors from ball lightning.

Berger[63] spent 30 years investigating lightning phenomena including ball lightning on Mt. San Salvatore in Switzerland and examining the documentary evidence from many ball lightning reports. Having never observed ball lightning, he concluded ball lightning does not exist. He suggested the solution to the ball lightning problem ("*Kugelblitz-Problem*") lies in the behavior of the retina of the eye ("*liegt im Verhalten der Netzhaut des Auges*") and the strange aftereffects ("*den merkwürdigen Nachwirkungen*") of bright flashes of light.

---

[61] Edward Argyle, "Ball Lightning as an Optical Illusion," *Nature* **230**, 179 (1971).

[62] Rayle, *Ball Lightning Characteristics*.

[63] K. Berger, "Kugelblitz und Blitsforschung," *Naturwissenschaften* **60**, 485 (1973) (in German).

Cooray and Cooray[64] suggest that persons reporting ball lightning may actually be experiencing visual hallucinations caused by epileptic seizures of the occipital lobes of the brain triggered by the rapidly changing electric and magnetic fields in the vicinity of lightning strikes.

Among the proponents of the reality of ball lightning was Walther Brand[65] who accumulated approximately 600 reports of ball lightning and compiled "215 of the most carefully written and best documented accounts (several of which comprise several ball lightnings) dating from the last hundred years." Brand concluded:

> [T]here have been numerous and well-documented reports of ball lightning which give the impression of absolute objectivity. Many ball lightnings were simultaneously observed by several people and similarly described; occasionally, certain people observed the phenomenon only after their attention was drawn to it by others. The objective existence of ball lightning must therefore be regarded as established.

Hill[66] recognized many scientists' skepticism given ball lightning's "peculiar physical behavior, coupled with the difficulty that has been encountered in attempts to simulate them under controlled conditions," but judged that "the number of well-attested cases now known seems to be large enough to warrant their consideration as genuine physical events having a certain measure of reproducibility."

---

[64] Gerald Cooray and Vernon Cooray, "Could Some Ball Lightning Observations be Optical Hallucinations Caused by Epileptic Seizures?" *The Open Atmospheric Science Journal* **2**, 101 (2008).

[65] Walther Brand, *Der Kugelblitz*.

[66] E. L. Hill, "Ball Lightning as a Physical Phenomenon," *Journal of Geophysical Research* **65**, 1947 (1960).

Jennison[67], of the Electronics Laboratory at the University of Kent, defended ball lightning accounts as describing real physical (not psychological or physiological) phenomena. Jennison referred to his own observation of ball lightning:

> I was seated near the front of the passenger cabin of an all-metal airliner (Eastern Airlines Flight EA 539) on a late night flight from New York to Washington. The aircraft encountered an electrical storm during which it was enveloped in a sudden bright and loud electrical discharge (0005 h EST, March 19, 1963). Some seconds after this a glowing sphere a little more than 20 cm in diameter emerged from the pilot's cabin and passed down the aisle of the aircraft approximately 50 cm from me, maintaining the same height and course for the whole distance over which it could be observed.

Chapman[68] criticized Argyle's afterimage hypothesis as inaccurately describing the observed behavior of afterimages and failing to account for instances where there are multiple observers of the same event. Davies[69], while recognizing the "continuing unsatisfactory attempts to give ball lightning a convincing physical basis," opined that Argyle's approach is little more than asking scientists "to adopt the philosophy that if a phenomenon is difficult to explain physically then it cannot be real."

2.2.2. Exotic States of Matter. Altschuler[70] hypothesized that ball lightning results from nuclear reactions (proton absorption or positron decay) of nitrogen, oxygen, and fluorine nuclei. Ashby and Whitehead[71] thought that ball lightning could be the

---

[67] R. C. Jennison, "Ball Lightning and After-Images," *Nature* **230**, 576 (1971).

[68] W. N. Chapman, "After-Images and Ball Lightning," *Nature* **230**, 576 (1971).

[69] P. C. W. Davies, "Ball Lightning or Spots Before the Eyes?" *Nature* **230**, 576 (1971).

[70] M. D. Altschuler, L. L. House, and E. Hildner, "Is Ball Lightning a Nuclear Phenomenon?" *Nature* **228**, 545 (1970).

[71] D. E. T. F. Ashby and C. Whitehead, "Is Ball Lightning Caused by Antimatter Meteorites?" *Nature* **230**, 180 (1971).

result of the annihilation of small (~5×10^{-10} g) amounts of "meteoritic antimatter from the upper atmosphere." Crawford[72] described evidence of photon flux from annihilation of positrons produced by cosmic rays consistent with the calculations of Ashby and Whitehead.

Gilman[73] proposed that ball lightning consists of Rydberg matter, highly excited atoms with large polarizabilities.

Rabinowitz[74] hypothesized that ball lightning is caused by astrophysical "little black holes" with a mass of approximately 10^{-3} kg that interact with the earth atmosphere, e.g., by ionizing air through gravitational tidal interaction.

2.2.3. Electrochemical and Combustion Theories. Cawood[75] described creating in his laboratory glowing, spherical assemblages of electrically charged aerosols and suggested that "globular lightning may owe its origin to an analogous effect, in which particulate matter, either liquid or solid, is charged to a very much higher potential."

---

[72] J. F. Crawford, "Antimatter and Ball Lightning," *Nature* **239**, 395 (1972).

[73] J. J. Gilman, "Cohesion in Ball Lightning," *Applied Physics Letters* **83**(11), 2283 (2003); J. J. Gilman, "Cohesion in Ball Lightning and Cook Plasmas," in *Shock Compression of Condensed Matter - 2003: Proceedings of the Conference of the American Physical Society Topical Group on Shock Compression of Condensed Matter, Portland, Oregon, 20-25 July 2003*, edited by M. D. Furnish, Y. M. Gupta, and J. W. Forbes (American Institute of Physics, Melville, New York, 2004), pp. 1257-1260.

[74] Mario Rabinowitz, "Ball Lightning: Manifestations of Cosmic Little Black Holes," *Astrophysics and Space Science* **277**, 409-426 (2001).

[75] W. Cawood and H. S. Patterson, "A Curious Phenomenon Shown by Highly Charged Aerosols," *Nature* **128**, 150 (1931).

Bychov[76] sought to explain ball lightning as "a highly charged polymer-dielectric structure" created by an electric discharge on natural materials resulting in an electrically charged, glowing "aggregation of natural polymers, such as lignin and cellulose, soot, polymeric silica and other natural dust particles." Ambramson[77] similarly suggested ball lightning results from the slow oxidation of "filamentary networks" of "nanoparticles" ejected into the air by lightning discharges on soil.

Barry[78] suggested that ball lightning was the result of an atmospheric electrical discharge acting on simple, natural hydrocarbons (e.g., methane or ethane) in the atmosphere at concentrations less than necessary for ordinary combustion. Barry hypothesized that ionization of simple hydrocarbons during a thunderstorm can lead to the creation of more complex hydrocarbons which can "clump together" to form small regions with increased hydrocarbon density. If the density becomes sufficiently large, a nearby electrical discharge could ignite these small regions, creating a visible "burning center" that would be perceived as ball lightning.

2.2.4. Plasma Dynamic and Electrodynamic Theories. . Endean[79] proposed that ball lightning is driven by electromagnetic energy inside a rotating electric dipole

---

[76] V. L. Bychkov, "Polymer-Composite Ball Lightning," *Philosophical Transactions of the Royal Society of London Series A* **360**, 37 (2002).

[77] J. Abrahamson and J. Dinniss, "Ball Lightning Caused by Oxidation of Nanoparticle Networks from Normal Lightning Strikes on Soil," *Nature* **403**, 519 (2000); J. Abrahamson, "Ball Lightning from Atmospheric Discharges via Metal Nanospheres Oxidation from Soils, Wood or Metals," *Philosophical Transactions of the Royal Society of London Series A* **360**, 61 (2002).

[78] J. Dale Barry, "Laboratory Ball Lightning," *Journal of Atmospheric and Terrestrial Physics* **30**, 313 (1968).

[79] V. G. Endean, "Ball Lightning as Electromagnetic Energy," *Nature* **263**, 753 (1976).

configuration of space charges initially attracted to a lightning leader stroke as it approaches the ground.

Wooding[80] suggested that ball lightning could be explained as a plasma vortex ring. Rañada, *et al.*,[81] proposed that ball lightning could be explained as "electromagnetic knots, an electromagentic field in which any pair of magnetic lines or any pair of electric lines form a link – a pair of linked curves."

Fryberger[82] proposed that the "driving engine" of ball lightning is "a vorton-antivorton plasma," and the energy of ball lightning "derives from nucleon decay catalyzed by this plasma."

Powell and Finkelstein[83] described a model of ball lightning as a plasma fireball driven by direct current electric fields created following a lightning strike.

Muldrew[84] proposed a model of ball lightning in which a lightning strike in the vicinity of some small solid object separates electrons from the object, which form an electron layer and a plasma layer around the positively charged object and trap electromagnetic energy within.

---

[80] E. R. Wooding, "Ball Lightning," *Nature* **199**, 272 (1963).

[81] Antonio F. Rañada, "Knotted Solutions of the Maxwell Equations in Vacuum," *Journal of Physics A* **23**, L815 (1990); Antonio F. Rañada and José L. Trueba, "Ball Lightning an Electromagnetic Knot?" *Nature* **383**, 32 (1996); Antonio F. Rañada, Mario Soler, and José L. Trueba, "Ball Lightning as a Force-Free Magnetic Knot," *Physical Review E* **62**, 7181 (2000).

[82] David Fryberger, *A Model for Ball Lightning*, Stanford Linear Accelerator Center Report No. SLAC-PUB-6473. (Stanford University, Stanford, California, 1994). (Presented at First International Workshop on the Unidentified Atmospheric Light Phenomena in Hessdalen, Hessdalen, Norway, March 23-27, 1994.)

[83] J. R. Powell and D. Finkelstein, "Ball Lightning," *American Scientist* **58**, 262 (1970).

[84] D. B. Muldrew, "The Physical Nature of Ball Lightning," *Geophysical Research Letters* **17**, 2277 (1990).

Boichenko[85] suggested that ball lightning could be weakly ionized plasma with gas temperature of approximately 0.5 eV (6000 K). Boichenko showed that the maximum lifetime of balls of such plasmas with diameters of 10-20 cm could have lifetimes of 0.2-1 s if the plasma is not a perfect black body.

Egorov and Stepanov[86] claimed to produce "artificial ball lightning" from drops of water and high-voltage (5.5 kV) discharges between a ring electrode and a central electrodes to form clouds of cold plasma ("plasmoids") which rose upward through the air for less than one second before disappearing. The resulting plasmoids appeared as luminous globes with diameters of approximately 14 cm, but whose behavior bore little resemblance to the reported behavior of ball lightning.

2.2.5. High-Frequency Electromagnetic Wave Interference (Kapitsa Models). Marchant[87] suggested that an instance of "globular lightning" in a house near Liverpool, England, might be the result of ordinary lightning discharge inducing a high-frequency current in telephone wires. He speculated that "this high-frequency current produced something like standing waves in the telephone lead" and that "[i]f an antinode of pressure was formed at the point *A* [where the ball lightning was first observed], something analogous to globular lightning might have been produced at this point and thus have given rise to the phenomena observed."

---

[85] A. M. Boichenko, "Ball Lightning with a Lifetime t≤1 s," *Technical Physics* **44**, 1247 (1999).

[86] A. I. Egorov and S. I. Stepanov, "Long-Lived Plasmoids Produced in Humid Air as Analogues of Ball Lightning," *Technical Physics* **47**, 1584 (2002).

[87] E. W. Marchant, "Globular Lightning," *Nature* **125**, 128 (1930).

Cerillo[88] hypothesized that the appearance of ball lightning inside enclosures could be explained as the possible consequence of natural electromagnetic oscillations of the cavity ("*posible consecuencia de oscilaciones electromagnéticas naturales de la cavidad*") so that, if there is electromagnetic resonance in the enclosure, there may exist one or several isolated regions within the enclosure where the electric field is sufficiently intense to produce excitation and ionization of the air ("*que si hay resonancia electromagnética en el recinto, se pueden predecir una o varias regiones definidas y aisladas entre si, donde el campo eléctrico puede ser lo suficientemente intenso para producir la excitación y ionización del medio*").

Kapitsa[89] hypothesized that ball lightning could be formed at the antinodes of standing electromagnetic waves created by interference of a downward-traveling radio-frequency electromagnetic wave and an upward-traveling wave reflected off the surface of the Earth. Strong electric fields at the antinodes would create plasma discharges through electric breakdown of the air. These plasma discharges would be perceived as ball lightning. Electromagnetic waves with wavelengths between 35 and 70 cm would correspond to observed ball lightning diameters of 10 to 20 cm.

---

[88] Manuel Cerrillo, "Sobre las posibles interpretaciones electromagneticas del fenomeno de las centellas," *Anuario* **1**, 151 (1943) (in Spanish).

[89] P. L. Kapitsa (П. Л. Капица), "О природе шаровой молнии" ("O prerode sharovoi molnii"), Dok. Akad. Nauk SSSR **101**, 245 (1955) (in Russian). (An English language translation of this article appears as P. L. Kapitsa, "The Nature of Ball Lightning," in Donald J. Ritchie, *Ball Lightning: A Collection of Soviet Research in English Translation* (Consultants Bureau, New York, 1961), pp. 11-16.)

Kogan-Beletskii[90] analyzed a ball lightning incident outside a high-flying airplane in terms of Kapitsa's model. In a variation on the Kapitsa model, Watson[91] showed that "a polarized electromagnetic standing wave can actually produce containment of charged particles in the neighbourhood of its electric nodes, and that this effect should be important in the initial stages of fireball formation."

Weinstein[92] also hypothesized that ball lightning could result from the creation of a plasma discharge at a localized region of intense electric field:

> During a thunderstorm, an open resonator, with one mirror formed by the Earth and the other by the cloud, may come into being, and electromagnetic oscillations are excited in this resonator. If the configuration is favorable, the resonator may have a high Q factor. Under certain conditions, a highly concentrated electromagnetic field can be generated; for example, if the resonator is formed by a flat segment of the Earth and the curved surface of the cloud, with the radius of curvature roughly equal to its height above the Earth, then near the surface of the Earth a focus will appear…, a high-frequency discharge will take place there, and ball lightning will appear.

Jennison[93] proposed that ball lightning is formed by a "phase locked loop of electromagnetic radiation in the intense field associated with lightning activity" during which there is "a particular wavelength of electromagnetic radiation which can form a

---

[90] G. I. Kogan-Beletskii (Г. И. Коган-Белечкий), "К вопросу о природе шаровой молнии" ("K voprosu o prirode sharovoi molnii"), *Priroda* **4**, 71 (1957) (in Russian). (An English translation of this article appears as G. I. Kogan-Beletskii, "The Nature of Ball Lightning" in Donald J. Ritchie, *Ball Lightning: A Collection of Soviet Research in English Translation* (Consultants Bureau, New York, 1961).)

[91] W. K. R. Watson, "A Theory of Ball Lightning Formation," *Nature* **185**, 449 (1960).

[92] Weinstein (Vaynshteyn), Lev Albertovich, *Open Resonators and Open Waveguides*, trans. Petr Beckmann, Boulder: Golem Press, 1969. (Translation of original Russian edition, Л. А. Вайнштейн, *Откртые резонаторы и открытые волноводе волноводы* (*Otkrytye rezonatory i otkrytye volnovody*), Sovetskoe Radio, Moskva, 1966.)

[93] R. C. Jennison, "Can Ball Lightning Exist in a Vacuum?," *Nature* **245**, 95 (1973).

stable standing wave which externally exhibits a spherical configuration and which excites the ambient gas to produce the glow by which it is seen."

Zheng[94] analyzed dimension, temperature, energy, and lifetime of ball lightning when described as a spherical standing wave of electromagnetic radiation trapped in a plasma shell.

Espinoza and Chubykolo[95] start from the free Maxwell equations in a vacuum and derive solutions whose spatial components have spherical and ring-like forms that do not change with time. They show that these solutions have characteristics of standing waves and draw the analogy to the Kapitsa model.

Some have objected to the standing wave model. Hill[96] pointed out that "no direct experimental evidence exists for the reality of [intense electromagnetic standing wave] fields…in nature, nor has any practicable way been found for the controlled production of fireballs in this manner."

Rayle states[97], "The radio-frequency excitation process proposed by Kapitza would agree well with the observed characteristics; unfortunately there is little evidence for the existence of sustained, intense, constant-frequency radiation associated with storms."

---

[94] X. H. Zheng, "Quantitative Analysis for Ball Lightning," *Physics Letters A* **148**, 463 (1990).

[95] Augusto Espinoza and Andrew Chubykalo, "Mathematical Foundation of Kapitsa's Hypothesis about the Origin and Structure of Ball Lightning," *Foundations of Physics* **33**, 863 (2003).

[96] E. L. Hill, "Ball Lightning as a Physical Phenomenon," *Journal of Geophysical Research* **65**, 1947 (1960).

[97] Rayle, *Ball Lightning Characteristics.*

Powell and Finkelstein[98] described their own experiments on microwave cavities and criticized the standing wave model on the grounds that "[f]ield strengths of ~1000 V/cm are required at several hundred megahertz at the focal point of the reflected rf waves, but in nature only $\approx 10^{-4}$ V/cm (bandwidth, 250 c/sec) are found."

Altschuler, House and Hildner[99] discounted the model because, he claimed it leads to the conclusion that "ball lightning could not enter metallic enclosures," which is contrary to reports such as by Jennison[100].

Kapitsa[101] himself recognized the problem posed by the lack of direct evidence for the existence of such intense standing waves:

> Although the proposed hypothesis [of intense standing waves] removes a number of the basic difficulties involved in the understanding of ball lightning, nevertheless it should be pointed out that this question is still not definitely settled, in as much as it is still necessary to show the existence in nature of electromagnetic oscillations capable of producing ball lightning. First of all, it is necessary to answer a question which occurs quite naturally; namely, why is it that up to this time there have been no literature references concerning radiation, during a storm, of electromagnetic oscillations in the wavelength region necessary for the formation of ball lightning?

Weinstein[102] also conceded, "at the present time it is not possible to answer the… question concerning the mechanism by which the electromagnetic oscillations maintaining the ball lightning are excited, i.e., the mechanism of converting the energy of

---

[98] J. R. Powell and D. Finkelstein, "Ball Lightning," *American Scientist* **58**, 262 (1970).

[99] M. D. Altschuler, L. L. House, and E. Hildner, "Is Ball Lightning a Nuclear Phenomenon?" *Nature* **228**, 545 (1970).

[100] R. C. Jennison, "Ball Lightning," *Nature* **224**, 895 (1969).

[101] P. L. Kapitsa (П. Л. Капица), "О природе шаровой молнии" ("O prerode sharovoi molnii"), Doklady Akademii. Nauk SSSR **101**, 245 (1955) (in Russian).

[102] Weinstein, Lev Albertovich, *Open Resonators and Open Waveguides*.

a stroke of ordinary lightning to the energy of high-frequency oscillations." Perhaps presciently, Weinstein ascribed the unknown mechanism to an "active substance *A*," a term strikingly similar to the term "active medium" commonly used by laser researchers. Various theoretical and experimental studies of the generation and maintenance of plasmas within resonant cavities and waveguides and by focused or intersecting beams of electromagnetic radiation lend considerable indirect support for the standing wave model.

Meyerand and Haught[103] (cited by Weinstein[104] in support of the standing wave theory) observed "a bright flash of light" indicating the electric breakdown of various gases from the intense electromagnetic fields of focused optical radiation from a ruby rod laser. Ramsden and Davies[105] observed a plasma front, initially formed at the focal region of a high-power pulse laser, moved along the beam path opposite to the direction of the beam.

Kapitsa[106] described a series of experiments involving a "filamentary high frequency discharge floating in the middle of a resonator." The apparatus consisted of a cylindrical resonator coupled through a waveguide to a HF generator that generated radiation with a wavelength of 19.3 cm at a maximum continuous power of 175 kW. Powers from 10 to 20 kW were fed into the discharge. A moveable piston within the

---

[103] R. G. Meyerand, Jr., and A. F. Haught, "Gas Breakdown at Optical Frequencies," *Physical Review Letters* **11**, 401 (1963).

[104] Weinstein, Lev Albertovich, *Open Resonators and Open Waveguides*.

[105] S. A. Ramsden and W. E. R. Davies, "Radiation Scattered from the Plasma Produced by a Focused Ruby Laser Beam," *Physics Review Letters* **13**, 227 (1964).

[106] P. L. Kapitza [Kapitsa], "Free Plasma Filament in a High Frequency Field at High Pressure," *Soviet Physics JETP* **30**, 973 (1970).

resonator allowed the resonant frequency to be tuned. A variety of gases was introduced into the resonator up to pressures of 5 atm, and the discharge was stabilized by imparting a circulatory motion in the gas within the resonator.

Kapitsa[107] performed extensive experimental and theoretical studies of the electrodynamic characteristics of the discharges produced. He concluded that the plasma discharge was hot based on measurements of intense ultraviolet radiation. At low powers and with pure gases, the discharge took a filamentary structure. At higher powers and with mixtures of gases, the discharge took a more ellipsoidal shape. Kaptiza found

> the length of the plasma filament is limited by half a wavelength of the high frequency field, because in such a case the greatest power input to the discharge is achieved. Experiment shows that after the plasma filament has attained this length a further increase in the power input leads to an increase in the cross section which also reaches a limiting value after which the filament begins to break up into two parts…. Thus, for a given frequency of the supply current there exists a limiting size of the filament.

Pershing and Bollen[108] studied the interaction between microwave radiation and air by using a dielectric lens to focus a microwave beam. They studied the dependence of the breakdown power threshold of air on microwave frequency and air pressure. They also studied the motion of plasma wave fronts with and without a reflecting surface. A metal plate oriented perpendicular or at 45º to the incident microwave beam was used to study the effect on the discharge resulting from the interference between the incident and reflected beams near a reflecting surface. They describe the results of a 1-D computer

---

[107] *Ibid*.

[108] Dean Pershing and W. Michael Bollen, *Microwave Interaction with Air*, Report No. MRC/WDC-R-097 (Mission Research Corporation, Alexandria, Virginia, 1985). (Report to Naval Research Laboratory, Washington, DC. Available at http://handle.dtic.mil/100.2/ADA158447.)

simulation code[109] used to model microwave breakdown that include nitrogen chemistry, wave optics, and hydrodynamic effects.

Woo and de Groot[110] performed theoretical investigations of microwave-atmospheric interactions for focused and reflected microwave beams. They also investigated collective plasma effects due to microwaves, such as parametric instabilities, resonant absorption, and the ponderomotive force.

Ohtsuki and Ofuruton[111] described producing "plasma fireballs" by microwave interference within an air-filled cylindrical cavity fed by a rectangular waveguide using a 2.45-GHz, 5-kW (maximum power) microwave oscillator.

Zhil'tsov, *et al.*,[112] used an apparatus similar to that of Ohtsuki and Ofuruton to study "spatially localized (with dimensions much less than the size of the discharge chamber) steady low-power microwave discharges of spheroidal shape."

---

[109] W. M. Bollen, C. L. Yee, and M. J. Nagurney, *High Power Microwave Interaction with Air*, Report No. MRC/WDC-R-025 (Mission Research Corporation, Alexandria, Virginia, 1982). (Final report to Naval Research Laboratory, Washington, DC. Available at http://handle.dtic.mil/100.2/ ADA193917. Alternate title, "Investigation of High-Power Microwave Breakdown in Air.")

[110] Wee Woo and J. S. DeGroot, *Analysis and Computations of Microwave-Atmospheric Interactions*, Report No. PRG-R-98, Final Report for the Period September 1, 1982 to August 31, 1983. (Plasma Research Group, University of California-Davis, Davis, California, 1984).

[111] Y. H. Ohtsuki and H. Ofuruton, "Plasma Fireballs Formed by Microwave Interference in Air," *Nature* **350**, 139 (1991). (See also, Y. H. Ohtsuki and H. Ofuruton, "Plasma Fireballs Formed by Microwave Interference in Air (Corrections)," *Nature* **353**, 868 (1991).)

[112] V. A. Zhil'tsov, É. A. Manykin, E. A. Petrenko, A. A. Skovoroda, J. F. Leitner, and P. H. Handel, "Spatially Localized Microwave Discharge in the Atmosphere," *JETP* **81**, 1072 (1995).

3. HANDEL'S MASER-SOLITON THEORY

Handel's Maser-Soliton Theory (MST)[113] describes ball lightning as a localized region of low-density plasma, a plasma "caviton," fed by a large (several cubic kilometers) atmospheric maser. The atmospheric maser is driven by a population inversion in closely spaced rotational energy levels of water molecules within a large active volume of moist air created by the strong electric field pulse coincident with a lightning strike or polarization catastrophe process[114]. Interference of the emitted microwave radiation within the volume of moist air creates an intense electric field leading to electrical breakdown in the air and creation of a plasma discharge. Nonlinear effects within the plasma discharge create a solitary plasma wave, a soliton, which is perceived as ball lightning.

3.1. MASER ACTION IN MOIST AIR INITIATED BY LIGHTNING

A population inversion in the rotational levels of the ground vibrational state may be achieved by a sudden, short electric field pulse such as that generated during a

---

[113] Peter H. Handel, "New Approach to Ball Lightning," in *Science of Ball Lightning (Fire Ball): First International Symposium on Ball Lightning (Fire Ball); 4-6 July 1988; Waseda University, Tokyo, Japan*, edited by Yoshi-Hiko Ohtsuki (World Scientific, Teaneck, New Jersey, 1989), pp. 254-259; Peter H. Handel and Jean-François Leitner, "Development of the Maser-Caviton Ball Lightning Theory," *Journal of Geophysical Research* **99**, 10689 (1994).

[114] Peter H. Handel, "Polarization Catastrophe Theory of Cloud Electricity - Speculation on a New Mechanism for Thunderstorm Electrification," *Journal of Geophysical Research* **90**, 5857 (1985).

lightning strike. A simple two-level model has been used[115] to show that a sufficiently intense electric field pulse may create a population inversion among water molecules. Consider a two-level quantum system with Hamiltonian $H = H_0 + V$, where H_0 is time-independent and V is a time-dependent perturbation term which accounts for an interaction. E.g., $V(t) = -\vec{p} \cdot \vec{\mathcal{E}}(t)$ represents the interaction of a molecule with dipole moment $\vec{p}$ and a time-dependent electric field $\vec{\mathcal{E}}$.

The wave-function ψ of the two-level system satisfies the time-dependent Schrödinger equation:

$$i\hbar \frac{d\phi}{dt} = H\phi \tag{3.1}$$

For the unperturbed system, there are two solutions (j = 1, 2):

$$i\hbar \frac{d\phi_j}{dt} = H_0\phi_j \,, \tag{3.2}$$

where the energy eigenvalues are found from

$$H_0\phi_j = E_j\phi_j \,. \tag{3.3}$$

And the general solution to the time dependent problem has the form:

$$\psi = \sum_{j=1}^{2} c_j(t)\phi_j \,, \tag{3.4}$$

---

[115] Peter H. Handel, "New Approach to Ball Lightning," in *Science of Ball Lightning (Fire Ball): First International Symposium on Ball Lightning (Fire Ball); 4-6 July 1988; Waseda University, Tokyo, Japan*, edited by Yoshi-Hiko Ohtsuki (World Scientific, Teaneck, New Jersey, 1989), pp. 254-259; Peter H. Handel and Glenn A. Carlson, "Rise Time of Maser-Caviton Ball Lightning Energy Spikes," *Proceedings Ninth International Symposium on Ball Lightning*, ISBL-06, 16-19 August 2006, Eindhoven, The Netherlands, Ed. G. C. Dijkhuis.

where the time-dependent coefficients $c_j(t) = c_j e^{-iEt/\hbar}$ are written in terms of time-independent magnitudes c_j and the energy eigenvalues E of ψ.

The probability of finding the system in eigenstate 2 of the unperturbed system is:

$$\left|\left\langle \phi_2 \left| \psi(\tau) \right\rangle\right|^2 = \frac{4\mu_{12}^2 \mathcal{E}^2}{4\mu_{12}^2 \mathcal{E}^2 + \left(E_2 - E_1\right)^2} \sin^2\left[\frac{\Omega t}{2}\right] \tag{3.5}$$

where $\mu_{jk} = \left\langle \phi_j \left| \vec{p} \right| \phi_k \right\rangle$ are the matrix elements for the dipole moment in the two-state basis set, E_1 and E_2 are the energy eigenvalues of the unperturbed states 1 and 2, respectively, and

$$\Omega = \sqrt{\left(\frac{E_2 - E_1}{\hbar}\right)^2 + \frac{4\mu_{12}^2 \mathcal{E}^2}{\hbar^2}}\,. \tag{3.6}$$

The population ratio R of eigenstate 2 and eigenstate 1 is

$$R = \frac{\left|\left\langle \phi_2 \left| \psi(\tau) \right\rangle\right|^2}{1 - \left|\left\langle \phi_2 \left| \psi(\tau) \right\rangle\right|^2} = \frac{\sin^2\left[\frac{\Omega t}{2}\right]}{\left(\frac{E_2 - E_1}{2\mu_{12}\mathcal{E}}\right)^2 + \cos^2\left[\frac{\Omega t}{2}\right]}\,. \tag{3.7}$$

A population inversion exists between states 1 and 2 when $R > 1$, which from (3.7) will occur for when the electric field is sufficiently strong such that such that the energy of the dipole exceeds the energy spacing between eigenstates 1 and 2:

$$\mathcal{E} > \frac{E_2 - E_1}{2\mu_{12}} \tag{3.8}$$

A sudden, short electric pulse of duration τ and amplitude E can produce a population ratio R

$$R = \frac{\left|W_{12} \sin r\tau\right|}{\left(\frac{1}{2} hf\right)^2 + \left(W_{12} \cos r\tau\right)^2}\,, \tag{3.9}$$

according to the solution of the Schrödinger equation for two close energy levels connected by the matrix element W_{12} corresponding to the applied electric field E. Here, $r = \sqrt{\omega^2/4 + |W_{12}/\hbar|^2}$ and h is Planck's constant. If the energy difference hf between the almost degenerate levels is small (i.e., $hf \ll W_{12}$), Equation (3.9) predicts a population inversion whenever the duration τ is close to $(2n+1)\pi/2r$. Many such pairs of closely-spaced energy levels exist in the high frequency spectrum of the asymmetric top water molecule. Most of the pairs of close-lying energy levels of the water molecule correspond to forbidden transitions, but become weakly allowed in the presence of a perturbing applied electric field.

The magnitude of the potential energy of an electric dipole with dipole moment d in an electric field E is $W_{12} \sim Ed$. The dipole moment of a water molecule d = 1.85 Debye = $1.85 \times 3.335641 \times 10^{-30}$ C·m = 6.17×10^{-30} C·m.

3.1.1. Water Vapor Lasers. There is considerable circumstantial support, both experimental and analytical, for the hypothesis that the volume of water vapor beneath a thunder cloud could constitute an active masing medium. Water vapor is known to provide an active lasing medium for both microwave and infrared radiation. Artificial water vapor lasers operate on over a hundred infrared lines from 7 to 220 microns[116]

---

[116] W. S. Benedict, "Identification of Water-Vapor Laser Lines," *Applied Physics Letters* **12**(5), 170 (1968); M. A. Pollack and W. J. Tomlinson, "Molecular Level Parameters and Proposed Identifications for the CW Water-Vapor Laser," *Applied Physics Letters* **12**(5), 173 (1968); William S. Benedict, Martin A. Pollack, and W. John Tomlinson III, "The Water-Vapor Laser," *IEEE Journal of Quantum Electronics* QE-5, 108 (1969).

including weakly allowed ro-vibrational transitions in the microwave region among low-lying vibrational states in H_2O[117].

The existence of natural water masers was unknown until Cheung, *et al.*,[118] reported the detection of the 1.35-cm line (22-GHz) corresponding to the $6_{16} \rightarrow 5_{23}$ transition in interstellar water. Knowles, *et al.*,[119] confirmed the maser nature of these emissions through their small size (< 1arc min diameter), extreme brightness temperature (> 50,000 K), and variability on the order of weeks. Since these initial discoveries, water masers have been detected in many interstellar environments[120] (e.g., late-type stars and star-forming regions) and in the nuclei of active galaxies[121].

3.1.2. Atmospheric Masers. A natural, low gain laser in the infrared bands within the CO_2-rich atmosphere of Mars was discovered by Mumma, *et al.*[122] A natural laser, also operating in the infrared, has also been found in the atmosphere of Venus.[123]

---

[117] B. Hartmann and B. Kleman, "On the Origin of the Water-Vapor Laser Lines," *Applied Physics Letters* **12**(5), 168 (1968).

[118] Cheung, D. M., Rank, C. H. Townes, D. D. Thornton, and W. J. Welch, "Detection of Water in Interstellar Regions by its Microwave Radiation," *Nature* **221**, 626 (1969).

[119] S. H. Knowles, C. H. Mayer, A. C. Cheung, D. M. Rank, and C. H. Townes, "Spectra, Variability, Size, and Polarization of H_2O Microwave Emission Sources in the Galaxy," *Science* **163**, 1055 (1969).

[120] Moshe Elitzur, *Astronomical Masers*, Dordrecht: Kluwer, 1992, Chapter 10.

[121] J. A. Braatz, C. Henkel, L. J. Greenhill, J. M. Moran, and A. S. Wilson, "A Green Bank Telescope Search for Water Masers in Nearby Active Galactic Nuclei," *Astrophysical Jounal* **617**, L29 (2004).

[122] Michael J. Mumma, David Buhl, Gordon Chin, Drake Deming, Fred Espenak, Theodor Kostiuk, David Zipoy, "Discovery of Natural Gain Amplification in the 10-micrometer Carbon Dioxide Laser Bands on Mars: A Natural Laser," *Science* **212**, 45 (1981).

[123] D. Deming, F. Espenak, D. Jennings, T. Kostiuk, M. Mumma, and D. Zipoy, "Observations of the 10-μm Natural Laser Emission from Mesospheres of Mars and Venus," *Icarus* **55**, 347 (1983).

In both cases solar energy drives the inversion by radiation pumping.[124]. Deming and Mumma[125] speculate creating an artificial laser sufficiently intense for interstellar communication by placing engineered mirrors in suitable orbits around Mars to amplify the power of the natural Martian laser.

Natural population inversions for CO_2 vibrational states have also been observed in the Earth's atmosphere at altitudes of 95-100 km at which the rate of molecular collisions that would thermalize excited states decreases below the pumping rate due to absorption of solar infrared radiation.[126] In addition, at higher altitudes, population inversions are also fed by O_2 and O_3 photodissociation in the ultraviolet.

Cosmovici, *et al*.,[127] claimed the first evidence of a planetary water maser in the atmosphere of Jupiter immediately following the impact of the Shoemaker-Levy 9 comet on Jupiter. On observing the water line at 22.235 GHz, they claimed water maser emission based on a narrow line width of 40 kHz and a brightness temperature of 20000 K. However, Cecchi-Pestellini and Scappini[128] disputed the Cosmovici results and claimed the observed water line emission was not maser emission, but rather, was intense

---

[124] Michael J. Mumma, *et al.*, "Discovery of Natural Gain Amplification in the 10-micrometer Carbon Dioxide Laser Bands on Mars: A Natural Laser," *Science* **212**, 45 (1981); Drake Deming and Michael J. Mumma, "Modeling of the 10-μm Natural Laser Emission from the Mesospheres of Mars and Venus," *Icarus* **55**, 356 (1983); F. W. Taylor, "Natural Lasers on Venus and Mars," *Nature* **306**, 640 (1983).

[125] Drake Deming and Michael J. Mumma, "Modeling of the 10-μm Natural Laser Emission from the Mesospheres of Mars and Venus," *Icarus* **55**, 356 (1983).

[126] G. M. Shved and V. P. Ogibalov, "Natural Population Inversion for the CO_2 Vibrational States in Earth's Atmosphere," *Journal of Atmospheric and Solar-Terrestrial Physics* **62**, 993 (2000).

[127] Cristiano B. Cosmovici, Stelio Montebugnoli, Alessandro Orfei, Sergej Pgrebenko, and Piere Colom, "First Evidence of Planetary Water Emission Induced by the Comet/Jupiter Catastrophic Impact," *Planetary and Space Science* **44**, 735 (1996).

[128] Cesare Cecchi-Pestellini and Flavio Scappini, "Modeling Water Emission Induced by the Shoemaker-Levy 9/Jupiter Catastrophic Impact," *Canadian Journal of Physics* **79**, 123 (2001).

water thermal emission produced by a high concentration of water deposited by the cometary impact.

3.2. MASER-CAVITON BALL LIGHTNING ENERGY SPIKES

The creation of a ball lightning discharge by an atmospheric maser requires the generation of a large amount of energy in a very short time. Sufficient energy must be generated by the atmospheric maser to ionize air, and the energy must be generated before molecular collisions destroy the population inversion that gives rise to the maser action.

Handel and his collaborators showed that maser action in a large volume of atmosphere could generate a large initial electromagnetic spike[129], and a similar spike at the demise of a ball lightning discharge[130]. Additionally, spiking has been proposed to

---

[129] Peter H. Handel and Glenn A. Carlson, "Rise Time of Maser-Caviton Ball Lightning Energy Spikes," *Proceedings Ninth International Symposium on Ball Lightning*, ISBL-06, 16-19 August 2006, Eindhoven, The Netherlands, Ed. G. C. Dijkhuis; Peter H. Handel, Glenn A. Carlson, and Jean-François Leitner, "Maser-Caviton Ball Lightning Interaction Spiking with Cold Emission," *Proceedings Ninth International Symposium on Ball Lightning*, ISBL-06, 16-19 August 2006, Eindhoven, The Netherlands, Ed. G. C. Dijkhuis; P. H. Handel, G. A. Carlson, M. Grace, J.-F. Leitner, "Electric Ponderomotive Forces Cause Explosive Ball Lightning Damages," *Proceedings Eighth International Symposium on Ball Lightning*, ISBL-04, 3-6 August 2004, National Central University, Chung-Li, Taiwan.

[130] Peter H. Handel and Jean-François Leitner, "Development of the Maser-Caviton Ball Lightning Theory," *Journal of Geophysical Research* **99**, 10689 (1994); Peter H. Handel, Glenn A. Carlson, and Jean-François Leitner, "Maser-Caviton Ball Lightning Interaction Spiking with Cold Emission," *Proceedings Ninth International Symposium on Ball Lightning*, ISBL-06, 16-19 August 2006, Eindhoven, The Netherlands, Ed. G. C. Dijkhuis; P. H. Handel, G. A. Carlson, M. Grace, J.-F. Leitner, "Electric Ponderomotive Forces Cause Explosive Ball Lightning Damages," *Proceedings Eighth International Symposium on Ball Lightning*, ISBL-04, 3-6 August 2004, National Central University, Chung-Li, Taiwan.

explain reports of humming sounds associated with ball lightning[131] and of the movement of solid objects by ball lightning.[132]

3.2.1. Spiking of an Atmospheric Maser. The analysis begins with the coupled rate equations for the photon number $n(t)$ and upper-level molecular population $N_2(t)$ within the active region of the maser:

Photon number:

$$\frac{d}{dt}n(t) = K\left[n(t)+1\right]N_2(t) - \frac{1}{\tau_c}n(t) - \frac{1}{\tau_b}n(t) \tag{3.10}$$

Upper level:

$$\frac{d}{dt}N_2(t) = -Kn(t)N_2(t) - \frac{1}{\tau_2}N_2(t) + R_p(t), \tag{3.11}$$

where τ_c is the cavity lifetime (the "cavity ringing time"), τ_2 ($>> \tau_c$) is the total lifetime of the upper level due to decay mechanisms, K is the coupling parameter that relates the energy transfer between the photons and the upper-level molecules, and $R_p(t)$ is an effective pumping rate of atoms into the upper level. Equations (3.10) and (3.11) are the standard rate equations[133] with the additional term $n(t)/\tau_b$ that represents the rate of depletion of photons resulting from the "load" represented by the visible ball lightning.

---

[131] Peter H. Handel, Glenn A. Carlson, and Jean-François Leitner, "Maser-Caviton Ball Lightning Interaction Spiking with Cold Emission," *Proceedings Ninth International Symposium on Ball Lightning*, ISBL-06, 16-19 August 2006, Eindhoven, The Netherlands, Ed. G. C. Dijkhuis.

[132] P. H. Handel, G. A. Carlson, M. Grace, J.-F. Leitner, "Electric Ponderomotive Forces Cause Explosive Ball Lightning Damages," *Proceedings Eighth International Symposium on Ball Lightning*, ISBL-04, 3-6 August 2004, National Central University, Chung-Li, Taiwan.

[133] A. E. Siegman, *An Introduction to Lasers and Masers*, New York: McGraw-Hill, 1971, p. 422.

The relaxation of the lower molecular population $N_1(t)$ is sufficiently fast that $N_1 \approx 0$ at all times; thus $N_2(t)$ also represents the population inversion. The upper-level lifetime τ_2 may be as long as a second or a minute if the upper-to-lower transition is one of the many well-known strongly forbidden transitions between pairs of nearly coincident rotational energy levels of the water molecule that may become weakly allowed under the influence of perturbing fields.

The effective pumping rate $R_p(t)$ allows for the case in which the upper-level population is replenished by various processes (e.g., by circulation of inverted air into the active region, by motion of inverted air from nodes to antinode of a standing wave, or by recuperation of a hole burned into an inhomogeneously broadened molecular transition in the frequency domain). Thus, a quasi-stationary, slowly decaying maser action can be sustained over a considerable interval of time[134].

The coupling parameter K may be shown to be[135]:

$$K = \frac{1}{\tau_{rad} p}, \tag{3.12}$$

where τ_{rad} is the spontaneous decay rate (the "radiative" decay rate) of the upper level and

$$p = \frac{8\pi V_c}{\lambda^3} \frac{\Delta\omega_a}{\omega_a} \tag{3.13}$$

is the cavity mode number, which is equal to the number of cavity modes within the molecular linewidth $\Delta\omega_a$. In (3.13), V_c is the cavity volume and ω_a, $\Delta\omega_a$, and λ are the

---

[134] Peter H. Handel and Jean-François Leitner, "Development of the Maser-Caviton Ball Lightning Theory," *Journal of Geophysical Research* **99**, 10689 (1994).

[135] Siegman, *Lasers*, p. 499.

frequency, linewidth, and wavelength, respectively, of the molecular transition corresponding to the upper maser level.

From Appendix A, we see that the pressure-broadened linewidths of the low-energy transitions (λ = 10 cm) for water are on the order of $\Delta\bar{\nu}/\bar{\nu} = \Delta\omega_a/\omega_a = 1$. Then, for an atmospheric maser volume of 1 km^3, the cavity mode number is on the order of $p = 10^{12}$, a much larger number than for ordinary laser cavities.[136]

For an atmospheric maser in open air, without cavity walls or reflecting objects or boundaries, the "cavity" lifetime τ_c is on the order of L/c, where L is the diameter or characteristic size of the active volume of air containing the inverted population, and c is the speed of light. The quality factor Q of such a cavity may be defined as [137]

$$Q = 2\pi\nu \frac{\left(\text{Energy stored in the cavity}\right)}{\left(\text{Rate of energy loss from the cavity}\right)}, \tag{3.14}$$

where ν is the frequency of the radiation within the cavity.

Let the energy stored in the cavity be represented by U. Then, for a mirrorless cavity and assuming no losses (absorption) inside the cavity, all the energy within the cavity leaves the cavity in the time it takes for light to traverse the cavity. If we take the characteristic length of the cavity as L, rate of energy loss from the cavity is simply

$$\left(\text{Rate of energy loss from the cavity}\right) = \frac{U\,c}{L}, \tag{3.15}$$

where c is the speed of light. The quality factor for a mirrorless cavity is then

---

[136] *Ibid*., p. 501.

[137] A. Maitland and M. H. Dunn, *Laser Physics*, Amsterdam: North-Holland, 1969, p. 101; Siegman, *An Introduction to Lasers and Masers*, p. 190.

$$Q_c = \frac{2\pi\nu L}{c}. \tag{3.16}$$

For a mirrorless cavity with $\nu = 1$ GHz and $L = 1$ km, the quality factor is very large, $\sim 10^4$ and the cavity lifetime is $\sim 10^{-5}$, better than for resonant cavities with copper walls[138].

Large amplitude spiking in the photon number that occurs during the initial "turn-on" phase of the maser can be analyzed by studying the behavior of (3.10) and (3.11) at threshold. [139] Before the ball lightning discharge has formed, $\tau_b = 0$, and the "threshold" value for the upper population $N_{2,th}$ by considering the steady state ("ss") solutions of (3.10) and (3.11) in the form:

$$n_{ss} = \frac{N_{2,ss}}{N_{2,th} - N_{2,ss}} \tag{3.17}$$

and

$$N_{2,ss} = \frac{R_p}{\frac{1}{\tau_2} + K n_{ss}}, \tag{3.18}$$

where

$$N_{2,th} \equiv \frac{1}{K\tau_c}. \tag{3.19}$$

From (3.17), we see that the photon number will be small until the upper-level population N_2 is brought very close to the threshold value $N_{2,th}$. From (3.18), we see that

---

[138] Peter H. Handel and Jean-François Leitner, "Development of the Maser-Caviton Ball Lightning Theory," *Journal of Geophysical Research* **99**, 10689 (1994).

[139] Siegman, *Lasers*, p. 510; Peter H. Handel, Glenn A. Carlson, and Jean-François Leitner, "Maser-Caviton Ball Lightning Interaction Spiking with Cold Emission," *Proceedings Ninth International Symposium on Ball Lightning*, ISBL-06, 16-19 August 2006, Eindhoven, The Netherlands, Ed. G. C. Dijkhuis.

when $N_2 << N_{2,th}$, the upper-level population is approximately directly proportional to the pumping rate R_p.

From (3.18), we see that the threshold pumping rate such that $N_{2,ss} = N_{2,th}$ is

$$R_{p,th} = \frac{N_{2,th}}{\tau_2} = \frac{1}{K\tau_2\tau_c}. \tag{3.20}$$

It is convenient to define a nondimensionalized pumping rate by

$$r \equiv \frac{R_p}{R_{p,th}}. \tag{3.21}$$

The situation is quite different when the upper-level population exceeds the threshold value. By rearranging (3.17), (3.18), and (3.19), we can write the steady-state photon number and upper-level population in the form[140]:

$$N_{2,ss} = \frac{n_{ss}}{n_{ss}+1} N_{2,th} \tag{3.22}$$

and

$$n_{ss} = \frac{R_p - N_{2,ss}/\tau_2}{KN_{2,ss}} = \frac{\tau_2 p}{\tau_{rad}}\left(\frac{N_{2,th}}{N_{2,ss}} r - 1\right), \tag{3.23}$$

where we relate the coupling parameter K and the cavity mode number p through (3.12) and (3.13).

From (3.23), we see that, above threshold (r, the magnitude of the photon number is on the same order of magnitude as the cavity mode number p, which was shown above to a very large number on the order of 10^{12}.

---

[140] Siegman, *Lasers*, p. 513.

An alternative approach to analyzing spiking at threshold is to recognize that, in the quasi-stationary regime, the time derivatives are zero in (3.10) and (3.11). If we then eliminate N_2 and solve the resulting quadratic equation for n, we find

$$n = \frac{p}{2}\left\{ r - 1 + \left[(r-1)^2 + \frac{4r}{p} \right]^{\frac{1}{2}} \right\}. \tag{3.24}$$

Since p is a large number $\sim 10^{12}$, (3.24) describes a very large increase in the number of photons n as r exceeds unity.

Spiking may also occur at the sudden demise of a ball lightning discharge, when τ_b in (3.10) becomes suddenly very large, causing r to quickly exceed unity. Handel, *et al.*,[141] have suggested that this final act of spiking can be very destructive, because the electric field amplitude and the photon number increase to very high levels, exerting large electrostatic forces on dielectrics in the vicinity of the former discharge without a sign of heating or burning.

3.2.2. Low-Temperature Ball Lightning Discharge. Handel, *et al.*, propose the spiking process to explain the much lower temperature of ball lightning and its apparent lack of buoyancy as compared to the arc discharge that is normally obtained at atmospheric pressure in the laboratory. After forming, the ball lightning continuously tries to extinguish, due to the absence of free electrons at the low temperatures at which ball lightning is observed and that often are only slightly higher the surrounding

---

[141] Peter H. Handel and Glenn A. Carlson, "Rise Time of Maser-Caviton Ball Lightning Energy Spikes," *Proceedings Ninth International Symposium on Ball Lightning*, ISBL-06, 16-19 August 2006, Eindhoven, The Netherlands, Ed. G. C. Dijkhuis; P. H. Handel, G. A. Carlson, M. Grace, J.-F. Leitner, "Electric Ponderomotive Forces Cause Explosive Ball Lightning Damages," *Proceedings Eighth International Symposium on Ball Lightning*, ISBL-04, 3-6 August 2004, National Central University, Chung-Li, Taiwan.

temperature, particularly in the case of orange-colored ball lightning. When the discharge attempts to end, however, the vanishing load generates the next spike. The spike consists of photons identical to the ones in the previous spike, because it is generated through stimulated emission initiated by photons still present in the standing wave. These new photons create an electric field with a maximum at exactly the same place in which the ball lightning was located. This explains ball lightning's apparent lack of buoyancy.

3.2.3. Humming Sounds from Ball Lightning. Handel, *et al*.,[142] suggest that low-frequency spiking or "humming" of the maser-soliton system could explain the few reports of "hissing, buzzing, or fluttering" sounds from ball lightning[143]. In Rayle's survey[144], 25 of 108 respondents answered "Yes" when asked, "Did you notice any sound from the ball [lightning]?"

On linearizing the rate equations (3.10) and (3.11) about the steady state solutions (3.17) and (3.18) (or (3.22) and (3.23)), we can write the linearized rate equations as

$$\frac{d\tilde{n}(t)}{dt} = \frac{(r-1)}{\tau_2}\tilde{N}(t) \tag{3.25}$$

and

$$\frac{d\tilde{N}(t)}{dt} = -\frac{\tilde{n}(t)}{\tau} - r\frac{\tilde{N}(t)}{\tau_2}, \tag{3.26}$$

where $\tau^{-1} = \tau_c^{-1} + \tau_b^{-1}$, r is defined in (3.21), and $\tilde{n}(t)$ and $\tilde{N}(t)$ are small-signal fluctuations about the steady-state solutions, i.e.,

---

[142] *Ibid*.

[143]Stenhoff, *Ball Lightning: An Unsolved Problem in Atmospheric Physics*, pp. 17, 79, 125, 151, 172.

$$n(t) = n_{ss}(t) + \tilde{n}(t) \tag{3.27}$$

and

$$N_2(t) = N_{2,ss}(t) + \tilde{N}(t). \tag{3.28}$$

If we now assume that the fluctuations vary as exp(*st*), then (3.27) and (3.28) lead to the secular determinant 1

$$0 = \begin{vmatrix} s & -\dfrac{(r-1)}{\tau_2} \\ \dfrac{1}{\tau} & s + \dfrac{r}{\tau_2} \end{vmatrix} \tag{3.29}$$

and the secular equation

$$s^2 + \frac{r}{\tau_2} s + \frac{(r-1)}{\tau\tau_2} = 0. \tag{3.30}$$

The roots s_1 and s_2 of (3.30) describe the exponential decay and oscillation frequencies of the fluctuations about the steady state:

$$s_1, s_2 = -\frac{r}{2\tau_2} \pm i\sqrt{\frac{(r-1)}{\tau\tau_2} - \left(\frac{r}{2\tau_2}\right)^2} \equiv -\gamma \pm i\omega \tag{3.31}$$

When $\tau_2 >> \tau$, such as when the lifetime τ_2 is for a long-lived strongly-forbidden rovibrational transitions of H_2O that becomes weakly allowed by the electric fields generated during a thunderstorm, then the expression under the radical in (3.31) is greater than zero and the complete solutions take the form of exponentially damped sinusoids:

$$n(t) = n_{ss}(t) + \tilde{n}e^{-\gamma t}\cos\omega t \tag{3.32}$$

and

---

[144] Rayle, *Ball Lightning Characteristics*.

$$N_2(t) = N_{2,ss}(t) + \tilde{N}e^{-\gamma t}\cos\omega t\,. \tag{3.33}$$

(We note here that the statement "the lifetime τ_2 is for a long-lived strongly-forbidden rovibrational transitions of H_2O that becomes weakly allowed by the electric fields generated during a thunderstorm" does not account for the fact that the relaxation lifetime τ_2 of the transition also includes the *nonradiative* lifetime due to collisions as well as the radiative lifetime. We will see below that, for air at atmospheric pressure, the nonradiative lifetime due to collisions is very short, on the order of 10^{-8} s to 10^{-10} s.)

The "humming" frequency ω is thus determined in first approximation by $r - 1$, τ_2, and τ through (3.31):

$$\omega = \sqrt{\frac{(r-1)}{\tau\tau_2} - \left(\frac{r}{2\tau_2}\right)^2}\,. \tag{3.34}$$

The humming frequency is thus determined in first approximation by $r-1$, τ_2 and τ_c through Eq. (17).

Handel and Leitner[145] reported the experimental "excitation of sound waves in LPO [localized plasma objects]."

3.3. PERCEIVED ENERGY OF BALL LIGHTNING

Various commentators have estimated the energy contained in ball lightning. One of the earliest is based on a "Letter to the Editor of 'The Daily Mail'" [London] from W. Morris published on November 5, 1936[146]:

---

[145] Peter H. Handel and Jean-François Leitner, "Development of the Maser-Caviton Ball Lightning Theory," *Journal of Geophysical Research*, **99**, 10689 (1994).

[146] p. 14.

> Sir, -- During a thunderstorm I saw a large, red hot ball come down from the sky. It struck our house, cut the telephone wire, burnt the window frame, and then buried itself in a tub of water which was underneath.
>
> The water boiled for some minutes afterwards, but when it was cool enough for me to search I could find nothing in it.

Sir Charles V. Boys[147] spoke of Mr. Morris' account to Prof. B. L. Goodlet and others at a meeting of The Institution of Electrical Engineers. According to Sir Boys, he "ascertained that the ball appeared to be the size of a large orange, and after 20 minutes the water was too hot for Mr. Morris to put his hands into it. The amount of water was about 4 gallons." (It is unclear how Sir Boys "ascertained" this information not included in the account published in the *The Daily Mail*.) Based on this information, Prof. Goodlet estimated the energy contained in the ball lightning, thus[148]:

> Water "too hot to put one's hands in" is probably over 60º C.; if the initial temperature [of the water] was 10º C. we get for the minimum energy 2000 lb.-deg. C. [*sic*] or 3800 kW-sec. If we assume that all the water in the butt[149] was raised to 100º C. and that 4 lb. of water was actually evaporated, the energy becomes 10940 kW-sec., which is identical with Prof. Thornton's estimate of the energy of a fireball – viz. 8 million ft.-lb.

"Prof. Thornton," to whom Prof. Goodlet refers, is Prof. W. M. Thornton[150] who proposed that ball lightning is a gaseous sphere of ozone, and the energy released is due to chemical decomposition of ozone.

---

[147] B. L. Goodlet, "Lightning," *I. E. E. Journal*, **81**, 31 (1937).

[148] *Ibid*., p. 55.

[149] Butt: "a large cask especially for wine, beer, or water." Merriam-Webster Online Dictionary, http://www.merriam-webster.com (Accessed December 31, 2011.)

[150] W. M. Thornton, "On Thunderbolts," *Philosophical Magazine Series 6* **21**, 630 (1911).

Barry[151] compiles various estimates of the energy density of ball lightning derived from *The Daily Mail* account. Depending on the assumptions made, the estimates range from 2.4×10^3 J·cm^{-3} to 1.9×10^3 J·cm^{-3}. Barry calculates this upper limit by assuming the diameter of a "large orange" is 10 cm.

Handel, *et al.*,[152] assert that the Maser-Soliton Theory can explain why the energy of the demise of ball lightning can be considerable in open air, but, in the case of ball lightning confined to a conducting enclosure, the total energy of the final spike is too small to produce any damage, or even to be noticed. For an enclosure volume $V =$ 10 m × 5 m × 3 m = 150 m^3 with an absolute humidity of $\rho = 20$ g/m^3 and a ball lightning frequency of $\nu = 2\times10^8$ Hz, an upper limit on the ball lightning energy may be estimated from the available water molecules ($M_W = 18$ g/mol):

$$\frac{V \rho N_A h \nu}{M_W} = 13.2 \text{ J}, \tag{3.35}$$

where Avogadro's number $N_A = 6\times10^{23}$ mol^{-1} and Planck's constant $h = 6.6\times10^{-34}$ J·s. Now, since not every water molecule will contribute a photon, we expect a ten times smaller result, 1.3 J, which is harmless.

However, for a volume of open air $V =$ 1 km^3, the ball lightning energy is 9000 kJ if only 10% of the water molecules contributes a photon, which is approximately the same order of magnitude as Prof. Goodlet's estimate. For a ball lightning of

---

[151] Barry, *Ball Lightning and Bead Lightning: Extreme Forms of Atmospheric Electricity*, Section 4.2.

[152] P. H. Handel, G. A. Carlson, M. Grace, J.-F. Leitner, "Electric Ponderomotive Forces Cause Explosive Ball Lightning Damages," *Proceedings Eighth International Symposium on Ball Lightning*, ISBL-04, 3-6 August 2004, National Central University, Chung-Li, Taiwan.

approximately 10 cm in diameter, the energy density is 5×10^4 J/cm^3, which is not wildly different from Barry's estimates of the energy density of ball lightning in open air.

3.4. PHASE SHIFTS AND THE MOTION OF BALL LIGHTNING

Handel, *et al*.,[153] use the Maser-Soliton Theory to explain ball lightning motion as the time dependence of the phase differences between the component waves that give rise to the ball lightning discharge. Gradients in the population inversion in the active region of the atmosphere result in maser radiation of slightly lower frequencies from regions with lesser population inversions and of slightly higher frequencies from regions with greater population inversions. The wave generated in the region where these two waves intersect has a non-zero group velocity, and so is observed to move opposite to the gradient population inversion.

Let ω be the "average" frequency of maser radiation generated in the active region. The population inversion across the region is not uniform. Where the population inversion slightly greater than the average, the maser radiation has a frequency slightly above average, i.e., $\omega + s$. Where the population inversion is slightly less than average, the maser radiation has a frequency slightly below average, i.e., $\omega - s$. If $\vec{k}$ is the wave vector pointing from the "higher" region to the "lower" region, the intersection $\vec{E}$ of the two waves can be written as

$$\vec{E} = \vec{E}_0\, \mathrm{e}^{i\left[\vec{k}\cdot\vec{r}-(\omega+s)t\right]} + \vec{E}_0\, \mathrm{e}^{i\left[-\vec{k}\cdot\vec{r}-(\omega-s)t\right]}, \tag{3.36}$$

---

[153] P. H. Handel, G. A. Carlson, and J.-F. Leitner, "Phase Shifts Considered as the Cause of the Motion of Ball Lightning," *Proceedings Second International Symposium on Unconventional Plasmas*, ISUP-06, 14-16 August 2006, Eindhoven, The Netherlands, Eds. G. C. Dijkhuis and H. Kikuchi.

where the waves are arbitrarily assumed to have equal magnitude.

Now, if we assume a vector $\vec{v}$ such that

$$\vec{k} \cdot \vec{v} = s\,, \tag{3.37}$$

we may write (3.36) in the form

$$\vec{E} = \vec{E}_0\, \mathrm{e}^{i\left[\vec{k}\cdot(\vec{r}-\vec{v}t)-\omega t\right]} + \vec{E}_0\, \mathrm{e}^{i\left[-\vec{k}\cdot(\vec{r}-\vec{v}t)-\omega t\right]} = 2\vec{E}_0 e^{i\omega t} \cos\left[\vec{k}\cdot\left(\vec{r}-\vec{v}t\right)\right], \tag{3.38}$$

which is a wave moving with velocity $\vec{v}$ defined by (3.37).

Thus the ball lightning will move at a velocity $\vec{v}$ in the direction opposed to the gradient of the population inversion.

3.5. BALL LIGHTNING IS A PLASMA SOLITON

In Handel's Maser-Soliton Theory[154], an atmospheric maser is created during a thunderstorm when a sudden electric field of a conventional lightning strike creates population inversion in water molecules within a large volume of the atmosphere. Maser action creates a standing electromagnetic wave between the thundercloud and the earth as in Kapitsa's model[155]. A standing wave of sufficient magnitude and frequency can result in the electric breakdown of air and the creation of a plasma soliton, or caviton[156].

The caviton is described by a nonlinear Schrödinger describing the interaction of the plasma and the electric field. The saturating ponderomotive force acting on plasma

---

[154] Peter H. Handel, "New Approach to Ball Lightning," in *Science of Ball Lightning (Fire Ball): First International Symposium on Ball Lightning (Fire Ball); 4-6 July 1988; Waseda University, Tokyo, Japan*, edited by Yoshi-Hiko Ohtsuki (World Scientific, Teaneck, New Jersey, 1989), pp. 254-259.

[155] P. L. Kapitsa (П. Л. Капица), "О природе шаровой молнии" ("O prerode sharovoi molnii"), *Doklady Akademii Nauk SSSR* **101**, 245 (1955) (in Russian).

[156] A. Y. Wong, "Cavitons," *Journal de Physique* **C6**, 27 (1977).

electrons is represented by exponential nonlinearity. The ponderomotive force drives electrons out of the plasma, and electrostatic attraction force the ions to follow. The result is a low-density region, or caviton, containing a trapped large-magnitude electric field. Initial studies of cavitons by Zakharov[157] showed they were unstable with respect to collapse, but Laedke and Spatschek[158] showed that three-dimensional cavitons are stable for sizes exceeding a certain minimum. This stable quasi-spherical configuration of trapped electromagnetic field surrounded by plasma is perceived as ball lightning.

---

[157] V. E. Zakharov, "Collapse of Langmuir Waves," *Soviet Physics JETP* **35**, 908 (1972).

[158] E. W. Laedke and K. H. Spatschek, "Stable Three-Dimensional Envelope Solitons," *Physical Review Letters* **52**, 279 (1984).

4. AN ATMOSPHERIC MASER IN THE AIR-EARTH SYSTEM

Given the precedents for Handel's Maser-Soliton Theory of ball lightning described in Section 3, it is reasonable to further investigate whether a thundercloud and the Earth's surface could act as mirrors of an open resonator so as to sufficiently amplify naturally-occurring microwave radiation emitted by water vapor to create a cause breakdown of the air and creation of a Laedke-Spatschek caviton that is perceived as ball lightning.

In this section, we develop a model to describe how the maser energy is concentrated into an isolated volume resulting in electric breakdown of the air and creation of a plasma discharge. The prototypical system (Figure 4-1) is comprised of the surface of the Earth and the thundercloud with the atmosphere in between composed of air and water vapor. The system is idealized as an open resonator with the thundercloud and surface of the Earth as reflecting surfaces and the water vapor serving as the active medium. The maser radiation forms a beam of width w with the narrowest part of the beam, the beam waist, denoted by w_0.

4.1. THE ATMOSPHERIC POTENTIAL GRADIENT

At standard atmospheric pressure and temperature, the magnitude of the electric field across small gaps leading to breakdown of air at atmospheric pressure is approximately 3000 kV/m[159].

---

[159] Vernon Cooray, *The Lightning Flash*, London: Institution of Electrical Engineers, 2003, Section 4.6.2.1; Yuri P. Raizer, *Gas Discharge Physics*, Berlin: Springer-Verlag, 1997, p. 135; J. R. Dwyer, "A Fundamental Limit on Electric Fields in Air," *Geophysical Research Letters* **30**, 2055 (2003).

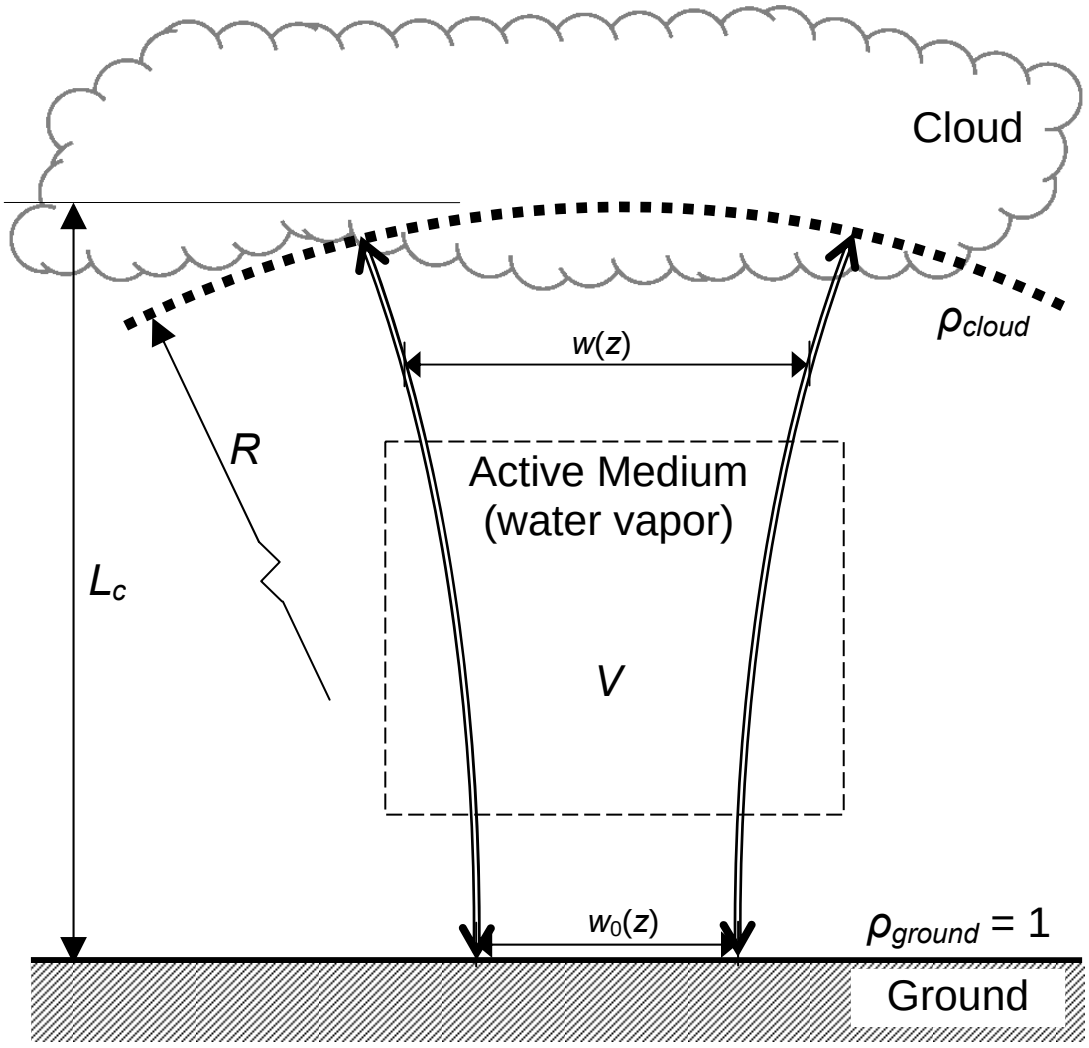

V = Volume of active medium (water vapor)
R = Radius of curvature
L_c = Distance of separation
ρ = Power reflectivity
$w(z)$ = Beam width
$w_0(z)$ = Beam waist

Figure 4-1: Prototypical Atmospheric Maser

Typical maximum electric field magnitudes developed in thunderclouds are on the order of 100 kV/m[160]. Marshall, *et al*.,[161] used balloons to perform electric field soundings in thunderstorms (elevations ~ 4-10 km) and found that electric fields "rarely" exceeded 150 kV/m.

Winn, *et* al.,[162] cited previously published reports of maximum electric fields ~10^3 kV/m and reported their own measurements of electric fields of such magnitude in six out of 61 cases, but they judged the occurrence of such very intense fields as "rare."

Uman, *et al*.,[163] measured ground-level electric fields at a distance of 15 meters from triggered lightning from natural thunderclouds using the rocket-and-wire technique. Peak electric fields for full strokes (leader-return) were ~75 kV/m. The duration of a stroke was ~0.2 ns. Miki, *et al*.,[164] measured ground-level electric fields at distances from 0.1 m to 1.6 m from triggered lightning. Peak vertical electric fields ranged from 176 kV/m to 1.5 MV/m (median of 577 kV/m), and peak horizontal electric fields ranged

---

[160] William P. Winn, G. W. Schwede, and C. B. Moore, "Measurements of Electric Fields in Thunderclouds," *Journal of Geophysical Research*, **79**, 1761 (1974); C. P. R. Saunders, "Thunderstorm Electrification," in *Handbook of Atmospheric Electrodynamics*, Volume 1, H. Volland (Ed.), Boca Raton: CRC Press 1995, p. 85.

[161] Thomas C. Marshall, Michael P. McCarthy, and W. David Rust, "Electric Field Magnitudes and Lightning Initiation in Thunderstorms," *Journal of Geophysical Research*, **100**, 709 (1995).

[162] William P. Winn, G. W. Schwede, and C. B. Moore, "Measurements of Electric Fields in Thunderclouds," *Journal of Geophysical Research*, **79**, 1761 (1974).

[163] M. A. Uman, J. Schoene, V. A. Rakov, K. J. Rambo, and G. H. Schnetzer, "Correlated Time Derivatives of Current, Electric Field Intensity, and Magnetic Flux Density for Triggered Lightning at 15 m," *Journal of Geophysical Research* **107**, 4160 (2002).

[164] Megumu Miki, Vladimire A. Rakov, Keith J. Rambo, George H. Schnetzer, and Martin A. Uman, "Electric Fields near Triggered Lightning Channels Measured with Pockels Sensors," *Journal of Geophyical Research* **107**, 4227 (2002)

from 495 kV/m to 1.2 MV/m (median of 821 kV/m). The vertical electric field peak at 15 m for a typical leader/return stroke is ~100 kV/m and ~50 kV at 30 m.[165]

Dwyer[166] argued that the magnitude of the electric field that can exist over a large volume of open air is constrained by a feedback mechanism mechanism of ionizations caused by high energy particles (gamma rays and positrons) generated during the breakdown avalanche. Dwyer performed Monte Carlo simulations of the runaway breakdown of air that included a variety of modes for producing and propagating high-energy electrons and photons, e.g, bremsstrahlung, Compton scattering, pair production, etc. The simulations sought to explain the high-energy particles (>> 10 keV) Dwyer, *et al*.,[167] had detected during the dart leader phase of rocket-triggered lightning and similar bursts of radiation reported by Moore[168] with energy greater than 1 MeV approximately 1 to 2 milliseconds before cloud-to-ground, negative lightning strikes. Dwyer argued the observation of high-energy radiation immediately before lightning strikes is evidence for runaway breakdown of air leading to the lightning discharge.

---

[165] Megumu Miki, Vladimire A. Rakov, Keith J. Rambo, George H. Schnetzer, and Martin A. Uman, "Electric Fields near Triggered Lightning Channels Measured with Pockels Sensors," *Journal of Geophysical Research* **107**, 4227 (2002) citing David. E. Crawford, Vladimir A. Rakov, Martin A. Uman, George H. Schnetzer, Keith J. Rambo, Michael V. Stapleton, and Richard J. Fisher, "The Close Lightning Environment: Dart-Leader Electric Field Change versus Distance," *Journal of Geophysical Research.* **106**, 14909 (2001).

[166] J. R. Dwyer, "A Fundamental Limit on Electric Fields in Air," *Geophysical Research Letters.* **30**, 2055 (2003).

[167] Dwyer, J. R, Martin A. Uman, Hamid K. Rassoul, Maher Al-Dayeh, LeeCaraway, Jason Jerauld, Vladimir A. Rakov, Douglas M. Jordan, Keith J. Rambo, VincentCorbin, Brian Wright, "Energetic Radiation Produced During Rocket-Triggered Lightning," *Science* **299**, 694 (2003).

[168] C. B. Moore, K. B. Eack, G. D. Aulich, and W. Rison, "Energetic Radiation Associated with Lightning Steppedl-Leaders," *Geophysical Research Letters* **28**, 2141 (2001).

From the results of his simulations, Dwyer[169] argued that there is a fundamental limit on the maximum static electric field strength achievable in a given volume of air that is imposed by a positive feedback mechanism of ionizations caused by high energy particles (gamma rays and positrons) generated during the breakdown avalanche. This limit may be on the order of 1000 kV/m, but depends on the size of the region over which the field exists:

$$\lambda = \frac{7200 \text{ kV}}{\left(E - 275 \text{ kV/m}\right)}, \quad 300 \text{ kV/m} < E < 2500 \text{ kV/m}, \tag{4.1}$$

where λ is the characteristic length of region over which the electric field E exists. The simulation assumes a pressure of 1 atm. At lower pressures P, the electric field strength scales by a factor P; lengths scale by a factor P^{-1}.

For a region of open air of length 100 m, the maximum electric field strength is limited by runaway breakdown to be approximately 350 kV/m. For a region of length 1 km, the maximum field strength is 282 kV/m. For a region of length 3 km, the maximum field strength is 277 kV/m. An electric field of strength 1000 kV/m could only be sustained in open air over a length of 10 m. Dwyer[170] states that his simulation may overestimate maximum electric field strengths close to the minimum threshold strength due to inaccuracies in the elastic scattering model assumed in his simulation.

---

[169] J. R. Dwyer, "A Fundamental Limit on Electric Fields in Air," *Geophysical Research Letters*. **30**, 2055 (2003).

[170] *Ibid*.

4.2. INTERACTION OF MICROWAVES WITH THE ATMOSPHERE

4.2.1. Absorption of Microwaves by Oxygen. In this dissertation, the properties of the atmosphere are taken, except where noted, from a NASA model[171] used for calibration of Deep Space Network antennae. Here, "standard" surface conditions are taken to be temperature $T = 295$ K, pressure $P = 1.013$ MPa, and elevation $h = 0$ km. Since ball lightning is associated with conventional lightning strikes during thunderstorms, a relative humidity of 100% is assumed throughout.

For microwave absorption below 100 GHz, the atmospheric constituents of concern are molecular oxygen (O_2) and water vapor. Since the relative concentrations of other atmospheric gases and pollutants (e.g., ozone, sulfur dioxide (SO_2), nitrogen dioxide (NO_2), nitrous oxide (N_2O)) are so small, their contribution to microwave absorption is negligible compared to oxygen and water vapor[172].

Diatomic molecules that are nonpolar, e.g., molecular nitrogen (N_2), ordinarily do not absorb microwaves[173]. Though molecular oxygen (O_2) is nonpolar and so lacks an electric dipole moment, its ground state electronic structure results in a pair of electrons with parallel spins. This "spin one" ground state gives the O_2 molecule a magnetic dipole

---

[171] S. Shambayati, "Atmosphere Attenuation and Noise Temperature at Microwave Frequencies," in *Low-Noise Systems in the Deep Space Network*, M. S. Reid (Ed.), Jet Propulsion Laboratory, California Institute of Technology, (2008). Available at http://descanso.jpl.nasa.gov/Monograph/series10_chapter.cfm.

[172] Ulaby, F. T., R. K. Moore, and A. K. Fung, *Microwave Remote Sensing: Active and Passive. Volume I, Microwave Remote Sensing Fundamentals and Radiometry*, Norwood: Artech House, 1986.

[173] C. H. Townes and A. L. Schawlow, *Microwave Spectroscopy*, New York: Dover Publications, 1975.

moment that interacts with "end-over-end" rotation of the molecule to allow rotational transitions in the microwave region[174], e.g., the rotational transition at 60 GHz[175].

Oxygen absorbs microwaves over a large number of absorption lines in the "60-GHz complex" from approximately 50 GHz to 70 GHz region[176]. At high pressures (~1 atm) these lines broaden to form a continuous absorption band centered around 60 GHz[177]. For frequencies less than 45 GHz, a "low-frequency approximation" of the absorption coefficient α_{OX} for microwaves in O_2 is[178]

$$\alpha_{OX}(f) = C(f)\gamma_0(h) f^2 \left(\frac{P}{1013}\right)^2 \left(\frac{300}{T}\right)^2 \times \left(\frac{1}{(f-60)^2 - \gamma^2(h)} + \frac{1}{f^2 + \gamma^2(h)}\right), \tag{4.2}$$

where α_{OX} is in dB/km, P is pressure in mbar (1 bar = 0.1 MPa), T is temperature in kelvin, f is frequency in GHz, $C(f)$ is given by

$$C(f) = 0.011\left(7.13\times10^{-7} f^4 - 9.2051\times10^{-5} f^3 + 3.280422\times10^{-3} f^2 - 0.01906468 f + 1.110303146\right). \tag{4.3}$$

The linewidth parameter γ in GHz is given by

$$\gamma = \gamma_0 \left(\frac{P}{1013}\right)\left(\frac{300}{T}\right)^{0.85}, \tag{4.4}$$

---

[174] *Ibid*.

[175] J. H. Van Vleck, "The Absorption of Microwaves by Oxygen," *Phyical Review* **71**, 413 (1947).

[176] F. T. Ulaby, R. K. Moore, and A. K. Fung, *Microwave Remote Sensing: Active and Passive. Volume I, Microwave Remote Sensing Fundamentals and Radiometry*.

[177] *Ibid*.

[178] S. Shambayati, "Atmosphere Attenuation and Noise Temperature at Microwave Frequencies."

where $\gamma_0 = 0.59$ GHz at the earth's surface where *P*= 1013 MPa.

Figure 4-2 shows the power absorption coefficient calculated using (4.2).

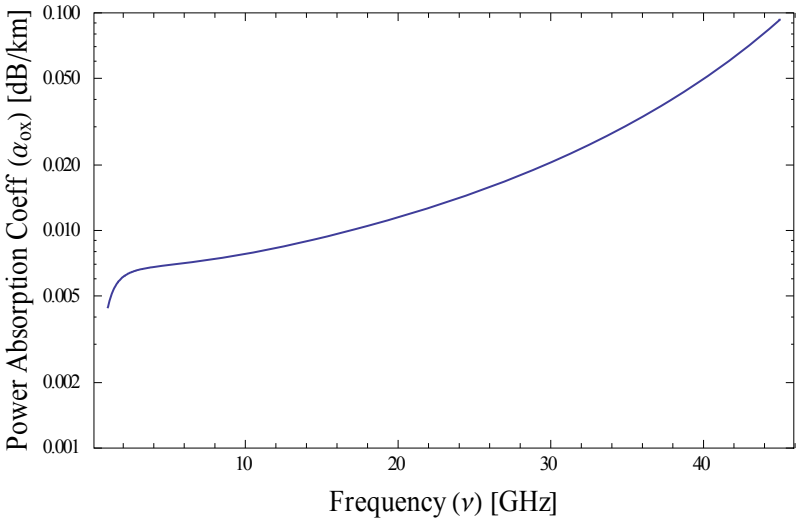

Figure 4-2: Power Absorption Coefficient for Oxygen at 1 atm, 300 K

4.2.2. Absorption of Microwaves by Water Vapor. The absorption coefficient α_{H_2O} in water vapor of microwaves below 100 GHz is given by[179]

$$\alpha_{H_2O}(f) = k_{H_2O}(f)\left[a_{H_2O}(f) + 1.2\times10^{-6}\right], \tag{4.5}$$

Where α_{H_2O} is in dB/km, f is frequency in GHz, and

$$k_{H_2O}(f) = 2f^2\rho_{H_2O}\left(\frac{300}{T}\right)^{1.5}\gamma_1 \quad , \tag{4.6}$$

$$a_{H_2O}(f) = \frac{300}{T}\left(\frac{1}{d_{H_2O}(f)}\right)\exp\left(-\frac{644}{T}\right) \quad , \tag{4.7}$$

---

[179] *Ibid*.

$$d_{H_2O}(f) = \left(22.2^2 - f^2\right)^2 + 4f^2\gamma_1{}^2 \quad . \tag{4.8}$$

The linewidth parameter for water vapor γ_1 in GHz is given by

$$\gamma_1 = 2.85\left(\frac{P}{1013}\right)\left(\frac{300}{T}\right)^{0.626}\left(1 + 0.018\frac{\rho_{H_2O}T}{1013}\right), \tag{4.9}$$

where the pressure P is in mbar and the temperature T is in Kelvin. The absolute humidity ρ_{H_2O} in (4.6) is given by[180]

$$\rho_{H_2O} = \rho_{RH}\frac{(216.5)(6.1)}{T}\left(10^{7.4475\frac{(T-273.15)}{(T-38.45)}}\right), \tag{4.10}$$

where ρ_{H_2O} is in g/m^3, the temperature T is in kelvin, and ρ_{RH} is the relative humidity ($0 \le \rho_{RH} \le 1$). (Equation (4.10) is a corrected version of Equation 6.2-10 by Shambayati.[181]) Microwave absorption due to the water vapor continuum[182], which is significant above 30 GHz, is ignored here.

Figure 4-3 shows the absorption coefficient calculated using (4.5).

---

[180] Stephen D. Slobin, personal email communication, February 14, 2012.

[181] Shambayati, "Atmosphere Attenuation and Noise Temperature at Microwave Frequencies."

[182] P. W. Rosenkranz, "Water Vapor Microwave Continuum Absorption: A Comparison of Measurements and Models," *Radio Science* **33**, 919 (1998); Vivienne H. Payne, Eli J. Mlawer, Karen E. Cady-Pereira, and Jean-Luc Moncet "Water Vapor Vontinuum Absorption in the Microwave," *IEEE Transactions in Geoscience and Remote Sensing* **49**, 2194 (2011).

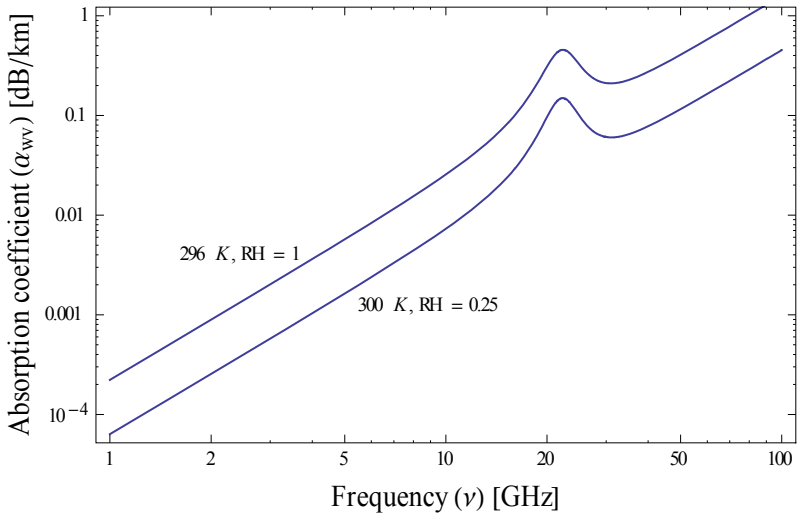

Figure 4-3: Power Absorption Coefficient for Water Vapor at 1 atm

4.2.3. The Microwave Breakdown of Air. The breakdown of air at microwave frequencies has been thoroughly reviewed in monographs of MacDonald[183]; Raĭzer, Shneider, and Yatsenko[184]; Raizer[185]; and Gurevich, Borisov, and Milikh[186]. Research of microwave breakdown of air seem to envision a diverging variety of applications of the work: avoidance of breakdown at radar antennae or other sources of microwave radiation

---

[183] A. D. MacDonald, *Microwave Breakdown in Gases*. New York: Wiley & Sons, 1966.

[184] I. U. P. Raĭzer, M. N. Shneider, and N. A. Yatsenko, *Radio-Frequency Capacitive Discharges*. Boca Raton: CRC Press, 1995.

[185] J. P. Raizer, *Gas Discharge Physics*. Berlin: Springer, 1997.

[186] A. V. Gurevich, N. D. Borisov, and G. M. Milikh, *Physics of microwave discharges: Artifically ionized regions in the atmosphere*. Amsterdam: Gordon and Breach, 1997.

to prevent unwanted attenuation of the emitted beam power[187], the intentional creation of "artificial ionospheric mirrors" for over-the-horizon communications[188], and applications in biomedicine[189], materials processing[190], and detection of concealed radioactive materials[191].

Some of the earliest work on microwave breakdown of gases was performed by Herlin and Brown[192]. They noted that breakdown of a gas at microwave frequencies is distinguishable from breakdown at constant field conditions[193] ("d.c." or direct current conditions) in that, while most electrons are generated through ionization by collisions of ions and electrons accelerated by the applied electric field, the secondary source of electrons due to collisions with walls is negligible in high-frequency microwave

---

[187] A. D., MacDonald, "High-Frequency Breakdown in Air at High Altitudes," *Proceedings of the* IRE **47**, 436 (1959); Joseph T. Mayhan, Ronald L. Fante, Robert O'Keefe, Richard Elkin, Jack Klugerman, and J. Yos, "Comparison of Various Microwave Breakdown Prediction Models," *Journal of Applied Physics* **42**, 5362 (1971); Wee Woo and J. S. DeGroot, "Microwave Absorption and Plasma Heating due to Microwave Breakdown in the Atmosphere," *Physics of Fluids* **27**, 475 (1984).

[188] J. Kim, S. P. Kuo, and Paul Kossey, "Modelling and Numerical Simulationof Microwave Pulse Propagation in an Air-Breakdown Environment," *Journal of Plasma Physics* **53**, 253 (1995).

[189] H. E. Porteanu, S. Kühn, and R. Gesche, "Ignition Delay for Atmospheric Pressure Microplasmas," *Contributions in Plasma Physics* **49, 21 (2009).**

[190] Sang Ki Nam and John P. Verboncoeur, "Global Model for High Power Microwave Breakdown at High Pressure in Air," *Computer Physics Communications* **180**, 628 (2009).

[191] Victor L. Granatstein and Gregory S. Nusinovich, "Detecting Excess Ionizing Radiation by Electromagnetic Breakdown of Air," *Journal of Applied Physics* **108**, 063304 (2010).

[192] See, for example, Melvin A. Herlin and Sanborn C. Brown, "Microwave Breakdown of a Gas in a Cylindrical Cavity of Arbitrary Length," *Physical Review* **74**, 1650 (1948); and Melvin A. Herlin and Sanborn C. Brown, "Breakdown of a Gas at Microwave Frequencies," *Physical Review* **74**, 291 (1948).

[193] *Ibid*.

experiments in which the field reverses so quickly that most electrons don't have enough time to travel to a wall.[194]

A dimensional analysis of microwave breakdown of gases shows that the breakdown electric field E_b is a function of four variables[195]:

$$E_b = E\left(u_i, l, \Lambda, \lambda\right), \tag{4.11}$$

where u_i is the ionization potential of the gas, l is the mean free path of an electron in the gas, Λ is the characteristic diffusion length for an electron in the gas, and λ is the wavelength of the microwave radiation. Since there are five variables and only two independent dimensions, voltage and length, the Π-Theorem[196] tells us there are three dimensionless quantities[197], for example:

$$\left(\frac{El}{u_i}, \quad \frac{\Lambda}{l}, \quad \frac{\Lambda}{\lambda}\right) \quad \text{or} \quad \left(\frac{E\Lambda}{u_i}, \quad \frac{E\lambda}{u_i}, \quad \frac{\lambda}{l}\right). \tag{4.12}$$

Since the ionization potential is constant for a specific gas, and the mean free path of an electron is inversely proportional to gas pressure with a constant of proportionalality fixed for a specified gas and electron energy, it is common to express the relevant

---

[194] See also, MacDonald, *Microwave Breakdown in Gases*, p. 2.

[195] *Ibid.*, p. 12.

[196] E. Buckingham, "On Physically Similar Systems: Illustrations of the Use of Dimensional Equations," *Physical Review* **4**, 345 (1914); P. W. Bridgman, *Dimensional Analysis*, New Haven: Yale University Press, 1931; L. I. Sedov, *Similarity and Dimensional Methods in Mechanics*, Trans. Ed. Maurice Holt, Trans. Morris Friedman, New York: Academic Press, 1959.

[197] MacDonald, *Microwave Breakdown in Gases*, p. 12.

variables in terms of dimensional "proper variables"[198] such as[199]

$$\left(\frac{E}{p}, \quad p\Lambda, \quad \frac{\Lambda}{\lambda}\right) \quad \text{or} \quad \left(E\Lambda, \quad E\lambda, \quad p\lambda\right). \tag{4.13}$$

Using these last triplets, Brown and MacDonald[200] identified regimes for applicability of diffusion theory in the "uniform field limit," the "mean free path limit," and the "oscillation amplitude limit." MacDonald[201] has calculated these limits for air.

The diffusion equation can be written as

$$D\nabla^2 n + \nu_i\, n = S\,, \tag{4.14}$$

where D is the diffusion coefficient for electrons, ν_i is the net ionization rate (ionization minus recombination), n is the electron density, and S is the rate electrons are introduced by an external source. For infinite parallel plates and a boundary condition $n = 0$,

$$n = \frac{A}{D}\sin\left(\frac{z}{\Lambda}\right), \tag{4.15}$$

where A is constant, z is the distance from one plate, and Λ is the characteristic diffusion length defined in (4.11) and, for infinite parallel plates, $\Lambda = \frac{L}{\pi}$.

The uniform field limit corresponds to the condition in which the wavelength of the alternating field is greater than the dimensions of the test volume. For infinite parallel

---

[198] *Ibid*., citing Sanford C. Brown, "Breakdown in Gases: Alternating and High-Frequency Fields," in S. Flügge, *Handbuk der Physik*, Berlin: Springer-Verlag, 1956, p. 531.

[199] *Ibid*.

[200] Sanborn C. Brown and A. D. MacDonald, "Limits for Diffusion Theory of High Frequency Gas Discharge Breakdown," *Physical Review* **76**, 1629 (1949).

[201] A. D., MacDonald, "High-Frequency Breakdown in Air at High Altitudes," *Proceedings of the IRE* **47**, 436 (1959).

plates, the limiting condition among the wavelength, the distance between the plates, and the diffusion length is

$$\frac{\lambda}{2} = \pi\Lambda\,, \tag{4.16}$$

where we use the relation $\lambda/2 = L$ to specify a uniform field between the plates. In terms of the proper variables in (4.13), we may express (4.16) as

$$p\lambda = 2\pi\left(p\Lambda\right). \tag{4.17}$$

This uniform field limit is depicted in Figure 4-4. Other lines in Figure 4-4 are discussed below.

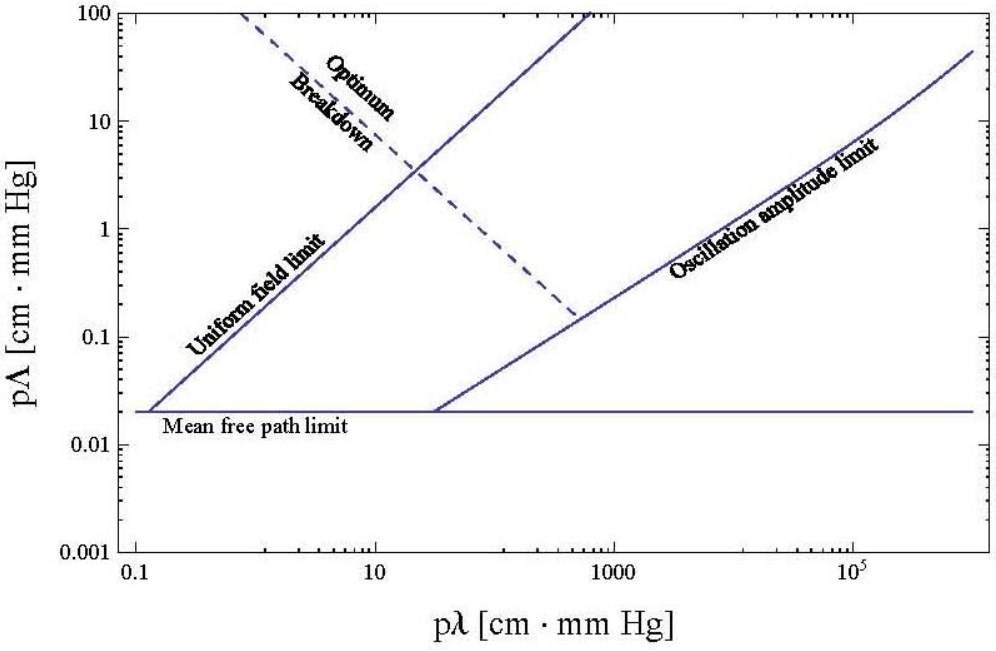

Figure 4-4: Limits of Diffusion Theory for Hydrogen Gas

The mean free path limit defines the condition where the mean free path becomes comparable to the test volume, i.e., $l = L$. For infinite parallel plates, L can be related to the diffusion length: $L = \Lambda$. Then, in terms of proper variables in (4.13), the mean free path limit can be written as

$$p\Lambda = pl \; . \tag{4.18}$$

The probability of collision is proportional to $1/pl$ for a given temperature[202] and depends on the electron energy.[203] Then for a specified gas temperature and electron energy pl is a constant, and the mean free path limit is a horizontal line on the $p\Lambda$-pl plot. The mean free path limit for hydrogen[204] is depicted in Figure 4-4.

The oscillation amplitude limit is defined by the condition under which the electron oscillation amplitude in the electric field allows the electrons to travel across the width of the test volume (or collide with the test volume walls) on every half-cycle. We can find the amplitude of oscillation by integrating Newton's Second Law for the electron in the oscillating electric field, and, on equating the amplitude with the half-width of the plate separation, we find[205]

$$\frac{L}{2} = \frac{\sqrt{2}eE}{m\omega\nu_m}, \tag{4.19}$$

where ν_m is the electron collision frequency, ω is the angular frequency of the electric field, m is the mass of the electron, and e is the electron charge. On substituting

---

[202] Vincenti and Kruger, *Introduction to Physical Gas Dynamics*, p. 13.

[203] Brown, Sanborn C., "Breakdown in Gases: Alternating and High-Frequency Fields," p. 539.

[204] Brown, "Breakdown in Gases: Alternating and High-Frequency Fields," p. 538.

[205] *Ibid.*

$\omega = 2\pi c/\lambda$ and $\nu_m = \bar{v}/l$, where $\bar{v}$ is the electron velocity, we can write (4.19) in terms of the proper variables in (4.13):

$$p\lambda = \left[\frac{\pi mc\bar{v}}{(pl)e\sqrt{2}}\right]\frac{(p\Lambda)}{(E/p)}. \tag{4.20}$$

The bracketed quantity in (4.20) is a constant for a given gas at a given temperature and pressure and for electrons of a given energy. (Recall the discussion following (4.18) above.) Equation (4.20) can be solved if the breakdown field has been determined experimentally. Beyond the oscillation limit, electrons leave the test volume (or collide with the walls), and the electric field to achieve breakdown must be sharply increased to make up for the loss.[206] The approximate oscillation amplitude limit for hydrogen[207] is depicted in Figure 4-4.

Brown and MacDonald[208] also identified the "optimum breakdown" condition at which breakdown occurs most easily between the low-pressure condition in which electrons oscillate many times between collisions giving them more time to diffuse out of the test volume (e.g., by diffusing into a wall) and the high-pressure condition in which the energy imparted to the electrons by the oscillating field readily dissipated by collisions.

---

[206] Brown, "Breakdown in Gases: Alternating and High-Frequency Fields," p. 569.

[207] *Ibid*., p. 538.

[208] Sanborn C. Brown and A. D. MacDonald, "Limits for Diffusion Theory of High Frequency Gas Discharge Breakdown," *Physical Review* **76**, 1629 (1949).

Breakdown will occur when the net ionization rate (ionization minus recombination) equals the diffusion rate of electrons out of the test volume. The solution to the one-dimensional time-dependent form of the diffusion equation (4.14) is

$$n = \frac{4S}{\pi} \frac{\cos(\pi z/L)}{\left[D(\pi/L)^2 - \nu_i \right]}, \tag{4.21}$$

and the breakdown condition can be written as $\nu_i / D = (\pi/L)^2$, or, since $1/\Lambda = \pi/L$ for infinite parallel plates, the breakdown condition is

$$\nu_i = \frac{D}{\Lambda^2}. \tag{4.22}$$

From linear diffusion theory (where Fick's Law is applicable), the diffusion coefficient can be approximated as[209]

$$D = \tfrac{1}{3} \bar{v} l, \tag{4.23}$$

where $\bar{u}$ is the average electron velocity. Then the breakdown condition (4.22) becomes

$$\nu_i = \frac{\bar{v} l}{3\Lambda^2} = \frac{\bar{v}^2}{3\Lambda^2 \nu_m}, \tag{4.24}$$

where $\nu_m = \bar{v}/l$.

In the low-pressure region, we also express the ionization rate in terms of the power *P* that goes into ionization:

$$\nu_i = \frac{P}{n u_i}, \tag{4.25}$$

---

[209] R. Byron Bird, Warren E. Stewart, and Edwin N. Lightfoot, *Transport Phenomena*, New York: Wiley & Sons, 1960, p. 510.

where u_i is the ionization energy and n is the electron density. From Newton's Second Law for electrons in an oscillating field and a collision frequency ν_m, the power absorbed by the electrons from the electric field is

$$P = \frac{ne^2 E_{eff}^2}{m\nu_m}, \tag{4.26}$$

Where the effective electric field $E_{eff} = E\sqrt{\nu_m^2 / \left(\omega^2 + \nu_m^2\right)}$ is the magnitude of a steady field that would produce the same energy transfer as the alternating field.[210]

Since $\nu_m \ll \omega$ in the low-pressure region, and since $\omega = 2\pi c/\lambda$, we can combine (4.25) and (4.26) to yield

$$\nu_i = \frac{\lambda^2 e^2 E^2 \nu_m}{\left(2\pi\right)^2 u_i mc^2}. \tag{4.27}$$

If we equate (4.24) and (4.27), we find

$$\nu_i = \frac{\bar{v}^2}{3\Lambda^2 \nu_m} = \frac{n\lambda^2 e^2 E^2 \nu_m}{\left(2\pi\right)^2 u_i mc^2}, \tag{4.28}$$

and, on solving (4.28) for E, we find the breakdown field in the low-pressure region[211]:

$$E = \frac{2\pi c}{\Lambda\lambda\nu_m}\left(\frac{2}{3}\bar{u}u_i\right)^{\frac{1}{2}}, \tag{4.29}$$

where $\bar{u} = m\bar{v}^2/2$.

---

[210] Sanborn C. Brown and A. D. MacDonald, "Limits for Diffusion Theory of High Frequency Gas Discharge Breakdown," *Physical Review* **76**, 1629 (1949).

[211] Brown, Sanborn C., "Breakdown in Gases: Alternating and High-Frequency Fields," p. 569.

In the high-pressure region, the power from the electric field by the electrons is dissipated by collisions:

$$\frac{\text{change in energy}}{\text{collision}} = \frac{P}{n\nu_m} = \frac{e^2E^2}{m\nu_m^2}\left(\frac{\nu_m^2}{\omega^2+\nu_m^2}\right), \tag{4.30}$$

where P is the power absorbed from the electric field by the electrons (see Equation (4.26)). The change in energy per collision can also be written as

$$\frac{\text{change in energy}}{\text{collision}} = \frac{2m}{M}\bar{u}\,, \tag{4.31}$$

where $\bar{u}$ is the average electron energy and M is the molecular mass. On equating (4.30) and (4.31), we find

$$\frac{e^2E^2}{m\nu_m^2}\left(\frac{\nu_m^2}{\omega^2+\nu_m^2}\right) = \frac{2m}{M}\bar{u}\,, \tag{4.32}$$

And, on solving for E,

$$E = \frac{m}{e}\left(\frac{2\bar{u}}{M}\right)^{\frac{1}{2}}\nu_m\,. \tag{4.33}$$

Then, on equating (4.29) and (4.33), we find

$$\frac{2\pi c}{\Lambda\lambda\nu_m}\left(\frac{2}{3}\bar{u}u_i\right)^{\frac{1}{2}} = \frac{m}{e}\left(\frac{2\bar{u}}{M}\right)^{\frac{1}{2}}\nu_m, \tag{4.34}$$

and

$$\Lambda\lambda\nu_m^2 = \frac{2\pi ce}{m}\left(\frac{M}{3}u_i\right)^{\frac{1}{2}}. \tag{4.35}$$

Now, the righthand side of (4.35) depends only on gas properties, and ν_m on the lefthand side is proportional to the pressure, so we can write (4.35) in terms of proper variables in (4.13) as

$$(p\Lambda)(p\lambda) = \frac{2\pi ce}{mC}\left(\frac{M}{3}u_i\right)^{\frac{1}{2}}, \tag{4.36}$$

where $C = v_m^2 / p^2$. Figure 4-4 depicts the optimum breakdown line for hydrogen[212].

Kroll and Watson[213] reported a previously unpublished equation for the threshold power flux for breakdown of air

$$P_B = 1.44\left(p_R^2 + 2.4\times10^{-6} f^2\right) \text{MW/cm}^2, \tag{4.37}$$

where p_R is the air pressure in units of standard atmospheric pressure (0.1013 MPa) and f is the frequency in GHz. They note however that their formula is based on data from "observations at microwave frequencies and pressures much below atmospheric ($p_R << 1$)."[214] To modify Equation (4.37) for pressure near standard atmospheric pressure, Kroll and Watson solved the Boltzmann equation including both single- and multi-photon ionization and detachment processes in nitrogen and oxygen. Their results of solving the classical Boltzmann equation showed that the breakdown power could be written in the form similar to (4.37) by introducing two correction factors K_H and K_L , "Hi-f" and "Lo-f" correction factors, respectively.

$$P = 1.44\left[p_R^2 K_L\left(\Lambda p_R, p_R\right) + 2.4\times10^{-6} f^2 K_H\left(\Lambda p_R, p_R\right)\right] \text{MW/cm}^2, \tag{4.38}$$

where Λ is measured in cm.

---

[212] Brown, "Breakdown in Gases: Alternating and High-Frequency Fields," p. 538.

[213] Norman Kroll and Kenneth M. Watson, "Theoretical Study of Ionization of Air by Intense Laser Pulses," *Physical Review A* **5**, 1883 (1972).

[214] *Ibid*.

From the plots provided by Kroll and Watson[215], we see that both K_H and K_L are essentially unity for $\Lambda p_R > 0.01$. And, recalling that Λ is approximately representative of the characteristic length of the test volume (e.g., we found above that $1/\Lambda = \pi/L$ for infinite parallel plates), the correction factors K_H and K_L are taken to be unity for this dissertation where the "test volume" is on the order of 1 km. This is consistent with the approach of other researchers[216] who have studied microwave breakdown of air at atmospheric pressures.

The electric field strength is related to the threshold power flux by

$$P_b = \frac{1}{2} c \epsilon_0 E^2 , \tag{4.39}$$

where c is the speed of light and ϵ_0 is the permittivity of free space. Then

$$E = \sqrt{\frac{2}{c\,\epsilon_0}\left(1.44\times10^4\right)\left(p_R^2 + 2.4\times10^{-6}\, f^2\right)}\; kV/\text{m} \tag{4.40}$$

The electric field strength for breakdown from (4.40) is depicted in Figure 4-5.

---

[215] *Ibid*.

[216] A. W. Ali, "On Laser Air Breakdown, Threshold Power and Laser Generated Channel Length," NRL Memorandum Report 5187, Washington: Naval Research Laboratory, 1983; Woo, Wee, and J. S. DeGroot, *Analysis and Computations of Microwave-Atmospheric Interactions*, Report No. PRG-R-98, Final Report for the Period September 1, 1982 to August 31, 1983. (Plasma Research Group, University of California-Davis, Davis, California, 1984). (Available from http://handle.dtic.mil/100.2/ADA149666); Granatstein, Victor L., and Gregory S. Nusinovich, "Detecting Excess Ionizing Radiation by Electromagnetic Breakdown of Air," *Journal of Applied Physics* **108**, 063304 (2010).

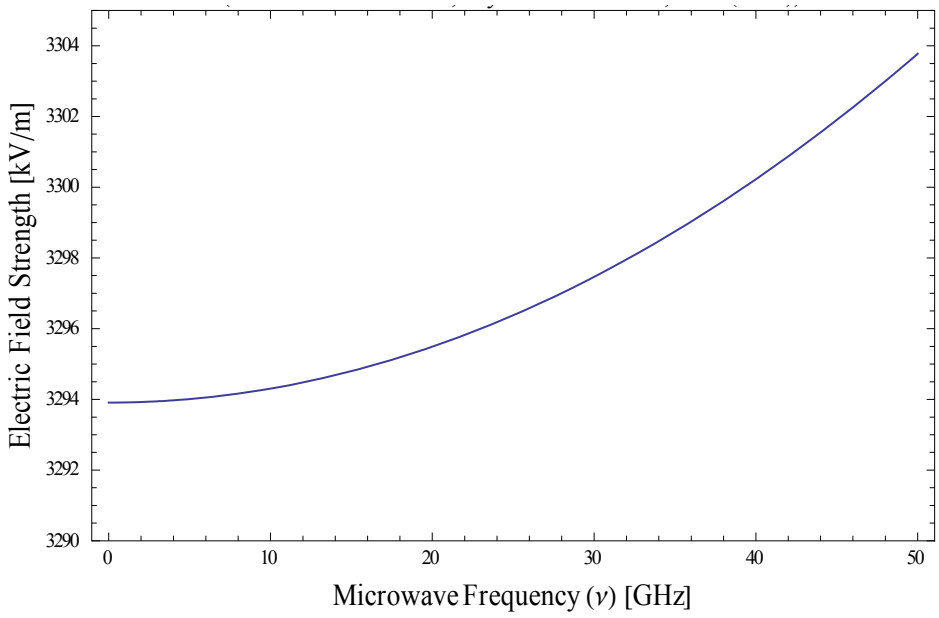

Figure 4-5: Electric Field Strength for Microwave Breakdown of Air at 1 Atm

4.3. MICROWAVE SPECTROSCOPY OF WATER VAPOR

4.3.1. Collisional Broadening of Spectral Lines. Radiation emitted and absorbed by molecules during transitions between energy levels is not observed to occur at fixed and definite frequencies. When measured by spectroscopic or another method, the energy levels of an atom or molecule (even isolated and stationary) appear as broadened spectral lines rather than as infinitesimally thin lines.

The broadening of spectral lines is not merely a complication when measuring molecular spectra. Broadening also effects the energy that one molecule "sees" another molecule to have. Molecules do not interact with other molecules at fixed and definite energies. Rather, they interact at energies corresponding to spectral lines that vary about average or center frequencies.

The width of the broadened lines is the cumulative effect of many sources[217]:

1. Natural line breadth
2. Doppler effect
3. Pressure broadening (intermolecular collision effects)
4. Saturation broadening
5. Collisions between molecules and the walls of a containing vessel.

Saturation broadening is ignored since, other than at the creation of the initial population inversion by lightning, the population inversion is not maintained by optical pumping. Also, wall effects are ignored since there are no walls.

Natural line breadth. According to the Heisenberg Uncertainty Principle, the energy levels of an atom or molecule that have a finite lifetime cannot be measured with arbitrary precision. The shorter the lifetime τ of a given state, the greater the uncertainty in the energy ΔE of that state.

The linewidth $\Delta\omega_{ki}$ for the naturally broadened line depends on the combined uncertainty of the upper and lower states of the transition and is found from the Einstein A coefficients[218]:

$$\Delta\omega_{ki} = \gamma_{ki} = \sum_{j<k} A_{kj} + \sum_{j<i} A_{ij} \,, \tag{4.41}$$

where the sums in (4.41) are taken over all transitions from state k to all lower states and from state i to all lower states.

---

[217] Townes and Schawlow, *Microwave Spectroscopy*, p. 336.

[218] A. Corney, *Atomic and Laser Spectroscopy*. Oxford: Clarendon Press, 1977, p. 235.

For transitions of water molecules of 1-cm wavelength, $A_{ij} < 10^{-8}$ sec^{-1}. Natural line broadening at microwave frequencies is negligible compared to pressure broadening at normal atmospheric pressure.

Doppler broadening. Doppler broadening results from a shift in the frequency of a spectral line due to the thermal motion of a molecule along the line of propagation of emitted or absorbed radiation. Doppler broadening is a type of *inhomogeneous* broadening in that the magnitude of broadening is different for different molecules depending on their direction and speed of motion.

The halfwidth at half-maximum of Doppler broadening is given by[219]:

$$\Delta\omega_{Doppler} = \omega\frac{V}{c}\sqrt{\ln 2}\,, \tag{4.42}$$

where $V = \sqrt{2kT/m}$ is the thermal velocity of the molecule of mass m at temperature T, c is the speed of light, and ω is the angular frequency of the radiation.

For water molecules at normal atmospheric temperatures (~300 K), $V/c \ll 1$, and, for microwave radiation with ω ~ 1 GHz, the Doppler broadening ~ 10 kHz. This amount of broadening is several orders of magnitude greater than the natural broadening, but, again, as will be shown below, is negligible compared to pressure broadening at normal atmospheric pressure.

Pressure broadening (intermolecular effects). The description of pressure broadening adopted here follows the "impact theory" line of analysis. To a hypothetical observer on a slow-moving, isolated water molecule, an electromagnetic field oscillating

---

[219] Townes and Schawlow, *Microwave Spectroscopy*, p. 337.

at some frequency v_0 appears as a pure sinusoidal wave. However, if the water molecule is one of many, then each collision between molecules will cause the pure sinusoid to undergo an apparent random jump in phase. Such collisional *dephasing*[220] causes spectral lines to spread out or *broaden* over a range of frequencies centered on v_0.

Lorentz[221] took an impact theoretic approach to the analysis of the line-broadening of radiation emitted by an oscillating electron, the sinusoidal motion of which is repeatedly interrupted by collisions which result in a random change in phase ("We shall suppose that immediately after a blow all directions of the displacement and the velocity of the electron are equally probable."). For a mean time between collisions of τ_c, the shape of the resulting frequency distribution, the *lineshape* $g(\omega)$, is Lorentzian[222]:

$$g(\omega) = \frac{1}{\pi} \frac{\gamma/2}{(\omega_0 - \omega)^2 + (\gamma/2)^2}, \tag{4.43}$$

where $\gamma \equiv 1/\tau_c$ is the linewidth (full width at half-maximum (FWHM)). For rotating molecules, the assumption of random phase after a collision is equivalent to assuming random orientation after a collision[223].

Van Vleck and Weisskopf[224] resolved the inconsistent results of Debye for nonresonant (i.e., zero frequency) absorption in liquids and Lorentz for a resonant

---

[220] Siegman, *Laser*, p. 89.

[221] H. A. Lorentz, "The Absorption and Emission Lines of Gaseous Bodies," *Proceedings of the Royal Academy of Amsterdam* **8**, 591 (1906).

[222] O. Svelto, *Principles of Lasers*, 4th Edition, Trans. D. C. Hanna, New York: Plenum Press, 1998 p. 35.

[223] Townes and Schawlow, *Microwave Spectroscopy*, p. 338.

[224] J. H. Van Vleck and V. F. Weisskopf, "On the Shape of Collision-Broadened Lines," *Reviews of Modern Physics*. **17**, 227 (1945).

oscillator by assuming that molecules are in thermodynamic equilibrium with the electromagnetic field after a collision. In which case, instead of completely random phases after collisions, the phases have a Boltzmann distribution after a collision. For rotating molecules, this is equivalent to assuming the molecules are oriented with respect to the electromagnetic field with a Boltzmann distribution. The resulting lineshape is

$$g(\nu)=\frac{1}{\pi}\left[\frac{\gamma}{(\nu_0-\nu)^2+\gamma^2}-\frac{\gamma}{(\nu_0+\nu)^2+\gamma^2}\right], \tag{4.44}$$

where ν_0 is the frequency of the oscillating (or rotating) molecule, and $\gamma = 1/\tau$ with the radiative damping rate denoted by $1/\tau$. For narrow lines ($\gamma << \nu_0$) and frequencies near the central peak ($\nu \approx \nu_0$), the second term in (4.44) may be neglected, and (4.44) reduces to the Lorentz lineshape (4.43). The Van Vleck-Weisskopf lineshape is needed when the line breadth $\Delta\nu$ is of the same order of magnitude as the resonant frequency[225] ν_0 such as is the case for microwave transitions of water vapor in air.[226]

Anderson[227]commented that the Lorentz and Van Vleck-Weisskopf pressure broadening theories suffer from the same limitation, i.e., both theories rely on a Fourier transform that "explicitly assumes that no [quantum] transitions are caused by collisions" and that a formula broadly applicable to high and low frequencies must include "the effects of both phase-shifts and of transitions." Anderson generalized the Fourier transform in the classical impact theory to account for quantum effects of the radiation

---

[225] *Ibid*.

[226] Townes and Schawlow, *Microwave Spectroscopy*, p. 345.

[227] P. W. Anderson, "Pressure Broadening in the Microwave and Infra-Red Regions," *Physical Review* **76**, 647 (1949).

field as described by Foley[228]. The resulting lineshape function is similar in form to the Lorentz lineshape, but with a shift δ in the central frequency[229]:

$$g(\nu) = \frac{1}{\pi} \frac{\gamma}{(\nu - \nu_0 - \delta)^2 + \gamma^2}, \tag{4.45}$$

where, as before, γ is the FWHM linewidth.

Applying the Anderson approach to the Van Vleck-Weisskopf lineshape (4.44) results in a similar shift in the central frequency[230]:

$$g(\nu) = \frac{1}{\pi} \frac{\nu}{\nu_0} \left[\frac{\gamma}{(\nu_0 - \nu - \delta)^2 + \gamma^2} + \frac{\gamma}{(\nu_0 + \nu + \delta)^2 + \gamma^2} \right]. \tag{4.46}$$

Equations (4.45) and (4.46) can also be derived by assuming the collision cross-section σ may be complex-valued[231]:

$$\sigma \equiv \sigma' + i\sigma'', \tag{4.47}$$

where the real quantities σ' and σ'' represent the effective cross-section for frequency shift and for broadening, respectively. The linewidth and frequency shift are related to the effective cross-sections by:

$$\delta = N\bar{v}\sigma', \tag{4.48}$$

---

[228] H. M. Foley, "The Pressure Broadening of Spectral Lines," *Phyical Review* 616 (1946).

[229] George Birnbaum, "Microwave Pressure Broadening and its Application to Intermolecular Forces," in *Advances in Chemical Physics*, edited by Joseph O. Hirschfelder, New York: Wiley Interscience, 1967, Vol. 12, p. 487.

[230] Townes and Schawlow, *Microwave Spectroscopy*., p. 356.

[231] Michel Baranger, "General Impact Theory of Pressure Broadening," *Physical Review* **112**, 855 (1958); A. Ben-Reuven, "Impact Broadening of Microwave Spectra," *Physical Review* **145**, 7 (1966); George Birnbaum, "Microwave Pressure Broadening and its Application to Intermolecular Forces"; Jeanna Buldyreva, Nina Lavrentieva, and Vitaly Starikov, *Collisional Line Broadening and Shifting of Atmospheric Gases: A Practical Guide for Line Shape Modelling by Current Semi-Classical Approaches*, London: Imperial College Press, 2011, p.6; Townes and Schawlow, *Microwave Spectroscopy*, p. 356.

and

$$\gamma = N\bar{v}\sigma'', \tag{4.49}$$

where N is the number of molecules per unit volume and $\bar{v}$ is the mean molecular velocity. (Note: In the Robert-Bonamy formalism[232], the halfwidth and line shift correspond to the real part and imaginary part, respectively, of (4.47).)

The Van Vleck-Weisskopf and the Anderson broadening theories represent the two extreme cases of "strong" and "weak" collisions, respectively.[233]. For strong collisions, the energy of collision kT is much greater than the spacing of energy levels, and the molecule has transition probabilities to many levels and the transition probability to a particular level is proportional to the Boltzmann factor of the level regardless of the initial level.[234] For weak collisions, the energy of collision is smaller than or of the same magnitude as the spacing of energy levels, and a molecule will have appreciable transition probabilities to only a few levels.[235]

The pressure-broadened line halfwidth $\gamma(p,T)$ [cm^{-1}] and frequency shift $\delta(p)$ [cm^{-1}] for a gas at pressure p [atm], temperature T [K], and partial pressure p_s [atm], may be calculated from the data in the HITRAN molecular spectroscopic

---

[232] Robert R. Gamache, Richard Lynch, and Steven P. Neshyba, "New developments in the theory of pressure-broadening and pressure-shifting of spectral lines of H_2O: The complex Robert-Bonamy formalism," *Journal of Quantitative Spectroscopy and Radiative Transfer* **59**, 319 (1998).

[233] Takeshi Oka, "Collision-Induced Transitions Between Rotational Levels," in Advances in Atomic and Molecular Physics, 9, edited by D. R. Bates (Elsevier, Burlington, 1974), p. 127.

[234] *Ibid*. citing J. H. Van Vleck and V. F. Weisskopf, "On the Shape of Collision-Broadened Lines," *Reviews of Modern Physics* **17**, 227 (1945).

[235] *Ibid*. citing P. W. Anderson, "Pressure Broadening in the Microwave and Infra-Red Regions," *Physical Review* **76**, 647 (1949).

database[236] for the air-broadening coefficient γ_{air}, the self-broadening coefficient γ_{self}, and the air-pressure induced shift δ_{air} at the reference temperature T_{ref} and reference pressure p_{ref}, and the temperature-dependence exponent of γ_{air}. The pressure-broadened line halfwidth is calculated as[237]

$$\gamma(p,T)=\left(\frac{T_{ref}}{T}\right)^{n_{air}}\left[\gamma_{air}\left(p_{ref},T_{ref}\right)\left(p-p_s\right)+\gamma_{self}\left(p_{ref},T_{ref}\right)p_s\right], \tag{4.50}$$

and the frequency shift is given by

$$\delta=\delta_{air}\left(p_{ref}\right)p\,. \tag{4.51}$$

(Note: There is ambiguity in the HITRAN documentation regarding whether the temperature correction in (4.50) should be applied to only the γ_{air} term or to both the γ_{air} and γ_{self} terms. Equation (4.50) is specified by the 1996 version of the HITRAN database, but the equation was removed from later versions. The issue need not be resolved here since all calculations herein are performed at $T = T_{ref} = 296$ K.)

---

[236] L. S. Rothman, I. E. Gordon, A. Barbe, D. Chris Benner, P. F. Bernath, M. Birk, V. Boudon, L. R. Brown, A. Campargue, J.-P. Champion, K. Chance, L. H. Coudert, V. Dana, V. M. Devi, S. Fally, J.-M. Flaud, R. R. Gamache, A. Goldman, D. Jacquemart, I. Kleiner, N. Lacome, W. J. Lafferty, J.-Y. Mandin, S. T. Massie, S. N. Mikhailenko, C. E. Miller, N. Moazzen-Ahmadi, O. V. Naumenko, A. V. Nikitin, J. Orphal, V. I. Perevalov, A. Perrin, A. Predoi-Cross, C. P. Rinsland, M. Rotger, M. Šimečková, M. A. H. Smith, K. Sung, S. A. Tashkun, J. Tennyson, R. A. Toth, A. C. Vandaele, J. Vander Auwera, "The HITRAN 2008 molecular spectroscopic database," *Journal of Quantitative Spectroscopy and Radiative Transfer* **110**, 533 (2009).

[237] L. S. Rothman, C. P. Rinsland, A. Goldman, S. T. Massie, D. P. Edwards, J. M. Flaud, A. Perrin, C. Camy-Peyret, V. Dana, J. Y. Mandin, J. Schroeder, A. McCann, R. R. Gamache, R. B. Wattson, K. Yoshino, K. V. Chance, K. W. Jucks, "L. R. Brown, V. Nemchinov, P. Varanasi,, "The HITRAN molecular spectroscopic database and HAWKS (HITRAN Atmospheric Workstation): 1996 Edition," *Journal of Quantitative Spectroscopy and Radiative Transfer* **60**, 665 (1998).

As pressure increases, the lineshape profile of a transition in the gas molecules will change from being doppler-broadened at low pressures to being pressure-broadened at high pressures[238]

$$\Delta\omega_{ji} = \gamma_{self,ji} P_{H_2O} + \gamma_{air,ji} P_{air}, \tag{4.52}$$

where P_{H_2O} and P_{air} are the partial pressures of water vapor and dry air, respectively, and $P_{atm} = P_{air} + P_{H_2O}$.

4.3.2. Nonradiative Vibrational and Rotational Relaxation. In a process known as *relaxation*[239], a molecule in an excited state may lose the excess energy by emitting radiation or by transferring the energy through collisions to its surroundings (e.g., confining surfaces) or to other molecules.

The relaxation of a gas can be described by the Bethe-Teller rate equation[240] :

$$\frac{dE_\alpha(T_\alpha)}{dt} = \frac{E_\alpha(T) - E_\alpha(T_\alpha)}{\tau_\alpha}, \tag{4.53}$$

---

[238] Siegman, *Lasers*, p. 167.

[239] Roy G. Gordon, William Klemperer, and Jeffrey I. Steinfeld, "Vibrational and Rotational Relaxation," *Annual Review of Chemical Physics* 19, 215 (1968); Don Secrest, "Theory of Rotational and Vibrational Energy Transfer in Molecules," *Annual Review of Physical Chemistry* 24, 379 (1973); Eric Weitz and George Flynn, "Laser Studies of Vibrational and Rotational Relaxation in Small Molecules," *Annual Review of Physical Chemistry* **25**, 275 (1974); Takeshi Oka, "Collision-Induced Transitions Between Rotational Levels," in *Annual Review of Physical Chemistry*, Vol. 9, edited by D. R. Bates, Burlington: Elsevier, 1974.

[240] H. A. Bethe and E. Teller, "Deviations from thermal equilibrium in shock waves." (Undated document accessed March 5, 2012, from http://www.fas.org/sgp/ othergov/doe/ lanl/lib-www/la-pubs/00367149.pdf.); Frank J. Zeleznik, "A Comparison of Rotational Collision Numbers Obtained from Different Definitions," NASA TN D-5321, National Aeronautics and Space Administration, Cleveland, Ohio (1969); R. N. Schwartz, Z. I. Slawsky, and K. F. Herzfeld, "Calculation of Vibrational Relaxation times," J. Chem. Phys. **20**, 1591 (1952); B. K. Annis and A. P. Malinauskas, "Temperature Dependence of Rotational Collision Numbers from Thermal Transpiration," *Journal of Chemical Physics* **54** (11), 4763 (1971); Walter G. Vincenti and Charles H. Kruger, Jr., *Introduction to Physical Gas Dynamics*. New York: Wiley and Sons,, 1965, p. 202; Tiwari, Surendra N., "Radiative energy transfer in molecular gases," NASA-CR-190057, National Aeronautics and Space Administration, Washington, DC, (1992), p. 28.

where E_α is the energy associated with a the molecular degrees of freedom designated by α (i.e., α designates "translational," "vibrational," or "rotational" degrees of freedom), T is the temperature corresponding to thermal equilibrium with the translational degrees of freedom, T_α is the instantaneous temperature corresponding to the α degrees of freedom, and τ_α is the relaxation time for the α degrees of freedom. Neither the temperatures T_α nor the relaxation times τ_α are necessarily equal for the different degrees of freedom.

When relaxation occurs through collisions, the relaxation process is sometimes described by the collision number Z_α, defined[241] as

$$Z_\alpha = \frac{\tau_\alpha}{\tau_c}, \tag{4.54}$$

where τ_α is the relaxation rate defined in (4.53) and τ_c is the mean time between collisions.

Fujii, Lindsay, and Urushihara[242] determined the vibrational self-relaxation time of water vapor to be $\sim 10^{-8}$ sec.

Roessler and Sahm[243] determined the rotational and vibrational self-relaxation times for water vapor at 50 ºC: $\tau_{rot} \sim 10^{-10}$ sec , $\tau_{vib} \sim 10^{-9}$ sec .

---

[241] Frank J. Zeleznik, "A Comparison of Rotational Collision Numbers Obtained from Different Definitions," NASA TN D-5321, National Aeronautics and Space Administration, Cleveland, Ohio (1969); B. K. Annis and A. P. Malinauskas, "Temperature Dependence of Rotational Collision Numbers from Thermal Transpiration," *Journal of Chemical Physics* **54** (11), 4763 (1971); Lambert, J. D., *Vibrational and Rotational Relaxatin in* Gases, Oxford: Clarendon Press (1977), p. 4.

[242] Y. Fujii, R. B. Lindsay, and K. Urushihara, "Ultrasonic Absorption and Relaxation Times in Nitrogen, Oxygen, and Water Vapor," *Journal of the Acoustical Society of America* **35**, 961 (1963).

[243] H. Roesler and K.-F. Sahm, "Vibrational and Rotational Relaxation in Water Vapor," *Journal of the Acoustical Society of America* **37**, 386 (1965).

Keeton and Bass[244] experimentally determined rotational and vibrational relaxation times of water vapor in argon (Ar) and in nitrogen (N_2) at 500 K. For water in nitrogen (45%H_2O:55%N_2), the vibrational relaxtion time for water was $\sim 10^{-8}\,\mathrm{sec}\cdot\mathrm{atm}$ and the vibrational relaxation time was $\sim 10^{-9}\,\mathrm{sec}\cdot\mathrm{atm}$.

Townes and Schawlow[245] assert that "almost all collisions which are effective in broadening a microwave line are also strong enough to leave the molecule more or less randomly in the upper or lower [energy] state" and make an order of magnitude argument that at normal temperatures (~300 K):

1. The time over which a collision occurs is much less than the period of oscillation of the microwave radiation emitted by the molecule.
2. The energy of interaction during a collision is much greater than the energy of transition at microwave frequencies.

These two arguments are equivalent to the assumptions made by Van Vleck and Weisskopf[246]:

1. "The collision is adiabatic, i.e., takes place of an interval of time which is short compared to the period of oscillation of the impressed field."

---

[244] Roy G. Keeton and H. E. Bass, "Vibrational and Rotational Relaxation of Water Vapor by Water Vapor, Nitrogen, and Argon at 500 K," *Journal of the Acoustical Society of America* **60**, 78 (1976).

[245] Townes and Schawlow, *Microwave Spectroscopy*, p. 352.

[246] J. H. Van Vleck and V. F. Weisskopf, "On the Shape of Collision-Broadened Lines," *Reviews of Modern Physics* **17**, 227 (1945).

2. A "strong collision… [is one] so powerful that the molecule has no 'hangover' or memory regarding its orientation or other distributional properties before the collision."

If collisions are both adiabatic and strong, molecules will have a Boltzmann distribution after a collision. Weitz and Flynn[247] assert that, for water vapor, collisional relaxation of rotational energy levels is inefficient compared to collisional relaxation of the translational velocity distribution. Citing spectroscopic studies showing water vapor linewidths narrow as foreign gases are added to the water vapor, they attribute the relative ineffiency to the large separation (~300 cm^{-1}) between adjacent rotational levels in high vibrational ($J \sim 12–15$) states for water vapor, "leading to very inefficient collisional relaxation of these levels at room temperature ($kT \approx 208$ cm^{-1})."

Molecules in excited energy states lose energy, or "relax," by *radiative relaxation*, the spontaneous emission of electromagnetic radiation, and by *nonradiative relaxation*, the transfer of energy by nonradiative means, e.g., by inelastic collisions with other particles, e.g., electrons or molecules (like or unlike). Nonradiative relaxation may also occur through collisions with containing walls or, in solids, by the emission of phonons, lattice vibrational quanta, to a solid lattice.

The collision rate of air molecules Θ_{air} may be calculated from simple kinetic theory[248]:

---

[247] E. Weitz and G. Flynn, "Laser Studies of Vibrational and Rotational Relaxation in Small Molecules," *Annual Reviews of Physical Chemistry* **25**, 275 (1974).

[248] Vincenti and Kruger, *Introduction to Physical Gas Dynamics*, p. 13.

$$\Theta_{air} = \frac{\langle v \rangle}{\lambda}, \tag{4.55}$$

where $\langle v \rangle$ is the mean speed of an air molecule and λ is the mean free path of an air molecule. The mean speed of air molecule assuming a Maxwell-Boltzmann distribution is

$$\langle v \rangle \cong 1.13\sqrt{\frac{2kT}{m}}, \tag{4.56}$$

and the mean free path of an air molecule at 296 K, atmospheric pressure, and 100% relative humidity is[249]

$$\lambda = 6.647 \times 10^{-8} \text{ m}. \tag{4.57}$$

The mass of an air molecule is

$$m = \frac{M_W}{N_A}, \tag{4.58}$$

where the molecular weight M_W =0.02896 kg·mol^{-1} and N_A = 6.023×10^{23} mol^{-1} is the Avogadro number. Then for air at T = 296 K, the collision rate is

$$\Theta_{air} = \frac{1.13}{\lambda}\sqrt{\frac{2kN_AT}{M_W}} = 2.2 \times 10^{8} \text{ s}^{-1}. \tag{4.59}$$

For the ro-vibrational transitions of interest here, the spacing of energy levels are on the order of 1 cm^{-1} which is much smaller than the 200-cm^{-1} thermal energy at 296 K. Thus, we assume here that all collisions are "strong" and that, as a consequence, the

---

[249] S. G. Jennings, "The Mean Free Path in Air," *Journal of Aerosol Science* **19**(2), 159 (1988).

relaxation rate between such closely-spaced energy levels is equal to the collision rate.[250]

Where, as here, the collisions between molecules at thermal energies ($kT \sim 0.025$ eV) induce transitions that correspond to microwave energies ($kT \sim 10^{-5}$ eV), molecular collisions are an effective relaxation mechanism. This is in accord with Corney[251]:

> For near-resonant collisons, where very little energy needs to be transferred to or from the thermal kinetic energy of the system, the cross-sectons tend to have very large values, on the order of 10^{-13} cm^2. If energy differences of the order of kT exist between the two sides of a [molecular] reaction…, the observed cross-sections are of the same order as the gas kinetic cross-sections, $\approx 10^{-15}$ cm^2, while for energy differences greater than a few tenths fo an eV the cross-sections tend to be very small, $\approx 10^{-20}$ cm^2.

4.4. ATMOSPHERIC MASER DYNAMICS

Four transitions listed in the HITRAN molecular spectroscopic database[252] are at wavelengths greater than 1 cm and are candidates for the MST maser transition:

1. The $4_{2,2} \rightarrow 5_{1,5}$ transition at 0.072059 cm–1 (13.9 cm)
2. The $4_{2,3} \rightarrow 3_{3,0}$ transition at 0.400572 cm^{-1} (2.50 cm)

---

[250] E. C. Morris, "Microwave Absorption by Gas Mixtures at Pressures up to Several Hundred Bars," *Australian Journal of Physics* **24**, 157 (1971); Gabrielle Cazzoli, Christina Puzzarini, Giovanni Buffa, Ottavio Tarrini, "Pressure-Broadening of Water Lines in the THz Frequency Region: Improvements and Confirmations for Spectroscopic Databases.: Part I," *Journal of Quantitative Spectroscopy & Radiative Transfer* **109**, 2820 (2008).

[251] Corney, *Atomic and Laser Spectroscopy*, p. 167.

[252] L. S. Rothman, I. E. Gordon, A. Barbe, D. Chris Benner, P. F. Bernath, M. Birk, V. Boudon, L. R. Brown, A. Campargue, J.-P. Champion, K. Chance, L. H. Coudert, V. Dana, V. M. Devi, S. Fally, J.-M. Flaud, R. R. Gamache, A. Goldman, D. Jacquemart, I. Kleiner, N. Lacome, W. J. Lafferty, J.-Y. Mandin, S. T. Massie, S. N. Mikhailenko, C. E. Miller, N. Moazzen-Ahmadi, O. V. Naumenko, A. V. Nikitin, J. Orphal, V. I. Perevalov, A. Perrin, A. Predoi-Cross, C. P. Rinsland, M. Rotger, M. Šimečková, M. A. H. Smith, K. Sung, S. A. Tashkun, J. Tennyson, R. A. Toth, A. C. Vandaele, J. Vander Auwera, "The HITRAN 2008 Molecular Spectroscopic Database," *Journal of Quantitative Spectroscopy and Radiative Transfer* **110**, 533 (2009).

3. The $6_{1,6} \rightarrow 5_{2,3}$ transition at 0.741691 cm^{-1} (1.35 cm)

4. The $5_{3,2} \rightarrow 4_{4,1}$ transition at 0.895092 cm^{-1} (1.12 cm)

The $6_{1,6} \rightarrow 5_{2,3}$ transition is between rotational levels in the ground state vibrational level, i.e., $\nu_1\nu_2\nu_3 = 000$, where $\nu_1\nu_2\nu_3$ represent the quantum numbers for the three normal vibrational modes of a water molecule: symmetric stretching, bending, asymmetric stretching, respectively. The other three transitions are between rotational levels in the $\nu_1\nu_2\nu_3 = 010$ vibrational band.

The lower maser level of each of these transitions lies well above the ground state and so is sparsely populated at normal temperatures (296 K). The $5_{2,3}$ level in the ground vibrational band has an energy corresponding to a wavenumber $\tilde{\nu} = 446.51$ cm^{-1}, which at 296 K gives a Boltzmann fraction relative to the ground state of $\exp(-hc\tilde{\nu}/kT)$ = 0.11. The $3_{3,0}$ level of the first excited vibrational band has an energy corresponding to a wavenumber $\tilde{\nu} = 1907.6$ cm^{-1}, which at 296 K gives a Boltzmann fraction relative to the ground state of $\exp(-hc\tilde{\nu}/kT) = 9\times10^{-5}$. The higher-lying $4_{4,1}$ and $5_{1,5}$ levels of the first excited vibrational band are even more sparsely populated.

In this dissertation, only the $4_{2,2} \rightarrow 5_{1,5}$ and $5_{3,2} \rightarrow 4_{4,1}$ transitions will be considered further.

4.4.1. "Optical" Pumping by the Electric Field Pulse of a Lightning Strike. The MST postulates that a lightning stroke creates a sudden, strong electric field pulse that in turn creates a population inversion in water molecules in a large volume of the atmosphere. Creating a population in this manner is similar to "optical" pumping[253] by

---

[253] Siegman, *Lasers*, p. 13; Svelto, *Principles of Lasers*, Section 6.2.

an incoherent light source, e.g., a flash lamp, emits emits broadband light which is absorbed at the particular frequencies characteristic of the medium. Like the flash lamp, a sudden, strong electric field is a broadband, incoherent source.

Lightning strikes may create population inversions among water molecules within a large volume of moist air.[254] At normal atmospheric conditions near the earth's surface, water molecules exist almost exclusively in the ground vibrational state.

The magnitude of the potential energy of an electric dipole with dipole moment d in an electric field E is $W_{12} \sim Ed$. The dipole moment of a water molecule $d = 1.85$ Debye $= 1.85 \times 3.335641 \times 10^{-30}$ C·m $= 6.17 \times 10^{-30}$ C·m.

Then, adopting a typical value of $E = 100$ kV/m for the maximum electric field, $W_{12} = Ed \sim 10^{-25}\,\mathrm{J}$. This may be compared to a typical separation of rotational energy levels $\Delta U = hv$ within a vibrational band of a water molecule corresponding to microwave frequencies $v \sim 10$ GHz or $\Delta U = \left(6.63 \times 10^{-34}\,\mathrm{J \cdot s}\right)\left(10^{10}\,\mathrm{Hz}\right) \approx 10^{-23}\,\mathrm{J}$.

$$\Delta E_{ROT} = \frac{h^2}{8\pi^2 I}\left[(J+1)(J+1+1) - J(J+1)\right] = \frac{h^2}{4\pi^2 I}(J+1)$$

The moments of inertia for a water molecule $I \approx 10^{-47}\,\mathrm{kg \cdot m^2}$. Then

$$\Delta E_{ROT} \approx \frac{\left(10^{-34}\right)^2}{10^{-47}} = 10^{-21}\,\mathrm{J}$$

---

[254] Peter H. Handel, "New Approach to Ball Lightning," in *Science of Ball Lightning (Fire Ball): First International Symposium on Ball Lightning (Fire Ball); 4-6 July 1988; Waseda University, Tokyo, Japan*, edited by Yoshi-Hiko Ohtsuki (World Scientific, Teaneck, New Jersey, 1989), pp. 254-259; Peter H. Handel and Glenn A. Carlson, "Rise Time of Maser-Caviton Ball Lightning Energy Spikes," *Proceedings Ninth International Symposium on Ball Lightning*, ISBL-06, 16-19 August 2006, Eindhoven, The Netherlands, Ed. G. C. Dijkhuis.

A more sophisticated model of a rotating rigid dipole acted on by an electric field also shows potential for a population inversion under the proper conditions.[255] For a rigid rotor with moment of inertia *I* and angular momentum *L*, the rotational kinetic energy is $L^2/2I$. The potential energy of a molecule with dipole moment *d* in an electric field *E* is dEx, where *x* is the cosine of the angle between the dipole and the field. The Hamiltonian is then

$$H = \frac{L^2}{2I} - dEx . \tag{4.60}$$

The time-dependent Schrödinger equation may be written in the dimensionless form

$$i\frac{\partial\phi(x,\tau)}{\partial\tau} = \left[\mathcal{L}^2 - \alpha x\right]\phi(x,\tau). \tag{4.61}$$

where $\tau = \hbar t/2I$ is a dimensionless time variable, $\mathcal{L} = L/\hbar$ is the angular momentum in units of $\hbar$, and $\alpha(\tau) = \frac{2dI}{\hbar^2}E(\tau)$ is a time-dependent parameter containing the time-dependent electric field. For water molecules in a typical thunderstorm,

$$\alpha \sim \frac{\left(10^{-30}\,\mathrm{C\cdot m}\right)\left(10^{-47}\,\mathrm{kg\cdot m^2}\right)\left(10^{5}\,\mathrm{V\cdot m^{-1}}\right)}{\left(10^{-34}\,\mathrm{J\cdot s}\right)^2} = 10^{-4}.$$

Persico and Van Leuven[256] showed that, for short times ($\tau \ll 1$), (4.61) may be solved and, for a rotor initially in the ground state ($l = 0$), the occupation probabilities W_l

---

[255] M. Persico and P. Van Leuven, "Short-Time Quantum Dynamics of a Driven Rigid Rotor," *Zeitschrift für Physik D*, **41**, 139 (1997).

[256] *Ibid*.

of the l-th rotational level produced by the electric field acting at the end of a dimensionless time interval $(0,T)$ are

$$W_l(T) = (2l+1)\, j_l^2\left(\beta(T)\right), \tag{4.62}$$

where j_l is the l-th spherical Bessel function of the first kind and $\beta(T) = \int_0^T \alpha(\tau')\, d\tau'$. We see from (4.62) that the ground state is completely depleted ($W_0 = 0$) when $\beta = \pi$, and the population of the first excited state ($l = 1$) is a maximum when $\beta \approx 2.08$ ($W_1(2.08) = 0.57$). A population inversion exists between the first excited state ($l = 1$) and the ground state when

$$\frac{2 j_1\left(\beta(T)\right)}{j_0\left(\beta(T)\right)} > 1, \tag{4.63}$$

i.e., when $\beta(T) \geq 1.317$ or, for a constant electric field, when

$$T\alpha(\tau) \geq \frac{2dI}{\hbar^2} ET \cong 1.317, \tag{4.64}$$

$$T \cong 1.317 \frac{\hbar^2}{2dEI} \sim \frac{\left(10^{-34}\,\mathrm{J\cdot s}\right)^2}{\left(10^{-30}\,\mathrm{C\cdot m}\right)\left(10^{5}\,\mathrm{V\cdot m^{-1}}\right)\left(10^{-47}\,\mathrm{kg\cdot m^{2}}\right)} = 10^4 \tag{4.65}$$

or

$$t \geq 1.317 \frac{\hbar}{dE} = 1.317 \frac{\left(1.054\times 10^{-34}\,\mathrm{J\cdot s}\right)}{\left(6.17\times 10^{-30}\,\mathrm{C\cdot m}\right)\left(10^{5}\,\mathrm{V\cdot m^{-1}}\right)} \sim 10^{-9}\ \mathrm{s} \tag{4.66}$$

4.4.2. Laser Rate Equations. Since the lower maser levels of the transitions listed above are sparsely populated at thermal equilibrium relative to the ground state, we will adopt a four-level maser model. All energy levels with energies less than the lower maser level E_1 will be grouped with the ground state E_0. All energy levels with energies greater than the upper maser level E_2 will be grouped into a single energy level E_3. Each

energy level has a corresponding population density of molecules N_i where $i = 0, 1, 2, 3$. The electromagnetic field oscillates in a single mode characterized by the photon number density ϕ.

Molecules are assumed to be "pumped" from the ground state ($i = 0$) to the uppermost energy level ($i = 3$) at a rate denoted by R_p. The lifetime of the molecules populating the upper maser level ($i = 2$) is assumed to be much greater than the lifetime of molecules populating levels $i = 1$ or 3. (We make this assumption even though, as will be shown below, the relaxation time due to collisions of water molecules in excited vibrational states is very short at normal atmospheric pressure.)

Consequently, energy levels $i = 0$ and $i = 1$ are assumed to be completely depopulated compared to level $i = 2$, and the population densities of levels $i = 1$ and 3 are taken as $N_1 \approx 0$ and $N_3 \approx 0$, and difference between the population densities of the maser levels, the *population inversion density*, is given by $N_2 - N_1 \approx N_2$. (For the sake of brevity, except where needed for clarity, we will, omit the term "density" in the following discussion and refer simply to the "photon number" and "population inversion.")

The four-level maser models for the $4_{2,2} \rightarrow 5_{1,5}$ and $5_{3,2} \rightarrow 4_{4,1}$ transitions are shown in Figure 4-6 and Figure 4-7, respectively. Data for the transitions are taken from the HITRAN 2008 molecular spectroscopic database[257] (see Appendix A).

---

[257] L. S. Rothman, I. E. Gordon, A. Barbe, D. Chris Benner, P. F. Bernath, M. Birk, V. Boudon, L. R. Brown, A. Campargue, J.-P. Champion, K. Chance, L. H. Coudert, V. Dana, V. M. Devi, S. Fally, J.-M. Flaud, R. R. Gamache, A. Goldman, D. Jacquemart, I. Kleiner, N. Lacome, W. J. Lafferty, J.-Y. Mandin, S. T. Massie, S. N. Mikhailenko, C. E. Miller, N. Moazzen-Ahmadi, O. V. Naumenko, A. V. Nikitin, J. Orphal, V. I. Perevalov, A. Perrin, A. Predoi-Cross, C. P. Rinsland, M. Rotger, M. Šimečková, M. A. H. Smith, K. Sung, S. A. Tashkun, J. Tennyson, R. A. Toth, A. C. Vandaele, J. Vander Auwera, "The HITRAN 2008 molecular spectroscopic database," *Journal of Quantitative Spectroscopy and Radiative Transfer* **110**, 533 (2009).

A four-level maser is described by the maser *rate equations* that describe the photon number density and population inversion density:

$$\frac{d\phi}{dt} = B\left(\phi + 1\right) N_2 - \frac{1}{\tau_c}\phi \tag{4.67}$$

$$\frac{dN_2}{dt} = R_p - B\phi N_2 - \frac{1}{\tau_2} N_2 \tag{4.68}$$

where B is the Einstein B coefficient for stimulated emission, τ_2 is the fluorescence lifetime of the upper laser level, and τ_c is the lifetime of a photon in the cavity. The constant 1 added to ϕ in (4.67) is the "extra photon" [258] that accounts for spontaneous emission that is fundamental to a maser as a quantum system. At the onset of maser oscillations, the contribution of spontaneous emission is negligible compared to the maser gain[259], but the extra photon is included in the rate equations to initiate growth in the radiation field from the initial zero-field condition.

The system of equations (4.67) and (4.68) are coupled and nonlinear. Though closed-form analytical solutions[260] have been identified for specific values of the pump rate R_p, numerical methods are required to solve the general problem. We undertake this task here.

Taking a similar path as Kleinman[261], we define the dimensionless variables

---

[258] Siegman, *Lasers*, p. 503.

[259] Svelto, *Principles of Lasers*, p. 251; D. A. Kleinman, "The Maser Rate Equations and Spiking," *Bell System Technical Journal* **43** (4), 1505 (1964).

[260] A. C. Reardon, "Exact Solutions of Laser Rate Equations," *Journal of Modern Optics* 38 (5), 857 (1991).

[261] D. A. Kleinman, "The Maser Rate Equations and Spiking," *Bell System Technical Journal* **43** (4), 1505 (1964).

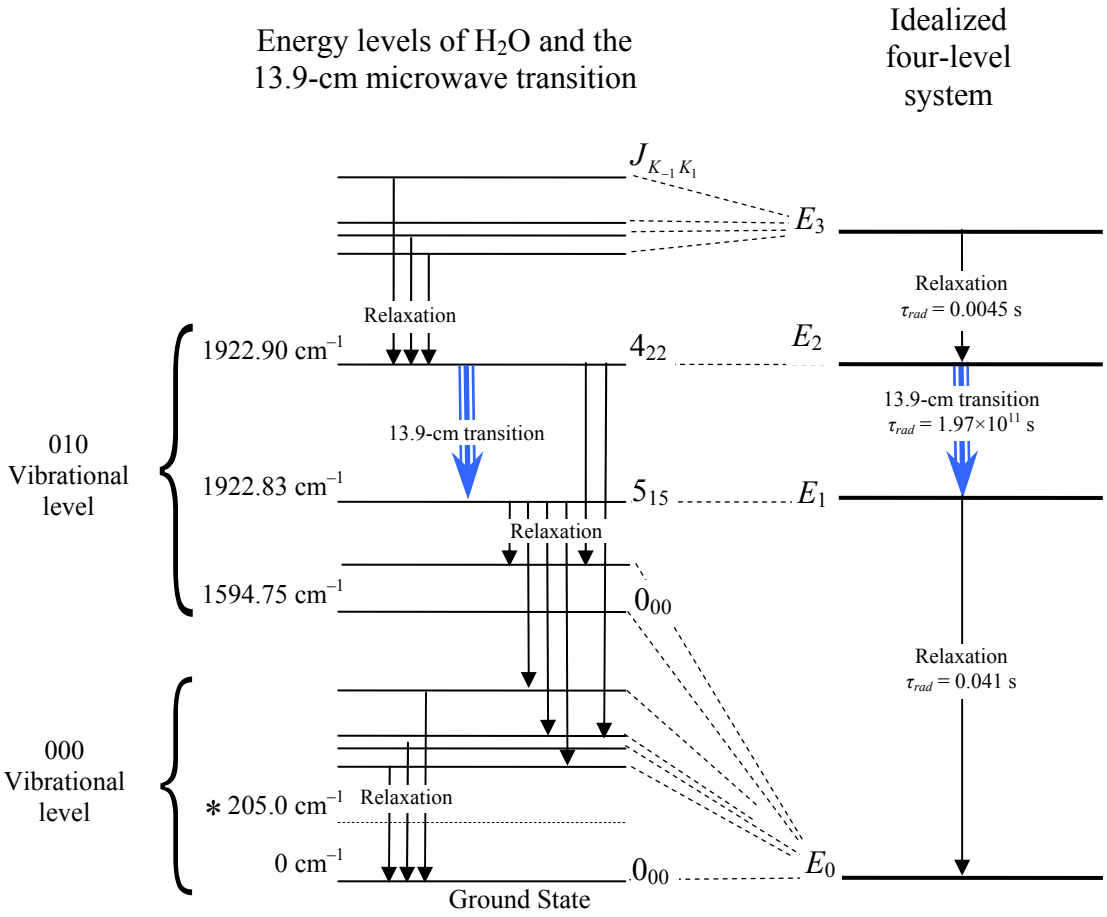

Figure 4-6: H_2O Energy Levels and an Idealized Four-Level System

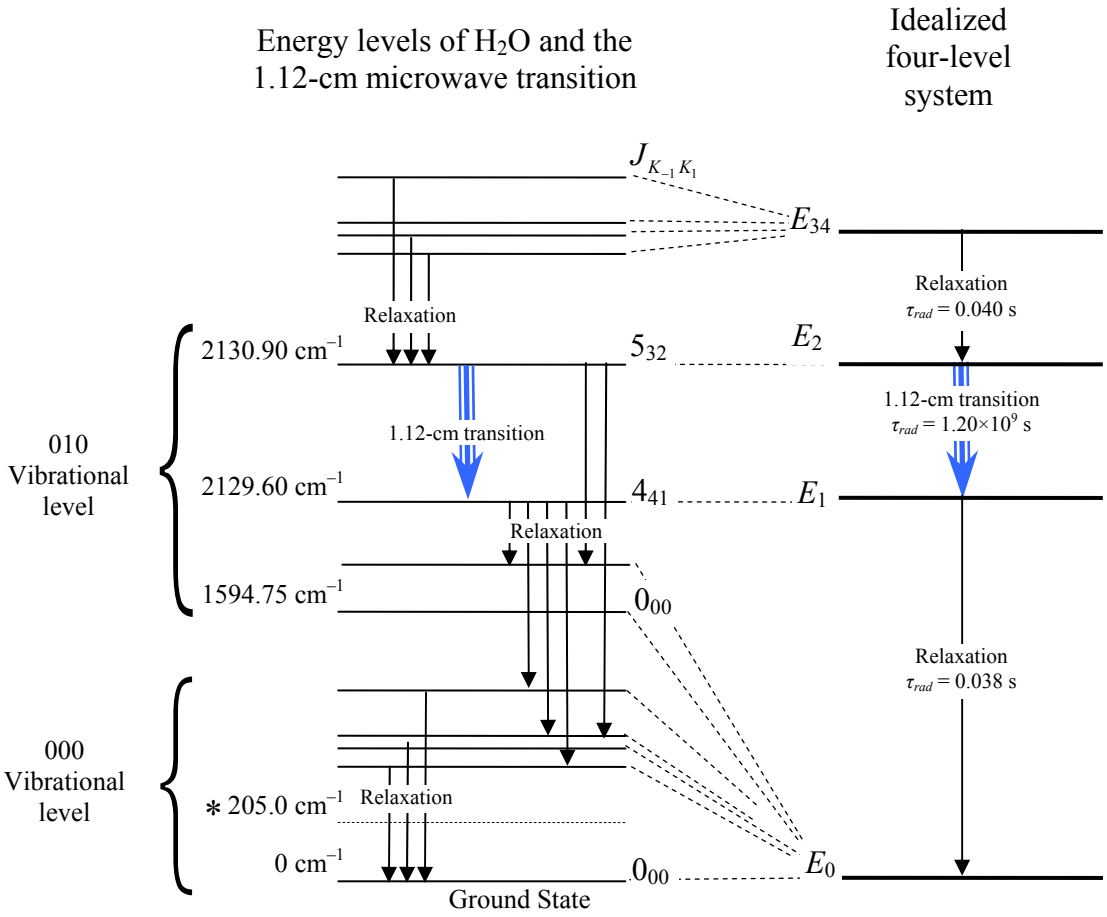

Figure 4-7: H_2O Energy Levels and an Idealized Four-Level System

$$\tau \equiv \frac{t}{\tau_c} \tag{4.69}$$

$$\eta \equiv N_2 B \tau_c \tag{4.70}$$

$$\rho \equiv \phi B \tau_2 \tag{4.71}$$

and the dimensionless parameters

$$\pi \equiv R_p B \tau_c \tau_2 \tag{4.72}$$

$$\mu \equiv \frac{\tau_c}{\tau_2} \tag{4.73}$$

$$\sigma \equiv B \tau_2 \,. \tag{4.74}$$

Using these dimensionless quantities, the maser rate equations (4.67) and (4.68) may be written in a form:

$$\frac{d\rho}{d\tau} = (\rho + \sigma)\eta - \rho \tag{4.75}$$

$$\frac{d\eta}{d\tau} = \mu(\pi - \eta - \rho\eta)\,, \tag{4.76}$$

where ρ represents the *photons*, η represents the *population inversion*, and τ represents the *time*, while μ represents the relative magnitude of the cavity lifetime (photon lifetime) and the relaxation lifetime (upper level total decay time), π represents the *pumping rate*, and σ represents *spontaneous emission*.

The critical inversion N_{crit} corresponding to the Schawlow-Townes[262] criterion for the onset of laser oscillation is then

---

[262] A. L. Schawlow and C. H. Townes, "Infrared and Optical Masers," *Physical Review* **112** (6), 1940 (1958).

$$N_{crit} = \frac{1}{B\tau_c}, \tag{4.77}$$

and the dimensionless inversion η in (4.70), the dimensionless pumping rate parameter π in (4.72), and the ratio of spontaneous lifetime and total decay lifetime of the upper level σ in (4.74) may be expressed in the respective equivalent forms

$$\eta = \frac{N_2}{N_{crit}}, \tag{4.78}$$

$$\pi = \frac{R_p \tau_2}{N_{crit}}, \tag{4.79}$$

and

$$\sigma = \frac{1}{\mu N_{crit}}. \tag{4.80}$$

Let $N_2^{(0)}$ represent the equilibrium value for the inversion with the pump on and with no photons in the cavity (i.e., $\phi = 0$). Then on setting $dN_2/dt = 0$ in (4.68),

$$N_2^{(0)} = R_p \tau_2 . \tag{4.81}$$

An equivalent meaning to (4.81) is that $R_p = N_2^{(0)}/\tau_2$ is the pump rate needed to exactly equal the rate at which the upper level population spontaneously decays. And, from (4.79), $\pi = 1$ corresponds to the pump rate that will produce the critical upper inversion for laser oscillation.

The steady state solution to (4.75) and (4.76) is

$$\eta_\infty = \frac{(\pi+1) - (\pi-1)\sqrt{1 + \dfrac{4\pi\sigma}{(\pi-1)^2}}}{2(1-\sigma)} \tag{4.82}$$

$$\rho_\infty = \frac{(\pi - 1)}{2}\left(1 + \sqrt{1 + \frac{4\pi\sigma}{(\pi - 1)^2}}\right), \tag{4.83}$$

where the corresponding signs of the radicals are selected such that $\eta_\infty, \rho_\infty \geq 0$.

We may examine the asymptotic forms of η_∞ and ρ_∞ as $\sigma \to 0$, depending on whether $\pi < 1$ or $\pi > 1$. From (4.82) and (4.83), when $\sigma \to 0$,

$$\left.\begin{aligned} \eta_\infty &\underset{\sigma\to 0}{\to} \pi - \rho_\infty \\ \rho_\infty &\underset{\sigma\to 0}{\to} \frac{\pi\sigma}{1-\pi} \end{aligned}\right\}, \quad \pi < 1 \tag{4.84}$$

$$\left.\begin{aligned} \eta_\infty &\underset{\sigma\to 0}{\to} 1 + \rho_\infty \\ \rho_\infty &\underset{\sigma\to 0}{\to} \pi - 1 + \frac{\pi\sigma}{\pi - 1} \end{aligned}\right\}, \quad \pi > 1, \tag{4.85}$$

where in (4.84) and (4.85), we use the small-value approximation $\sqrt{1+x} \approx 1 + \frac{1}{2}x$, for $x \ll 1$. Thus, for $\pi < 1$, i.e., the pump rate alone is insufficient to create the critical inversion, and laser oscillation does not occur. For $\pi > 1$, i.e., the pump rate alone is sufficient to create the critical inversion needed for laser oscillation, the steady state inversion is the critical inversion.

4.4.3. Einstein *B* Coefficient for Stimulated Emission. The Einstein *B* coefficient is related to the Einstein *A* coefficient for spontaneous emission by the relations:

$$B_\nu = \frac{A}{m(\nu)} = \frac{c^3}{8\pi\nu^2} A \tag{4.86}$$

$$B_{\omega} = \frac{A}{m(\omega)} = \frac{\pi^2 c^3}{\omega^2} A \tag{4.87}$$

depending on whether the electromagnetic field is characterized by the frequency v or the angular frequency ω ($= 2\pi v$) . Spectral mode density m is number of modes per unit volume per unit frequency (or per angular frequency) range. The factors multiplying A in (4.86) and (4.87) are determined by recognizing that the number of modes per unit volume are equal for corresponding frequency and angular frequency ranges. Thus, $m(v)$ and $m(\omega)$ are related by:

$$m(v)\,dv = \frac{8\pi}{c^3} v^2 dv = \frac{1}{\pi^2 c^3} \omega^2 d\omega = m(\omega)\,d\omega\,. \tag{4.88}$$

In this dissertation, we will express the electromagnetic field in terms of frequency v, so we will calculate the Einstein B coefficient from (4.86). The Einstein A coefficients for thousands of transitions for the water molecule are tabulated in HITRAN molecular spectroscopic database.[263]

Table 4-1 lists the Einstein A and B coefficients for the $4_{2,2} \rightarrow 5_{1,5}$ and $5_{3,2} \rightarrow 4_{4,1}$ transitions.

---

[263] Marie Šimečková, David Jacquemart, Laurence S. Rothman, Robert R. Gamache, and Aaron Godman, "Einstein *A*-coefficients and Statistical Weights for Molecular Absorption Transitions in the HITRAN Database," *Journal of Quantitative Spectroscopy and Radiative Transfer* **98**, 130 (2006).

Table 4-1: Einstein *B* coefficient for stimulated emission

Transition	Einstein *A* coefficient [s^{-1}]	Einstein *B* coefficient (B_v) [$m^3 \cdot s^{-2}$]
$4_{2,2} \rightarrow 5_{1,5}$	5.088×10^{-12}	1.1688×10^{-6}
$5_{3,2} \rightarrow 4_{4,1}$	8.314×10^{-9}	1.5310×10^{-5}

4.4.4. Fluorescence Lifetime. The *fluorescence lifetime* of an excited molecular level can be determined by measuring the decay of the fluorescent emission from a sample of suitable material using a pulsed light source.[264] A collection of molecules in the sample absorb energy from the light source and enter an excited state. The excited molecules decay by emitting radiation or transferring it nonradiatively through, for example, collisions with other molecules. The fluorescence lifetime τ_j of an energy level j includes both the radiative and the nonradiative decays:

$$\frac{1}{\tau_j} = \sum_{i<j} \left(\frac{1}{\tau_{rad,ji}} + \frac{1}{\tau_{nr,ji}} \right), \tag{4.89}$$

where $\tau_{rad,j}$ and $\tau_{nr,ji}$ denote the radiative and nonradiative lifetimes, respectively, of the transition from level j to level i and the sum is taken over all states i that are lower in energy than level j.

[264] Siegman, *Lasers*, p. 119.

The reciprocal of the radiative lifetime of the $i \rightarrow j$ transition is "exactly the same thing as the *Einstein A coefficient* for that transition"[265]:

$$\frac{1}{\tau_{rad,ji}} = A_{ji}\,. \tag{4.90}$$

Thus,

$$\frac{1}{\tau_j} = \sum_{i<j}\left(A_{ji} + \frac{1}{\tau_{nr,ji}} \right). \tag{4.91}$$

Einstein A coefficients for thousands of transitions for the water molecule are tabulated in HITRAN molecular spectroscopic database. The nonradiative lifetime is found from the width $\Delta\omega_{ji}$ of the pressure-broadened spectral line for the transition according to (4.52):

$$\Delta\omega_{ji} = \gamma_{self,ji} P_{H_2O} + \gamma_{air,ji} P_{air}\,. \tag{4.92}$$

The sum of the Einstein A coefficients in (4.91) for the $4_{2,2} \rightarrow 5_{1,5}$ and $5_{3,2} \rightarrow 4_{4,1}$ transitions are taken from the tables in Appendix A and are listed in Table 4-2. We see clearly that, at atmospheric pressure, the fluorescence lifetime is dominated by the relaxation due to molecular collisions.

---

[265] *Ibid*. p. 121 (italics in original); Corney, *Atomic and Laser Spectroscopy*, p. 104.

Table 4-2: Radiative and Nonradiative Lifetimes

Transition ($j \rightarrow i$)	$\sum_{i<j} A_{ji}$ [s^{-1}]	$\sum_{i<j} \frac{1}{\tau_{nr,ji}} = \Delta\omega_{pressure}$ [s^{-1}]	$\frac{1}{\tau_j} = \sum_{i<j}\left(A_{ji} + \frac{1}{\tau_{nr,ji}}\right)$ [s^{-1}]
$4_{2,2} \rightarrow 5_{1,5}$	24.173	3.01653×10^{9}	3.01653×10^{9}
$5_{3,2} \rightarrow 4_{4,1}$	25.088	2.67968×10^{9}	2.67968×10^{9}

4.4.5. Cavity Lifetime τ_c and Quality Factor Q. The cavity decay time τ_c in (4.67) characterizes the loss of photons from the maser cavity due to transmission through the cavity boundaries with various degrees of reflectivity, diffraction at edges of mirrors or apertures, geometric effects as mirrors reflect light at angles such that the light leaves the cavity, and internal losses such as absorption and scattering.

The cavity lifetime for radiation of frequency v is related to the quality factor[266] Q:

$$\tau_c = \frac{Q}{2\pi v}. \tag{4.93}$$

For an unbounded region of open air, the quality factor was found (see (3.16)) to be

$$Q = \frac{2\pi v L}{c}, \tag{4.94}$$

where c is the speed of light. The cavity lifetime, then, equals the cavity transit time:

---

[266] Maitland and Dunn, *Laser Physics*, p. 105.

$$\tau_c = \frac{1}{2\pi\nu}\frac{2\pi\nu L}{c} = \frac{L}{c}. \tag{4.95}$$

For a cavity bounded by two mirrors with power reflectivities R_1 and R_2 and fractional internal power losses per pass T the cavity lifetime is[267]

$$\tau_c = -\frac{2L}{c\ln\left[R_1R_2\left(1-T\right)^2\right]}, \tag{4.96}$$

where L is the length of the cavity and c is the speed of light.

Müller and Weber[268] noted that a cavity lifetime of the form (4.96) "cannot be valid in any case" since, if $R_1R_2\left(1-T\right)^2 < e^{-1}$, the cavity lifetime becomes less than the cavity roundtrip time, which is impossible for an empty resonator ($T = 0$). However, they agree with (4.96) in the low power loss limit ($\left(1-T\right)^2 R_1R_2 \ll 1$):

$$\tau_c = \frac{L}{c}\frac{1}{1-\left(1-T\right)^2 R_1R_2}. \tag{4.97}$$

Equation (4.97) also agrees with the expression for the empty cavity given by Shimoda.[269]

For a medium with a power aborption coefficient α defined by the Beers-Lambert Law, $I\left(L\right) = I_0e^{-\alpha L}$, the cavity time constant is[270]

$$\tau_c = \frac{1}{\alpha c}, \tag{4.98}$$

---

[267] Svelto, *Principles of Lasers*, p. 168.

[268] W. Muller and H. Weber, "Decay Time of Optical Resonators," *Optics Communications* **23**, 440 (1977).

[269] Koichi Shimoda, *Introduction to Laser Physics*, Second Edition, Berlin: Springer-Verlag, 1991, p. 106.

[270] Maitland and Dunn, *Laser Physics*, p. 105.

and the corresponding quality factor for radiation with frequency v is

$$Q_\alpha = \frac{2\pi\nu}{\alpha c}. \tag{4.99}$$

For a loss that can be expressed as a fractional power loss per pass through the cavity, δ, the cavity time constant is[271]

$$\tau_c = \frac{L/c}{\delta}, \tag{4.100}$$

and the corresponding quality factor is

$$Q_\delta = 2\pi\nu\frac{L/c}{\delta} \tag{4.101}$$

The preceding results are summarized in Table 4-3.

Table 4-3 : Cavity Lifetimes and Quality Factors

Cavity Description	Cavity time constant τ_c	Quality factor Q
Unbounded cavity (L = Length)	$\frac{L}{c}$	$2\pi\nu L/c$
Cavity w/ mirrors and absorptive medium (R = mirror reflectivity, $R \ll 1$; T = fractional power loss per pass)	$\frac{L/c}{1-(1-T)^2 R_1 R_2}$	$\frac{2\pi\nu L/c}{1-(1-T)^2 R_1 R_2}$
Absorptive medium (α = power absorption coefficient)	$\frac{1}{\alpha c}$	$\frac{2\pi\nu/c}{\alpha}$
Absorptive medium (δ = power loss per pass)	$\frac{L/c}{\delta}$	$\frac{2\pi\nu L/c}{\delta}$

[271] *Ibid*.

4.4.6. Cavity Lifetime τ_c for Open Resonant Cavities. In terms of geometric optics, open resonant cavities are characterized as *stable* if "a ray within … the resonantor remains within the resonator after any number of round trips" and *unstable* if all rays "walk out" of the resonator.[272]

Resonant cavities formed from a pair of mirrors with power reflectivities R_1 and R_2 separated by a distance L can be characterized by the normalized curvature or g parameter[273]:

$$g_i = 1 - \frac{L}{R_i}, \quad (i = 1, 2). \tag{4.102}$$

In (4.102), by convention, $R_i > 0$ denotes a concave mirror, and $R_i < 0$ denotes a convex mirror. A cavity can be mapped to a point on a g_1g_2-plane (Figure 4-8), and a stable resonant cavity is defined by $0 \le g_1 g_2 \le 1$. A cavity that lies within the shaded region is stable, and one that lies without is unstable. Unstable resonators are further classified as a "positive branch" resonator if $g_1g_2 > 0$ and as "negative branch" resonator if $g_1g_2 < 0$.

The magnitude of diffractive losses of the lowest-order mode in an open cavity can be estimated by the Fresnel number for the cavity:

$$N_F = \frac{a^2}{L\lambda}, \tag{4.103}$$

where L is the distance between the mirrors, a is the radius of the mirrors, and λ is the wavelength of the radiation. A cavity that is large compared to the radiation

---

[272] *Ibid*., p. 123.

[273] A. E. Siegman, "Unstable Optical Resonators for Laser Applications," *Proceedings of the IEEE* **53**, 277 (1965); H. Kogelnik and T. Li, "Laser Beams and Resonators," *Applied Optics* **5**, 1550 (1966).

wavelength ($L \approx a \gg \lambda$) has a large Fresnel number ($N_F \gg 1$). For large Fresnel number, the diffraction losses of the low order modes are small for a resonator that lies well within the stable region in Figure 4-8 and increase near the boundary of the stable region at $g_1 g_2 = 1$.[274]

The fractional amplitude loss per pass γ of an electromagnetic mode m through a symmetric ($R_1 = R_2 = R$) stable resonator ($g_1 = g_2 = g$) is found by solving the Fresnel-Huygens integral equation[275]:

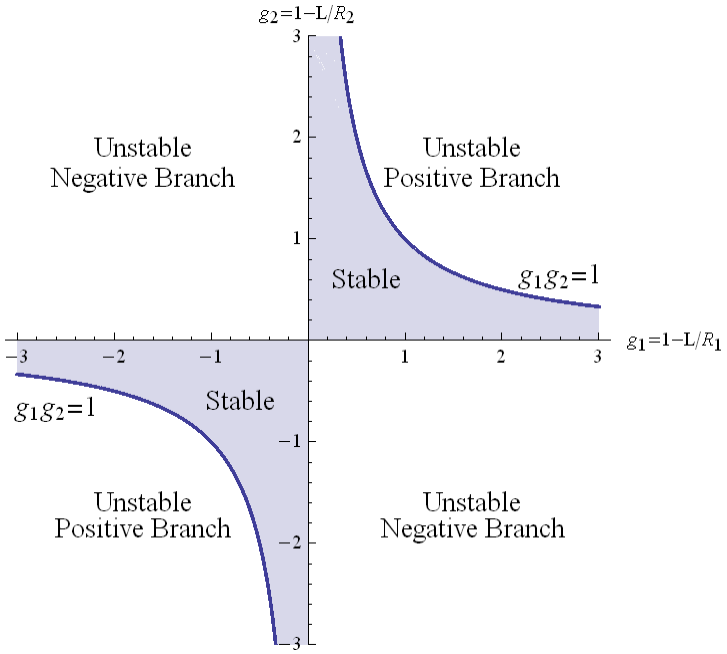

Figure 4-8: Open Resonator Stability Diagram

---

[274] Maitland and Dunn, *Laser Physics*, p. 125.

[275] H. Kogelnik and T. Li, "Laser Beams and Resonators," *Applied Optics* **5**, 1550 (1966).

$$\gamma_m \Phi_m(r_1)\sqrt{r_1} = \int_0^R K_m(r_1, r_2)\Phi_m(r_2)\sqrt{r_2}\, dr_2 , \tag{4.104}$$

where

$$K_m(r_1, r_2) = \frac{i^{m+1}}{d} J_m\left(k\frac{r_1 r_2}{d}\right)\sqrt{r_1 r_2}\exp\left[-\frac{igk}{2d}\left(r_1^2 + r_2^2\right)\right], \tag{4.105}$$

$\Phi(r)$ is the radial distribution of the field on each mirror, J_m is a Bessel function of the first kind and m-th order, R is the radius of the mirror, d is the distance between the mirrors, $k = 2\pi/\lambda$, and λ is the wavelength of the wave. The lowest order mode corresponds to $m = 0$. The fractional power loss is given by γ^2.

Equation (4.104) was solved by an iterative method[276]. The results[277] show that γ^2 is a rapidly decreasing function of N_F for $0 \le g \le 1$. In particular, $\gamma^2 \ll 0.001$ for all resonators with $N_F > 40$ for all $0 \le g \le 1$. For g < 0.95, $\gamma^2 \ll 0.001$ for all resonators with $N_F > 4$. For this dissertation where $N_F \sim 10^4$, we will ignore diffractive losses from the stable cavity.

4.4.7. Progagation of Maser Radiation: The Beam Waist. The steady state electric field within a resonant cavity satisfies the scalar wave equation

$$\nabla^2 E + k^2 E = 0 , \tag{4.106}$$

where $k = \omega/c$.

---

[276] Tingye Li, "Diffraction Loss and Selection of Modes in Maser Resonators with Circular Mirrors," *Bell System Technical Journal* **44**, 917 (1965).

[277] *Ibid*., Figure 4.

A wave propagating in the +z-direction can be represented by the *paraxial approximation*:

$$E = u(x, y, z)\exp(-ikz), \tag{4.107}$$

where $u(x,y,z)$ is a slowly-varying function, i.e., $(\nabla u)/u \ll k$. On substituting (4.107) into (4.107), we obtain the *paraxial wave equation:*

$$\nabla_{\perp}^2 u - 2ik\frac{\partial u}{\partial z} = 0, \tag{4.108}$$

where $\nabla_{\perp}^2$ is the Laplacian in the transverse coordinates x and y.

The differential equation (4.108) can be expressed as an equivalent integral equation[278]:

$$u(x, y, z) = \frac{i}{\lambda L}\iint_S dx_1\, dy_1\, u(x_1, y_1, z_1)\exp\left[-ik\frac{(x-x_1)^2 + (y-y_1)^2}{2L}\right], \tag{4.109}$$

where $\lambda = k/2\pi$, $L = z - z_1$, and S represents surface at $z = z_1$ over which the field is defined.

When S extends to infinity, a solution to (4.109) takes a Gaussian form[279]

$$u(x, y, z) \propto \exp\left[-ik\frac{(x^2 + y^2)}{2q}\right], \tag{4.110}$$

where $q = q(z)$ is a complex-valued *beam parameter*. The beam parameter can be resolved into real and imaginary parts:

---

[278] Svelto, *Principles of Lasers*, p. 147.

[279] *Ibid*, p. 149.

$$\frac{1}{q}=\frac{1}{R}-i\frac{\lambda}{\pi w^2}, \tag{4.111}$$

where $R = R(z)$ is the radius of curvature of the spherical wave (i.e., on a surface of constant phase) represented by (4.110) and $w = w(z)$ is the width of the beam, i.e., the amplitude of the fundamental mode at a distance w away from the z-axis is $1/e$ times the value on the axis. The parameter w is sometimes referred to as the "spot size."

If we assume the Gaussian beam (4.110) is propagating in $+z$-direction and $R = \infty$ at $z = 0$, we can express the spot size and radius of curvature as

$$w^2\left(z\right)=w_0^2\left[1+\left(\frac{z}{b}\right)^2\right] \tag{4.112}$$

and

$$R\left(z\right)=z\left[1+\left(\frac{b}{z}\right)^2\right], \tag{4.113}$$

where b is the *confocal* parameter[280] defined by

$$b=\pi w_0^2/\lambda\,. \tag{4.114}$$

The minimum spot size w_0, the *beam waist*, is located at $z = 0$. The field amplitude take the form[281]

$$u\left(x,y,z\right)=\frac{w_0}{w}\exp\left[-\frac{\left(x^2+y^2\right)}{w^2}\right]\exp\left[-ik\frac{\left(x^2+y^2\right)}{2R}\right]\exp j\phi\,, \tag{4.115}$$

where $\phi=\tan^{-1}\left(z/b\right)$.

---

[280] H. Kogelnik and T. Li, "Laser Beams and Resonators," *Applied Optics* **5**, 1550 (1966).

[281] Svelto, *Principles of Lasers*, p. 152.

Table 4-4 lists the confocal parameter and the location of the beam waist for some of the various resonator configurations tabulated by Kogelnik and Li.[282] In Table 4-4, L is the distance between the mirrors, and R_1 and R_2 are the radii of curvature of the mirrors.

Table 4-4: Confocal Parameter and Beam Waist Location

Optical System	Confocal Parameter	Beam Waist Location (Relative to R_1)
Half-Symmetric ($R_1 = R$, $R_2 = \infty$)	$2\sqrt{L(R-L)}$	L
Symmetric ($R_1 = R_2 = R$)	$\sqrt{L(2R-L)}$	$\frac{L}{2}$
Asymmetric ($R_1 \neq R_2$)	$2\frac{\sqrt{L(R_1-L)(R_2-L)(R_1+R_2-L)}}{R_1+R_2-2L}$	$\frac{L(R_2-L)}{R_1+R_2-2L}$

Note that the asymmetric case in Table 4-4 includes the half-symmetric and symmetric cases as limiting cases:

$$\text{Half-symmetric case: } \lim_{R_1\to\infty}\frac{L(R_2-L)}{R_1+R_2-2L}=0 \tag{4.116}$$

and

$$\text{Symmetric case: } \lim_{R_1,R_2\to R}\frac{L(R_2-L)}{R_1+R_2-2L}=\frac{L}{2}. \tag{4.117}$$

---

[282] H. Kogelnik and T. Li, "Laser Beams and Resonators," *Applied Optics* **5**, 1550 (1966).

It is also instructive to note that the confocal parameter and beam waist location for the asymmetric case can be written in terms of the g parameters as

$$\frac{b}{L} = \frac{2\sqrt{g_1 g_2 \left(1 - g_1 g_2\right)}}{g_1 + g_2 - 2 g_1 g_2} \tag{4.118}$$

and

$$\frac{z_0}{L} = \frac{\left(1 - g_1\right) g_2}{g_1 + g_2 - 2 g_1 g_2} . \tag{4.119}$$

where z_0 denotes the location of the beam waist.

Thus, the location of the beam waist can be mapped onto the $g_1 g_2$ plane for various values of z_0/L as shown in Figure 4-9 through Figure 4-12. In Figure 4-9 through Figure 4-12, the stability limit curve $g_1 g_2 = 1$ is denoted by a heavy dashed line. Also, in addition to the curves shown above for $\frac{1}{2} \le t/L \le 1$, there is a set of corresponding curves for $0 \le t/L < \frac{1}{2}$ reflected across the line $g_1 = g_2$. For the symmetric cavities considered here, the beam waist is at the planar mirror (i.e., at the ground).

4.4.8. Maser Spiking. Statz and Mars[283] and Kleinman[284] have shown that the maser rate equations (4.67) and (4.68) (or (4.75) and (4.76)) may be used to describe the "spiking" oscillations of the photon and molecule populations exhibited by real masers

---

[283] H. Statz and G. deMars, "Transients and oscillation pulses in masers," in *Quantum Electronics, Proceedings of the First International Quantum Electronics Conference*, Highview, NY, 1959, edited by Charles H. Townes (Columbia University, New York, 1960), p. 530.

[284] D. A. Kleinman, "The Maser Rate Equations and Spiking," *Bell System Technical Journal* **43** (4), 1505 (1964).

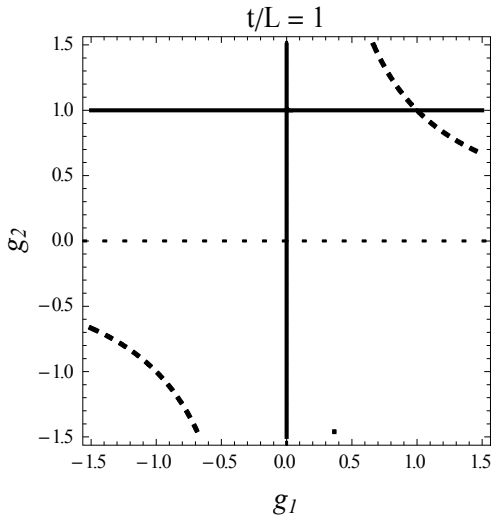

Figure 4-9: Beam Waist at *t*/*L* = 1

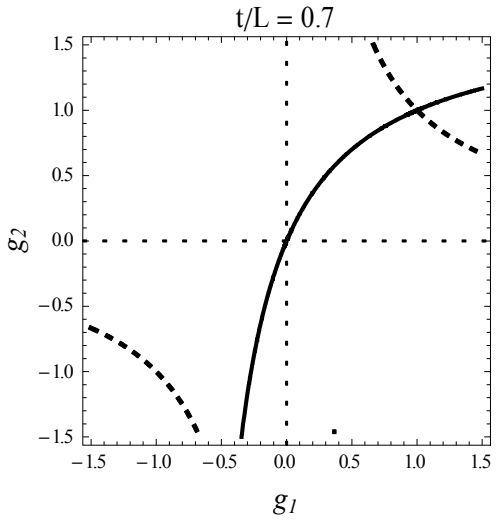

Figure 4-10: Beam Waist at *t*/*L* = 0.7

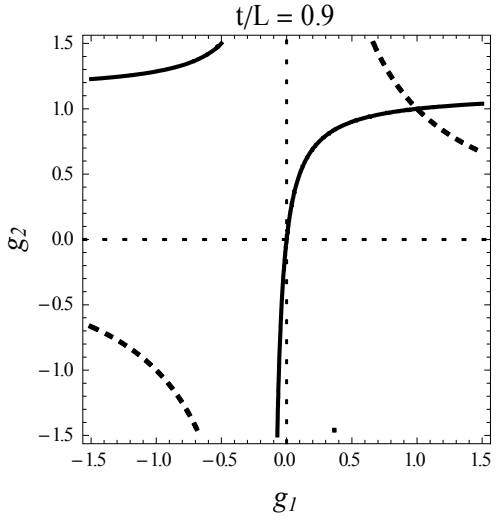

Figure 4-11: Beam Waist at *t*/*L* = 0.9

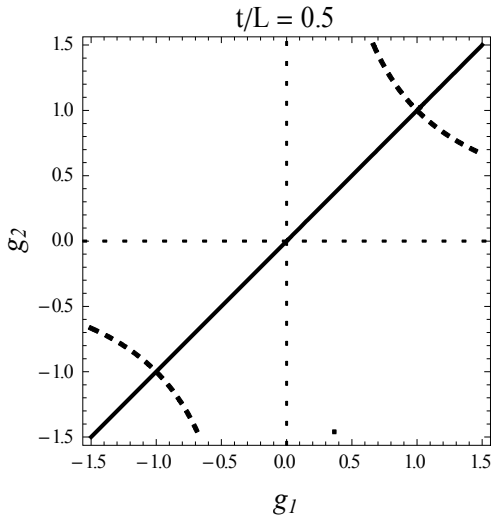

Figure 4-12: Beam Waist at *t*/*L* = 0.5

and lasers under certain pump conditions. Figure 4-13 depicts a "typical" example of spiking of the photon number calculated from the rate equations.

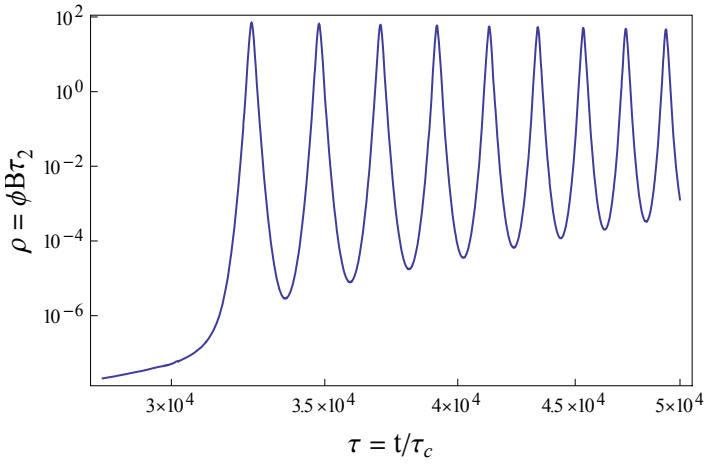

Figure 4-13: Spiking of Photon Number Calculated from Rate Equations

We saw previously that the the linearized rate equations had solutions of the form

$$f(t) = c_1 \exp(s_1 t) + c_2 \exp(s_2 t), \tag{4.120}$$

where c_1 and c_2 are constants and s_1 and s_2 are roots of the secular determinant (3.31):

$$s_1, s_2 = -\frac{r}{2\tau_2} \pm i\sqrt{\frac{(r-1)}{\tau\tau_2} - \left(\frac{r}{2\tau_2}\right)^2} \equiv -\gamma \pm i\omega \tag{4.121}$$

where $r \equiv R_p / R_{p,th}$ and the threshold pump rate $R_{p,th} = N_{2,th}/\tau_2$.

At atmospheric pressure and temperature, the collision rate is $\tau_\delta \sim 10^{-10}$ s, and the damping constant in (4.121) is

$$\gamma = -\frac{r}{2\tau_2} \sim 10^{10} \text{ s} \tag{4.122}$$

Consequently, within less than a microsecond, any spike that might occur is *nonradiatively* damped through molecular collisions, and the maser achieves the steady state output level proportional to the pumping rate expressed in (4.85).

4.5. PUMPING RATE TO ACHIEVE BREAKDOWN OF AIR

We are now ready to calculate the pumping rate needed to create a population inversion sufficient to cause the electrical breakdown of air in the atmosphere.

Letting L be the characteristic length of our maser geometry (e.g., height, width), the total energy in the maser radiation is proportional to L^3 and the area of the maser beam at the beam waist is proportional to L^2. Then the energy deposited per unit area at the beam waist is proportional to L, i.e., the larger the size of the maser in the atmosphere, the greater the energy per unit area deposited at the beam waist, and the more likely to achieve breakdown.

However, the greater the maser volume, the smaller the strength of the electric field that can be sustained within that volume. Very strong electric fields cannot be maintained in large volumes of open air because electron avalanche initiated by cosmic radiation is more likely to occur the larger the volume of open air that is available. And the weaker the electric field, the weaker is its ability to create large population inversions.

Thus, there are competing effects depending on the size of the atmospheric maser: Large masers can radiate more energy than small masers, but high strength electric fields cannot be sustained in large masers.

Referring to Figure 4-1, we assume the bottom of the thundercloud is at a height above the surface L_c = 1000 m and the power reflectivity of the cloud ρ_{cloud} = 0.86. The

volume of the active medium $V = L_{am}^3$, which we will allow to vary up to $L_{am} \approx L_c$. The radius of curvature the upper mirror (the cloud) will be accounted for through the *g* parameter, which will be allowed to vary over the range $0 \le g_2 \le 1$. The ground is assumed to have a power reflectivity $\rho_{ground} = 1$ and to be planar so that $g_1 = 1$.

Since the ground is assumed to be planar, the ground and cloud comprise a half-symmetric stable resonator. The beam waist is located on the ground and can be calculated from (4.114):

$$w_0 = \sqrt{\frac{\lambda b}{\pi}}, \tag{4.123}$$

where the confocal parameter *b* is defined in terms of the *g* parameters in (4.118):

$$b = 2L_c \frac{\sqrt{g_1 g_2 (1 - g_1 g_2)}}{g_1 + g_2 - 2g_1 g_2}. \tag{4.124}$$

We assume that the beam waist is narrower than the width of the active medium (i.e., $w_0 < L_{am}$) so that we can write the energy density of the maser beam at the beam waist in terms of the energy density of the maser beam in the active medium as

$$u_{waist} = \left(\frac{L_{am}}{w_0} \right)^2 u_{am} \tag{4.125}$$

where the energy density in the active medium is simply the steady state photon number density ϕ_∞ from (4.83) times the energy per photon *hv*:

$$u_{am} = h\nu\phi_\infty, \tag{4.126}$$

and the average energy density of an electric field with amplitude E is given by[285]

$$u = \tfrac{1}{2}\epsilon_0 E^2 . \tag{4.127}$$

Now, we can combine (4.125), (4.126), and (4.127) to relate the photon number density in the active medium to the electric field strength E_0 at the beam waist:

$$E_0 = \left(\frac{L_{am}}{w_0}\right)\sqrt{\frac{2h\nu\phi}{\epsilon_0}} . \tag{4.128}$$

The electric field at the beam waist will cause electrical breakdown of the air if E_0 equals the breakdown field at the beam waist given by Kroll and Watson in (4.40). We then solve for the pumping rate R_p such that $E_0 = E_{bd}$ or

$$\left(\frac{L_{am}}{w_0}\right)\sqrt{\frac{2h\nu\phi}{\epsilon_0}} = \sqrt{\frac{2}{c\,\epsilon_0}\left(1.44\times10^4\right)\left(p_R^2 + 2.4\times10^{-6}\,\nu^2\right)} . \tag{4.129}$$

We use the symbolic mathematics package Mathematica® to solve (4.129). The Mathematica notebooks (.nb files) for both the $4_{2,2} \rightarrow 5_{1,5}$ and $5_{3,2} \rightarrow 4_{4,1}$ transitions are provided in Appendix C. The results shown in Figure 4-14 and Figure 4-15.

We see that that in all cases, except for very nearly hemispherical clouds for which $g_2 = 1 - L/R_2 \approx 0$ and, therefore, the beam waist $w_0 \approx 0$ (the maser beam is focused to a point), the pumping rates required to achieve electrical breakdown of air at the beam waist are on the order of 10^5 to 10^7.

---

[285] David J. Griffiths, *Introduction to Electrodynamics*, 3rd Edition. Upper Saddle River: Prentice-Hall, 1999, p. 381.

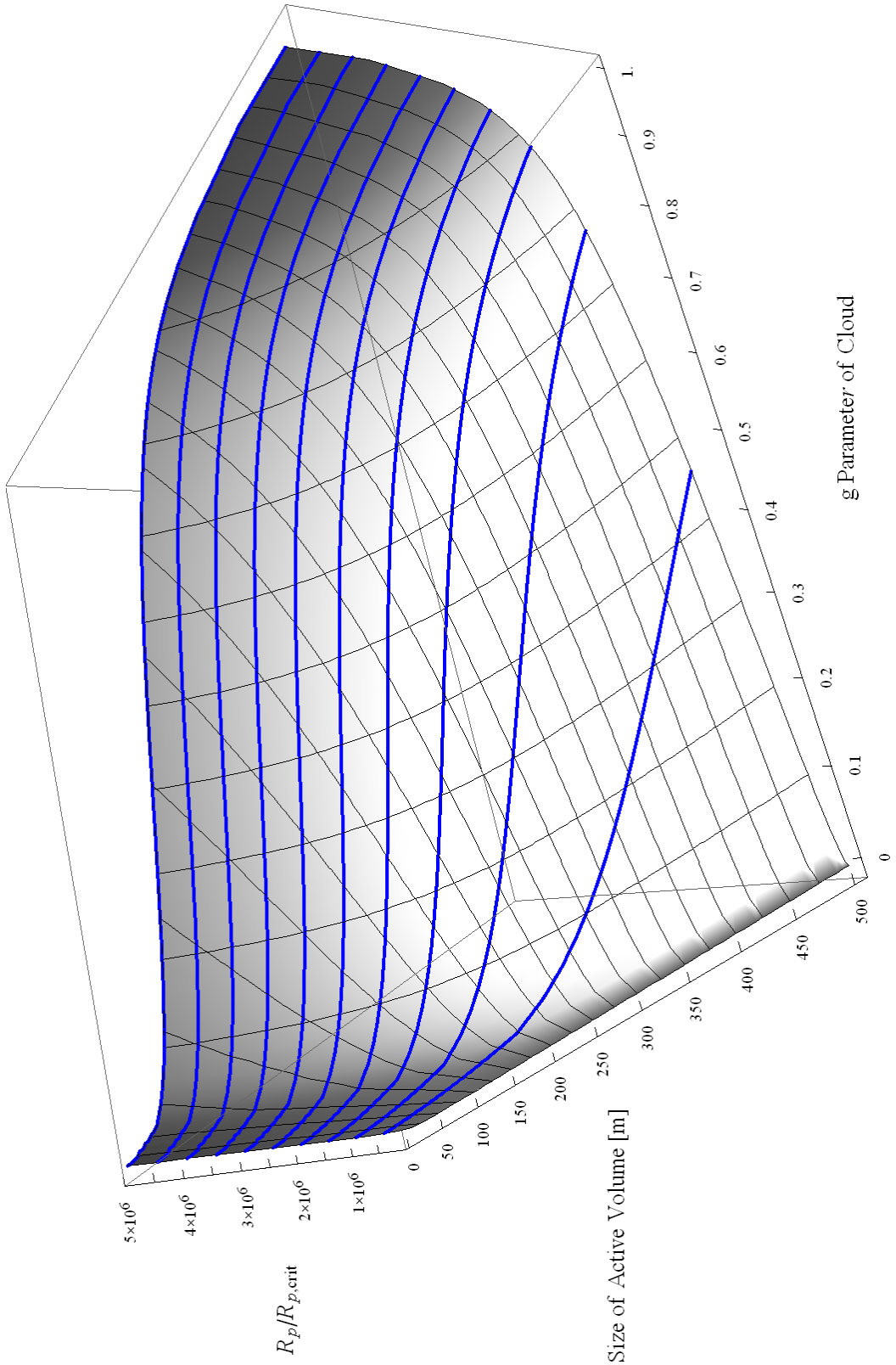

Figure 4-14: Pumping Ratio to Achieve Electrical Breakdown of Air ($5_{32} \rightarrow 4_{41}$, L = 1000 m, ρ_{cloud} = 0.86)

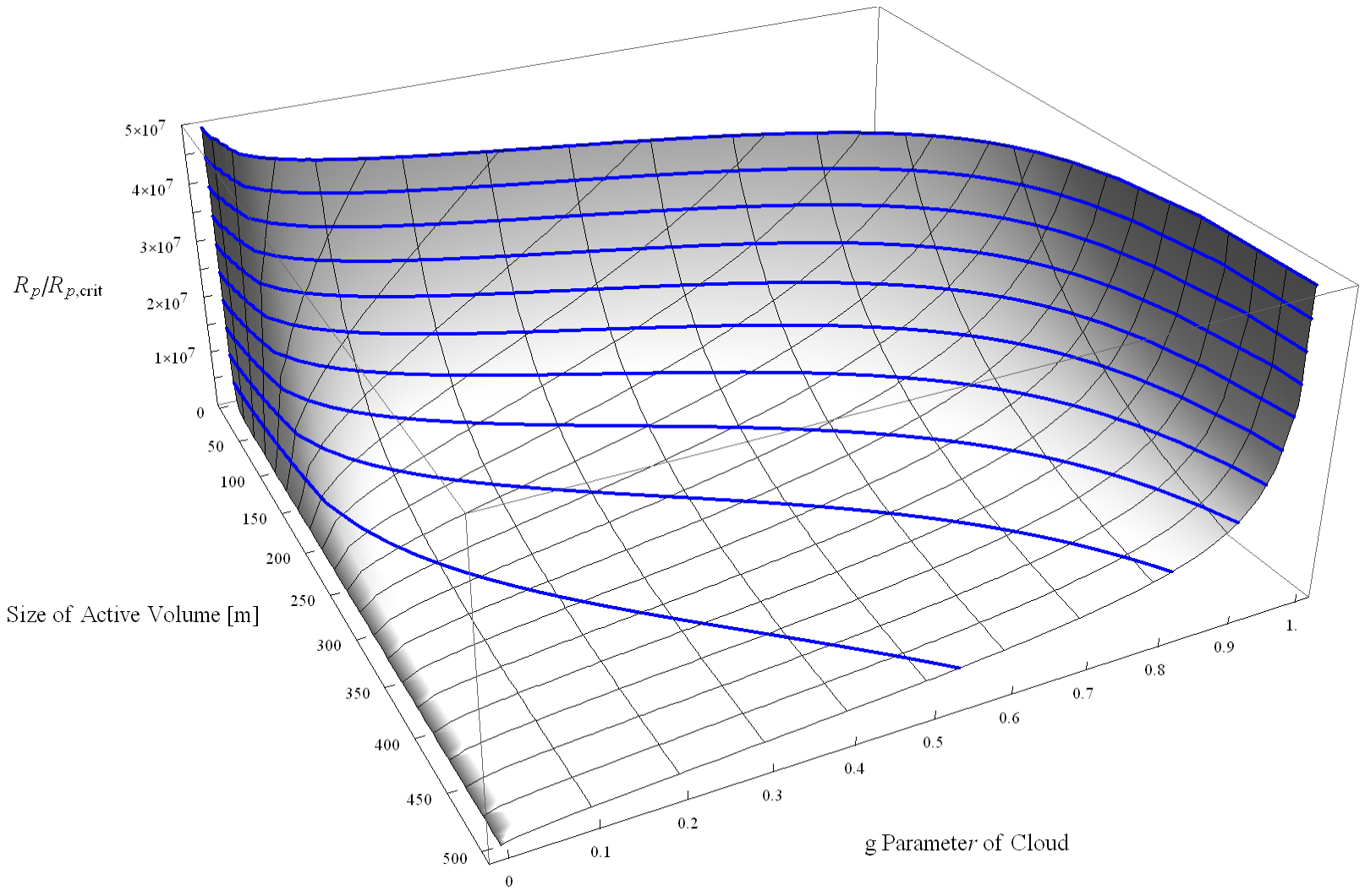

Figure 4-15: Pumping Ratio to Achieve Electrical Breakdown of Air
($4_{22} \rightarrow 5_{15}$, L = 1000 m, ρ_{cloud} = 0.86)

5. CONCLUSIONS AND RECOMMENDATIONS FOR FUTURE WORK

This dissertation developed details of Handel's Maser-Soliton Theory of ball lightning. The atmosphere between a thundercloud and the Earth's surface was modeled as an idealized stable open resonator with water vapor as the active medium and the thundercloud and Earth's surface as reflecting surfaces. The stable resonator generates a maser beam that narrows to the beam waist at the Earth's surface, which is assumed to be planar.

Two candidate rotational transitions were identified within the $\nu_1\nu_2\nu_3 = 010$ vibrational band of water having wavelengths of 13.9 cm and 1.12 cm, and relevant spectroscopic parameters were retrieved from the HITRAN 2008 molecular spectroscopic database.

The maser was modeled as a continuously pumped four-level maser that includes the effects of nonradiative relaxation due to molecular collisions and of microwave absorption in atmospheric oxygen. Maser spiking was shown to be highly unlikely to occur due to the high rate of collisional relaxation at normal atmospheric pressure, so that the electrical breakdown of air must be achieved by the steady state output of the atmospheric maser.

A parametric analysis was performed to relate the size of the atmospheric maser to the pumping rate needed to create a steady state population inversion sufficient to generate maser radiation intense enough at the beam waist to result in the electrical breakdown of air.

The analysis suggests that electric field intensities at the beam waist sufficient to cause electrical breakdown of air could only be created through huge pumping rates ($\sim 10^5$

to 10^7 times the critical pumping rate) and only for the most highly curved clouds ($g \approx 0$) that give the narrowest beam waists.

Experimental programs for the investigation of Handel's Maser Soliton Theory of Ball Lightning have been proposed.[286] Further work is recommended in the following areas:

- Identification of candidate transitions. Currently identified transitions give rise to an atmospheric maser only for huge pumping levels due to the high rate of collisional relaxation at normal atmospheric pressure. A search for candidate transitions should be undertaken to identify transitions more resistant to collisional relaxation.
- Study of maser operating modes other than steady state continuous wave operation. Other modes of operation include gain-switching in which a large initial population inversion is created, but not continuously replensished, and Q-switching in which the configuration of the maser cavity changes such that a population inversion initially below the critical value exceeds the critical value for the cavity after the change.
- Study of optical pumping by lightning. The population inversion was assumed here to be created by a strong electric field pulse due to a lightning strike. The details of this pumping mechanism need further investigation. Calculations of the time-dependent response of rotating dipoles, in general, and the water molecule,

---

[286] Peter H. Handel and Glenn A. Carlson, "Rise Time of Maser-Caviton Ball Lightning Energy Spikes," Proceedings Ninth International Symposium on Ball Lightning, ISBL-06, 16-19 August 2006, Eindhoven, The Netherlands, Ed. G. C. Dijkhuis.; Peter H. Handel, unpublished.proposal.

in particular, while lengthy, are feasible. Such calculations would establish useful information on the boundaries of the feasibility of pulsed electric fields creating population inversions in water molecules.

- Large-scale experiments. The maser-soliton theory of ball lightning necessarily involves large volumes of open air. Small bench scale experiments are inadequate to demonstrate or refute the theory. Outdoor experiments or experiments within very large enclosures (e.g., within large aircraft hangars) are necessary and recommended.

APPENDIX A: Water Lines Data from HITRAN Molecular Spectroscopic Database

(Excerpts for transitions with wavenumber < 100 cm^{-1})

Definitions and units associated with the HITRAN database

Variable	Definition	Units	Comments
ν	Transition wavenumber	cm^{-1}	Line position in vacuum
S	Intensity	cm^{-1} /(molecule cm^{-2})	At 296 K
A	Einstein A-coefficient	s^{-1}	
γ_{air}	Air-broadened half-width	cm^{-1} atm^{-1}	HWHM at 296 K
γ_{self}	Self-broadened half-width	cm^{-1} atm^{-1}	HWHM at 296 K
E''	Lower-state energy	cm^{-1}	Referenced to zero for lowest possible level
n_{air}	Temperature-dependence exponent for γ_{air}	Unitless	$\gamma_{air}(T) = \gamma_{air}(T_0)(T/T_0)^{n_{air}}$, $T_0 = 296$ K
δ_{air}	Air pressure-induced shift	cm^{-1} atm^{-1}	At 296 K
v', v''	Upper- and lower-state ‘‘global’’ quanta	Unitless	$v = v_1 v_2 v_3$
q', q''	Upper- and lower-state ‘‘local’’ quanta	Unitless	$q \equiv J\ K_{-1}K_1 \equiv J_{K_{-1},K_1}$
g', g''	Upper- and lower-state statistical weights	Unitless	Includes state-independent factors in HITRAN

ν	S	A	γ_{air}	γ_{self}	E''	n_{air}	δ_{air}	v'	v''	q'	q''	g'	g''
0.072059	2.043E-30	5.088E-12	0.0919	0.429	1922.8291	0.71	0.00370	0 1 0	0 1 0	4 2 2	5 1 5	9	11
0.400572	2.352E-28	1.009E-09	0.0869	0.466	1907.6158	0.71	-0.00310	0 1 0	0 1 0	4 2 3	3 3 0	27	21
0.741691	4.394E-25	1.991E-09	0.0900	0.385	446.5107	0.77	-0.00103	0 0 0	0 0 0	6 1 6	5 2 3	39	33
0.895092	3.600E-28	8.314E-09	0.0801	0.439	2129.5991	0.81	-0.00030	0 1 0	0 1 0	5 3 2	4 4 1	33	27
2.261694	1.233E-26	1.953E-07	0.0951	0.466	1819.3351	0.76	-0.00290	0 1 0	0 1 0	4 1 4	3 2 1	27	21
3.210930	1.532E-27	4.608E-07	0.0774	0.429	2126.4077	0.66	0.00150	0 1 0	0 1 0	4 4 0	5 3 3	9	11
4.002621	1.429E-26	1.473E-06	0.0983	0.466	1739.4836	0.73	0.00560	0 1 0	0 1 0	2 2 0	3 1 3	5	7
4.656998	1.168E-28	5.455E-07	0.0399	0.253	3080.1790	0.21	0.01345	0 0 0	0 0 0	14 6 9	15 3 12	87	93
6.114567	7.785E-23	3.631E-06	0.0998	0.525	136.1639	0.78	-0.00301	0 0 0	0 0 0	3 1 3	2 2 0	7	5
6.975432	1.657E-27	3.366E-06	0.0690	0.423	2399.1655	0.67	-0.00550	0 1 0	0 1 0	5 5 1	6 4 2	11	13
7.761580	6.153E-27	4.627E-06	0.0671	0.423	2398.3816	0.61	-0.00460	0 1 0	0 1 0	5 5 0	6 4 3	33	39
8.253712	2.674E-28	2.442E-06	0.0546	0.300	2872.5808	0.39	-0.00519	0 0 0	0 0 0	14 4 10	15 3 13	29	31
8.671100	5.941E-28	3.208E-06	0.0446	0.268	2739.4287	0.23	0.01506	0 0 0	0 0 0	13 6 8	14 3 11	27	29
8.769334	6.965E-29	3.973E-06	0.0470	0.328	3101.1423	0.53	-0.01030	0 1 0	0 1 0	7 7 1	8 6 2	15	17
8.787797	2.098E-28	3.998E-06	0.0460	0.328	3101.1238	0.53	-0.01020	0 1 0	0 1 0	7 7 0	8 6 3	45	51
9.795577	1.782E-27	7.007E-06	0.0603	0.384	2724.1672	0.57	-0.00720	0 1 0	0 1 0	6 6 1	7 5 2	39	45
9.921489	6.094E-28	7.279E-06	0.0563	0.384	2724.0415	0.56	-0.00930	0 1 0	0 1 0	6 6 0	7 5 3	13	15
10.714931	2.528E-24	6.118E-06	0.0683	0.296	1282.9192	0.70	-0.01900	0 0 0	0 0 0	10 2 9	9 3 6	63	57
10.845940	9.105E-23	1.161E-05	0.0932	0.507	315.7795	0.76	-0.00200	0 0 0	0 0 0	5 1 5	4 2 2	11	9
11.045233	1.594E-28	3.217E-05	0.0937	0.439	3381.7041	0.72	0.00620	0 2 0	0 2 0	3 2 1	4 1 4	21	27
11.215351	5.400E-26	1.050E-05	0.0894	0.423	2042.7534	0.72	0.00200	0 1 0	0 1 0	5 2 3	6 1 6	33	39
12.682023	8.304E-22	3.062E-05	0.0961	0.637	212.1564	0.76	-0.00308	0 0 0	0 0 0	4 1 4	3 2 1	27	21
13.013490	2.854E-25	8.213E-06	0.0678	0.382	1525.1361	0.61	-0.00037	0 0 0	0 0 0	10 3 7	11 2 10	21	23
13.439649	1.047E-28	7.306E-05	0.0876	0.429	3722.7310	0.73	0.00370	0 2 0	0 2 0	6 2 5	5 3 2	39	33
14.199487	4.010E-27	4.263E-05	0.0504	0.384	2905.4336	0.44	0.00080	0 1 0	0 1 0	8 5 4	7 6 1	51	45
.588315	4.817E-24	2.117E-05	0.0580	0.264	1045.0583	0.62	0.00516	0 0 0	0 0 0	7 5 3	6 6 0	15	13

ν	S	A	γ_{air}	γ_{self}	E''	n_{air}	δ_{air}	v'	v''	q'	q''	g'	g''
14.634232	1.874E-28	3.872E-05	0.0406	0.328	3306.2957	0.45	0.00120	0 1 0	0 1 0	9 6 4	8 7 1	19	17
14.648500	7.145E-23	2.782E-05	0.0668	0.329	742.0763	0.65	0.00320	0 0 0	0 0 0	6 4 3	5 5 0	39	33
14.701423	1.432E-27	4.735E-05	0.0535	0.384	2905.4307	0.46	0.00120	0 1 0	0 1 0	8 5 3	7 6 2	17	15
14.718126	5.688E-28	3.941E-05	0.0406	0.328	3306.2952	0.45	0.00140	0 1 0	0 1 0	9 6 3	8 7 2	57	51
14.777502	1.483E-23	2.202E-05	0.0585	0.270	1045.0580	0.62	0.00545	0 0 0	0 0 0	7 5 2	6 6 1	45	39
14.943711	8.679E-22	5.413E-05	0.0871	0.467	285.4186	0.71	-0.00275	0 0 0	0 0 0	4 2 3	3 3 0	27	21
15.449727	1.317E-25	6.772E-05	0.0908	0.466	1907.4514	0.81	-0.00190	0 1 0	0 1 0	4 2 2	3 3 1	9	7
15.707169	2.740E-23	3.440E-05	0.0692	0.346	742.0731	0.69	0.00327	0 0 0	0 0 0	6 4 2	5 5 1	13	11
15.833930	1.094E-22	4.764E-05	0.0764	0.396	488.1342	0.70	0.00025	0 0 0	0 0 0	5 3 3	4 4 0	11	9
16.294303	2.216E-23	1.357E-05	0.0854	0.487	586.4792	0.76	0.00056	0 0 0	0 0 0	6 2 4	7 1 7	13	15
16.628261	1.107E-26	8.494E-05	0.0596	0.423	2552.8799	0.49	-0.00120	0 1 0	0 1 0	7 4 4	6 5 1	15	13
16.797230	3.171E-24	2.598E-05	0.0507	0.204	1394.8143	0.62	0.00544	0 0 0	0 0 0	8 6 3	7 7 0	51	45
16.827724	1.061E-24	2.612E-05	0.0508	0.206	1394.8142	0.62	0.00553	0 0 0	0 0 0	8 6 2	7 7 1	17	15
17.219532	1.309E-28	1.180E-04	0.0983	0.466	3299.9910	0.73	0.00560	0 2 0	0 2 0	2 2 0	3 1 3	5	7
17.488526	1.886E-28	2.962E-03	0.1035	0.468	3779.4932	0.77	0.00680	0 0 1	0 0 1	1 1 0	1 0 1	3	3
17.690312	2.227E-26	2.864E-05	0.0594	0.335	2533.7932	0.44	0.00183	0 0 0	0 0 0	14 3 12	13 4 9	87	81
18.037596	9.611E-28	3.211E-03	0.1035	0.468	3680.4536	0.77	0.00680	1 0 0	1 0 0	1 1 0	1 0 1	9	9
18.235622	2.002E-25	1.615E-04	0.0834	0.439	2005.9171	0.71	-0.00290	0 1 0	0 1 0	5 2 4	4 3 1	11	9
18.295144	9.395E-29	6.457E-05	0.0348	0.301	3752.4163	0.47	-0.00030	0 1 0	0 1 0	10 7 4	9 8 1	63	57
18.481764	9.293E-28	2.323E-04	0.0949	0.464	3316.1450	0.79	0.00200	0 2 0	0 2 0	3 1 2	2 2 1	21	15
18.574102	2.159E-28	1.215E-04	0.0865	0.439	3482.0645	0.67	0.00440	0 2 0	0 2 0	3 3 0	4 2 3	21	27
18.577385	5.285E-20	3.477E-03	0.1039	0.486	23.7944	0.77	0.00654	0 0 0	0 0 0	1 1 0	1 0 1	9	9
19.077007	3.046E-26	2.756E-05	0.0508	0.297	2414.7234	0.31	0.01519	0 0 0	0 0 0	12 6 7	13 3 10	75	81
19.281910	4.472E-26	1.335E-04	0.0634	0.423	2552.8574	0.63	0.00260	0 1 0	0 1 0	7 4 3	6 5 2	45	39
19.736723	5.557E-28	2.537E-05	0.0491	0.282	3244.6008	0.27	0.01532	0 0 0	0 0 0	14 7 8	15 4 11	87	93
19.803988	6.399E-27	8.251E-05	0.0800	0.328	2670.7898	0.78	-0.00250	0 1 0	0 1 0	9 2 8	8 3 5	19	17

ν	S	A	γ_{air}	γ_{self}	E''	n_{air}	δ_{air}	v'	v''	q'	q''	g'	g''
19.849710	2.215E-25	1.820E-04	0.0729	0.429	2251.8625	0.58	-0.00410	0 1 0	0 1 0	6 3 4	5 4 1	39	33
20.704358	5.694E-22	1.093E-04	0.0803	0.419	488.1077	0.81	-0.00078	0 0 0	0 0 0	5 3 2	4 4 1	33	27
21.540438	2.352E-25	4.558E-05	0.0456	0.171	1789.0428	0.62	0.00533	0 0 0	0 0 0	9 7 3	8 8 0	19	17
21.545092	7.059E-25	4.561E-05	0.0456	0.171	1789.0428	0.62	0.00535	0 0 0	0 0 0	9 7 2	8 8 1	57	51
21.948720	3.027E-23	5.515E-03	0.1035	0.468	1618.5571	0.77	0.00680	0 1 0	0 1 0	1 1 0	1 0 1	9	9
24.172303	1.154E-27	6.358E-03	0.0976	0.464	3825.2131	0.79	0.00850	0 0 1	0 0 1	2 1 1	2 0 2	15	15
24.522496	6.415E-28	6.645E-03	0.0976	0.464	3725.9419	0.79	0.00850	1 0 0	1 0 0	2 1 1	2 0 2	5	5
25.063676	1.742E-28	1.531E-04	0.0894	0.423	3601.8586	0.72	0.00200	0 2 0	0 2 0	5 2 3	6 1 6	33	39
25.085124	3.483E-20	7.083E-03	0.1022	0.463	70.0908	0.79	0.00500	0 0 0	0 0 0	2 1 1	2 0 2	5	5
25.577525	1.635E-25	7.211E-05	0.0494	0.302	1960.2075	0.33	0.01243	0 0 0	0 0 0	11 5 7	12 2 10	23	25
25.846413	5.787E-28	8.595E-05	0.0655	0.260	3136.4126	0.61	0.00160	0 1 0	0 1 0	10 3 7	11 2 10	21	23
25.867995	2.808E-27	2.343E-03	0.1004	0.468	3196.0933	0.79	-0.00020	0 2 0	0 2 0	2 0 2	1 1 1	5	3
26.472072	2.106E-26	9.050E-03	0.1035	0.468	3175.4414	0.77	0.00680	0 2 0	0 2 0	1 1 0	1 0 1	9	9
28.054466	1.821E-24	8.727E-05	0.0550	0.333	1690.6644	0.39	0.01291	0 0 0	0 0 0	10 5 6	11 2 9	63	69
28.488075	1.612E-25	9.852E-05	0.0445	0.300	2246.8850	0.27	0.01042	0 0 0	0 0 0	12 5 8	13 2 11	75	81
28.685368	1.912E-23	1.044E-02	0.1024	0.464	1664.9646	0.72	0.00570	0 1 0	0 1 0	2 1 1	2 0 2	5	5
28.814601	1.408E-25	9.344E-05	0.0417	0.152	2225.4692	0.61	0.00425	0 0 0	0 0 0	10 8 3	9 9 0	63	57
28.815294	4.694E-26	9.346E-05	0.0417	0.152	2225.4692	0.61	0.00425	0 0 0	0 0 0	10 8 2	9 9 1	21	19
29.056415	8.368E-28	8.441E-04	0.0887	0.439	3597.8660	0.81	0.00040	0 2 0	0 2 0	5 2 3	4 3 2	33	27
29.997525	8.265E-24	4.090E-03	0.1004	0.468	1634.9670	0.79	-0.00020	0 1 0	0 1 0	2 0 2	1 1 1	5	3
30.100724	4.144E-26	1.126E-04	0.0829	0.384	2181.0898	0.76	0.00180	0 1 0	0 1 0	6 2 4	7 1 7	13	15
30.107865	5.786E-24	1.153E-03	0.0949	0.464	1742.3055	0.79	0.00200	0 1 0	0 1 0	3 1 2	2 2 1	21	15
30.227777	2.855E-23	2.184E-04	0.0792	0.416	1050.1577	0.78	-0.00250	0 0 0	0 0 0	9 2 8	8 3 5	19	17
30.560189	1.433E-21	5.686E-04	0.0894	0.470	285.2193	0.81	-0.00177	0 0 0	0 0 0	4 2 2	3 3 1	9	7
30.791725	1.165E-24	8.451E-04	0.0876	0.429	2130.4944	0.73	0.00370	0 1 0	0 1 0	6 2 5	5 3 2	39	33
30.894277	1.848E-25	7.275E-04	0.0812	0.429	2251.6953	0.80	0.00030	0 1 0	0 1 0	6 3 3	5 4 2	13	11

ν	S	A	γ_{air}	γ_{self}	E''	n_{air}	δ_{air}	v'	v''	q'	q''	g'	g''
32.290571	1.915E-25	5.624E-04	0.0799	0.384	2462.8752	0.80	-0.00240	0 1 0	0 1 0	8 2 7	7 3 4	51	45
32.366233	1.609E-21	8.973E-04	0.0844	0.458	383.8425	0.71	-0.00372	0 0 0	0 0 0	5 2 4	4 3 1	11	9
32.648432	4.849E-28	5.817E-03	0.1004	0.468	3693.2935	0.79	-0.00020	1 0 0	1 0 0	2 0 2	1 1 1	5	3
32.953690	2.532E-20	5.872E-03	0.1006	0.495	37.1371	0.79	-0.00190	0 0 0	0 0 0	2 0 2	1 1 1	5	3
33.384874	1.269E-26	1.578E-02	0.0976	0.464	3221.9612	0.79	0.00850	0 2 0	0 2 0	2 1 1	2 0 2	5	5
33.387973	2.121E-27	1.346E-04	0.0477	0.237	3211.2129	0.32	-0.00672	0 0 0	0 0 0	15 4 11	16 3 14	93	99
33.512176	9.775E-28	6.487E-03	0.1004	0.468	3791.7009	0.79	-0.00020	0 0 1	0 0 1	2 0 2	1 1 1	15	9
35.647259	1.911E-26	1.809E-04	0.0406	0.256	2550.8826	0.24	0.00886	0 0 0	0 0 0	13 5 9	14 2 12	27	29
35.772292	1.695E-27	1.691E-02	0.1011	0.444	3755.9287	0.81	0.00440	0 0 1	0 0 1	1 1 1	0 0 0	9	3
35.950288	2.397E-25	1.119E-03	0.0828	0.423	2282.5896	0.77	-0.00170	0 1 0	0 1 0	7 2 6	6 3 3	15	13
36.020583	3.068E-27	1.570E-02	0.0962	0.466	3791.3721	0.80	0.00510	1 0 0	1 0 0	3 1 2	3 0 3	21	21
36.032888	6.208E-28	1.546E-02	0.0962	0.466	3890.8293	0.80	0.00510	0 0 1	0 0 1	3 1 2	3 0 3	7	7
36.055643	6.425E-28	1.908E-02	0.0939	0.466	3926.8623	0.80	0.00410	0 0 1	0 0 1	3 2 1	3 1 2	7	7
36.240477	9.255E-28	1.737E-02	0.1011	0.444	3657.0530	0.81	0.00440	1 0 0	1 0 0	1 1 1	0 0 0	3	1
36.604150	1.645E-19	1.652E-02	0.1046	0.546	136.7617	0.80	0.00333	0 0 0	0 0 0	3 1 2	3 0 3	21	21
36.729767	1.016E-25	1.341E-04	0.0585	0.343	2105.8679	0.44	0.01336	0 0 0	0 0 0	11 6 6	12 3 9	23	25
37.012219	2.506E-24	1.571E-04	0.0615	0.364	1437.9688	0.48	0.01172	0 0 0	0 0 0	9 5 5	10 2 8	19	21
37.137125	5.042E-20	1.852E-02	0.0895	0.500	0.0000	0.81	0.00431	0 0 0	0 0 0	1 1 1	0 0 0	3	1
37.321736	2.384E-28	1.759E-03	0.0811	0.423	4015.5151	0.77	0.00160	0 2 0	0 2 0	7 3 4	6 4 3	45	39
37.371073	3.278E-27	2.080E-02	0.0939	0.466	3827.3926	0.80	0.00410	1 0 0	1 0 0	3 2 1	3 1 2	21	21
37.728850	1.541E-27	1.539E-02	0.0972	0.464	3849.3855	0.77	0.00380	0 0 1	0 0 1	2 2 0	2 1 1	15	15
38.077573	2.206E-27	1.104E-03	0.0406	0.301	3526.6274	0.34	-0.00030	0 1 0	0 1 0	10 6 5	9 7 2	63	57
38.247168	1.135E-22	1.068E-04	0.0792	0.455	744.1627	0.70	-0.00036	0 0 0	0 0 0	7 2 5	8 1 8	45	51
38.318561	1.855E-27	2.492E-02	0.0933	0.439	4027.8040	0.83	0.00560	0 0 1	0 0 1	4 2 2	4 1 3	27	27
38.333629	6.255E-27	1.321E-03	0.0479	0.328	3101.1423	0.36	-0.00070	0 1 0	0 1 0	9 5 5	8 6 2	19	17
38.378671	7.469E-28	1.131E-03	0.0404	0.301	3526.6250	0.34	0.00020	0 1 0	0 1 0	10 6 4	9 7 3	21	19

ν	S	A	γ_{air}	γ_{self}	E''	n_{air}	δ_{air}	v'	v''	q'	q''	g'	g''
38.464169	2.543E-20	2.671E-03	0.0970	0.538	134.9016	0.79	-0.00145	0 0 0	0 0 0	3 1 2	2 2 1	21	15
38.472291	1.707E-24	1.580E-04	0.0625	0.341	1774.7512	0.55	-0.00402	0 0 0	0 0 0	11 3 8	12 2 11	69	75
38.532352	7.781E-27	1.961E-04	0.0385	0.129	2701.8884	0.58	0.00315	0 0 0	0 0 0	11 9 3	10 10 0	23	21
38.532455	2.334E-26	1.961E-04	0.0385	0.129	2701.8884	0.58	0.00315	0 0 0	0 0 0	11 9 2	10 10 1	69	63
38.637531	2.440E-21	1.398E-03	0.0727	0.412	610.3412	0.58	-0.00246	0 0 0	0 0 0	6 3 4	5 4 1	39	33
38.698365	5.097E-28	2.783E-03	0.0949	0.464	3788.6943	0.79	0.00200	1 0 0	1 0 0	3 1 2	2 2 1	21	15
38.756501	9.913E-28	2.488E-02	0.0933	0.439	3927.8027	0.83	0.00560	1 0 0	1 0 0	4 2 2	4 1 3	9	9
38.790556	1.793E-19	2.291E-02	0.0996	0.502	173.3658	0.80	0.00314	0 0 0	0 0 0	3 2 1	3 1 2	21	21
38.972245	1.107E-22	9.308E-04	0.0504	0.282	1216.1946	0.44	0.00237	0 0 0	0 0 0	8 5 4	7 6 1	51	45
39.111258	1.995E-22	1.165E-03	0.0628	0.304	888.6327	0.49	0.00070	0 0 0	0 0 0	7 4 4	6 5 1	15	13
39.504874	8.814E-28	1.717E-02	0.0972	0.464	3750.4646	0.77	0.00380	1 0 0	1 0 0	2 2 0	2 1 1	5	5
39.721778	3.832E-23	9.869E-04	0.0554	0.295	1216.1898	0.46	0.00325	0 0 0	0 0 0	8 5 3	7 6 2	17	15
39.922262	2.035E-26	1.498E-03	0.0502	0.328	3101.1238	0.41	0.00200	0 1 0	0 1 0	9 5 4	8 6 3	57	51
40.220788	2.429E-23	2.263E-02	0.1011	0.444	1594.7462	0.81	0.00440	0 1 0	0 1 0	1 1 1	0 0 0	3	1
40.282490	5.585E-20	2.851E-02	0.0925	0.500	275.4970	0.83	0.00487	0 0 0	0 0 0	4 2 2	4 1 3	9	9
40.516781	8.720E-23	2.279E-02	0.0962	0.466	1731.8967	0.80	0.00510	0 1 0	0 1 0	3 1 2	3 0 3	21	21
40.530332	1.389E-25	1.859E-03	0.0574	0.384	2724.1672	0.41	-0.00240	0 1 0	0 1 0	8 4 5	7 5 2	51	45
40.554762	5.976E-24	8.698E-04	0.0465	0.236	1590.6908	0.45	0.00325	0 0 0	0 0 0	9 6 4	8 7 1	19	17
40.692949	1.805E-23	8.789E-04	0.0468	0.242	1590.6902	0.45	0.00341	0 0 0	0 0 0	9 6 3	8 7 2	57	51
40.788989	2.311E-25	2.182E-03	0.0716	0.423	2399.1655	0.55	-0.00560	0 1 0	0 1 0	7 3 5	6 4 2	15	13
40.895231	2.442E-28	1.190E-03	0.0325	0.282	3997.5083	0.36	-0.00070	0 1 0	0 1 0	11 7 4	10 8 3	69	63
40.987981	4.835E-20	1.885E-02	0.1009	0.497	95.1759	0.77	0.00151	0 0 0	0 0 0	2 2 0	2 1 1	5	5
42.411751	2.534E-25	5.416E-04	0.0647	0.396	2205.6528	0.52	-0.00321	0 0 0	0 0 0	13 3 11	12 4 8	27	25
42.638365	7.142E-22	1.528E-03	0.0693	0.769	888.5988	0.63	0.00203	0 0 0	0 0 0	7 4 3	6 5 2	45	39
43.243627	6.896E-22	1.056E-03	0.0813	0.445	842.3566	0.80	-0.00169	0 0 0	0 0 0	8 2 7	7 3 4	51	45
43.628963	5.236E-23	2.559E-04	0.0623	0.355	1079.0796	0.52	0.00856	0 0 0	0 0 0	8 4 5	9 1 8	51	57

ν	S	A	γ_{air}	γ_{self}	E''	n_{air}	δ_{air}	v'	v''	q'	q''	g'	g''
44.099344	5.696E-21	2.304E-03	0.0826	0.475	508.8121	0.73	-0.00289	0 0 0	0 0 0	6 2 5	5 3 2	39	33
44.463240	1.422E-26	2.861E-02	0.1011	0.444	3151.6301	0.81	0.00440	0 2 0	0 2 0	1 1 1	0 0 0	3	1
44.540102	2.631E-24	9.818E-04	0.0415	0.203	2009.8052	0.47	0.00277	0 0 0	0 0 0	10 7 4	9 8 1	63	57
44.563633	8.780E-25	9.835E-04	0.0415	0.204	2009.8051	0.48	0.00285	0 0 0	0 0 0	10 7 3	9 8 2	21	19
44.853568	3.814E-23	2.518E-04	0.0684	0.387	882.8904	0.56	0.00878	0 0 0	0 0 0	7 4 4	8 1 7	15	17
45.384176	5.547E-26	3.184E-02	0.0962	0.466	3289.2427	0.80	0.00510	0 2 0	0 2 0	3 1 2	3 0 3	21	21
45.970574	1.914E-26	3.544E-04	0.0369	0.228	2872.2744	0.23	0.00544	0 0 0	0 0 0	14 5 10	15 2 13	87	93
46.071708	5.443E-28	3.978E-02	0.0919	0.429	4149.8994	0.83	0.00690	0 0 1	0 0 1	5 2 3	5 1 4	11	11
46.240884	3.189E-27	1.997E-04	0.0559	0.337	2880.8345	0.36	0.01326	0 0 0	0 0 0	13 7 7	14 4 10	27	29
46.383900	2.673E-27	4.028E-02	0.0919	0.429	4049.5361	0.83	0.00690	1 0 0	1 0 0	5 2 3	5 1 4	33	33
46.921638	1.004E-22	3.756E-02	0.0939	0.466	1772.4135	0.80	0.00410	0 1 0	0 1 0	3 2 1	3 1 2	21	21
47.053149	1.420E-19	4.285E-02	0.0997	0.500	399.4575	0.83	0.00414	0 0 0	0 0 0	5 2 3	5 1 4	33	33
47.431396	3.034E-23	4.423E-02	0.0933	0.439	1875.4697	0.83	0.00560	0 1 0	0 1 0	4 2 2	4 1 3	9	9
47.648678	6.444E-26	3.091E-03	0.0673	0.384	2724.0415	0.66	0.00380	0 1 0	0 1 0	8 4 4	7 5 3	17	15
47.866740	7.954E-24	3.271E-04	0.0572	0.348	1293.0182	0.47	0.00839	0 0 0	0 0 0	9 4 6	10 1 9	19	21
48.059315	9.332E-22	2.268E-03	0.0820	0.454	661.5489	0.77	-0.00165	0 0 0	0 0 0	7 2 6	6 3 3	15	13
49.153021	6.016E-24	4.667E-03	0.0887	0.439	2004.8157	0.81	0.00040	0 1 0	0 1 0	5 2 3	4 3 2	33	27
49.836372	2.731E-23	3.129E-02	0.0972	0.464	1693.6499	0.77	0.00380	0 1 0	0 1 0	2 2 0	2 1 1	5	5
50.571326	3.128E-27	3.976E-04	0.0359	0.112	3216.1931	0.55	0.00420	0 0 0	0 0 0	12 10 3	11 11 0	75	69
50.571341	1.043E-27	3.977E-04	0.0359	0.112	3216.1931	0.55	0.00420	0 0 0	0 0 0	12 10 2	11 11 1	25	23
50.894815	4.081E-27	1.002E-02	0.0933	0.466	3387.6807	0.77	-0.00220	0 2 0	0 2 0	4 1 3	3 2 2	9	7
51.006290	1.150E-25	1.288E-03	0.0378	0.180	2471.2551	0.47	0.00146	0 0 0	0 0 0	11 8 4	10 9 1	23	21
51.010127	3.449E-25	1.287E-03	0.0378	0.180	2471.2551	0.47	0.00147	0 0 0	0 0 0	11 8 3	10 9 2	69	63
51.325430	5.835E-26	2.993E-02	0.0926	0.464	3237.9172	0.79	-0.00020	0 2 0	0 2 0	3 0 3	2 1 2	21	15
51.434485	1.527E-21	3.597E-03	0.0821	0.445	610.1145	0.80	-0.00100	0 0 0	0 0 0	6 3 3	5 4 2	13	11
52.161047	6.586E-28	2.613E-02	0.0953	0.464	3833.5767	0.79	0.00660	0 0 1	0 0 1	2 2 1	2 1 2	5	5

ν	S	A	γ_{air}	γ_{self}	E''	n_{air}	δ_{air}	v'	v''	q'	q''	g'	g''
52.181647	2.361E-28	2.480E-02	0.0885	0.429	4195.9707	0.83	0.00220	0 0 1	0 0 1	5 3 2	5 2 3	11	11
52.510729	2.281E-22	2.896E-04	0.0755	0.409	704.2141	0.64	0.00778	0 0 0	0 0 0	6 4 3	7 1 6	39	45
52.785684	1.310E-27	3.580E-02	0.0932	0.439	3875.0171	0.76	0.00410	1 0 0	1 0 0	4 1 3	4 0 4	9	9
53.105671	7.341E-23	6.091E-02	0.0919	0.429	2000.8632	0.83	0.00690	0 1 0	0 1 0	5 2 3	5 1 4	33	33
53.173048	2.395E-27	3.570E-02	0.0932	0.439	3974.6309	0.76	0.00410	0 0 1	0 0 1	4 1 3	4 0 4	27	27
53.245262	2.626E-23	2.910E-04	0.0685	0.379	1201.9216	0.58	0.00891	0 0 0	0 0 0	8 5 4	9 2 7	51	57
53.444280	6.938E-20	3.737E-02	0.0950	0.532	222.0528	0.76	0.00127	0 0 0	0 0 0	4 1 3	4 0 4	9	9
53.650041	2.714E-28	1.102E-03	0.0518	0.290	3758.3972	0.28	0.00188	0 0 0	0 0 0	17 4 14	16 5 11	35	33
53.797445	3.358E-27	2.846E-02	0.0953	0.464	3734.8970	0.79	0.00660	1 0 0	1 0 0	2 2 1	2 1 2	15	15
54.083530	1.653E-27	5.252E-02	0.1011	0.468	3779.4932	0.81	0.00630	0 0 1	0 0 1	2 1 2	1 0 1	5	3
54.443223	8.035E-27	5.298E-02	0.1011	0.468	3680.4536	0.81	0.00630	1 0 0	1 0 0	2 1 2	1 0 1	15	9
54.660115	1.706E-27	5.882E-04	0.0587	0.237	3386.3794	0.55	-0.00430	0 1 0	0 1 0	11 3 8	12 2 11	69	75
54.835280	1.465E-22	4.104E-02	0.0926	0.464	1677.0614	0.79	-0.00020	0 1 0	0 1 0	3 0 3	2 1 2	21	15
54.925704	1.271E-25	4.129E-04	0.0501	0.328	2337.6670	0.70	-0.00090	0 1 0	0 1 0	7 2 5	8 1 8	45	51
55.405255	1.830E-19	3.080E-02	0.0987	0.544	79.4964	0.79	0.00358	0 0 0	0 0 0	2 2 1	2 1 2	15	15
55.702029	4.349E-19	5.617E-02	0.1030	0.498	23.7944	0.81	0.00532	0 0 0	0 0 0	2 1 2	1 0 1	15	9
56.475227	7.747E-27	4.955E-02	0.0926	0.464	3734.8970	0.79	-0.00020	1 0 0	1 0 0	3 0 3	2 1 2	21	15
56.488084	1.055E-23	4.861E-04	0.0517	0.322	1524.8480	0.40	0.00693	0 0 0	0 0 0	10 4 7	11 1 10	63	69
56.510180	3.149E-28	5.678E-04	0.0406	0.200	3567.2551	0.26	-0.00705	0 0 0	0 0 0	16 4 12	17 3 15	33	35
56.553439	3.830E-27	2.611E-03	0.0699	0.260	3535.8706	0.65	-0.00640	0 1 0	0 1 0	12 3 10	11 4 7	75	69
57.168982	7.917E-22	2.534E-04	0.0887	0.467	325.3479	0.70	0.00593	0 0 0	0 0 0	4 3 2	5 0 5	27	33
57.252656	1.686E-27	5.307E-02	0.0926	0.464	3833.5767	0.79	-0.00020	0 0 1	0 0 1	3 0 3	2 1 2	7	5
57.265273	4.060E-19	5.067E-02	0.0979	0.554	79.4964	0.79	-0.00110	0 0 0	0 0 0	3 0 3	2 1 2	21	15
57.271513	2.166E-22	3.075E-04	0.0819	0.447	446.6966	0.65	0.00527	0 0 0	0 0 0	5 3 3	6 0 6	11	13
57.329393	8.042E-28	5.620E-02	0.0869	0.423	4350.6992	0.81	0.00230	0 0 1	0 0 1	6 3 3	6 2 4	39	39
57.364001	1.984E-26	7.137E-02	0.0933	0.439	3438.5754	0.83	0.00560	0 2 0	0 2 0	4 2 2	4 1 3	9	9

ν	S	A	γ_{air}	γ_{self}	E''	n_{air}	δ_{air}	v'	v''	q'	q''	g'	g''
58.018107	2.218E-27	5.382E-02	0.0885	0.429	4095.9199	0.83	0.00220	1 0 0	1 0 0	5 3 2	5 2 3	33	33
58.018537	3.602E-23	4.965E-02	0.0932	0.439	1817.4512	0.76	0.00410	0 1 0	0 1 0	4 1 3	4 0 4	9	9
58.053411	7.428E-25	7.086E-03	0.0697	0.384	2572.1392	0.58	-0.00560	0 1 0	0 1 0	8 3 6	7 4 3	51	45
58.122478	6.745E-26	6.368E-02	0.0939	0.466	3334.6270	0.80	0.00410	0 2 0	0 2 0	3 2 1	3 1 2	21	21
58.483903	1.872E-27	6.613E-04	0.0341	0.193	3211.0562	0.22	0.00321	0 0 0	0 0 0	15 5 11	16 2 14	31	33
58.504320	1.972E-22	6.262E-02	0.1011	0.468	1618.5571	0.81	0.00630	0 1 0	0 1 0	2 1 2	1 0 1	15	9
58.687026	5.136E-28	6.762E-02	0.0869	0.423	4249.5244	0.81	0.00230	1 0 0	1 0 0	6 3 3	6 2 4	13	13
58.775425	3.043E-20	8.040E-02	0.0888	0.487	602.7735	0.81	0.00241	0 0 0	0 0 0	6 3 3	6 2 4	13	13
58.914053	1.369E-21	6.677E-03	0.0708	0.402	757.7802	0.55	-0.00432	0 0 0	0 0 0	7 3 5	6 4 2	15	13
58.925831	9.439E-28	8.507E-02	0.0871	0.384	4426.0664	0.82	0.00650	1 0 0	1 0 0	7 3 4	7 2 5	45	45
59.262234	7.211E-28	7.197E-02	0.0894	0.423	4190.2622	0.77	0.00750	1 0 0	1 0 0	6 2 4	6 1 5	13	13
59.862385	3.937E-26	1.854E-03	0.0350	0.151	2972.8274	0.46	0.00146	0 0 0	0 0 0	12 9 4	11 10 1	75	69
59.862999	1.312E-26	1.854E-03	0.0350	0.151	2972.8274	0.46	0.00147	0 0 0	0 0 0	12 9 3	11 10 2	25	23
59.867711	3.706E-20	7.474E-02	0.0885	0.510	542.9058	0.77	0.00258	0 0 0	0 0 0	6 2 4	6 1 5	13	13
59.942258	1.321E-27	7.256E-02	0.0894	0.423	4290.7573	0.77	0.00750	0 0 1	0 0 1	6 2 4	6 1 5	39	39
59.946767	4.831E-20	9.029E-02	0.0894	0.498	782.4099	0.82	0.00361	0 0 0	0 0 0	7 3 4	7 2 5	45	45
60.340872	1.698E-27	4.555E-02	0.0879	0.439	4066.1226	0.82	0.00260	0 0 1	0 0 1	4 3 1	4 2 2	27	27
61.077728	3.008E-27	4.592E-02	0.0939	0.466	3895.5881	0.75	0.00640	0 0 1	0 0 1	3 2 2	3 1 3	21	21
61.467416	4.561E-26	8.969E-02	0.0919	0.429	3565.4551	0.83	0.00690	0 2 0	0 2 0	5 2 3	5 1 4	33	33
61.527410	8.324E-28	6.377E-03	0.0359	0.282	3770.7246	0.25	-0.00280	0 1 0	0 1 0	11 6 6	10 7 3	23	21
61.682163	1.442E-23	2.094E-02	0.0933	0.466	1813.7876	0.77	-0.00220	0 1 0	0 1 0	4 1 3	3 2 2	9	7
61.749582	1.718E-24	3.558E-04	0.0651	0.368	1813.2235	0.53	0.00979	0 0 0	0 0 0	10 6 5	11 3 8	63	69
61.815817	3.322E-28	4.227E-02	0.0843	0.429	4195.9707	0.78	0.00320	1 0 0	0 0 1	5 4 2	5 2 3	11	11
61.864285	1.847E-26	5.349E-02	0.0972	0.464	3255.3462	0.77	0.00380	0 2 0	0 2 0	2 2 0	2 1 1	5	5
62.252189	2.373E-26	7.559E-03	0.0434	0.301	3321.0132	0.27	-0.00120	0 1 0	0 1 0	10 5 6	9 6 3	63	57
62.301394	1.561E-19	8.123E-02	0.0891	0.461	446.5107	0.83	0.00050	0 0 0	0 0 0	5 3 2	5 2 3	33	33

ν	S	A	γ_{air}	γ_{self}	E''	n_{air}	δ_{air}	v'	v''	q'	q''	g'	g''
62.335797	1.690E-27	4.895E-02	0.0939	0.466	3796.5398	0.75	0.00640	1 0 0	1 0 0	3 2 2	3 1 3	7	7
62.433120	2.570E-27	6.673E-03	0.0372	0.282	3770.7114	0.24	-0.00120	0 1 0	0 1 0	11 6 5	10 7 4	69	63
62.475855	1.077E-25	7.130E-02	0.1011	0.468	3175.4414	0.81	0.00630	0 2 0	0 2 0	2 1 2	1 0 1	15	9
62.701709	3.188E-23	3.244E-04	0.0729	0.399	920.2101	0.68	-0.00184	0 0 0	0 0 0	8 2 6	9 1 9	17	19
62.735152	4.420E-22	3.869E-04	0.0748	0.441	586.2436	0.60	0.00405	0 0 0	0 0 0	6 3 4	7 0 7	39	45
62.842349	3.236E-28	1.043E-03	0.0425	0.237	3587.6670	0.33	0.01360	0 1 0	0 1 0	11 5 7	12 2 10	23	25
62.873096	1.083E-21	7.264E-03	0.0604	0.336	1059.8354	0.41	-0.00030	0 0 0	0 0 0	8 4 5	7 5 2	51	45
63.166581	1.962E-22	1.642E-04	0.0948	0.488	222.0528	0.75	0.00633	0 0 0	0 0 0	3 3 1	4 0 4	7	9
63.191039	5.858E-26	8.968E-03	0.0563	0.328	2920.1321	0.33	-0.00430	0 1 0	0 1 0	9 4 6	8 5 3	19	17
63.277327	2.229E-26	6.593E-02	0.0932	0.439	3375.2981	0.76	0.00410	0 2 0	0 2 0	4 1 3	4 0 4	9	9
63.338898	6.260E-23	6.284E-03	0.0514	0.301	1411.6420	0.36	0.00261	0 0 0	0 0 0	9 5 5	8 6 2	19	17
63.430813	2.786E-28	1.137E-03	0.0359	0.214	3877.0889	0.27	0.00870	0 1 0	0 1 0	12 5 8	13 2 11	75	81
63.493769	3.475E-25	5.703E-04	0.0551	0.298	2042.3741	0.46	-0.00590	0 0 0	0 0 0	12 3 9	13 2 12	25	27
63.498697	9.805E-24	2.672E-03	0.0708	0.396	1899.0083	0.65	-0.00534	0 0 0	0 0 0	12 3 10	11 4 7	75	69
63.993782	2.917E-20	1.147E-02	0.0886	0.458	382.5169	0.81	-0.00128	0 0 0	0 0 0	5 2 3	4 3 2	33	27
64.022941	9.125E-20	5.264E-02	0.0953	0.465	142.2785	0.75	0.00424	0 0 0	0 0 0	3 2 2	3 1 3	7	7
64.385069	2.625E-23	5.631E-03	0.0440	0.251	1810.5880	0.34	0.00214	0 0 0	0 0 0	10 6 5	9 7 2	63	57
64.493751	1.927E-24	1.009E-02	0.0811	0.423	2398.3816	0.77	0.00160	0 1 0	0 1 0	7 3 4	6 4 3	45	39
64.791872	3.381E-28	7.641E-04	0.0334	0.097	3766.3875	0.52	0.00532	0 0 0	0 0 0	13 11 2	12 12 1	81	75
64.878549	8.884E-24	5.767E-03	0.0451	0.265	1810.5834	0.34	0.00287	0 0 0	0 0 0	10 6 4	9 7 3	21	19
64.926902	1.825E-23	9.792E-02	0.0894	0.423	2146.2639	0.77	0.00750	0 1 0	0 1 0	6 2 4	6 1 5	13	13
65.081065	6.003E-28	1.210E-02	0.0887	0.439	4030.8389	0.81	0.00040	1 0 0	1 0 0	5 2 3	4 3 2	33	27
65.186465	1.316E-27	1.486E-02	0.0854	0.429	3719.4929	0.74	0.00120	0 2 0	0 2 0	6 2 4	5 3 3	13	11
65.244196	1.012E-22	4.837E-02	0.0983	0.464	1677.0614	0.74	0.00435	0 1 0	0 1 0	2 2 1	2 1 2	15	15
65.294285	1.349E-27	7.324E-02	0.0879	0.439	3966.5593	0.82	0.00260	1 0 0	1 0 0	4 3 1	4 2 2	9	9
65.685931	2.021E-22	7.050E-03	0.0561	0.317	1411.6115	0.41	0.00468	0 0 0	0 0 0	9 5 4	8 6 3	57	51

ν	S	A	γ_{air}	γ_{self}	E''	n_{air}	δ_{air}	v'	v''	q'	q''	g'	g''
66.470953	9.022E-27	9.292E-03	0.0496	0.301	3320.9297	0.41	0.00420	0 1 0	0 1 0	10 5 5	9 6 4	21	19
67.208651	1.082E-22	2.944E-04	0.0821	0.443	542.9058	0.72	0.00606	0 0 0	0 0 0	5 4 2	6 1 5	11	13
67.245953	8.094E-21	1.211E-01	0.0869	0.466	982.9118	0.79	0.00428	0 0 0	0 0 0	8 3 5	8 2 6	17	17
67.277860	2.937E-28	1.163E-01	0.0883	0.328	4725.0625	0.79	0.00950	0 0 1	0 0 1	8 3 5	8 2 6	51	51
67.388202	7.561E-28	5.378E-02	0.0870	0.466	3962.9177	0.80	0.00400	0 0 1	0 0 1	3 3 0	3 2 1	7	7
67.528607	1.054E-24	5.654E-03	0.0390	0.216	2254.2844	0.36	0.00158	0 0 0	0 0 0	11 7 5	10 8 2	23	21
67.621942	3.169E-24	5.676E-03	0.0392	0.220	2254.2837	0.36	0.00176	0 0 0	0 0 0	11 7 4	10 8 3	69	63
68.062986	7.353E-20	8.228E-02	0.0893	0.453	315.7795	0.82	0.00083	0 0 0	0 0 0	4 3 1	4 2 2	9	9
68.409775	3.281E-27	1.131E-03	0.0492	0.260	3314.8557	0.39	0.01310	0 1 0	0 1 0	10 5 6	11 2 9	63	69
68.413319	1.434E-24	7.586E-04	0.0466	0.292	1774.6165	0.34	0.00449	0 0 0	0 0 0	11 4 8	12 1 11	23	25
68.895124	6.831E-28	2.134E-02	0.0851	0.439	4066.1226	0.79	-0.00040	1 0 0	0 0 1	4 4 1	4 2 2	27	27
68.927344	9.936E-28	3.402E-02	0.0933	0.466	3858.8755	0.77	-0.00220	1 0 0	1 0 0	4 1 3	3 2 2	9	7
69.195617	4.994E-20	3.345E-02	0.0936	0.495	206.3014	0.77	-0.00346	0 0 0	0 0 0	4 1 3	3 2 2	9	7
69.531870	9.872E-27	7.054E-03	0.0728	0.282	3253.7380	0.72	-0.00620	0 1 0	0 1 0	11 3 9	10 4 6	23	21
69.553843	7.468E-28	2.231E-02	0.0895	0.429	4095.9199	0.73	0.00070	0 0 1	1 0 0	5 2 4	5 2 3	33	33
69.740662	1.411E-25	1.176E-02	0.0720	0.328	2771.6902	0.67	-0.00650	0 1 0	0 1 0	9 3 7	8 4 4	19	17
70.282732	2.444E-23	1.375E-01	0.0871	0.384	2392.5925	0.82	0.00650	0 1 0	0 1 0	7 3 4	7 2 5	45	45
70.375014	9.340E-27	1.192E-01	0.0989	0.464	3825.2131	0.79	0.00690	0 0 1	0 0 1	3 1 3	2 0 2	21	15
70.580891	3.908E-27	6.066E-02	0.0870	0.466	3864.7639	0.80	0.00400	1 0 0	1 0 0	3 3 0	3 2 1	21	21
70.597716	5.010E-27	1.189E-01	0.0989	0.464	3725.9419	0.79	0.00690	1 0 0	1 0 0	3 1 3	2 0 2	7	5
70.969602	1.280E-27	2.805E-03	0.0324	0.130	3512.4048	0.43	0.00228	0 0 0	0 0 0	13 10 4	12 11 1	27	25
70.969700	3.839E-27	2.805E-03	0.0324	0.130	3512.4048	0.43	0.00228	0 0 0	0 0 0	13 10 3	12 11 2	81	75
71.138168	2.040E-27	3.885E-02	0.0933	0.466	3956.6658	0.77	-0.00220	0 0 1	0 0 1	4 1 3	3 2 2	27	21
71.398987	1.605E-23	1.318E-01	0.0869	0.423	2211.1907	0.81	0.00230	0 1 0	0 1 0	6 3 3	6 2 4	13	13
71.596646	1.070E-26	1.305E-01	0.0894	0.423	3713.0828	0.77	0.00750	0 2 0	0 2 0	6 2 4	6 1 5	13	13
72.128919	4.836E-22	1.139E-02	0.0723	0.392	1059.6467	0.66	0.00234	0 0 0	0 0 0	8 4 4	7 5 3	17	15

ν	S	A	γ_{air}	γ_{self}	E''	n_{air}	δ_{air}	v'	v''	q'	q''	g'	g''
72.187672	2.689E-19	1.255E-01	0.0998	0.470	70.0908	0.79	0.00472	0 0 0	0 0 0	3 1 3	2 0 2	7	5
72.364133	1.427E-27	1.139E-03	0.0317	0.179	3567.1743	0.22	0.00240	0 0 0	0 0 0	16 5 12	17 2 15	99	105
72.630570	8.939E-23	5.189E-04	0.0681	0.390	744.0637	0.57	0.00329	0 0 0	0 0 0	7 3 5	8 0 8	15	17
72.790754	1.129E-27	7.323E-02	0.0869	0.439	3977.2615	0.66	0.00600	0 0 1	0 0 1	4 2 3	4 1 4	9	9
73.091333	3.318E-25	6.356E-03	0.0355	0.192	2740.4209	0.36	0.00054	0 0 0	0 0 0	12 8 5	11 9 2	75	69
73.107934	1.107E-25	6.364E-03	0.0355	0.192	2740.4209	0.36	0.00057	0 0 0	0 0 0	12 8 4	11 9 3	25	23
73.227979	4.086E-27	7.246E-02	0.0864	0.429	3976.3081	0.68	0.00100	1 0 0	1 0 0	5 1 4	5 0 5	33	33
73.262212	2.123E-19	6.702E-02	0.0884	0.481	212.1564	0.80	0.00197	0 0 0	0 0 0	3 3 0	3 2 1	21	21
73.403993	2.556E-27	6.492E-02	0.0864	0.466	3956.6658	0.72	0.00360	0 0 1	0 0 1	3 3 1	3 2 2	21	21
73.739790	5.597E-27	7.568E-02	0.0869	0.439	3877.5752	0.66	0.00600	1 0 0	1 0 0	4 2 3	4 1 4	27	27
73.755991	8.364E-28	7.290E-02	0.0864	0.429	4076.1433	0.68	0.00100	0 0 1	0 0 1	5 1 4	5 0 5	11	11
73.960041	1.426E-25	1.158E-02	0.0784	0.301	2998.7664	0.72	-0.00590	0 1 0	0 1 0	10 3 8	9 4 5	63	57
74.109615	2.155E-19	7.606E-02	0.0889	0.508	325.3479	0.68	-0.00003	0 0 0	0 0 0	5 1 4	5 0 5	33	33
74.303893	4.973E-23	8.022E-02	0.0939	0.466	1739.4836	0.75	0.00640	0 1 0	0 1 0	3 2 2	3 1 3	7	7
74.519119	1.169E-22	1.317E-01	0.0989	0.464	1664.9646	0.79	0.00690	0 1 0	0 1 0	3 1 3	2 0 2	7	5
74.878837	3.345E-21	1.470E-02	0.0708	0.405	931.2372	0.58	-0.00557	0 0 0	0 0 0	8 3 6	7 4 3	51	45
74.976740	3.848E-24	1.659E-01	0.0883	0.328	2595.8130	0.79	0.00950	0 1 0	0 1 0	8 3 5	8 2 6	17	17
75.096476	7.354E-28	7.048E-02	0.0835	0.439	4050.0522	0.64	0.00460	0 0 1	0 0 1	4 3 2	4 2 3	9	9
75.307084	4.836E-26	1.214E-01	0.0904	0.466	3299.9910	0.70	0.00050	0 2 0	0 2 0	4 0 4	3 1 3	9	7
75.523901	2.989E-19	8.088E-02	0.0895	0.504	224.8384	0.66	0.00437	0 0 0	0 0 0	4 2 3	4 1 4	27	27
76.335675	1.466E-27	7.270E-02	0.0864	0.466	3858.8755	0.72	0.00360	1 0 0	1 0 0	3 3 1	3 2 2	7	7
76.525608	8.370E-23	1.367E-01	0.0885	0.429	2053.9688	0.83	0.00220	0 1 0	0 1 0	5 3 2	5 2 3	33	33
76.617546	6.030E-26	1.392E-03	0.0568	0.301	2688.0801	0.52	0.00990	0 1 0	0 1 0	8 4 5	9 1 8	51	57
76.734946	2.026E-23	4.005E-04	0.0751	0.409	982.9118	0.67	0.00633	0 0 0	0 0 0	7 5 3	8 2 6	15	17
77.042242	6.679E-28	2.050E-02	0.0875	0.429	4076.8960	0.69	0.00500	1 0 0	0 0 1	5 3 2	5 1 5	33	33
77.316227	8.026E-21	1.811E-01	0.0837	0.439	1282.9192	0.69	0.00412	0 0 0	0 0 0	9 4 5	9 3 6	57	57

ν	S	A	γ_{air}	γ_{self}	E''	n_{air}	δ_{air}	v'	v''	q'	q''	g'	g''
77.651578	1.551E-27	1.318E-01	0.0796	0.384	4348.4150	0.64	0.00890	1 0 0	1 0 0	7 2 5	7 1 6	45	45
77.967519	1.132E-22	1.503E-01	0.0904	0.466	1739.4836	0.70	0.00050	0 1 0	0 1 0	4 0 4	3 1 3	9	7
78.029628	6.087E-26	1.401E-01	0.0989	0.464	3221.9612	0.79	0.00690	0 2 0	0 2 0	3 1 3	2 0 2	7	5
78.195775	7.810E-20	1.358E-01	0.0808	0.483	704.2141	0.64	0.00069	0 0 0	0 0 0	7 2 5	7 1 6	45	45
78.227843	6.706E-26	7.808E-02	0.0953	0.464	3237.9172	0.79	0.00660	0 2 0	0 2 0	2 2 1	2 1 2	15	15
78.303574	9.059E-22	1.947E-01	0.0836	0.471	1538.1497	0.71	0.00666	0 0 0	0 0 0	10 4 6	10 3 7	21	21
78.477457	5.695E-27	1.676E-01	0.0904	0.466	3796.5398	0.70	0.00050	1 0 0	1 0 0	4 0 4	3 1 3	9	7
78.615564	2.674E-23	7.714E-03	0.0738	0.402	1616.4531	0.72	-0.00522	0 0 0	0 0 0	11 3 9	10 4 6	23	21
78.706679	1.418E-26	4.574E-03	0.0565	0.315	3360.6003	0.34	-0.00396	0 0 0	0 0 0	16 4 13	15 5 10	99	93
78.830860	1.080E-27	5.237E-02	0.0795	0.429	4165.4736	0.58	0.00520	0 0 1	0 0 1	5 3 3	5 2 4	33	33
78.917917	7.905E-20	7.939E-02	0.0869	0.459	206.3014	0.72	0.00239	0 0 0	0 0 0	3 3 1	3 2 2	7	7
79.006604	6.895E-26	5.301E-04	0.0604	0.357	2533.7932	0.40	0.00878	0 0 0	0 0 0	12 7 6	13 4 9	75	81
79.042848	1.089E-26	1.744E-01	0.0904	0.466	3895.5881	0.70	0.00050	0 0 1	0 0 1	4 0 4	3 1 3	27	21
79.133356	2.836E-25	1.875E-02	0.0684	0.328	2919.6331	0.67	0.00470	0 1 0	0 1 0	9 4 5	8 5 4	57	51
79.153918	4.104E-26	1.280E-03	0.0641	0.328	2490.3542	0.56	0.00900	0 1 0	0 1 0	7 4 4	8 1 7	15	17
79.523933	5.361E-27	1.134E-01	0.0835	0.439	3951.3149	0.64	0.00460	1 0 0	1 0 0	4 3 2	4 2 3	27	27
79.774278	2.981E-19	1.728E-01	0.0929	0.499	142.2785	0.70	-0.00002	0 0 0	0 0 0	4 0 4	3 1 3	9	7
80.096493	1.105E-22	9.969E-02	0.0864	0.429	1920.7666	0.68	0.00100	0 1 0	0 1 0	5 1 4	5 0 5	33	33
80.177014	8.845E-27	1.645E-03	0.0507	0.282	2903.1460	0.47	0.00980	0 1 0	0 1 0	9 4 6	10 1 9	19	21
80.997619	1.156E-20	1.858E-01	0.0796	0.444	1201.9216	0.65	0.00481	0 0 0	0 0 0	9 3 6	9 2 7	57	57
81.016012	1.008E-26	7.819E-03	0.0328	0.162	3266.7644	0.35	0.00068	0 0 0	0 0 0	13 9 5	12 10 2	27	25
81.018867	3.023E-26	7.817E-03	0.0328	0.162	3266.7644	0.35	0.00069	0 0 0	0 0 0	13 9 4	12 10 3	81	75
81.077372	3.322E-27	1.331E-03	0.0570	0.282	3058.3984	0.48	0.01100	0 1 0	0 1 0	9 5 5	10 2 8	19	21
81.617912	7.345E-21	1.911E-01	0.0801	0.397	1050.1577	0.71	0.00063	0 0 0	0 0 0	8 4 4	8 3 5	17	17
82.154605	2.864E-19	1.235E-01	0.0835	0.456	300.3623	0.64	0.00360	0 0 0	0 0 0	4 3 2	4 2 3	27	27
82.640731	1.570E-24	1.168E-03	0.0422	0.251	2042.3107	0.32	0.00298	0 0 0	0 0 0	12 4 9	13 1 12	75	81

ν	S	A	γ_{air}	γ_{self}	E''	n_{air}	δ_{air}	v'	v''	q'	q''	g'	g''
82.862335	3.708E-23	1.692E-01	0.0796	0.384	2309.7302	0.64	0.00890	0 1 0	0 1 0	7 2 5	7 1 6	45	45
83.015920	3.940E-23	1.374E-01	0.0879	0.439	1922.9011	0.82	0.00260	0 1 0	0 1 0	4 3 1	4 2 2	9	9
83.341095	6.053E-28	8.624E-02	0.0824	0.423	4408.0288	0.78	0.00050	0 0 1	0 0 1	6 4 2	6 3 3	39	39
83.390554	3.670E-26	6.864E-02	0.0910	0.439	3482.0645	0.71	-0.00350	0 2 0	0 2 0	5 1 4	4 2 3	33	27
83.437158	2.992E-26	9.755E-04	0.0712	0.301	2512.3757	0.68	-0.00210	0 1 0	0 1 0	8 2 6	9 1 9	17	19
83.500580	1.257E-25	2.351E-02	0.0545	0.301	3141.0461	0.30	-0.00700	0 1 0	0 1 0	10 4 7	9 5 4	63	57
84.049143	6.564E-25	7.663E-04	0.0878	0.429	1920.7666	0.70	0.00710	0 1 0	0 1 0	4 3 2	5 0 5	27	33
84.455676	5.195E-22	1.872E-02	0.0728	0.398	1131.7756	0.67	-0.00572	0 0 0	0 0 0	9 3 7	8 4 4	19	17
84.627179	1.958E-25	1.019E-03	0.0791	0.423	2041.7806	0.65	0.00280	0 1 0	0 1 0	5 3 3	6 0 6	11	13
84.782898	5.795E-24	3.858E-02	0.0854	0.429	2126.4077	0.74	0.00120	0 1 0	0 1 0	6 2 4	5 3 3	13	11
84.881965	1.662E-27	2.087E-02	0.0337	0.260	4038.4036	0.16	-0.00080	0 1 0	0 1 0	12 6 7	11 7 4	75	69
84.973332	3.385E-22	2.247E-02	0.0580	0.348	1255.9116	0.33	-0.00114	0 0 0	0 0 0	9 4 6	8 5 3	19	17
85.155559	1.557E-27	1.524E-01	0.0795	0.429	4065.1318	0.58	0.00520	1 0 0	1 0 0	5 3 3	5 2 4	11	11
85.348358	1.476E-26	2.203E-01	0.0871	0.384	3967.4885	0.82	0.00650	0 2 0	0 2 0	7 3 4	7 2 5	45	45
85.505590	5.739E-27	2.375E-02	0.0422	0.282	3565.0037	0.17	-0.00290	0 1 0	0 1 0	11 5 7	10 6 4	23	21
85.631813	1.035E-20	2.587E-02	0.0825	0.454	756.7248	0.77	-0.00030	0 0 0	0 0 0	7 3 4	6 4 3	45	39
85.784761	8.800E-22	2.442E-01	0.0795	0.463	1813.2235	0.64	0.00855	0 0 0	0 0 0	11 4 7	11 3 8	69	69
85.892885	4.410E-22	1.485E-02	0.0743	0.407	1360.2354	0.72	-0.00540	0 0 0	0 0 0	10 3 8	9 4 5	63	57
85.947586	1.462E-22	7.167E-04	0.0613	0.349	920.1684	0.52	0.00252	0 0 0	0 0 0	8 3 6	9 0 9	51	57
86.203091	2.196E-26	2.349E-01	0.0928	0.466	3791.3721	0.73	0.00680	1 0 0	1 0 0	4 1 4	3 0 3	27	21
86.272337	5.162E-24	2.312E-01	0.0820	0.301	2818.3982	0.65	0.01380	0 1 0	0 1 0	9 3 6	9 2 7	57	57
86.419532	1.607E-22	1.198E-01	0.0869	0.439	1821.5968	0.66	0.00600	0 1 0	0 1 0	4 2 3	4 1 4	27	27
86.432202	4.454E-27	2.325E-01	0.0928	0.466	3890.8293	0.73	0.00680	0 0 1	0 0 1	4 1 4	3 0 3	9	7
86.468475	6.718E-26	1.292E-01	0.0864	0.429	3478.9866	0.68	0.00100	0 2 0	0 2 0	5 1 4	5 0 5	33	33
86.650766	2.191E-27	2.396E-01	0.0883	0.328	4173.2256	0.79	0.00950	0 2 0	0 2 0	8 3 5	8 2 6	17	17
86.809323	4.210E-25	1.232E-03	0.0467	0.237	2327.9143	0.36	-0.00563	0 0 0	0 0 0	13 3 10	14 2 13	81	87

ν	S	A	γ_{air}	γ_{self}	E''	n_{air}	δ_{air}	v'	v''	q'	q''	g'	g''
87.247521	5.852E-28	2.278E-02	0.0360	0.260	4038.3518	0.16	0.00260	0 1 0	0 1 0	12 6 6	11 7 5	25	23
87.335810	1.707E-22	2.190E-02	0.0498	0.316	1631.3831	0.27	0.00261	0 0 0	0 0 0	10 5 6	9 6 3	63	57
87.371563	5.795E-23	6.668E-04	0.0650	0.348	1114.5500	0.61	-0.00307	0 0 0	0 0 0	9 2 7	10 1 10	57	63
87.454300	9.741E-28	1.852E-01	0.0843	0.384	4484.9922	0.76	0.00040	1 0 0	1 0 0	7 4 3	7 3 4	45	45
87.675392	1.710E-27	1.132E-01	0.0817	0.429	3977.4563	0.55	0.00530	1 0 0	1 0 0	5 2 4	5 1 5	11	11
87.689595	3.240E-26	1.252E-01	0.0939	0.466	3299.9910	0.75	0.00640	0 2 0	0 2 0	3 2 2	3 1 3	7	7
87.759364	8.201E-20	1.650E-01	0.0788	0.454	416.2088	0.58	0.00473	0 0 0	0 0 0	5 3 3	5 2 4	11	11
88.076729	1.165E-18	2.465E-01	0.0939	0.555	136.7617	0.73	0.00455	0 0 0	0 0 0	4 1 4	3 0 3	27	21
88.152193	2.071E-26	2.093E-01	0.0796	0.384	3879.3364	0.64	0.00890	0 2 0	0 2 0	7 2 5	7 1 6	45	45
88.229037	7.133E-24	1.983E-02	0.0424	0.270	2054.3687	0.25	0.00245	0 0 0	0 0 0	11 6 6	10 7 3	23	21
88.280654	1.128E-22	1.097E-01	0.0870	0.466	1819.3351	0.80	0.00400	0 1 0	0 1 0	3 3 0	3 2 1	21	21
88.577978	2.363E-27	8.558E-02	0.0817	0.429	4076.8960	0.55	0.00530	0 0 1	0 0 1	5 2 4	5 1 5	33	33
88.650184	2.172E-22	1.661E-04	0.0878	0.451	399.4575	0.79	0.00551	0 0 0	0 0 0	4 4 1	5 1 4	27	33
88.651316	2.050E-25	1.170E-03	0.0759	0.384	2309.7302	0.64	0.00750	0 1 0	0 1 0	6 4 3	7 1 6	39	45
88.756052	3.771E-27	2.318E-01	0.0989	0.468	3796.9817	0.75	0.00370	0 0 1	0 0 1	2 2 1	1 1 0	5	3
88.781855	1.078E-26	2.114E-03	0.0450	0.260	3135.7649	0.40	0.00840	0 1 0	0 1 0	10 4 7	11 1 10	63	69
88.880521	5.355E-20	2.122E-01	0.0836	0.476	842.3566	0.76	-0.00004	0 0 0	0 0 0	7 4 3	7 3 4	45	45
89.114445	1.001E-26	2.240E-01	0.0869	0.423	3784.6792	0.81	0.00230	0 2 0	0 2 0	6 3 3	6 2 4	13	13
89.583278	9.017E-20	1.203E-01	0.0812	0.467	326.6255	0.55	0.00326	0 0 0	0 0 0	5 2 4	5 1 5	11	11
89.700113	4.897E-22	2.468E-01	0.0928	0.466	1731.8967	0.73	0.00680	0 1 0	0 1 0	4 1 4	3 0 3	27	21
89.701069	2.212E-23	2.091E-02	0.0446	0.288	2054.3452	0.24	0.00435	0 0 0	0 0 0	11 6 5	10 7 4	69	63
89.833256	3.729E-28	2.227E-02	0.0592	0.439	4135.0176	0.51	0.00060	0 0 1	1 0 0	4 4 0	4 4 1	27	27
90.000206	1.398E-25	4.135E-04	0.0934	0.439	1817.4512	0.75	0.00570	0 1 0	0 1 0	3 3 1	4 0 4	7	9
90.203073	1.866E-26	2.415E-01	0.0989	0.468	3698.4912	0.75	0.00370	1 0 0	1 0 0	2 2 1	1 1 0	15	9
90.366595	1.775E-27	9.576E-02	0.0808	0.429	4153.9380	0.62	-0.00060	0 0 1	1 0 0	5 3 3	5 3 2	33	33
90.534720	2.222E-24	1.900E-02	0.0371	0.238	2522.2651	0.25	0.00173	0 0 0	0 0 0	12 7 6	11 8 3	75	69

ν	S	A	γ_{air}	γ_{self}	E''	n_{air}	δ_{air}	v'	v''	q'	q''	g'	g''
90.671326	6.665E-28	1.833E-01	0.0741	0.423	4296.5635	0.52	0.00760	0 0 1	0 0 1	6 3 4	6 2 5	13	13
90.767529	1.763E-27	1.011E-01	0.0784	0.429	4165.4736	0.58	0.00420	1 0 0	0 0 1	5 4 1	5 2 4	33	33
90.843319	7.455E-25	1.920E-02	0.0375	0.245	2522.2615	0.24	0.00217	0 0 0	0 0 0	12 7 5	11 8 4	25	23
91.069302	4.094E-25	1.288E-03	0.0715	0.384	2180.6431	0.60	0.00450	0 1 0	0 1 0	6 3 4	7 0 7	39	45
91.151320	2.372E-27	1.022E-02	0.0305	0.140	3831.1792	0.35	0.00145	0 0 0	0 0 0	14 10 5	13 11 2	87	81
91.151804	7.907E-28	1.022E-02	0.0305	0.140	3831.1792	0.35	0.00146	0 0 0	0 0 0	14 10 4	13 11 3	29	27
91.479091	4.191E-25	2.908E-01	0.0805	0.282	3162.2590	0.71	0.00770	0 1 0	0 1 0	10 4 6	10 3 7	21	21
92.461421	2.449E-25	2.482E-01	0.0928	0.466	3289.2427	0.73	0.00680	0 2 0	0 2 0	4 1 4	3 0 3	27	21
92.529898	1.010E-18	2.580E-01	0.1105	0.522	42.3717	0.75	0.00212	0 0 0	0 0 0	2 2 1	1 1 0	15	9
92.846723	1.117E-22	1.130E-01	0.0910	0.439	1908.0164	0.71	-0.00350	0 1 0	0 1 0	5 1 4	4 2 3	33	27
93.096007	1.896E-24	5.537E-04	0.0695	0.400	1538.1497	0.57	0.00540	0 0 0	0 0 0	9 6 4	10 3 7	19	21
93.459919	6.545E-23	2.732E-02	0.0587	0.353	1631.2456	0.41	0.00630	0 0 0	0 0 0	10 5 5	9 6 4	21	19
93.519028	3.397E-27	2.016E-01	0.0741	0.423	4199.3911	0.52	0.00760	1 0 0	1 0 0	6 3 4	6 2 5	39	39
93.663832	4.123E-23	1.257E-01	0.0864	0.466	1813.7876	0.72	0.00360	0 1 0	0 1 0	3 3 1	3 2 2	7	7
93.730614	6.927E-28	2.099E-01	0.0824	0.423	4308.2114	0.78	0.00050	1 0 0	1 0 0	6 4 2	6 3 3	13	13
94.095940	3.905E-24	2.953E-01	0.0800	0.301	2904.6704	0.69	0.00390	0 1 0	0 1 0	9 4 5	9 3 6	57	57
94.261884	2.738E-27	2.969E-01	0.0820	0.301	4399.5420	0.65	0.01380	0 2 0	0 2 0	9 3 6	9 2 7	57	57
94.830942	3.791E-25	3.242E-01	0.0783	0.260	3441.0396	0.64	0.01170	0 1 0	0 1 0	11 4 7	11 3 8	69	69
94.946803	1.194E-27	1.305E-01	0.0786	0.423	4095.3152	0.58	-0.00140	1 0 0	1 0 0	6 1 5	6 0 6	13	13
95.032245	5.611E-23	3.275E-01	0.0750	0.455	2205.6528	0.51	0.00735	0 0 0	0 0 0	12 5 7	12 4 8	25	25
95.112506	6.577E-26	1.982E-02	0.0337	0.211	3032.6904	0.25	0.00152	0 0 0	0 0 0	13 8 6	12 9 3	27	25
95.172208	1.975E-25	1.985E-02	0.0337	0.210	3032.6897	0.25	0.00160	0 0 0	0 0 0	13 8 5	12 9 4	81	75
95.199019	2.146E-26	3.363E-02	0.0515	0.282	3564.7051	0.44	0.00640	0 1 0	0 1 0	11 5 6	10 6 5	69	63
95.279733	2.172E-27	1.293E-01	0.0786	0.423	4195.4775	0.58	-0.00140	0 0 1	0 0 1	6 1 5	6 0 6	39	39
95.413328	1.076E-26	2.345E-01	0.0980	0.468	3791.7009	0.78	0.00870	0 0 1	0 0 1	2 2 0	1 1 1	15	9
95.541244	3.815E-23	3.409E-01	0.0754	0.453	2533.7932	0.56	0.01090	0 0 0	0 0 0	13 5 8	13 4 9	81	81

ν	S	A	γ_{air}	γ_{self}	E''	n_{air}	δ_{air}	v'	v''	q'	q''	g'	g''
95.624475	8.510E-28	3.303E-02	0.0741	0.439	4030.8389	0.67	0.00410	0 0 1	1 0 0	4 3 1	4 3 2	27	27
95.808644	5.267E-26	2.354E-01	0.0885	0.429	3626.9224	0.83	0.00220	0 2 0	0 2 0	5 3 2	5 2 3	33	33
96.067309	1.760E-19	2.164E-01	0.0731	0.464	552.9114	0.52	0.00493	0 0 0	0 0 0	6 3 4	6 2 5	39	39
96.209196	6.177E-20	1.362E-01	0.0796	0.471	446.6966	0.58	-0.00075	0 0 0	0 0 0	6 1 5	6 0 6	13	13
96.231285	3.627E-20	2.274E-01	0.0822	0.467	661.5489	0.78	0.00054	0 0 0	0 0 0	6 4 2	6 3 3	13	13
96.675802	5.958E-27	2.453E-01	0.0980	0.468	3693.2935	0.78	0.00870	1 0 0	1 0 0	2 2 0	1 1 1	5	3
96.799373	1.479E-22	1.924E-01	0.0835	0.439	1908.0164	0.64	0.00460	0 1 0	0 1 0	4 3 2	4 2 3	27	27
96.905357	5.419E-28	8.666E-02	0.0630	0.423	4394.4644	0.51	0.00040	0 0 1	1 0 0	6 4 2	6 4 3	39	39
97.282359	2.177E-25	3.009E-01	0.0806	0.439	3381.7041	0.54	0.00350	0 2 0	0 2 0	5 0 5	4 1 4	33	27
97.406583	4.202E-28	1.177E-01	0.0799	0.429	4248.1528	0.75	0.00060	0 0 1	0 0 1	5 4 1	5 3 2	11	11
97.865219	6.048E-28	1.059E-01	0.0782	0.429	4150.2871	0.71	0.00310	0 0 1	1 0 0	5 3 2	5 3 3	11	11
98.221099	7.026E-27	1.566E-01	0.0910	0.439	3951.3149	0.71	-0.00350	1 0 0	1 0 0	5 1 4	4 2 3	33	27
98.312602	1.693E-25	1.727E-03	0.0384	0.217	2327.8840	0.31	0.00190	0 0 0	0 0 0	13 4 10	14 1 13	27	29
98.387508	1.560E-27	9.977E-02	0.0779	0.439	4126.4634	0.76	0.00070	0 0 1	0 0 1	4 4 0	4 3 1	27	27
98.732910	2.399E-26	3.760E-01	0.0806	0.439	3877.5752	0.54	0.00350	1 0 0	1 0 0	5 0 5	4 1 4	33	27
98.805394	2.327E-20	7.003E-02	0.0857	0.493	503.9681	0.74	-0.00174	0 0 0	0 0 0	6 2 4	5 3 3	13	11
98.881704	4.817E-27	3.684E-01	0.0806	0.439	3977.2615	0.54	0.00350	0 0 1	0 0 1	5 0 5	4 1 4	11	9
99.026795	3.234E-19	2.624E-01	0.0992	0.535	37.1371	0.78	0.00544	0 0 0	0 0 0	2 2 0	1 1 1	5	3
99.095238	3.547E-19	1.569E-01	0.0894	0.509	300.3623	0.71	-0.00384	0 0 0	0 0 0	5 1 4	4 2 3	33	27
99.169761	4.885E-22	3.518E-01	0.0806	0.439	1821.5968	0.54	0.00350	0 1 0	0 1 0	5 0 5	4 1 4	33	27
99.237033	4.830E-28	7.279E-02	0.0854	0.429	4150.2871	0.74	0.00120	1 0 0	1 0 0	6 2 4	5 3 3	13	11
99.668082	5.667E-28	1.098E-01	0.0762	0.439	4125.1489	0.69	0.00010	0 0 1	0 0 1	4 4 1	4 3 2	9	9
99.784824	9.053E-23	3.452E-01	0.0703	0.438	2105.8679	0.46	0.00709	0 0 0	0 0 0	12 4 8	12 3 9	25	25
99.846941	1.521E-27	1.677E-01	0.0910	0.439	4050.0522	0.71	-0.00350	0 0 1	0 0 1	5 1 4	4 2 3	11	9
99.987138	6.947E-22	3.521E-01	0.0754	0.459	1899.0083	0.51	0.00167	0 0 0	0 0 0	11 5 6	11 4 7	69	69
99.998587	1.973E-26	4.160E-02	0.0576	0.282	3387.4009	0.38	-0.01100	0 1 0	0 1 0	11 4 8	10 5 5	23	21

APPENDIX B: Spectroscopic Data for the $4_{2,2} \rightarrow 5_{1,5}$ and $5_{3,2} \rightarrow 4_{4,1}$ Transitions

Table B-1: Transitions from (v_1 v_2 v_3) = (010), (J K_{-1} K_1) = (4 2 2)

Note: Column headings are defined in Appendix A.

ν	S	A	γ_{air}	γ_{self}	E''	n_{air}	δ_{air}	v'	v''	q'	q''	g'	g''
0.072059	2.043E-30	5.088E-12	0.0919	0.429	1922.830	0.71	0.00370	**0 1 0**	0 1 0	**04 02 02**	05 01 05	9	11
15.450	1.317E-25	6.772E-05	0.0908	0.466	1907.450	0.81	-0.00190	**0 1 0**	0 1 0	**04 02 02**	03 03 01	9	7
47.431	3.034E-23	4.423E-02	0.0933	0.439	1875.470	0.83	0.00560	**0 1 0**	0 1 0	**04 02 02**	04 01 03	9	9
183.417	1.259E-22	4.946E-01	0.0959	0.466	1739.480	0.81	0.00640	**0 1 0**	0 1 0	**04 02 02**	03 01 03	9	7
1180.83	5.043E-24	3.812E-03	0.0852	0.375	742.073	0.80	-0.00300	**0 1 0**	0 0 0	**04 02 02**	05 05 01	9	11
1418.93	1.947E-20	6.664E+00	0.0862	0.474	503.968	0.74	0.00132	**0 1 0**	0 0 0	**04 02 02**	05 03 03	9	11
1539.06	3.271E-20	7.343E+00	0.0900	0.426	383.843	0.77	-0.00170	**0 1 0**	0 0 0	**04 02 02**	04 03 01	9	9
1596.28	1.072E-21	1.960E-01	0.0925	0.445	326.626	0.71	0.00201	**0 1 0**	0 0 0	**04 02 02**	05 01 05	9	11
1637.68	3.362E-21	5.290E-01	0.0924	0.423	285.219	0.75	-0.00155	**0 1 0**	0 0 0	**04 02 02**	03 03 01	9	7
1647.40	5.001E-20	7.595E+00	0.0933	0.465	275.497	0.77	0.00585	**0 1 0**	0 0 0	**04 02 02**	04 01 03	9	9
1780.62	1.404E-20	1.303E+00	0.0953	0.423	142.279	0.76	0.00485	**0 1 0**	0 0 0	**04 02 02**	03 01 03	9	7
	Sum =	24.173	1.007	4.831									

Table B-2: Transitions to (v_1 v_2 v_3) = (010), (J K_{-1} K_1) = (4 2 2)

Note: Column headings are defined in Appendix A.

ν	S	A	γ_{air}	γ_{self}	E''	n_{air}	δ_{air}	v'	v''	q'	q''	g'	g''
83.02	3.940E-23	1.374E-01	0.0879	0.439	1922.9	0.82	0.00260	0 1 0	**0 1 0**	04 03 01	**04 02 02**	9	9
203.51	2.081E-22	1.886E+00	0.0877	0.439	1922.9	0.80	0.00160	0 1 0	**0 1 0**	05 03 03	**04 02 02**	11	9
483.24	4.556E-25	1.617E-02	0.0833	0.439	1922.9	0.84	0.00100	0 1 0	**0 1 0**	05 05 01	**04 02 02**	11	9
1377.09	1.285E-23	5.271E+00	0.0890	0.433	1922.9	0.75	-0.00499	0 2 0	**0 1 0**	03 01 03	**04 02 02**	7	9
1515.67	5.768E-23	2.228E+01	0.0936	0.426	1922.9	0.78	-0.00452	0 2 0	**0 1 0**	04 01 03	**04 02 02**	9	9
1559.58	1.965E-24	6.574E-01	0.0925	0.465	1922.9	0.71	-0.00387	0 2 0	**0 1 0**	05 01 05	**04 02 02**	11	9
1577.61	1.243E-24	6.686E-01	0.0866	0.403	1922.9	0.77	0.00180	0 2 0	**0 1 0**	03 03 01	**04 02 02**	7	9
1675.83	1.429E-23	6.745E+00	0.0868	0.434	1922.9	0.77	0.00179	0 2 0	**0 1 0**	04 03 01	**04 02 02**	9	9
1796.59	1.690E-23	7.500E+00	0.0849	0.384	1922.9	0.75	0.00103	0 2 0	**0 1 0**	05 03 03	**04 02 02**	11	9
1873.64	1.251E-25	9.488E-02	0.0976	0.459	1922.9	0.77	-0.00795	1 0 0	**0 1 0**	03 01 03	**04 02 02**	7	9
1967.93	1.134E-26	9.488E-03	0.0983	0.465	1922.9	0.77	-0.00946	0 0 1	**0 1 0**	03 00 03	**04 02 02**	7	9
2004.90	6.535E-25	4.414E-01	0.0950	0.469	1922.9	0.77	-0.00785	1 0 0	**0 1 0**	04 01 03	**04 02 02**	9	9
2012.31	5.567E-26	4.870E-02	0.0896	0.441	1922.9	0.75	-0.00124	1 0 0	**0 1 0**	03 03 01	**04 02 02**	7	9
2040.02	7.141E-25	6.420E-01	0.0938	0.445	1922.9	0.76	-0.00227	0 0 1	**0 1 0**	03 02 01	**04 02 02**	7	9
2054.56	3.082E-26	1.788E-02	0.0936	0.471	1922.9	0.71	-0.00576	1 0 0	**0 1 0**	05 01 05	**04 02 02**	11	9
2108.95	5.446E-25	4.070E-01	0.0892	0.427	1922.9	0.77	-0.00246	1 0 0	**0 1 0**	04 03 01	**04 02 02**	9	9
2127.15	2.860E-25	2.174E-01	0.0923	0.451	1922.9	0.73	-0.00429	0 0 1	**0 1 0**	04 02 03	**04 02 02**	9	9
2127.60	3.546E-27	2.207E-03	0.0829	0.374	1922.9	0.81	0.00065	0 2 0	**0 1 0**	05 05 01	**04 02 02**	11	9
2153.24	1.686E-26	1.075E-02	0.0941	0.478	1922.9	0.72	-0.00601	0 0 1	**0 1 0**	05 00 05	**04 02 02**	11	9
2227.39	3.122E-25	2.129E-01	0.0881	0.448	1922.9	0.74	-0.00235	1 0 0	**0 1 0**	05 03 03	**04 02 02**	11	9
2273.07	1.565E-24	1.112E+00	0.0924	0.431	1922.9	0.80	-0.00341	0 0 1	**0 1 0**	05 02 03	**04 02 02**	11	9
2301.92	3.122E-27	2.779E-03	0.0861	0.411	1922.9	0.79	-0.00090	0 0 1	**0 1 0**	04 04 01	**04 02 02**	9	9
2422.66	3.135E-26	2.529E-02	0.0860	0.436	1922.9	0.77	-0.00111	0 0 1	**0 1 0**	05 04 01	**04 02 02**	11	9

Table B-2 (Continued)

ν	S	A	γ_{air}	γ_{self}	E''	n_{air}	δ_{air}	v'	v''	q'	q''	g'	g''
2897.86	9.037E-26	1.639E-01	0.0957	0.465	1922.9	0.75	-0.00708	0 3 0	**0 1 0**	03 01 03	**04 02 02**	7	9
3038.79	4.397E-25	6.822E-01	0.0932	0.448	1922.9	0.77	-0.00451	0 3 0	**0 1 0**	04 01 03	**04 02 02**	9	9
3142.46	2.154E-26	4.595E-02	0.0880	0.439	1922.9	0.76	0.00115	0 3 0	**0 1 0**	03 03 01	**04 02 02**	7	9
3240.36	1.771E-25	3.124E-01	0.0880	0.439	1922.9	0.82	-0.00027	0 3 0	**0 1 0**	04 03 01	**04 02 02**	9	9
3361.30	1.876E-25	2.914E-01	0.0878	0.439	1922.9	0.80	-0.00100	0 3 0	**0 1 0**	05 03 03	**04 02 02**	11	9
3453.88	2.618E-25	6.746E-01	0.0966	0.439	1922.9	0.76	-0.00647	1 1 0	**0 1 0**	03 01 03	**04 02 02**	7	9
3543.73	5.002E-25	1.357E+00	0.0986	0.439	1922.9	0.77	-0.00891	0 1 1	**0 1 0**	03 00 03	**04 02 02**	7	9
3588.02	5.244E-25	1.134E+00	0.0950	0.439	1922.9	0.78	-0.00969	1 1 0	**0 1 0**	04 01 03	**04 02 02**	9	9
3616.35	3.772E-25	1.066E+00	0.0882	0.439	1922.9	0.76	-0.00096	1 1 0	**0 1 0**	03 03 01	**04 02 02**	7	9
3626.80	1.493E-23	4.242E+01	0.0874	0.439	1922.9	0.76	-0.00385	0 1 1	**0 1 0**	03 02 01	**04 02 02**	7	9
3710.49	2.767E-24	6.401E+00	0.0896	0.439	1922.9	0.73	-0.00461	0 1 1	**0 1 0**	04 02 03	**04 02 02**	9	9
3716.83	4.881E-24	1.133E+01	0.0884	0.439	1922.9	0.82	-0.00355	1 1 0	**0 1 0**	04 03 01	**04 02 02**	9	9
3729.24	1.464E-25	2.799E-01	0.0935	0.439	1922.9	0.72	-0.00859	0 1 1	**0 1 0**	05 00 05	**04 02 02**	11	9
3831.84	4.034E-25	8.142E-01	0.0881	0.439	1922.9	0.80	-0.00398	1 1 0	**0 1 0**	05 03 03	**04 02 02**	11	9
3860.50	1.638E-23	3.356E+01	0.0858	0.439	1922.9	0.80	-0.00800	0 1 1	**0 1 0**	05 02 03	**04 02 02**	11	9
3919.10	1.041E-26	2.686E-02	0.0856	0.439	1922.9	0.79	-0.00499	0 1 1	**0 1 0**	04 04 01	**04 02 02**	9	9
4040.28	1.174E-25	2.634E-01	0.0874	0.439	1922.9	0.77	-0.00236	0 1 1	**0 1 0**	05 04 01	**04 02 02**	11	9
5084.53	1.428E-25	7.975E-01	0.0920	0.394	1922.9	0.77	-0.01600	0 2 1	**0 1 0**	03 00 03	**04 02 02**	7	9
5180.71	3.070E-24	1.780E+01	0.0877	0.450	1922.9	0.76	-0.00494	0 2 1	**0 1 0**	03 02 01	**04 02 02**	7	9
5191.71	1.230E-25	7.162E-01	0.0884	0.381	1922.9	0.76	-0.00188	1 2 0	**0 1 0**	03 03 01	**04 02 02**	7	9
5268.47	1.545E-24	7.205E+00	0.0898	0.424	1922.9	0.73	-0.00578	0 2 1	**0 1 0**	04 02 03	**04 02 02**	9	9
5288.54	1.896E-25	8.910E-01	0.0886	0.439	1922.9	0.82	-0.00499	1 2 0	**0 1 0**	04 03 01	**04 02 02**	9	9
5405.72	6.455E-25	2.593E+00	0.0884	0.422	1922.9	0.80	-0.00528	1 2 0	**0 1 0**	05 03 03	**04 02 02**	11	9
5416.09	3.268E-24	1.318E+01	0.0862	0.372	1922.9	0.80	-0.01900	0 2 1	**0 1 0**	05 02 03	**04 02 02**	11	9
5633.63	2.771E-26	1.209E-01	0.0875	0.358	1922.9	0.77	-0.00335	0 2 1	**0 1 0**	05 04 01	**04 02 02**	11	9

Table B-2 (Continued)

ν	S	A	γ_{air}	γ_{self}	E''	n_{air}	δ_{air}	v'	v''	q'	q''	g'	g''
6587.47	3.227E-26	3.025E-01	0.0860	0.457	1922.9	0.77	-0.02400	0 3 1	**0 1 0**	03 00 03	**04 02 02**	7	9
6703.10	2.207E-25	2.142E+00	0.0880	0.390	1922.9	0.76	-0.00602	0 3 1	**0 1 0**	03 02 01	**04 02 02**	7	9
6935.70	2.663E-25	1.761E+00	0.0866	0.439	1922.9	0.80	-0.01010	0 3 1	**0 1 0**	05 02 03	**04 02 02**	11	9
7097.27	1.009E-24	1.098E+01	0.0891	0.439	1922.9	0.76	-0.00850	1 1 1	**0 1 0**	03 02 01	**04 02 02**	7	9
7110.12	1.210E-25	1.028E+00	0.0966	0.439	1922.9	0.78	-0.01458	2 1 0	**0 1 0**	04 01 03	**04 02 02**	9	9
7182.53	3.227E-25	2.797E+00	0.0910	0.439	1922.9	0.73	-0.00962	1 1 1	**0 1 0**	04 02 03	**04 02 02**	9	9
7326.34	1.271E-24	9.378E+00	0.0879	0.439	1922.9	0.80	-0.01250	1 1 1	**0 1 0**	05 02 03	**04 02 02**	11	9
8191.92	3.750E-27	5.436E-02	0.0885	0.439	1922.9	0.76	-0.00711	0 4 1	**0 1 0**	03 02 01	**04 02 02**	7	9
8423.88	7.500E-27	7.316E-02	0.0871	0.439	1922.9	0.80	-0.01115	0 4 1	**0 1 0**	05 02 03	**04 02 02**	11	9
11951.00	4.650E-27	1.435E-01	0.0928	0.300	1922.9	0.76	-0.01424	2 2 1	**0 1 0**	03 02 01	**04 02 02**	7	9
12178.20	6.780E-27	1.382E-01	0.0924	0.400	1922.9	0.80	-0.01805	2 2 1	**0 1 0**	05 02 03	**04 02 02**	11	9
	Sum =	2.213E+02	5.303	25.426									

Table B-3: Transitions from (v_1 v_2 v_3) = (010), (J K_{-1} K_1) = (5 1 5)

Note: Column headings are defined in Appendix A.

ν	S	A	γ_{air}	γ_{self}	E''	n_{air}	δ_{air}	v'	v''	q'	q''	g'	g''
105.378	1.891E-22	4.313E-01	0.085	0.44	1817.45	0.61	0.00600	**0 1 0**	0 1 0	**05 01 05**	04 00 04	11	9
1165.05	2.268E-23	1.474E-02	0.084	0.40	757.78	0.61	-0.00565	**0 1 0**	0 0 0	**05 01 05**	06 04 02	11	13
1312.71	1.506E-23	6.051E-03	0.086	0.40	610.114	0.62	-0.00082	**0 1 0**	0 0 0	**05 01 05**	05 04 02	11	11
1320.06	1.726E-21	6.766E-01	0.093	0.48	602.774	0.70	-0.00225	**0 1 0**	0 0 0	**05 01 05**	06 02 04	11	13
1434.69	1.323E-24	3.507E-04	0.090	0.41	488.134	0.66	-0.00587	**0 1 0**	0 0 0	**05 01 05**	04 04 00	11	9
1476.13	3.560E-20	8.165E+00	0.070	0.41	446.697	0.33	-0.00118	**0 1 0**	0 0 0	**05 01 05**	06 00 06	11	13
1506.62	2.506E-20	5.163E+00	0.083	0.43	416.209	0.50	-0.00360	**0 1 0**	0 0 0	**05 01 05**	05 02 04	11	11
1607.05	1.795E-21	2.582E-01	0.095	0.46	315.780	0.70	-0.00005	**0 1 0**	0 0 0	**05 01 05**	04 02 02	11	9
1700.78	9.519E-20	9.721E+00	0.086	0.46	222.053	0.57	0.00505	**0 1 0**	0 0 0	**05 01 05**	04 00 04	11	9
	Sum =	2.444E+01	0.772	3.879									

Table B-4: Transitions to (v_1 v_2 v_3) = (010), (J K_{-1} K_1) = (5 1 5)

Note: Column headings are defined in Appendix A.

ν	S	A	γ_{air}	γ_{self}	E''	n_{air}	δ_{air}	v'	v''	q'	q''	g'	g''
0.072059	3.940E-23	5.088E-12	0.0919	0.429	1922.83	0.71	0.00370	0 1 0	**0 1 0**	04 02 02	**05 01 05**	9	11
101.32	2.081E-22	1.740E-01	0.0817	0.429	1922.83	0.55	0.00530	0 1 0	**0 1 0**	05 02 04	**05 01 05**	11	11
118.95	4.556E-25	6.527E-01	0.0696	0.429	1922.83	0.35	0.00190	0 1 0	**0 1 0**	06 00 06	**05 01 05**	13	11
206.79	1.285E-23	2.025E-04	0.0879	0.429	1922.83	0.73	0.00370	0 1 0	**0 1 0**	04 04 00	**05 01 05**	9	11
288.36	5.768E-23	5.869E-01	0.0908	0.429	1922.83	0.74	0.00280	0 1 0	**0 1 0**	06 02 04	**05 01 05**	13	11
328.87	1.965E-24	1.060E-02	0.0853	0.429	1922.83	0.69	0.00380	0 1 0	**0 1 0**	05 04 02	**05 01 05**	11	11
476.34	1.243E-24	6.106E-02	0.0826	0.429	1922.83	0.67	0.00570	0 1 0	**0 1 0**	06 04 02	**05 01 05**	13	11
1452.47	1.429E-23	1.643E+01	0.0834	0.434	1922.83	0.57	-0.00570	0 2 0	**0 1 0**	04 00 04	**05 01 05**	9	11
1573.11	1.690E-23	4.882E-01	0.0916	0.404	1922.83	0.70	0.00305	0 2 0	**0 1 0**	04 02 02	**05 01 05**	9	11
1675.69	1.251E-25	4.937E+00	0.0772	0.392	1922.83	0.45	0.00241	0 2 0	**0 1 0**	05 02 04	**05 01 05**	11	11
1677.22	1.134E-26	2.051E+01	0.0683	0.373	1922.83	0.32	0.00178	0 2 0	**0 1 0**	06 00 06	**05 01 05**	13	11
1861.85	6.535E-25	9.074E-01	0.0903	0.454	1922.83	0.68	0.00391	0 2 0	**0 1 0**	06 02 04	**05 01 05**	13	11
1946.04	5.567E-26	4.745E-03	0.0837	0.391	1922.83	0.62	0.00576	0 2 0	**0 1 0**	05 04 02	**05 01 05**	11	11
1952.19	7.141E-25	4.519E-01	0.0878	0.469	1922.83	0.58	-0.00711	1 0 0	**0 1 0**	04 00 04	**05 01 05**	9	11
2043.73	3.082E-26	6.905E-02	0.0935	0.468	1922.83	0.70	0.00003	1 0 0	**0 1 0**	04 02 02	**05 01 05**	9	11
2054.43	5.446E-25	7.493E-01	0.0856	0.458	1922.83	0.52	-0.00560	0 0 1	**0 1 0**	04 01 04	**05 01 05**	9	11
2093.22	2.860E-25	1.050E-02	0.0815	0.396	1922.83	0.58	0.00659	0 2 0	**0 1 0**	06 04 02	**05 01 05**	13	11
2142.30	3.546E-27	1.975E-01	0.0820	0.442	1922.83	0.51	-0.00040	1 0 0	**0 1 0**	05 02 04	**05 01 05**	11	11
2172.49	1.686E-26	4.871E-01	0.0743	0.415	1922.83	0.34	-0.00263	1 0 0	**0 1 0**	06 00 06	**05 01 05**	13	11
2227.07	3.122E-25	9.379E-02	0.0887	0.479	1922.83	0.63	-0.00346	0 0 1	**0 1 0**	05 01 04	**05 01 05**	11	11
2272.99	1.565E-24	1.183E+00	0.0738	0.414	1922.83	0.33	-0.00190	0 0 1	**0 1 0**	06 01 06	**05 01 05**	13	11
2325.32	3.122E-27	2.224E-03	0.0900	0.470	1922.83	0.69	0.00132	0 0 1	**0 1 0**	05 03 02	**05 01 05**	11	11

Table B-4 (Continued)

Note: Column headings are defined in Appendix A.

ν	S	A	γ_{air}	γ_{self}	E''	n_{air}	δ_{air}	v'	v''	q'	q''	g'	g''
2326.70	3.135E-26	4.469E-02	0.0912	0.485	1922.83	0.70	-0.00050	1 0 0	**0 1 0**	06 02 04	**05 01 05**	13	11
2464.41	9.037E-26	2.080E-02	0.0821	0.435	1922.83	0.55	0.00296	0 0 1	**0 1 0**	06 03 04	**05 01 05**	13	11
2479.11	3.816E-27	2.727E-03	0.0849	0.422	1922.83	0.62	0.00425	1 0 0	**0 1 0**	06 04 02	**05 01 05**	13	11
2968.91	4.801E-25	7.108E-01	0.0873	0.447	1922.83	0.58	-0.00733	0 3 0	**0 1 0**	04 00 04	**05 01 05**	9	11
3110.88	3.453E-26	5.613E-02	0.0898	0.455	1922.83	0.68	0.00488	0 3 0	**0 1 0**	04 02 02	**05 01 05**	9	11
3195.16	4.276E-25	5.076E-01	0.0697	0.429	1922.83	0.35	-0.00133	0 3 0	**0 1 0**	06 00 06	**05 01 05**	13	11
3215.36	1.715E-25	2.437E-01	0.0818	0.429	1922.83	0.55	0.00232	0 3 0	**0 1 0**	05 02 04	**05 01 05**	11	11
3398.83	3.857E-26	5.181E-02	0.0909	0.429	1922.83	0.74	0.00010	0 3 0	**0 1 0**	06 02 04	**05 01 05**	13	11
3530.74	1.150E-24	2.408E+00	0.0863	0.429	1922.83	0.57	-0.01000	1 1 0	**0 1 0**	04 00 04	**05 01 05**	9	11
3630.15	1.783E-23	3.946E+01	0.0821	0.429	1922.83	0.52	-0.00809	0 1 1	**0 1 0**	04 01 04	**05 01 05**	9	11
3635.02	5.527E-24	1.227E+01	0.0925	0.429	1922.83	0.71	-0.00248	1 1 0	**0 1 0**	04 02 02	**05 01 05**	9	11
3732.97	6.979E-26	1.336E-01	0.0822	0.429	1922.83	0.55	-0.00109	1 1 0	**0 1 0**	05 02 04	**05 01 05**	11	11
3750.63	1.303E-25	2.131E-01	0.0702	0.429	1922.83	0.35	-0.00503	1 1 0	**0 1 0**	06 00 06	**05 01 05**	13	11
3809.09	1.815E-24	3.619E+00	0.0908	0.429	1922.83	0.63	-0.00475	0 1 1	**0 1 0**	05 01 04	**05 01 05**	11	11
3848.89	2.263E-23	3.898E+01	0.0700	0.429	1922.83	0.33	-0.00451	0 1 1	**0 1 0**	06 01 06	**05 01 05**	13	11
3918.12	5.164E-26	9.218E-02	0.0914	0.429	1922.83	0.74	-0.00299	1 1 0	**0 1 0**	06 02 04	**05 01 05**	13	11
3928.44	2.078E-26	4.407E-02	0.0881	0.429	1922.83	0.69	-0.00079	0 1 1	**0 1 0**	05 03 02	**05 01 05**	11	11
4067.35	1.452E-25	2.793E-01	0.0822	0.429	1922.83	0.55	0.00134	0 1 1	**0 1 0**	06 03 04	**05 01 05**	13	11
5071.75	5.527E-26	2.388E-01	0.0866	0.243	1922.83	0.57	-0.01100	1 2 0	**0 1 0**	04 00 04	**05 01 05**	9	11
5173.89	4.881E-24	2.195E+01	0.0780	0.435	1922.83	0.52	-0.02100	0 2 1	**0 1 0**	04 01 04	**05 01 05**	9	11
5291.91	1.226E-25	3.992E-01	0.0705	0.351	1922.83	0.35	-0.00665	1 2 0	**0 1 0**	06 00 06	**05 01 05**	13	11
5356.90	3.994E-25	1.575E+00	0.0770	0.470	1922.83	0.63	-0.01500	0 2 1	**0 1 0**	05 01 04	**05 01 05**	11	11

Table B-4 (Continued)

Note: Column headings are defined in Appendix A.

ν	S	A	γ_{air}	γ_{self}	E''	n_{air}	δ_{air}	v'	v''	q'	q''	g'	g''
5390.88	5.285E+24	1.786E+01	0.0710	0.355	1922.83	0.33	-0.00300	0 2 1	**0 1 0**	06 01 06	**05 01 05**	13	11
5500.17	1.686E+26	7.009E-02	0.0884	0.429	1922.83	0.69	-0.00214	0 2 1	**0 1 0**	05 03 02	**05 01 05**	11	11
5640.38	3.022E+26	1.118E-01	0.0860	0.428	1922.83	0.55	0.01300	0 2 1	**0 1 0**	06 03 04	**05 01 05**	13	11
5708.88	2.824E+27	1.070E-02	0.0714	0.510	1922.83	0.35	-0.01034	2 0 0	**0 1 0**	06 00 06	**05 01 05**	13	11
6680.66	2.965E+25	2.223E+00	0.0831	0.387	1922.83	0.52	-0.01023	0 3 1	**0 1 0**	04 01 04	**05 01 05**	9	11
6896.83	3.469E+25	1.919E+00	0.0709	0.429	1922.83	0.33	-0.00741	0 3 1	**0 1 0**	06 01 06	**05 01 05**	13	11
7053.47	1.412E+25	1.180E+00	0.0880	0.429	1922.83	0.57	-0.01450	2 1 0	**0 1 0**	04 00 04	**05 01 05**	9	11
7102.32	1.343E+24	1.138E+01	0.0846	0.410	1922.83	0.52	-0.01268	1 1 1	**0 1 0**	04 01 04	**05 01 05**	9	11
7316.05	2.158E+24	1.343E+01	0.0723	0.430	1922.83	0.33	-0.01072	1 1 1	**0 1 0**	06 01 06	**05 01 05**	13	11
8147.51	7.500E+27	8.362E-02	0.0837	0.429	1922.83	0.52	-0.01130	0 4 1	**0 1 0**	04 01 04	**05 01 05**	9	11
8363.30	1.130E+26	9.190E-02	0.0715	0.429	1922.83	0.33	-0.00886	0 4 1	**0 1 0**	06 01 06	**05 01 05**	13	11
10442.40	1.300E+01	7.696E-01	0.0888	0.429	1922.83	0.52	-0.01727	2 1 1	**0 1 0**	04 01 04	**05 01 05**	9	11
10652.40	1.400E+01	6.002E-01	0.0762	0.429	1922.83	0.33	-0.01693	2 1 1	**0 1 0**	06 01 06	**05 01 05**	13	11
12154.60	1.500E+01	1.601E-01	0.0774	0.400	1922.83	0.33	-0.01838	2 2 1	**0 1 0**	06 01 06	**05 01 05**	13	11
	Sum =	221.198	4.780	24.705									

Table B-5: Transitions from (v_1 v_2 v_3) = (010), (J K_{-1} K_1) = (5 3 2)

Note: Column headings are defined in Appendix A.

ν	S	A	γ_{air}	γ_{self}	E''	n_{air}	δ_{air}	v'	v''	q'	q''	g'	g''
0.895092	3.600E-28	8.314E-09	0.0801	0.439	2129.600	0.81	-0.00030	**0 1 0**	0 1 0	**05 03 02**	04 04 01	33	27
76.526	8.370E-23	1.367E-01	0.0885	0.429	2053.970	0.83	0.00220	**0 1 0**	0 1 0	**05 03 02**	05 02 03	33	33
209.728	1.831E-23	5.714E-02	0.0887	0.429	1920.770	0.75	0.00530	**0 1 0**	0 1 0	**05 03 02**	05 00 05	33	33
222.478	6.485E-22	2.070E+00	0.0833	0.439	1908.020	0.73	0.00310	**0 1 0**	0 1 0	**05 03 02**	04 02 03	33	27
1085.440	2.187E-24	1.664E-03	0.0767	0.354	1045.060	0.75	-0.01304	**0 1 0**	0 0 0	**05 03 02**	06 06 01	33	39
1373.770	2.649E-20	7.920E+00	0.0755	0.369	756.725	0.61	0.00305	**0 1 0**	0 0 0	**05 03 02**	06 04 03	33	39
1520.150	3.408E-20	6.121E+00	0.0781	0.355	610.341	0.65	0.00130	**0 1 0**	0 0 0	**05 03 02**	05 04 01	33	33
1577.580	3.248E-21	4.752E-01	0.0849	0.435	552.911	0.64	0.00415	**0 1 0**	0 0 0	**05 03 02**	06 02 05	33	39
1642.390	3.033E-21	3.509E-01	0.0816	0.373	488.108	0.71	-0.00020	**0 1 0**	0 0 0	**05 03 02**	04 04 01	33	27
1683.980	4.951E-20	4.920E+00	0.0881	0.442	446.511	0.79	-0.00046	**0 1 0**	0 0 0	**05 03 02**	05 02 03	33	33
1805.150	1.279E-21	8.103E-02	0.0895	0.447	325.348	0.67	0.00528	**0 1 0**	0 0 0	**05 03 02**	05 00 05	33	33
1830.130	5.123E-20	2.954E+00	0.0840	0.404	300.362	0.64	0.00312	**0 1 0**	0 0 0	**05 03 02**	04 02 03	33	27
	Sum =	25.088	0.999	4.915									

Table B-6: Transitions to (v_1 v_2 v_3) = (010), (J K_{-1} K_1) = (5 3 2)

Note: Column headings are defined in Appendix A.

ν	S	A	γ_{air}	γ_{self}	E''	n_{air}	δ_{air}	v'	v''	q'	q''	g'	g''
30.79	2.081E-22	8.451E-04	0.0876	0.429	2130.49	0.73	0.00370	0 1 0	**0 1 0**	06 02 05	**05 03 02**	39	33
121.37	4.556E-25	3.434E-01	0.0799	0.429	2130.49	0.75	0.00060	0 1 0	**0 1 0**	05 04 01	**05 03 02**	33	33
267.89	1.285E-23	4.996E+00	0.0790	0.429	2130.49	0.72	0.00090	0 1 0	**0 1 0**	06 04 03	**05 03 02**	39	33
603.47	5.768E-23	1.794E-02	0.0763	0.340	2130.49	0.76	-0.00100	0 1 0	**0 1 0**	06 06 01	**05 03 02**	39	33
1348.49	1.965E-24	2.724E-01	0.0890	0.415	2130.49	0.67	-0.00821	0 2 0	**0 1 0**	05 00 05	**05 03 02**	33	33
1351.57	1.243E-24	1.186E+01	0.0810	0.402	2130.49	0.63	-0.00426	0 2 0	**0 1 0**	04 02 03	**05 03 02**	27	33
1496.43	1.429E-23	1.774E+01	0.0875	0.430	2130.49	0.74	-0.00124	0 2 0	**0 1 0**	05 02 03	**05 03 02**	33	33
1605.68	1.690E-23	1.726E+00	0.0786	0.366	2130.49	0.66	-0.00645	0 2 0	**0 1 0**	06 02 05	**05 03 02**	39	33
1616.27	1.251E-25	3.093E-01	0.0773	0.363	2130.49	0.73	-0.00201	0 2 0	**0 1 0**	04 04 01	**05 03 02**	27	33
1738.49	1.134E-26	4.316E+00	0.0746	0.343	2130.49	0.67	-0.00085	0 2 0	**0 1 0**	05 04 01	**05 03 02**	33	33
1820.82	6.535E-25	2.043E-01	0.0868	0.427	2130.49	0.65	-0.00767	1 0 0	**0 1 0**	04 02 03	**05 03 02**	27	33
1845.81	5.567E-26	1.149E-02	0.0900	0.439	2130.49	0.68	-0.00952	1 0 0	**0 1 0**	05 00 05	**05 03 02**	33	33
1885.02	7.141E-25	6.860E+00	0.0738	0.359	2130.49	0.65	-0.00150	0 2 0	**0 1 0**	06 04 03	**05 03 02**	39	33
1897.31	3.082E-26	7.140E-03	0.0916	0.441	2130.49	0.73	-0.00928	0 0 1	**0 1 0**	04 01 03	**05 03 02**	27	33
1965.43	5.446E-25	3.487E-01	0.0895	0.444	2130.49	0.79	-0.00433	1 0 0	**0 1 0**	05 02 03	**05 03 02**	33	33
1995.97	2.860E-25	4.889E-01	0.0836	0.412	2130.49	0.70	-0.00363	0 0 1	**0 1 0**	04 03 01	**05 03 02**	27	33
2004.52	3.546E-27	4.159E-02	0.0795	0.376	2130.49	0.72	-0.00405	1 0 0	**0 1 0**	04 04 01	**05 03 02**	27	33
2068.90	1.686E-26	4.794E-02	0.0824	0.443	2130.49	0.65	-0.00848	1 0 0	**0 1 0**	06 02 05	**05 03 02**	39	33
2113.81	3.122E-25	7.475E-01	0.0811	0.397	2130.49	0.62	-0.00539	0 0 1	**0 1 0**	05 03 03	**05 03 02**	33	33
2125.75	1.565E-24	6.873E-03	0.0776	0.377	2130.49	0.66	-0.00416	1 0 0	**0 1 0**	05 04 01	**05 03 02**	33	33
2160.26	3.122E-27	2.483E-02	0.0869	0.453	2130.49	0.72	-0.00840	0 0 1	**0 1 0**	06 01 05	**05 03 02**	39	33
2263.97	3.135E-26	3.673E-03	0.0766	0.389	2130.49	0.62	-0.00469	1 0 0	**0 1 0**	06 04 03	**05 03 02**	39	33

Table B-6 (Continued)

Note: Column headings are defined in Appendix A.

ν	S	A	γ_{air}	γ_{self}	E''	n_{air}	δ_{air}	v'	v''	q'	q''	g'	g''
2277.53	4.397E-25	1.1680	0.0867	0.435	2130.49	0.77	-0.00345	0 0 1	**0 1 0**	06 03 03	**05 03 02**	39	33
2338.20	2.154E-26	0.0018	0.0778	0.357	2130.49	0.74	-0.00417	0 0 1	**0 1 0**	05 05 01	**05 03 02**	33	33
2483.08	1.771E-25	0.0236	0.0751	0.374	2130.49	0.68	-0.00410	0 0 1	**0 1 0**	06 05 01	**05 03 02**	39	33
2890.90	1.876E-25	0.3837	0.0806	0.408	2130.49	0.66	-0.00582	0 3 0	**0 1 0**	04 02 03	**05 03 02**	27	33
3033.54	2.618E-25	0.5226	0.0849	0.374	2130.49	0.69	-0.00144	0 3 0	**0 1 0**	05 02 03	**05 03 02**	33	33
3145.97	5.002E-25	0.0364	0.0877	0.429	2130.49	0.73	0.00070	0 3 0	**0 1 0**	06 02 05	**05 03 02**	39	33
3211.69	5.244E-25	0.0357	0.0807	0.429	2130.49	0.76	-0.00125	0 3 0	**0 1 0**	04 04 01	**05 03 02**	27	33
3333.84	3.772E-25	0.2705	0.0800	0.429	2130.49	0.75	-0.00196	0 3 0	**0 1 0**	05 04 01	**05 03 02**	33	33
3411.17	1.493E-23	1.8390	0.0855	0.429	2130.49	0.68	-0.00717	1 1 0	**0 1 0**	04 02 03	**05 03 02**	27	33
3424.34	2.767E-24	0.0161	0.0904	0.429	2130.49	0.70	-0.01129	1 1 0	**0 1 0**	05 00 05	**05 03 02**	33	33
3477.79	4.881E-24	1.0420	0.0919	0.429	2130.49	0.73	-0.00901	0 1 1	**0 1 0**	04 01 03	**05 03 02**	27	33
3480.27	1.464E-25	0.3160	0.0791	0.429	2130.49	0.72	-0.00201	0 3 0	**0 1 0**	06 04 03	**05 03 02**	39	33
3523.07	4.034E-25	0.2794	0.0888	0.429	2130.49	0.69	-0.00672	0 1 1	**0 1 0**	05 01 05	**05 03 02**	33	33
3555.69	1.638E-23	0.7885	0.0880	0.429	2130.49	0.78	-0.00598	1 1 0	**0 1 0**	05 02 03	**05 03 02**	33	33
3597.08	1.041E-26	33.8300	0.0809	0.429	2130.49	0.70	-0.00309	0 1 1	**0 1 0**	04 03 01	**05 03 02**	27	33
3626.16	1.174E-25	0.9698	0.0811	0.429	2130.49	0.76	-0.00485	1 1 0	**0 1 0**	04 04 01	**05 03 02**	27	33
3660.02	1.428E-25	0.0165	0.0882	0.429	2130.49	0.73	-0.00272	1 1 0	**0 1 0**	06 02 05	**05 03 02**	39	33
3716.02	3.070E-24	25.2700	0.0813	0.429	2130.49	0.62	-0.00645	0 1 1	**0 1 0**	05 03 03	**05 03 02**	33	33
3744.25	1.230E-25	0.4373	0.0887	0.429	2130.49	0.72	-0.00808	0 1 1	**0 1 0**	06 01 05	**05 03 02**	39	33
3746.90	1.545E-24	1.8510	0.0804	0.429	2130.49	0.75	-0.00489	1 1 0	**0 1 0**	05 04 01	**05 03 02**	33	33

Table B-6 (Continued)

Note: Column headings are defined in Appendix A.

ν	S	A	γ_{air}	γ_{self}	E''	n_{air}	δ_{air}	v'	v''	q'	q''	g'	g''
3871.80	1.896E-25	2.675E+01	0.0793	0.429	2130.49	0.77	-0.00527	0 1 1	**0 1 0**	06 03 03	**05 03 02**	39	33
3892.05	6.455E-25	2.710E+00	0.0796	0.429	2130.49	0.72	-0.00534	1 1 0	**0 1 0**	06 04 03	**05 03 02**	39	33
4121.22	3.268E-24	1.450E-01	0.0784	0.429	2130.49	0.68	-0.00395	0 1 1	**0 1 0**	06 05 01	**05 03 02**	39	33
4967.65	2.771E-26	2.355E-01	0.0860	0.367	2130.49	0.68	-0.00900	1 2 0	**0 1 0**	04 02 03	**05 03 02**	27	33
5023.98	3.227E-26	5.646E-01	0.0921	0.531	2130.49	0.73	-0.01011	0 2 1	**0 1 0**	04 01 03	**05 03 02**	27	33
5065.65	2.207E-25	4.138E-02	0.0890	0.429	2130.49	0.69	-0.00787	0 2 1	**0 1 0**	05 01 05	**05 03 02**	33	33
5111.21	2.663E-25	2.981E-01	0.0882	0.429	2130.49	0.78	-0.00742	1 2 0	**0 1 0**	05 02 03	**05 03 02**	33	33
5168.97	1.009E-24	1.436E+01	0.0880	0.470	2130.49	0.70	0.00100	0 2 1	**0 1 0**	04 03 01	**05 03 02**	27	33
5223.60	1.210E-25	6.120E-02	0.0813	0.429	2130.49	0.76	-0.00643	1 2 0	**0 1 0**	04 04 01	**05 03 02**	27	33
5288.54	3.227E-25	1.078E+01	0.0920	0.434	2130.49	0.62	-0.01800	0 2 1	**0 1 0**	05 03 03	**05 03 02**	33	33
5294.35	1.271E-24	4.245E-02	0.0889	0.429	2130.49	0.72	-0.00896	0 2 1	**0 1 0**	06 01 05	**05 03 02**	39	33
5443.31	3.750E-27	1.360E+01	0.0860	0.352	2130.49	0.77	-0.00200	0 2 1	**0 1 0**	06 03 03	**05 03 02**	39	33
5488.63	7.500E-27	6.850E-02	0.0799	0.429	2130.49	0.72	-0.00680	1 2 0	**0 1 0**	06 04 03	**05 03 02**	39	33
5654.00	1.999E-24	5.786E-02	0.0815	0.652	2130.49	0.75	-0.00910	2 0 0	**0 1 0**	05 04 01	**05 03 02**	33	33
5738.86	1.350E-25	9.086E-02	0.0760	0.350	2130.49	0.68	-0.01700	0 2 1	**0 1 0**	06 05 01	**05 03 02**	39	33
6713.55	4.650E-27	1.760E+00	0.0814	0.326	2130.49	0.70	-0.00593	0 3 1	**0 1 0**	04 03 01	**05 03 02**	27	33
6833.56	6.780E-27	1.378E+00	0.0820	0.350	2130.49	0.62	-0.00918	0 3 1	**0 1 0**	05 03 03	**05 03 02**	33	33
6986.39	6.780E-27	1.675E+00	0.0803	0.429	2130.49	0.77	-0.00764	0 3 1	**0 1 0**	06 03 03	**05 03 02**	39	33
7064.04	6.780E-27	7.577E+00	0.0823	0.390	2130.49	0.70	-0.00918	1 1 1	**0 1 0**	04 03 01	**05 03 02**	27	33
7334.61	6.780E-27	6.809E+00	0.0819	0.380	2130.49	0.77	-0.01034	1 1 1	**0 1 0**	06 03 03	**05 03 02**	39	33
8232.58	6.780E-27	8.038E-02	0.0818	0.429	2130.50	0.70	-0.00735	0 4 1	**0 1 0**	04 03 01	**05 03 02**	27	33
8352.88	6.780E-27	6.770E-02	0.0824	0.429	2130.50	0.62	-0.01055	0 4 1	**0 1 0**	05 03 03	**05 03 02**	33	33

Table B-7: Transitions from (v_1 v_2 v_3) = (010), (J K_{-1} K_1) = (4 4 1)

Note: Column headings are defined in Appendix A.

ν	S	A	γ_{air}	γ_{self}	E''	n_{air}	δ_{air}	v'	v''	q'	q''	g'	g''
124.784	8.505E-23	2.429E-01	0.0762	0.439	2004.82	0.69	0.00010	**0 1 0**	0 1 0	**04 04 01**	04 03 02	27	27
128.736	1.243E-25	3.623E-04	0.0865	0.429	2000.86	0.79	0.00470	**0 1 0**	0 1 0	**04 04 01**	05 01 04	27	33
221.983	1.126E-21	4.371E+00	0.0698	0.466	1907.62	0.61	-0.00240	**0 1 0**	0 1 0	**04 04 01**	03 03 00	27	21
308.002	8.307E-25	3.475E-03	0.0889	0.439	1821.60	0.75	0.00510	**0 1 0**	0 1 0	**04 04 01**	04 01 04	27	27
357.186	4.226E-24	1.764E-02	0.0900	0.466	1772.41	0.81	0.00570	**0 1 0**	0 1 0	**04 04 01**	03 01 02	27	21
1387.52	4.186E-20	1.453E+01	0.0502	0.270	742.076	0.34	0.00078	**0 1 0**	0 0 0	**04 04 01**	05 05 00	27	33
1620.79	1.181E-21	1.799E-01	0.0831	0.377	508.812	0.76	0.00119	**0 1 0**	0 0 0	**04 04 01**	05 03 02	27	33
1730.14	2.188E-23	2.231E-03	0.0874	0.424	399.458	0.74	0.00490	**0 1 0**	0 0 0	**04 04 01**	05 01 04	27	33
1747.08	1.687E-20	1.616E+00	0.0766	0.359	382.517	0.66	-0.00126	**0 1 0**	0 0 0	**04 04 01**	04 03 02	27	27
1844.18	7.907E-20	5.263E+00	0.0696	0.337	285.419	0.59	-0.00331	**0 1 0**	0 0 0	**04 04 01**	03 03 00	27	21
1904.76	2.021E-23	1.069E-03	0.0918	0.433	224.838	0.69	0.00518	**0 1 0**	0 0 0	**04 04 01**	04 01 04	27	27
1956.23	1.113E-22	4.834E-03	0.0916	0.486	173.366	0.74	0.00483	**0 1 0**	0 0 0	**04 04 01**	03 01 02	27	21
	Sum =	26.232	0.962	4.925									

Table B-8: Transitions to (v_1 v_2 v_3) = (010), (J K_{-1} K_1) = (4 4 1)

Note: Column headings are defined in Appendix A.

ν	S	A	γ_{air}	γ_{self}	E''	n_{air}	δ_{air}	v'	v''	q'	q''	g'	g''
0.895092	2.081E-22	8.314E-09	0.0801	0.439	2129.6	0.81	-0.00030	0 1 0	**0 1 0**	05 03 02	**04 04 01**	33	27
276.54	4.556E-25	9.012E+00	0.0539	0.439	2129.6	0.41	-0.00710	0 1 0	**0 1 0**	05 05 00	**04 04 01**	33	27
1205.03	1.285E-23	1.502E-02	0.0889	0.430	2129.6	0.78	-0.00666	0 2 0	**0 1 0**	03 01 02	**04 04 01**	21	27
1252.11	5.768E-23	3.442E-03	0.0910	0.426	2129.6	0.68	-0.00702	0 2 0	**0 1 0**	04 01 04	**04 04 01**	27	27
1371.04	1.965E-24	2.822E+01	0.0608	0.296	2129.6	0.48	0.00112	0 2 0	**0 1 0**	03 03 00	**04 04 01**	21	27
1435.86	1.243E-24	4.271E-03	0.0865	0.416	2129.6	0.73	-0.00631	0 2 0	**0 1 0**	05 01 04	**04 04 01**	33	27
1468.27	1.429E-23	7.590E+00	0.0682	0.297	2129.6	0.59	0.00121	0 2 0	**0 1 0**	04 03 02	**04 04 01**	27	27
1593.13	1.690E-23	7.051E-01	0.0753	0.320	2129.6	0.68	0.00213	0 2 0	**0 1 0**	05 03 02	**04 04 01**	33	27
1805.75	1.251E-25	5.226E-01	0.0677	0.383	2129.6	0.58	-0.00432	1 0 0	**0 1 0**	03 03 00	**04 04 01**	21	27
1827.07	1.134E-26	1.197E-02	0.0849	0.399	2129.6	0.70	-0.00657	0 0 1	**0 1 0**	03 02 02	**04 04 01**	21	27
1901.24	6.535E-25	1.602E-01	0.0746	0.375	2129.6	0.66	-0.00329	1 0 0	**0 1 0**	04 03 02	**04 04 01**	27	27
1919.94	5.567E-26	6.833E-02	0.0880	0.425	2129.6	0.74	-0.00894	1 0 0	**0 1 0**	05 01 04	**04 04 01**	33	27
1920.91	7.141E-25	8.553E+00	0.0487	0.252	2129.6	0.34	-0.00924	0 2 0	**0 1 0**	05 05 00	**04 04 01**	33	27
1936.52	3.082E-26	6.666E-03	0.0856	0.405	2129.6	0.77	-0.00498	0 0 1	**0 1 0**	04 02 02	**04 04 01**	27	27
2024.34	5.446E-25	1.409E-02	0.0802	0.393	2129.6	0.76	-0.00479	1 0 0	**0 1 0**	05 03 02	**04 04 01**	33	27
2035.87	2.860E-25	5.649E-03	0.0830	0.396	2129.6	0.67	-0.00661	0 0 1	**0 1 0**	05 02 04	**04 04 01**	33	27
2095.25	3.546E-27	1.495E+00	0.0589	0.318	2129.6	0.51	-0.00438	0 0 1	**0 1 0**	04 04 00	**04 04 01**	27	27
2215.67	1.686E-26	2.950E-01	0.0648	0.322	2129.6	0.55	-0.00102	0 0 1	**0 1 0**	05 04 02	**04 04 01**	33	27
2252.30	3.122E-25	6.533E-01	0.0495	0.267	2129.6	0.35	-0.00623	1 0 0	**0 1 0**	05 05 00	**04 04 01**	33	27
2935.85	1.565E-24	9.026E-01	0.0560	0.288	2129.6	0.46	-0.00328	0 3 0	**0 1 0**	03 03 00	**04 04 01**	21	27
3033.04	3.122E-27	2.185E-01	0.0653	0.294	2129.6	0.60	0.00017	0 3 0	**0 1 0**	04 03 02	**04 04 01**	27	27
3156.96	3.135E-26	1.701E-02	0.0803	0.439	2129.6	0.81	-0.00328	0 3 0	**0 1 0**	05 03 02	**04 04 01**	33	27
3409.20	9.037E-26	3.550E+00	0.0672	0.439	2129.6	0.55	-0.00662	1 1 0	**0 1 0**	03 03 00	**04 04 01**	21	27

Table B-8 (Continued)

Note: Column headings are defined in Appendix A.

ν	S	A	γ_{air}	γ_{self}	E''	n_{air}	δ_{air}	v'	v''	q'	q''	g'	g''
3414.65	3.816E-27	2.017E-01	0.0842	0.439	2129.6	0.70	-0.00662	0 1 1	**0 1 0**	03 02 02	**04 04 01**	21	27
3505.41	4.801E-25	4.360E-01	0.0759	0.439	2129.6	0.61	-0.00438	1 1 0	**0 1 0**	04 03 02	**04 04 01**	27	27
3523.43	3.453E-26	4.398E-02	0.0848	0.439	2129.6	0.77	-0.00585	0 1 1	**0 1 0**	04 02 02	**04 04 01**	27	27
3549.13	4.276E-25	4.929E-01	0.0542	0.439	2129.6	0.41	-0.01018	0 3 0	**0 1 0**	05 05 00	**04 04 01**	33	27
3620.06	1.715E-25	1.879E-02	0.0817	0.439	2129.6	0.67	-0.01159	0 1 1	**0 1 0**	05 02 04	**04 04 01**	33	27
3712.43	3.857E-26	7.203E+01	0.0600	0.439	2129.6	0.51	-0.00630	0 1 1	**0 1 0**	04 04 00	**04 04 01**	27	27
3833.36	1.150E-24	1.343E+01	0.0647	0.439	2129.6	0.55	-0.00522	0 1 1	**0 1 0**	05 04 02	**04 04 01**	33	27
3896.98	1.783E-23	4.601E-02	0.0553	0.439	2129.6	0.41	-0.01370	1 1 0	**0 1 0**	05 05 00	**04 04 01**	33	27
4968.47	5.527E-24	5.622E-02	0.0844	0.379	2129.6	0.70	-0.00805	0 2 1	**0 1 0**	03 02 02	**04 04 01**	21	27
4985.04	6.979E-26	4.633E-01	0.0676	0.273	2129.6	0.55	-0.00805	1 2 0	**0 1 0**	03 03 00	**04 04 01**	21	27
5075.82	1.303E-25	7.980E-02	0.0851	0.308	2129.6	0.77	-0.00743	0 2 1	**0 1 0**	04 02 02	**04 04 01**	27	27
5305.57	1.815E-24	3.005E+01	0.0660	0.261	2129.6	0.51	-0.02000	0 2 1	**0 1 0**	04 04 00	**04 04 01**	27	27
5426.77	2.263E-23	6.258E+00	0.0651	0.262	2129.6	0.55	-0.00665	0 2 1	**0 1 0**	05 04 02	**04 04 01**	33	27
5777.39	5.164E-26	3.269E-02	0.0581	0.320	2129.6	0.41	-0.02000	2 0 0	**0 1 0**	05 05 00	**04 04 01**	33	27
6877.00	2.078E-26	4.348E+00	0.0610	0.250	2129.6	0.51	-0.00952	0 3 1	**0 1 0**	04 04 00	**04 04 01**	27	27
6928.32	1.452E-25	1.653E+00	0.0695	0.320	2129.6	0.55	-0.01274	2 1 0	**0 1 0**	03 03 00	**04 04 01**	21	27
6998.36	5.527E-26	8.654E-01	0.0655	0.439	2129.6	0.55	-0.00808	0 3 1	**0 1 0**	05 04 02	**04 04 01**	33	27
7175.92	4.881E-24	1.748E+01	0.0625	0.439	2129.6	0.51	-0.01320	1 1 1	**0 1 0**	04 04 00	**04 04 01**	27	27
7294.77	1.226E-25	4.782E+00	0.0667	0.439	2129.6	0.55	-0.01134	1 1 1	**0 1 0**	05 04 02	**04 04 01**	33	27
8429.90	3.994E-25	1.674E-01	0.0616	0.439	2129.6	0.51	-0.01113	0 4 1	**0 1 0**	04 04 00	**04 04 01**	27	27
	Sum =	214.959	3.033	16.099									

APPENDIX C: Mathematica® Notebooks for $4_{2,2} \rightarrow 5_{1,5}$ and $5_{3,2} \rightarrow 4_{4,1}$ Cases

In[112]:=
```
(* 422 → 515 transition  *)

(* Clear memory and define symbol objects  *)
Remove["Global`*"]
Needs["Notation`"];
Symbolize[ n_ ]; Symbolize[ ϕ_ ]; Symbolize[ rp_ ]; Symbolize[ g_ ]; Symbolize[ _0 ];
Symbolize[ _air ]; Symbolize[ _wv ]; Symbolize[ _atm ]; Symbolize[ α_ ]; Symbolize[ k_B ];
Symbolize[ _ox ]; Symbolize[ P_h0 ]; Symbolize[ T_p ]; Symbolize[ T_US ]; Symbolize[ T_h0 ];
Symbolize[ g_1 ]; Symbolize[ g_2 ]; Symbolize[ B_ν ]; Symbolize[ A_ν ]; Symbolize[ τ_ ];
Symbolize[ N_crit ]; Symbolize[ R_p,crit ]; Symbolize[ E_bd ]; Symbolize[ sumA_ν ];
Symbolize[ ∇ ]; Symbolize[ MW_air ]; Symbolize[ η_∞ ]; Symbolize[ ρ_∞ ]; Symbolize[ E_0 ];
Symbolize[ ρ_cloud ]; Symbolize[ b ]; Symbolize[ w_0 ]; Symbolize[ R_p ]; Symbolize[ T_atm ];
Symbolize[ L_c ]; Symbolize[ fL_am ];
```

In[122]:=
```
(* Resonant cavity  *)
Lc = 1000;                          (* Elevation of cloud deck [m] (cavity length)  *)
ρcloud = 86 / 100;                  (* Power reflectivity of cloud  *)
g1 = 1;                             (* g parameter for ground (R = ∞)  *)
(*
g2=1/2;                                                  (* g parameter for cloud  *)
Lam=100;
(* Length of active medium (V = Lam^3) *)
*)

(* Atmospheric conditions  *)
RH = 1;                             (* Atmospheric relative humidity  *)
Tatm = 296;                         (* Standard atmospheric temperature [K]  *)
Patm = 0.101325`30;                 (* Standard atmospheric pressure [MPa]  *)
Psat = 0.0026212`30;                (* Saturation pressure of H2O at 296 K [MPa]  *)

(* Maser transition  *)

(*
(* 532 → 441 transition  *)
ν̄=0.805092`30;
(* Transition wavenumber [cm^-1]  *)
γair=0.0801`30;
(* Line broadening coefficient air [cm^-1·atm^-1]  *)
γself=0.439`30;
(* Line broadening coefficient self [cm^-1·atm^-1]  *)
Aν =8.319`30*^-9;                                   (* Einstein A coefficient [s^-1]  *)
sumAν=25.088`30;                                    (* Sum of Aij, j<i  *)
*)

(* 422 → 515 transition  *)
ν̄ = 0.072059`30;            (* Transition wavenumber [cm^-1]  *)
γair = 0.0919`30;           (* Line broadening coefficient air [cm^-1·atm^-1]  *)
γself = 0.429`30;           (* Line broadening coefficient self [cm^-1·atm^-1]  *)
Aν = 5.088`30*^-12;         (* Einstein A coefficient [s^-1]  *)
sumAν = 24.173`30;          (* Sum of Aij, j<i  *)


λ = 1 / (100 ν̄);                    (* Transition wavelength [m]  *)
ν = c / λ;                          (* Transition frequency [Hz]  *)
```

In[136]:=
```
tiny = 1*^-15;
large = 1*^15;
prec = 30;

c = 299 792 458;                    (* Speed of light [m·s^-1] *)
ε0 = 8.85418782`30*^-12;            (* Permittivity of free space [m^-3·kg^-1·s^4·A^2] *)
h = 6.626068`30*^-34;               (* Planck constant [m^2·kg·s^-1] *)
kB = 1.3806503`30*^-23;             (* Boltzmann constant [m^2·kg·s^-2·K^-1] *)
q = 1.60217646`30*^-19;             (* Elementary electric charge [coulomb] *)
nA = 6.0221415`30*^23;              (* Avogadro number [mol^-1] *)

MWair = 28.9586`30;                 (* Molecular weight of air [g·mol^-1] *)
                                      (* Ref: Lemmon,
J. Phys. Chem. Ref. Data, 29, 331 (2000) *)


(* Electric field strength at beam waist.
  Energy density is proportional to 1/w0^2.  Field is proportional to 1/w0. *)

E0[g1_, g2_, p_, σ_, Lam_] := SetPrecision[(Lam/w0[g1, g2]) Sqrt[2 h ν ρω[p, σ]/(ε0 Bν τ2)], prec]
```

In[147]:=
```
(* Electric field (Ebd (kV)) for breakdown of air at microwave frequencies. *)
(* Ref: Norman Kroll and Kenneth M.Watson,
"Theoretical Study of Ionization of Air by Intense Laser Pulses,"
        Physical Review A 5,1883 (1972). *)

Ebd[v_] := SetPrecision[Sqrt[2/(c ϵ0) (1.44*^4) (1 + 2.4*^-6 v^2)], prec]

Plot[Ebd[v], {v, 0, 50}, PlotRange → {3290, 3305}, Frame → True, PlotLabel →
  "Electric field (Ebd (kV)) for breakdown of air (1 atm) at microwave frequencies.
(Ref: Kroll and Watson, Physical Review A 5, 1883 (1972))",
 FrameLabel → {Style["Microwave Frequency (v) [GHz]", 14],
   Style["Electric Field Strength [kV/m]", 14]}]
```

Out[148]=

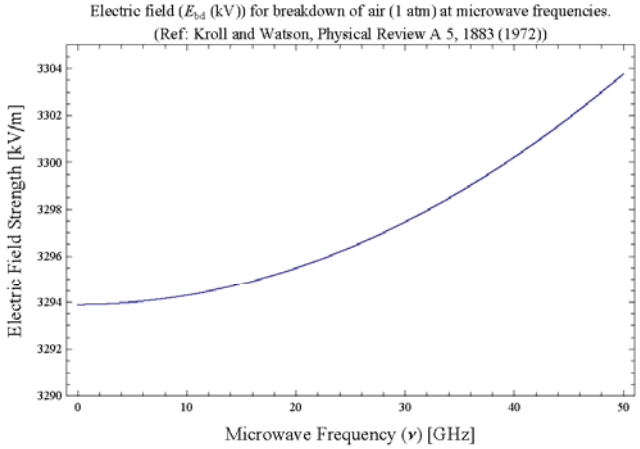

In[149]:=
```
(*  Absorption coefficient of water vapor

      αwv[ν,P,T,RH] = Power absorption coefficient [Np/m]
       ν = Frequency [GHz]
       P = Pressure [MPa]
       T = Temperature [K]
       RH = Relative humidity [-],  0 ≤ RH ≤ 1

    Ref:  S.Shambayati, Atmosphere Attenutation and Noise Temperature at
    Microwave Frequencies," in Low-Noise Systems in the Deep Space Network,
    M. S. Reid (Ed.), Jet Propulsion Laboratory, California Institute of Technology,
    (2008). Available at http://descanso.jpl.nasa.gov/Monograph/series10_chapter.cfm.

    Note that αwv is a *power* absorption coefficient (Ref. F. T. Ulaby, R. K. Moore,
    A. K. Fung, Microwave Remote Sensing: Active and Passive, Vol. I: "Microwave Remote
    Sensing Fundamentals and Radiometry," Addison-Wesley (1981).
  *)

αwv[ν_, P_, T_, RH_] :=
 SetPrecision[(1*^4 Log10[Exp[1]])^-1 kwv[ν, P, T, RH] (awv[ν, P, T, RH] + 1.2*^-6), prec]

kwv[ν_, P_, T_, RH_] := 2 ν^2 ρwv[T, RH] (300/T)^1.5 γwv[P, T, RH]

awv[ν_, P_, T_, RH_] := 300/T (1/dwv[ν, P, T, RH]) Exp[-644/T]

dwv[ν_, P_, T_, RH_] := (22.2^2 - ν^2)^2 + 4 ν^2 γwv[P, T, RH]^2

γwv[P_, T_, RH_] := 2.85 (P/0.101325) (300/T)^0.626 (1 + 0.018 ρwv[T, RH] T/1013)

ρwv[T_, RH_] := RH (216.5) (6.1)/T 10^7.4475 ((T-273.15)/(T-38.45))

(* Mass density of water vapor [g/cm^3]  *)

Nwv[T_, RH_] := ρwv[T, RH] (1*^6)/MWair nA

(* Number density of water vapor [m^-3]  *)

LogLogPlot[(1*^4 Log10[Exp[1]]) αwv[ν, Patm, 300, 0.25], {ν, 1, 100},
 PlotLabel → "Water vapor absorption coefficient", Frame → True, FrameLabel →
  {"Frequency (ν) [GHz]", "Absorption coefficient (αwv) [dB/km]"}, ImageSize → 250]
```

General::ovfl : Overflow occurred in computation. >>

Out[156]=

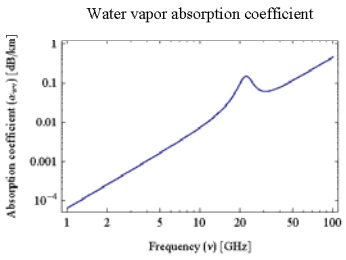

In[157]:=
```
(*  Absorption coefficient of oxygen. Valid for ν < 45 GHz.

        αox[ν,h,P,T] = Power absorption coefficient [Np/m]
        ν = Frequency [GHz]
        P = Pressure [MPa]
        T = Temperature [K]
        h = Elevation above mean sea level [km]

        Ref:  S.Shambayati, Atmosphere Attenutation and Noise Temperature at
      Microwave Frequencies," in Low-Noise Systems in the Deep Space Network,
      M. S. Reid (Ed.), Jet Propulsion Laboratory, California Institute of Technology,
      (2008). Available at http://descanso.jpl.nasa.gov/Monograph/series10_chapter.cfm.

      Note that αox is a *power* absorption coefficient (Ref. F. T. Ulaby, R. K. Moore,
      A. K. Fung, Microwave Remote Sensing: Active and Passive, Vol. I: "Microwave Remote
      Sensing Fundamentals and Radiometry," Addison-Wesley (1981).
    *)

Ph0 = 0.101325`30;
Th0 = 296;
h0 = 0;
αox[ν_, h_, P_, T_] := SetPrecision[(1*^4 Log10[Exp[1]])^-1 Cox[ν] γ0[h]
    ν^2 (P/0.101325)^2 (300/T)^2 (1/((ν - 60)^2 - γox[h, P, T]^2) + 1/(ν^2 + γox[h, P, T]^2)), prec]
Cox[ν_] := 0.011 (7.13*^-7 ν^4 - 9.2051*^-5 ν^3 + 3.280422*^-3 ν^2 - 0.01906468 ν + 1.110303146)
γox[h_, P_, T_] := γ0[h] (P/0.101325) (300/Tp[h])^0.85
γ0[h_] := Piecewise[{{0.59, P[h] > 0.0333},
   {0.59 (1 + 0.0031 (0.0333 - P[h])), (0.0025 < P[h] && P[h] ≤ 0.0333)}, {1.18, P[h] ≤ 0.0025}}]
P[h_] := Ph0 Exp[(8.387 (h0 - h))/((8.387 - 0.0887 h0) (8.387 - 0.0887 h0))]
Tp[h_] := Piecewise[{{Th0 + (h - h0)/2 (Tus[h0 + 2] - Th0), (h0 ≤ h && h <= h0 + 2)},
   {Tus[h], (h0 + 2 ≤ h && h ≤ 20)}, {217, 20 < h < 30}}, 217]
Tus[h_] := Piecewise[{{288.16 - 6.5 h, 288.16 - 6.5 h > 217},
   {217, 288.16 - 6.5 h ≤ 217 && h < 20}}, 197 + h]
Block[{h0 = 1}, {ListPlot[{Table[{Tp[h], h}, {h, h0, 30, 0.1}],
    Table[{Tus[h], h}, {h, h0, 30, 0.1}]}, DataRange → {200, 300},
   Joined → True, AxesOrigin → {200, 0}, PlotRange → {0, 35}, Frame → True,
   PlotLabel → "JPL/DSN model & U.S. std atmos temperature",
   FrameLabel → {"Temperature [K]", "Height above MSL [km]"}, ImageSize → 250],
  LogPlot[(1*^4 Log10[Exp[1]]) αox[ν, 0, Patm, 300], {ν, 1, 45}, PlotRange → {0.001, 0.1},
   Frame → True, PlotLabel → "O2 power absorption coefficient",
   FrameLabel → {"Frequency (ν) [GHz]", "Absorption coeff (αox) [dB/km]"}
   , ImageSize → 250]}]
```

Out[167]=

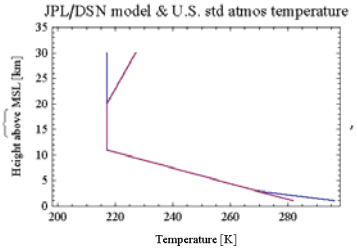
JPL/DSN model & U.S. std atmos temperature
Height above MSL [km]
Temperature [K]

,

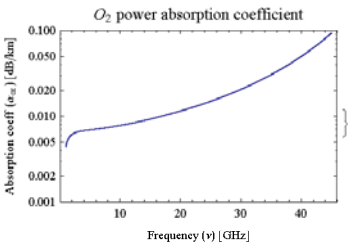
O_2 power absorption coefficient
Absorption coeff (α_{o2}) [dB/km]
Frequency (ν) [GHz]

In[168]:=
```
(* Maser cavity *)
B_ν = A_ν c^3 / (8 π ν^2);                                   (* Einstein B coefficient *)
τ_α = 1 / (α_ox[ν / 1*^9, 0, P_atm, T_atm] c);               (* O2 absorption lifetime τ_α *)
τ_ρ = -2 L_c / (c Log[ρ_cloud]);                             (* Cavity lifetime for reflectivity *)
τ_c = (1/τ_α + 1/τ_ρ)^-1;
(* Cavity lifetime for absorption and reflectivity *)

τ_rad = 1 / sumA_ν;                                          (* Radiative relaxation time τ_rad = 1/Sum[A_ij] *)
τ_nr = 1 / (100 c (γ_air (P_atm - P_sat)/P_atm + γ_self P_sat/P_atm));
(* Nonradiative relaxation time τ_nr = 1/Δν(broadening) *)
τ_2 = (1/τ_rad + 1/τ_nr)^-1;                                 (* Total upper level relaxation lifetime *)

μ = τ_c / τ_2;
(* Ratio of cavity lifetime to total relaxation lifetime *)
σ = B_ν τ_2;                                                 (* Ratio of total relaxation lifetime
                                                                to spontaneous emission lifetime *)
N_crit = 1 / (B_ν τ_c);                                      (* Critical population inversion *)
R_p,crit = 1 / (B_ν τ_c τ_2);                                (* Critical pumping rate (to achieve N_crit) *)

(* Maser beam *)
b[g1_, g2_] := 2 L_c Sqrt[g1 g2 (1 - g1 g2)] / (g1 + g2 - 2 g1 g2)   (* Confocal parameter *)
w_0[g1_, g2_] := Sqrt[c / (π ν) b[g1, g2]]                   (* Beam waist [m] *)
Print["w_0=3.236 at g2 = ", FindRoot[w_0[1, g] == 3.236, {g, tiny}]]
Plot[Sqrt[c / (π ν) b[1, g2]], {g2, 0, 1}, Frame → True, FrameLabel → {"g_2", "w_0"},
 PlotLabel → "Beam Waist w_0 = Sqrt[λ/π b[1, g2]] ", ImageSize → 250]
```

```
w_0=3.236 at g2 = {g → 0.0138545}
```

Beam Waist $w_0 = \sqrt{\frac{\lambda}{\pi}\, b[1, g2]}$

Out[182]=

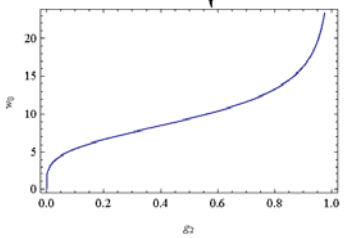

In[183]:=
```
(* Steady state solutions to maser rate equations  *)
```

$$\eta ss1[p\_, \sigma\_] := \frac{(p+1) - (p-1)\sqrt{1 + \frac{4\,p\,\sigma}{(p-1)^2}}}{2\,(1-\sigma)}$$

$$\eta ss2[p\_, \sigma\_] := \frac{(p+1) + (p-1)\sqrt{1 + \frac{4\,p\,\sigma}{(p-1)^2}}}{2\,(1-\sigma)}$$

$$\rho ss1[p\_, \sigma\_] := \frac{(p-1)}{2}\left(1 + \sqrt{1 + \frac{4\,p\,\sigma}{(p-1)^2}}\right)$$

$$\rho ss2[p\_, \sigma\_] := \frac{(p-1)}{2}\left(1 - \sqrt{1 + \frac{4\,p\,\sigma}{(p-1)^2}}\right)$$

```
ρ∞[p_, σ_] := Piecewise[{{ρss2[p, σ], p < 1}, {ρss1[p, σ], p > 1}}]
η∞[p_, σ_] := Piecewise[{{ηss2[p, σ], p < 1}, {ηss1[p, σ], p > 1}}]

{Plot[η∞[p, σ], {p, 0, 2}, ImageSize → 250,
  Frame → True, FrameLabel → {"π = Rp/Rp,crit", "n = N2/Ncrit"},
  PlotLabel → "Steady State Population Inversion"],
 Plot[ρ∞[p, σ], {p, 0, 2}, ImageSize → 250, Frame → True,
  FrameLabel → {"π = Rp/Rp,crit", "ρ = ϕBτ2"}, PlotLabel → "Steady State Photon Number"]}
```

Out[189]=

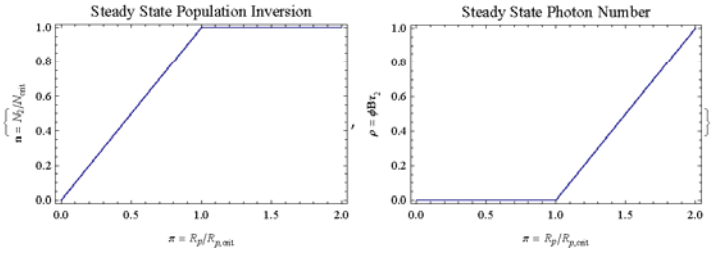

In[190]:=
```
Print["∇ = ", ∇ // N]
Print["ν = ", ν // N]
Print[]
Print["Bν = ", Bν // N]
Print["ν/(Bν τ2) = ", ν/(Bν τ2) // N]
Print["μ = τc/τ2 = ", μ // N]
Print["σ = Bν τ2 = ", σ // N]
Print[]
Print["τa = ", τa // N]
Print["τρ = ", τρ // N]
Print["τc = (1/τρ + 1/τa)^-1 = ", τc // N]
Print["τnr = ", τnr // N]
Print["τrad = ", τrad // N]
Print["τ2 = (1/τrad + 1/τnr)^-1 = ", τ2 // N]
Print[]
Print["Ncrit = 1/(Bν τc) = ", Ncrit // N]
Print["Rp,crit = 1/(Bν τc τ2) ", Rp,crit // N]
```

$\overline{\nu} = 0.072059$

$\nu = 2.16027 \times 10^{9}$

$B_\nu = 1.16883 \times 10^{-6}$

$\frac{\nu}{B_\nu \tau_2} = 5.57525 \times 10^{24}$

$\mu = \frac{\tau_c}{\tau_2} = 130745.$

$\sigma = B_\nu \tau_2 = 3.87475 \times 10^{-16}$

$\tau_\alpha = 0.00215532$

$\tau_\rho = 0.0000442326$

$\tau_c = (\frac{1}{\tau_\rho} + \frac{1}{\tau_\alpha})^{-1} = 0.000043343$

$\tau_{nr} = 3.31507 \times 10^{-10}$

$\tau_{rad} = 0.0413685$

$\tau_2 = (\frac{1}{\tau_{rad}} + \frac{1}{\tau_{nr}})^{-1} = 3.31507 \times 10^{-10}$

$N_{crit} = \frac{1}{B_\nu \tau_c} = 1.97392 \times 10^{10}$

$R_{p,crit} = \frac{1}{B_\nu \tau_c \tau_2} 5.95438 \times 10^{19}$

In[207]:=
```
(* This function returns the value for the pumping
 ratio such that the electric field strength at the beam waist
 equals the field strength to cause breakdown of the air.  *)
fp[(λ_)?NumericQ, (g2_)?NumericQ] :=
 Block[{p}, p /. FindRoot[E₀[g1, g2, p, σ, λ] / 1000 == E_bd[ν / 1*^9],
     {p, 1 + tiny}, WorkingPrecision → prec]]

(* Test the function *)
g2 = 3 / 4;
λ = 200;
FindRoot[E₀[g1, g2, p, σ, λ] / 1000 == E_bd[ν / 1*^9], {p, 2}, WorkingPrecision → prec] // N
fp[200, g2] // N
ρ∞[fp[200, g2], σ] // N
Print["E₀[g1,g2,fp[200,g2],σ,λ] = ", E₀[g1, g2, fp[200, g2], σ, λ] / 1000 // N, " kV/m"]
Print["E_bd[ν = ", ν / 1*^9 // N, " GHz] = ", E_bd[ν / 1*^9] // N, " kV/m"]

fp[10, 3 / 4] // N
fp[100, 3 / 4] // N
fp[500, 3 / 4] // N

tickRange = {7.96*^6, 1.99*^8, 1.99*^10};

Show[{LogLinearPlot[E_bd[ν / 1*^9], {p, 1*^3, 5*^11}, Frame → True, PlotRange → {0, 4000},
   PlotStyle → {Black, Dashed}, FrameTicks → {{Automatic, Automatic}, {tickRange, None}},
   FrameLabel → {"Pumping Ratio", "Electric Field (kV/m)"},
   PlotLabel → "Test Case: λ = {10,100,500}, g2 = 3/4"],
  LogLinearPlot[E₀[g1, g2, p, σ, 10] / 1000, {p, 1*^3, 5*^11}, Frame → True, PlotRange →
    {0, 4000}, PlotStyle → Red, FrameTicks → {{Automatic, Automatic}, {tickRange, None}},
   FrameLabel → {"Pumping Ratio", "Electric Field (kV/m)"},
   PlotLabel → "Test Case: λ = {10,100,500}, g2 = 3/4"], LogLinearPlot[
   E₀[g1, g2, p, σ, 100] / 1000, {p, 1*^3, 5*^11}, Frame → True, PlotRange → {0, 4000},
   PlotStyle → Blue, FrameTicks → {{Automatic, Automatic}, {tickRange, None}},
   FrameLabel → {"Pumping Ratio", "Electric Field (kV/m)"},
   PlotLabel → "Test Case: λ = {10,100,500}, g2 = 3/4"], LogLinearPlot[
   E₀[g1, g2, p, σ, 500] / 1000, {p, 1*^3, 5*^11}, Frame → True, PlotRange → {0, 4000},
   PlotStyle → Green, FrameTicks → {{Automatic, Automatic}, {tickRange, None}},
   FrameLabel → {"Pumping Ratio", "Electric Field (kV/m)"},
   PlotLabel → "Test Case: λ = {10,100,500}, g2 = 3/4"]}]
```

Out[210]= $\{p \to 4.97415 \times 10^7\}$

Out[211]= 4.97415×10^7

Out[212]= 4.97415×10^7

E₀[g1,g2,fp[200,g2],σ,λ] = 3293.93 kV/m

E_bd[ν = 2.16027 GHz] = 3293.93 kV/m

Out[215]= 1.98966×10^{10}

Out[216]= 1.98966×10^8

Out[217]= 7.95864×10^6

Out[219]=

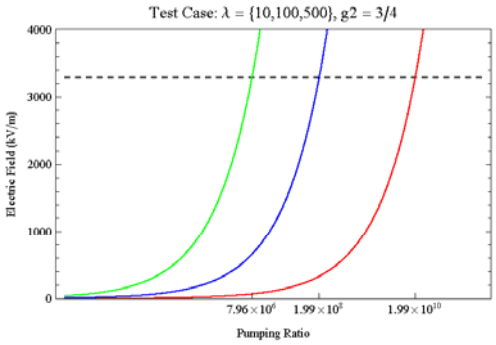

In[220]:=
```
Plot[{fp[Lc / 4, g2], fp[Lc / 3, g2], fp[Lc / 2, g2]}, {g2, 0, 1 - tiny}, PlotPoints → 20,
 PlotRange → Automatic, Frame → True, FrameLabel → {"g Parameter of Cloud", "Rp/Rp,crit"},
 Epilog → {Inset[Style["Lam=Lc/4"], {0.5, 2.3*^7}],
   Inset[Style["Lam=Lc/3"], {0.65, 1.85*^7}], Inset[Style["Lam=Lc/2"], {0.8, 1.4*^7}]}]
```

Out[220]=

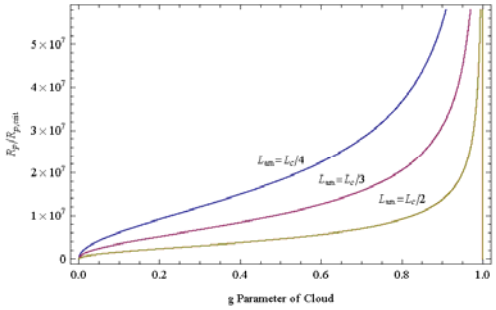

In[221]:=
```
Plot[{fp[λ, 0.9], fp[λ, 0.7], fp[λ, 0.5]}, {λ, Lc / 2, Lc},
 PlotPoints → 20, PlotRange → Automatic, Frame → True,
 FrameLabel → {"Length of Active Medium [m]", "Rp/Rp,crit"},
 Epilog → {Inset[Style["g2=0.9"], {650, 9.5*^6}],
   Inset[Style["g2=0.7"], {620, 5.7*^6}], Inset[Style["g2=0.5"], {600, 4*^6}]}]
```

Out[221]=

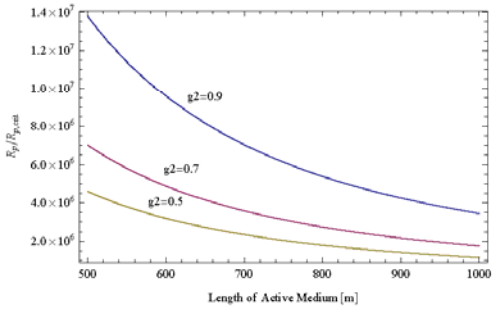

14| WaterLine_422-515.nb

In[222]:=
```
Plot3D[fp[λ, g2], {λ, 5, L_C / 2}, {g2, 0, 0.9999}, PlotPoints → 50,
 PlotRange → {0, 5*^7}, ClippingStyle → None, ViewPoint → {2, -1, 1.2},
 AxesEdge → {{-1, -1}, {1, -1}, {-1, -1}}, ImageSize → 800,
 ColorFunction → Function[{x, y, z}, RGBColor[Exp[-z / 2], Exp[-z / 2], Exp[-z / 2]]],
 RegionFunction → Function[{x, y, z}, (y < x / 100)],
 AxesLabel → {Rotate[Style["Size of Active Volume [m]", 14], 0 Degree], Rotate[Style["
              g Parameter of Cloud", 14], 0 Degree],
   Rotate[Style["R_p/R_p,crit     ", 14], 0 Degree]}, MeshFunctions -> {#1 &, #2 &, #3 &},
 Mesh → {50 {0, 0.5, 1, 1.5, 2, 2.5, 3, 3.5, 4, 4.5, 5, 5.5, 6, 6.5, 7, 7.5, 8, 8.5, 9, 9.5, 10},
   {0, 0.1, 0.2, 0.3, 0.4, 0.5, 0.6, 0.7, 0.8, 0.9, 1.0},
   5*^7 {0, 0.1, 0.2, 0.3, 0.4, 0.5, 0.6, 0.7, 0.8, 0.9, 1.0}},
 MeshStyle → {Black, Black, Directive[Blue, Thick]}, Ticks →
  {50 {0, 1, 2, 3, 4, 5, 6, 7, 8, 9, 10}, {0, 0.1, 0.2, 0.3, 0.4, 0.5, 0.6, 0.7, 0.8, 0.9, 1.0},
   {{0.5*^7, ""}, {1*^7, "1x10^7"}, {1.5*^7, ""}, {2*^7, "2x10^7"}, {2.5*^7, ""},
    {3*^7, "3x10^7"}, {3.5*^7, ""}, {4*^7, "4x10^7"}, {4.5*^7, ""}, {5*^7, "5x10^7"}}}]
```

Out[222]=

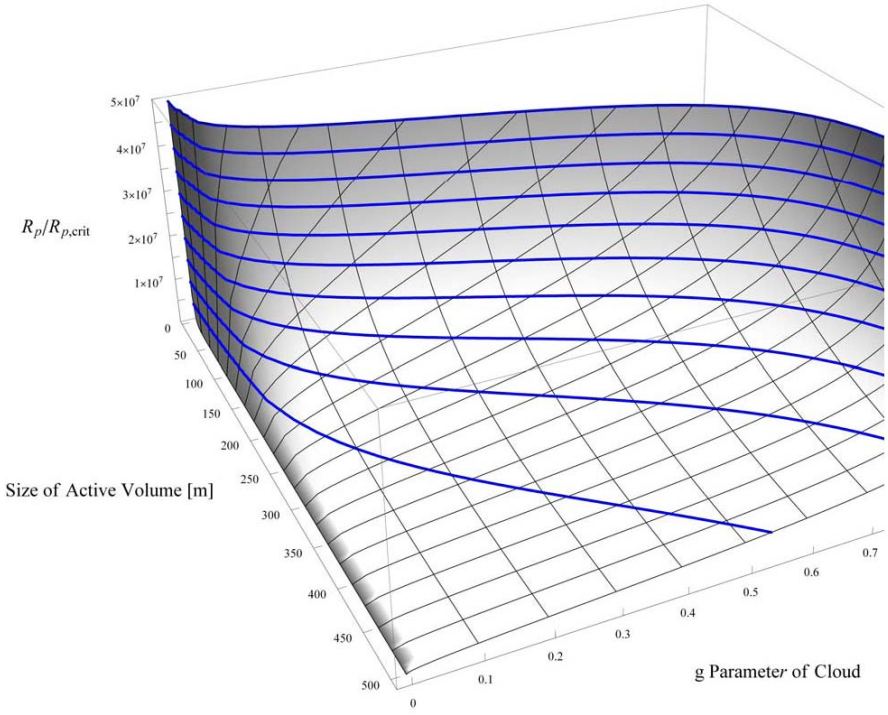

In[223]:=
```
(* 532 → 441 transition  *)

(* Clear memory and define symbol objects  *)
Remove["Global`*"]
Needs["Notation`"];
Symbolize[ n_ ]; Symbolize[ ϕ_ ]; Symbolize[ rp_ ]; Symbolize[ g_ ]; Symbolize[ _0 ];
Symbolize[ _air ]; Symbolize[ _wv ]; Symbolize[ _atm ]; Symbolize[ α_ ]; Symbolize[ k_B ];
Symbolize[ _ox ]; Symbolize[ P_h0 ]; Symbolize[ T_p ]; Symbolize[ T_US ]; Symbolize[ T_h0 ];
Symbolize[ g_1 ]; Symbolize[ g_2 ]; Symbolize[ B_ν ]; Symbolize[ A_ν ]; Symbolize[ τ_ ];
Symbolize[ N_crit ]; Symbolize[ R_p,crit ]; Symbolize[ E_bd ]; Symbolize[ sumA_ν ];
Symbolize[ ∇ ]; Symbolize[ MW_air ]; Symbolize[ η_∞ ]; Symbolize[ ρ_∞ ]; Symbolize[ E_0 ];
Symbolize[ ρ_cloud ]; Symbolize[ b ]; Symbolize[ w_0 ]; Symbolize[ R_p ]; Symbolize[ T_atm ];
Symbolize[ L_c ]; Symbolize[ fL_am ];
```

In[233]:=
```
(* Resonant cavity  *)
L_c = 1000;                          (* Elevation of cloud deck [m] (cavity length)  *)
ρ_cloud = 86 / 100;                  (* Power reflectivity of cloud  *)
g1 = 1;                              (* g parameter for ground (R = ∞)  *)
(*
g2=1/2;                                                  (* g parameter for cloud  *)
L_am=100;
(* Length of active medium (V = L_am^3) *)
*)

(* Atmospheric conditions  *)
RH = 1;                              (* Atmospheric relative humidity  *)
T_atm = 296;                         (* Standard atmospheric temperature [K]  *)
P_atm = 0.101325`30;                 (* Standard atmospheric pressure [MPa]  *)
P_sat = 0.0026212`30;                (* Saturation pressure of H2O at 296 K [MPa]  *)

(* Maser transition  *)

(* 532 → 441 transition  *)
ν̄ = 0.805092`30;                     (* Transition wavenumber [cm^-1]  *)
γ_air = 0.0801`30;                   (* Line broadening coefficient air [cm^-1 · atm^-1]  *)
γ_self = 0.439`30;                   (* Line broadening coefficient self [cm^-1 · atm^-1]  *)
A_ν = 8.319`30*^-9;                  (* Einstein A coefficient [s^-1]  *)
sumA_ν = 25.088`30;                  (* Sum of A_ij, j<i  *)

(*
(* 422 → 515 transition  *)
ν̄=0.072059`30;                       (* Transition wavenumber [cm^-1]  *)
γ_air=0.0919`30;                     (* Line broadening coefficient air [cm^-1 · atm^-1]  *)
γ_self=0.429`30;                     (* Line broadening coefficient self [cm^-1 · atm^-1]  *)
A_ν =5.088`30*^-12;                  (* Einstein A coefficient [s^-1]  *)
sumA_ν=24.173`30;                    (* Sum of A_ij, j<i  *)
*)

λ = 1 / (100 ν̄);                     (* Transition wavelength [m]  *)
ν = c / λ;                           (* Transition frequency [Hz]  *)
```

In[247]:=
```
tiny = 1*^-15;
large = 1*^15;
prec = 30;

c = 299 792 458;                    (* Speed of light [m·s^-1] *)
ε0 = 8.85418782`30*^-12;            (* Permittivity of free space [m^-3·kg^-1·s^4·A^2] *)
h = 6.626068`30*^-34;               (* Planck constant [m^2·kg·s^-1] *)
kB = 1.3806503`30*^-23;             (* Boltzmann constant [m^2·kg·s^-2·K^-1] *)
q = 1.60217646`30*^-19;             (* Elementary electric charge [coulomb] *)
nA = 6.0221415`30*^23;              (* Avogadro number [mol^-1] *)

MWair = 28.9586`30;                 (* Molecular weight of air [g·mol^-1] *)
                                      (* Ref: Lemmon,
J. Phys. Chem. Ref. Data, 29, 331 (2000) *)


(* Electric field strength at beam waist.
  Energy density is proportional to 1/w0^2.  Field is proportional to 1/w0.  *)

E0[g1_, g2_, p_, σ_, Lam_] := SetPrecision[(Lam/w0[g1, g2]) Sqrt[2 h ν ρm[p, σ]/(ε0 Bν τ2)], prec]
```

In[258]:=
```
(* Electric field (Ebd (kV)) for breakdown of air at microwave frequencies. *)
(* Ref: Norman Kroll and Kenneth M.Watson,
"Theoretical Study of Ionization of Air by Intense Laser Pulses,"
        Physical Review A 5,1883 (1972). *)

Ebd[v_] := SetPrecision[Sqrt[2/(c ϵ0) (1.44*^4) (1 + 2.4*^-6 v^2)], prec]

Plot[Ebd[v], {v, 0, 50}, PlotRange → {3290, 3305}, Frame → True, PlotLabel →
  "Electric field (Ebd (kV)) for breakdown of air (1 atm) at microwave frequencies.
(Ref: Kroll and Watson, Physical Review A 5, 1883 (1972))",
 FrameLabel → {Style["Microwave Frequency (v) [GHz]", 14],
   Style["Electric Field Strength [kV/m]", 14]}]
```

Out[259]=

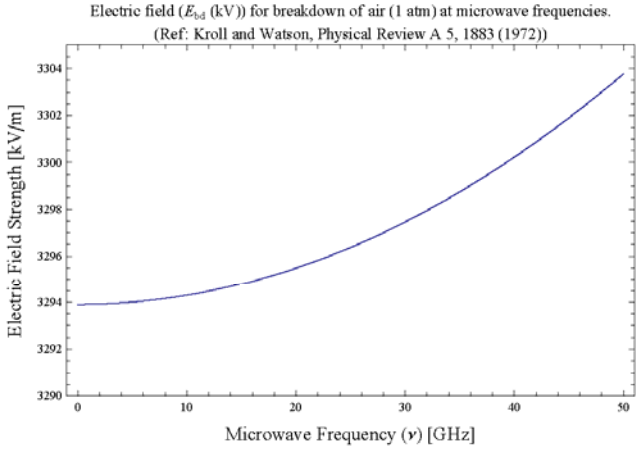

In[260]:=
```
(*  Absorption coefficient of water vapor

      αwv[ν,P,T,RH] = Power absorption coefficient [Np/m]
       ν = Frequency [GHz]
       P = Pressure [MPa]
       T = Temperature [K]
       RH = Relative humidity [-],  0 ≤ RH ≤ 1

    Ref:  S.Shambayati, Atmosphere Attenutation and Noise Temperature at
    Microwave Frequencies," in Low-Noise Systems in the Deep Space Network,
    M. S. Reid (Ed.), Jet Propulsion Laboratory, California Institute of Technology,
    (2008). Available at http://descanso.jpl.nasa.gov/Monograph/series10_chapter.cfm.

    Note that αwv is a *power* absorption coefficient (Ref. F. T. Ulaby, R. K. Moore,
    A. K. Fung, Microwave Remote Sensing: Active and Passive, Vol. I: "Microwave Remote
    Sensing Fundamentals and Radiometry," Addison-Wesley (1981).
  *)

αwv[ν_, P_, T_, RH_] :=
 SetPrecision[(1*^4 Log10[Exp[1]])^-1 kwv[ν, P, T, RH] (awv[ν, P, T, RH] + 1.2*^-6), prec]

kwv[ν_, P_, T_, RH_] := 2 ν^2 ρwv[T, RH] (300/T)^1.5 γwv[P, T, RH]

awv[ν_, P_, T_, RH_] := 300/T (1/dwv[ν, P, T, RH]) Exp[-644/T]

dwv[ν_, P_, T_, RH_] := (22.2^2 - ν^2)^2 + 4 ν^2 γwv[P, T, RH]^2

γwv[P_, T_, RH_] := 2.85 (P/0.101325) (300/T)^0.626 (1 + 0.018 ρwv[T, RH] T/1013)

ρwv[T_, RH_] := RH (216.5) (6.1)/T 10^7.4475 ((T-273.15)/(T-38.45))

(* Mass density of water vapor [g/cm^3]  *)

Nwv[T_, RH_] := ρwv[T, RH] (1*^6)/MWair nA

(* Number density of water vapor [m^-3]  *)

LogLogPlot[(1*^4 Log10[Exp[1]]) αwv[ν, Patm, 300, 0.25], {ν, 1, 100},
 PlotLabel → "Water vapor absorption coefficient", Frame → True, FrameLabel →
  {"Frequency (ν) [GHz]", "Absorption coefficient (αwv) [dB/km]"}, ImageSize → 250]
```

General::ovfl : Overflow occurred in computation. >>

Out[267]=

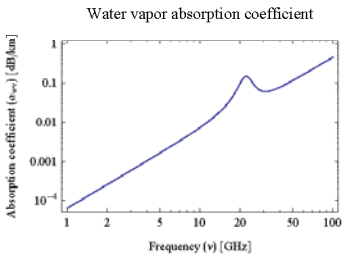

In[268]:=
```
(*  Absorption coefficient of oxygen. Valid for ν < 45 GHz.

        α_ox[ν,h,P,T] = Power absorption coefficient [Np/m]
        ν = Frequency [GHz]
        P = Pressure [MPa]
        T = Temperature [K]
        h = Elevation above mean sea level [km]

        Ref:  S.Shambayati, Atmosphere Attenutation and Noise Temperature at
      Microwave Frequencies," in Low-Noise Systems in the Deep Space Network,
      M. S. Reid (Ed.), Jet Propulsion Laboratory, California Institute of Technology,
      (2008). Available at http://descanso.jpl.nasa.gov/Monograph/series10_chapter.cfm.

      Note that α_ox is a *power* absorption coefficient (Ref. F. T. Ulaby, R. K. Moore,
      A. K. Fung, Microwave Remote Sensing: Active and Passive, Vol. I: "Microwave Remote
      Sensing Fundamentals and Radiometry," Addison-Wesley (1981).
    *)

P_h0 = 0.101325`30;
T_h0 = 296;
h_0 = 0;
α_ox[ν_, h_, P_, T_] := SetPrecision[(1*^4 Log10[Exp[1]])^-1 C_ox[ν] γ_0[h]
    ν^2 (P/0.101325)^2 (300/T)^2 (1/((ν - 60)^2 - γ_ox[h, P, T]^2) + 1/(ν^2 + γ_ox[h, P, T]^2)), prec]
C_ox[ν_] := 0.011 (7.13*^-7 ν^4 - 9.2051*^-5 ν^3 + 3.280422*^-3 ν^2 - 0.01906468 ν + 1.110303146)
γ_ox[h_, P_, T_] := γ_0[h] (P/0.101325) (300/T_p[h])^0.85
γ_0[h_] := Piecewise[{{0.59, P[h] > 0.0333},
   {0.59 (1 + 0.0031 (0.0333 - P[h])), (0.0025 < P[h] && P[h] ≤ 0.0333)}, {1.18, P[h] ≤ 0.0025}}]
P[h_] := P_h0 Exp[8.387 (h_0 - h)/((8.387 - 0.0887 h_0) (8.387 - 0.0887 h_0))]
T_p[h_] := Piecewise[{{T_h0 + (h - h_0)/2 (T_us[h_0 + 2] - T_h0), (h_0 ≤ h && h <= h_0 + 2)},
   {T_us[h], (h_0 + 2 ≤ h && h ≤ 20)}, {217, 20 < h < 30}}, 217]
T_us[h_] := Piecewise[{{288.16 - 6.5 h, 288.16 - 6.5 h > 217},
   {217, 288.16 - 6.5 h ≤ 217 && h < 20}}, 197 + h]
Block[{h_0 = 1}, {ListPlot[{Table[{T_p[h], h}, {h, h_0, 30, 0.1}],
    Table[{T_us[h], h}, {h, h_0, 30, 0.1}]}, DataRange → {200, 300},
   Joined → True, AxesOrigin → {200, 0}, PlotRange → {0, 35}, Frame → True,
   PlotLabel → "JPL/DSN model & U.S. std atmos temperature",
   FrameLabel → {"Temperature [K]", "Height above MSL [km]"}, ImageSize → 250],
  LogPlot[(1*^4 Log10[Exp[1]]) α_ox[ν, 0, P_atm, 300], {ν, 1, 45}, PlotRange → {0.001, 0.1},
   Frame → True, PlotLabel → "O2 power absorption coefficient",
   FrameLabel → {"Frequency (ν) [GHz]", "Absorption coeff (α_ox) [dB/km]"}
   , ImageSize → 250]}]
```

Out[278]=

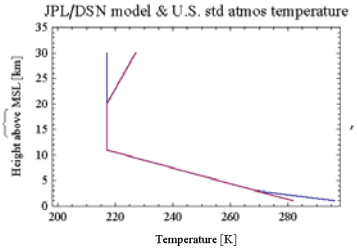

,

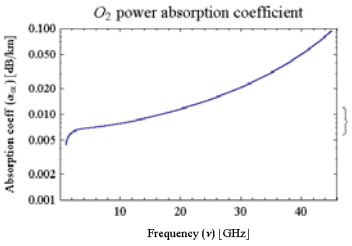

}

In[279]:=
```
(* Maser cavity *)

Bν = Aν c^3 / (8 π ν^2);                                   (* Einstein B coefficient *)

τα = 1 / (αox[ν / 1*^9, 0, Patm, Tatm] c);                 (* O2 absorption lifetime τα *)

τρ = -2 Lc / (c Log[ρcloud]);                              (* Cavity lifetime for reflectivity *)

τc = (1/τα + 1/τρ)^-1;
(* Cavity lifetime for absorption and reflectivity *)

τrad = 1 / sumAν;                                          (* Radiative relaxation time τrad = 1/Sum[Aij] *)

τnr = 1 / (100 c (γair (Patm - Psat)/Patm + γself Psat/Patm));
(* Nonradiative relaxation time τnr = 1/Δν(broadening) *)

τ2 = (1/τrad + 1/τnr)^-1;                                  (* Total upper level relaxation lifetime *)

μ = τc / τ2;
(* Ratio of cavity lifetime to total relaxation lifetime *)
σ = Bν τ2;                                                 (* Ratio of total relaxation lifetime
                                                              to spontaneous emission lifetime *)

Ncrit = 1 / (Bν τc);                                       (* Critical population inversion *)

Rp,crit = 1 / (Bν τc τ2);                                  (* Critical pumping rate (to achieve Ncrit) *)

(* Maser beam *)

b[g1_, g2_] := 2 Lc Sqrt[g1 g2 (1 - g1 g2)] / (g1 + g2 - 2 g1 g2)
                                                           (* Confocal parameter *)

w0[g1_, g2_] := Sqrt[c / (π ν) b[g1, g2]]                  (* Beam waist [m] *)

Print["w0=3.236 at g2 = ", FindRoot[w0[1, g] == 3.236, {g, tiny}]]

Plot[Sqrt[c / (π ν) b[1, g2]], {g2, 0, 1}, Frame → True, FrameLabel → {"g2", "w0"},
 PlotLabel → "Beam Waist w0 = Sqrt[λ/π b[1, g2]] ", ImageSize → 250]
```

```
w0=3.236 at g2 = {g → 0.636857}
```

Beam Waist $w_0 = \sqrt{\frac{\lambda}{\pi}\, b[1, g2]}$

Out[293]=

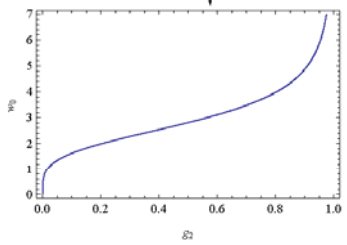

In[294]:=
```
(* Steady state solutions to maser rate equations  *)

ηss1[p_, σ_] := ((p + 1) - (p - 1) Sqrt[1 + 4 p σ/(p - 1)^2])/(2 (1 - σ))

ηss2[p_, σ_] := ((p + 1) + (p - 1) Sqrt[1 + 4 p σ/(p - 1)^2])/(2 (1 - σ))

ρss1[p_, σ_] := ((p - 1)/2) (1 + Sqrt[1 + 4 p σ/(p - 1)^2])

ρss2[p_, σ_] := ((p - 1)/2) (1 - Sqrt[1 + 4 p σ/(p - 1)^2])

ρ∞[p_, σ_] := Piecewise[{{ρss2[p, σ], p < 1}, {ρss1[p, σ], p > 1}}]
η∞[p_, σ_] := Piecewise[{{ηss2[p, σ], p < 1}, {ηss1[p, σ], p > 1}}]

{Plot[η∞[p, σ], {p, 0, 2}, ImageSize → 250,
  Frame → True, FrameLabel → {"π = Rp/Rp,crit", "n = N2/Ncrit"},
  PlotLabel → "Steady State Population Inversion"],
 Plot[ρ∞[p, σ], {p, 0, 2}, ImageSize → 250, Frame → True,
  FrameLabel → {"π = Rp/Rp,crit", "ρ = ϕBτ2"}, PlotLabel → "Steady State Photon Number"]}
```

Out[300]=

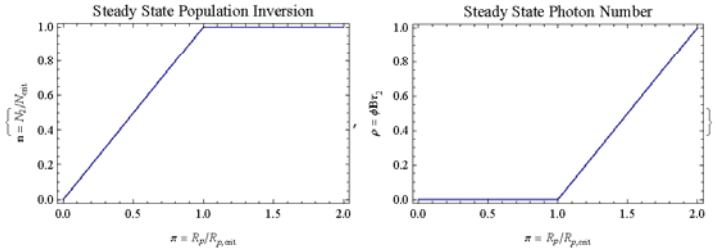

In[301]:=
```
Print["∇ = ", ∇ // N]
Print["v = ", v // N]
Print[]
Print["Bv = ", Bv // N]
Print["v/(Bv τ2) = ", v/(Bv τ2) // N]
Print["μ = τc/τ2 = ", μ // N]
Print["σ = Bv τ2 = ", σ // N]
Print[]
Print["τa = ", τa // N]
Print["τρ = ", τρ // N]
Print["τc = (1/τρ + 1/τa)^-1 = ", τc // N]
Print["τnr = ", τnr // N]
Print["τrad = ", τrad // N]
Print["τ2 = (1/τrad + 1/τnr)^-1 = ", τ2 // N]
Print[]
Print["Ncrit = 1/(Bv τc) = ", Ncrit // N]
Print["Rp,crit = 1/(Bv τc τ2) ", Rp,crit // N]
```

$\overline{\nu} = 0.805092$

$\nu = 2.41361 \times 10^{10}$

$B_\nu = 0.0000153095$

$\frac{\nu}{B_\nu \tau_2} = 4.22462 \times 10^{24}$

$\mu = \frac{\tau_c}{\tau_2} = 113467.$

$\sigma = B_\nu \tau_2 = 5.71318 \times 10^{-15}$

$\tau_\alpha = 0.000991558$

$\tau_\rho = 0.0000442326$

$\tau_c = (\frac{1}{\tau_\rho} + \frac{1}{\tau_\alpha})^{-1} = 0.0000423436$

$\tau_{nr} = 3.73179 \times 10^{-10}$

$\tau_{rad} = 0.0398597$

$\tau_2 = (\frac{1}{\tau_{rad}} + \frac{1}{\tau_{nr}})^{-1} = 3.73179 \times 10^{-10}$

$N_{crit} = \frac{1}{B_\nu \tau_c} = 1.54259 \times 10^{9}$

$R_{p,crit} = \frac{1}{B_\nu \tau_c \tau_2} \; 4.13365 \times 10^{18}$

In[318]:=
```
(* This function returns the value for the pumping
 ratio such that the electric field strength at the beam waist
 equals the field strength to cause breakdown of the air.  *)
fp[(λ_)?NumericQ, (g2_)?NumericQ] :=
 Block[{p}, p /. FindRoot[E₀[g1, g2, p, σ, λ] / 1000 == E_bd[ν / 1*^9],
     {p, 1 + tiny}, WorkingPrecision → prec]]

(* Test the function *)
g2 = 3 / 4;
λ = 200;
FindRoot[E₀[g1, g2, p, σ, λ] / 1000 == E_bd[ν / 1*^9], {p, 2}, WorkingPrecision → prec] // N
fp[200, g2] // N
ρ∞[fp[200, g2], σ] // N
Print["E₀[g1,g2,fp[200,g2],σ,λ] = ", E₀[g1, g2, fp[200, g2], σ, λ] / 1000 // N, " kV/m"]
Print["E_bd[ν = ", ν / 1*^9 // N, " GHz] = ", E_bd[ν / 1*^9] // N, " kV/m"]

fp[10, 3 / 4] // N
fp[100, 3 / 4] // N
fp[500, 3 / 4] // N

tickRange = {9.41*^5, 2.35*^7, 2.35*^9};

Show[{LogLinearPlot[E_bd[ν / 1*^9], {p, 1*^3, 5*^11}, Frame → True, PlotRange → {0, 4000},
   PlotStyle → {Black, Dashed}, FrameTicks → {{Automatic, Automatic}, {tickRange, None}},
   FrameLabel → {"Pumping Ratio", "Electric Field (kV/m)"},
   PlotLabel → "Test Case: λ = {10,100,500}, g2 = 3/4"],
  LogLinearPlot[E₀[g1, g2, p, σ, 10] / 1000, {p, 1*^3, 5*^11}, Frame → True, PlotRange →
    {0, 4000}, PlotStyle → Red, FrameTicks → {{Automatic, Automatic}, {tickRange, None}},
   FrameLabel → {"Pumping Ratio", "Electric Field (kV/m)"},
   PlotLabel → "Test Case: λ = {10,100,500}, g2 = 3/4"], LogLinearPlot[
   E₀[g1, g2, p, σ, 100] / 1000, {p, 1*^3, 5*^11}, Frame → True, PlotRange → {0, 4000},
   PlotStyle → Blue, FrameTicks → {{Automatic, Automatic}, {tickRange, None}},
   FrameLabel → {"Pumping Ratio", "Electric Field (kV/m)"},
   PlotLabel → "Test Case: λ = {10,100,500}, g2 = 3/4"], LogLinearPlot[
   E₀[g1, g2, p, σ, 500] / 1000, {p, 1*^3, 5*^11}, Frame → True, PlotRange → {0, 4000},
   PlotStyle → Green, FrameTicks → {{Automatic, Automatic}, {tickRange, None}},
   FrameLabel → {"Pumping Ratio", "Electric Field (kV/m)"},
   PlotLabel → "Test Case: λ = {10,100,500}, g2 = 3/4"]}]
```

Out[321]= $\{p \to 5.88356 \times 10^6\}$

Out[322]= 5.88356×10^6

Out[323]= 5.88356×10^6

$E_0[g1,g2,fp[200,g2],\sigma,\lambda]$ = 3296.21 kV/m

$E_{bd}[\nu$ = 24.1361 GHz] = 3296.21 kV/m

Out[326]= 2.35342×10^9

Out[327]= 2.35342×10^7

Out[328]= 941370.

Out[330]=

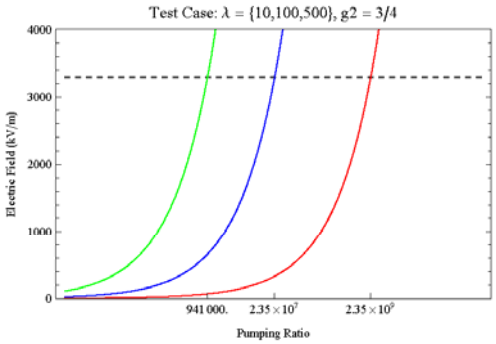

In[331]:=
```
Plot[{fp[Lc / 4, g2], fp[Lc / 3, g2], fp[Lc / 2, g2]}, {g2, 0, 1 - tiny}, PlotPoints → 20,
 PlotRange → Automatic, Frame → True, FrameLabel → {"g Parameter of Cloud", "Rp/Rp,crit"},
 Epilog → {Inset[Style["Lam=Lc/4"], {0.5, 2.8*^6}],
   Inset[Style["Lam=Lc/3"], {0.65, 2.2*^6}], Inset[Style["Lam=Lc/2"], {0.8, 1.6*^6}]}]
```

Out[331]=

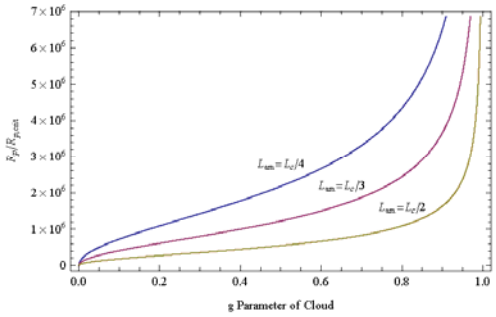

In[332]:=
```
Plot[{fp[λ, 0.9], fp[λ, 0.7], fp[λ, 0.5]}, {λ, Lc / 2, Lc},
 PlotPoints → 20, PlotRange → Automatic, Frame → True,
 FrameLabel → {"Length of Active Medium [m]", "Rp/Rp,crit"},
 Epilog → {Inset[Style["g2=0.9"], {650, 1.1*^6}],
   Inset[Style["g2=0.7"], {620, 6.5*^5}], Inset[Style["g2=0.5"], {600, 4.8*^5}]}]
```

Out[332]=

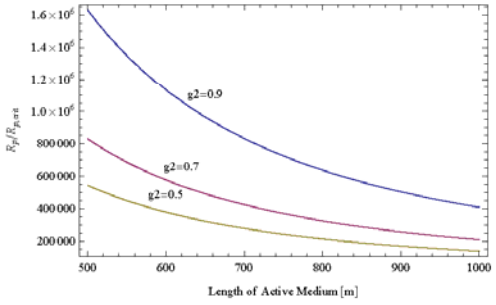

In[333]:=
```
Plot3D[fp[λ, g2], {λ, 5, L_c / 2}, {g2, 0, 0.9999}, PlotPoints → 50,
 PlotRange → {0, 5*^6}, ClippingStyle → None, ViewPoint → {2, -1, 1.2},
 AxesEdge → {{-1, -1}, {1, -1}, {-1, -1}}, ImageSize → 800,
 ColorFunction → Function[{x, y, z}, RGBColor[Exp[-z / 2], Exp[-z / 2], Exp[-z / 2]]],
 RegionFunction → Function[{x, y, z}, (y < x / 100)],
 AxesLabel → {Rotate[Style["Size of Active Volume [m]", 14], 0 Degree], Rotate[Style["
              g Parameter of Cloud", 14], 0 Degree],
   Rotate[Style["R_p/R_p,crit     ", 14], 0 Degree]}, MeshFunctions -> {#1 &, #2 &, #3 &},
 Mesh → {50 {0, 0.5, 1, 1.5, 2, 2.5, 3, 3.5, 4, 4.5, 5, 5.5, 6, 6.5, 7, 7.5, 8, 8.5, 9, 9.5, 10},
   {0, 0.1, 0.2, 0.3, 0.4, 0.5, 0.6, 0.7, 0.8, 0.9, 1.0},
   5*^6 {0, 0.1, 0.2, 0.3, 0.4, 0.5, 0.6, 0.7, 0.8, 0.9, 1.0}},
 MeshStyle → {Black, Black, Directive[Blue, Thick]}, Ticks →
  {50 {0, 1, 2, 3, 4, 5, 6, 7, 8, 9, 10}, {0, 0.1, 0.2, 0.3, 0.4, 0.5, 0.6, 0.7, 0.8, 0.9, 1.0},
   {{0.5*^6, ""}, {1*^6, "1x10^6"}, {1.5*^6, ""}, {2*^6, "2x10^6"}, {2.5*^6, ""},
    {3*^6, "3x10^6"}, {3.5*^6, ""}, {4*^6, "4x10^6"}, {4.5*^6, ""}, {5*^6, "5x10^6"}}}]
```

Out[333]=

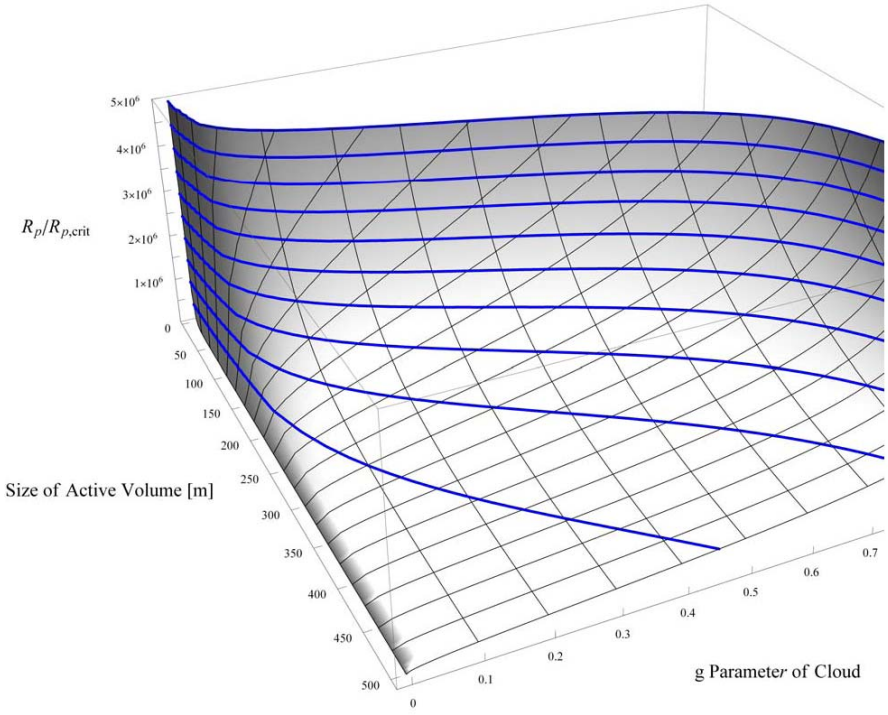

BIBLIOGRAPHY

1. Abrahamson, J., and J. Dinniss, "Ball Lightning Caused by Oxidation of Nanoparticle Networks from Normal Lightning Strikes on Soil," *Nature* **403**, 519 (2000).

2. Abrahamson, J., "Ball Lightning from Atmospheric Discharges via Metal Nanospheres Oxidation from Soils, Wood or Metals," *Philosophical Transactions of the Royal Society of London, Series A* **360**, 61 (2002).

3. Ali, A. W., "On Laser Air Breakdown, Threshold Power and Laser Generated Channel Length," NRL Memorandum Report 5187, Washington: Naval Research Laboratory, 1983.

4. Altschuler, M. D., L. L. House, and E. Hildner, "Is Ball Lightning a Nuclear Phenomenon?," *Nature* **228**, 545 (1970).

5. Anderson, P. W., "Pressure Broadening in the Microwave and Infra-Red Regions," *Physical Review* **76**, 647 (1949).

6. Annis, B. K., and A. P. Malinauskas, "Temperature Dependence of Rotational Collision Numbers from Thermal Transpiration," *Journal of Chemical Physics* **54** (11), 4763 (1971).

7. Argyle, Edward, "Ball Lightning as an Optical Illusion," *Nature* **230**, 179 (1971).

8. Ashby, D. E. T. F., and C. Whitehead, "Is Ball Lightning Caused by Antimatter Meteorites?," *Nature* **230**, 180 (1971).

9. Baker, Charles E., and Richard S. Brokaw, "Thermal Conductivities of Gaseous H_2O, D_2O, and the Equimolar H_2O-D_2O Mixture," *Journal of Chemical Physics* **40**, 1523 (1964).

10. Baranger, Michel, "General Impact Theory of Pressure Broadening," *Physical Review* **112**, 855 (1958).

11. Barnes, Peter W., Ian R. Sims, and Ian W. M. Smith,"Relaxation of H_2O from its $|04\rangle^-$ vibrational state in collisions with H_2O, Ar, H_2, N_2, and O_2," *Journal of Chemical Physics* **120**, 5592 (2004).

12. Barry, J. Dale, "Laboratory Ball Lightning," *Journal of Atmospheric and Terrestrial Physics* **30**, 313 (1968).

13. Barry, J. D., *Ball Lightning and Bead Lightning: Extreme Forms of Atmospheric Electricity*, New York: Plenum Press, 1980.

14. Bass, Henry E., John R. Olson, and Robert C. Amme, “Vibrational Relaxation in H_2O Vapor in the Temperature Range 373-946 K,” *Journal of the Acoustical Society of America* **56**, 1455 (1974).

15. Bass, H. E., Roy G. Keeton, and David Williams, “Vibrational and Rotational Relaxation in Mixtures of Water Vapor and Oxygen,” *Journal of the Acoustical Society of America* **60**, 74 (1976).

16. Ben-Reuven, A., "Impact Broadening of Microwave Spectra," *Physical Review* **145**, 7 (1966).

17. Benedict, W. S., "Identification of Water-Vapor Laser Lines," *Applied Physics Letters* **12**(5), 170 (1968).

18. Benedict, William S., Martin A. Pollack, and W. John Tomlinson III, "The Water-Vapor Laser," *IEEE Journal of Quantum Electronics* **QE-5**, 108 (1969).

19. Berger, K., “Kugelblitz und Blitsforschung,” *Naturwissenschaften* **60**, 485 (1973) (in German).

20. Bethe, H. A., and E. Teller, “Deviations from Thermal Equilibrium in Shock Waves.” (Undated document accessed March 5, 2012, from http://www.fas.org/sgp/ othergov/doe/ lanl/lib-www/la-pubs/00367149.pdf.)

21. Bird, R. Byron, Warren E. Stewart, and Edwin N. Lightfoot, *Transport Phenomena*, New York: Wiley & Sons, 1960.

22. Birnbaum, George, "Microwave Pressure Broadening and its Application to Intermolecular Forces," in *Advances in Chemical Physics*, Vol. 12, edited by Joseph O. Hirschfelder, NewYork: Wiley Interscience, 1967.

23. Boichenko, A. M., "Ball Lightning with a Lifetime t≤1 s," *Technical Physics* **44**, 1247 (1999).

24. Bollen, W. M., C. L. Yee, and M. J. Nagurney, *High Power Microwave Interaction with Air*, Report No. MRC/WDC-R-025 (Mission Research Corporation, Alexandria, Virginia, 1982). (Final report to Naval Research Laboratory, Washington, DC. Available at http://handle.dtic.mil/100.2/ ADA193917. Alternate title, "Investigation of High-Power Microwave Breakdown in Air.")

25. Braatz, J. A., C. Henkel, L. J. Greenhill, J. M. Moran, and A. S. Wilson, “A Green Bank Telescope Search for Water Masers in Nearby Active Galactic Nuclei,” *Astrophysical Jounal* **617**, L29 (2004).

26. Brand, Walther, *Der Kugelblitz* (Henri Grand, Hamburg, 1923) (in German). (An English translation exists at Walther Brand, *Ball Lightning*, NASA Technical Translation, No. NASA-TT-F-13228 (National Aeronautics and Space Administration, Washington, DC, February 1971).)

27. Bridgman, P. W., *Dimensional Analysis*, New Haven: Yale University Press, 1931.

28. Brown, Sanborn C., "Breakdown in Gases: Alternating and High-Frequency Fields," in S. Flügge, *Handbuk der Physik*, Berlin: Springer-Verlag, 1956, pp. 531-575.

29. Brown, Sanborn C., and A. D. MacDonald, "Limits for Diffusion Theory of High Frequency Gas Discharge Breakdown," *Physical Review* **76**, 1629 (1949).

30. Buckingham, E., "On Physically Similar Systems: Illustrations of the Use of Dimensional Equations," *Physical Review* **4**, 345 (1914).

31. Buldyreva, Jeanna, Nina Lavrentieva, and Vitaly Starikov, *Collisional Line Broadening and Shifting of Atmospheric Gases: A Practical Guide for Line Shape Modelling by Current Semi-Classical Approaches*. London: Imperial College Press, 2011.

32. Bychkov, V. L., "Polymer-Composite Ball Lightning," *Philosophical Transactions of the Royal Society of London, Series A* **360**, 37 (2002).

33. Cawood, W., and H. S. Patterson, "A Curious Phenomenon Shown by Highly Charged Aerosols," *Nature* **128**, 150 (1931).

34. Cazzoli, Gabrielle, Christina Puzzarini, Giovanni Buffa, Ottavio Tarrini, "Pressure-Broadening of Water Lines in the THz Frequency Region: Improvements and Confirmations for Spectroscopic Databases: Part I," *Journal of Quantitative Spectroscopy & Radiative Transfer* **109**, 2820 (2008).

35. Cecchi-Pestellini, Cesare, and Flavio Scappini, "Modeling Water Emission Induced by the Shoemaker-Levy 9/Jupiter Catastrophic Impact," *Canadian Journal of Physics* **79**, 123 (2001).

36. Cerrillo, Manuel, "Sobre las posibles interpretaciones electromagneticas del fenomeno de las centellas," *Anuario* **1**, 151 (1943) (in Spanish).

37. Chalmers, J. Alan, *Atmospheric Electricity* (Pergamon Press, New York, 1967).

38. Chapman, W. N., "After-Images and Ball Lightning," *Nature* **230**, 576 (1971).

39. Cheung, D. M., Rank, C. H. Townes, D. D. Thornton, and W. J. Welch, "Detection of Water in Interstellar Regions by its Microwave Radiation," *Nature* **221**, 626 (1969).

40. Cooray, Gerald, and Vernon Cooray, "Could Some Ball Lightning Observations be Optical Hallucinations Caused by Epileptic Seizures?" *The Open Atmospheric Science Journal* **2**, 101 (2008).

41. Cooray, Vernon, *The Lightning Flash*, Institution of Electrical Engineers, London, (2003).

42. Corney, A., *Atomic and Laser Spectroscopy*. Oxford: Clarendon Press, 1977.

43. Cosmovici, Cristiano B., Stelio Montebugnoli, Alessandro Orfei, Sergej Pogrebenko, and Pierre Colom, "First Evidence of Planetary Water Emission Induced by the Comet/Jupiter Catastrophic Impact," *Planetary and Space Science* **44**, 735 (1996).

44. Crawford, David E., Vladimir A. Rakov, Martin A. Uman, George H. Schnetzer, Keith J. Rambo, Michael V. Stapleton, and Richard J. Fisher, "The Close Lightning Environment: Dart-Leader Electric Field Change versus Distance," *Journal of Geophysical Research* **106**, 14909 (2001).

45. Crawford, J. F., "Antimatter and Ball Lightning," *Nature* **239**, 395 (1972).

46. Davies, P. C. W., "Ball Lightning or Spots Before the Eyes?," *Nature* **230**, 576 (1971).

47. De Sanctis, M., and C. Quimbay, "Derivation of the Rabi Equations by Means of the Pauli Matrices," Electronic J. Th. Phys. **20**, 235 (2009).

48. Deming, D., F. Espenak, D. Jennings, T. Kostiuk, M. Mumma, and D. Zipoy, "Observations of the 10-μm Natural Laser Emission from Mesospheres of Mars and Venus," *Icarus* **55**, 347 (1983).

49. Deming, Drake, and Michael J. Mumma, "Modeling of the 10-μm Natural Laser Emission from the Mesospheres of Mars and Venus," *Icarus* **55**, 356 (1983).

50. Dwyer, J. R. "A Fundamental Limit on Electric Fields in Air," *Geophysical Research Letters.* **30**, 2055 (2003).

51. Dwyer, J. R, Martin A. Uman, Hamid K. Rassoul, Maher Al-Dayeh, LeeCaraway, Jason Jerauld, Vladimir A. Rakov, Douglas M. Jordan, Keith J. Rambo, Vincent Corbin, Brian Wright, "Energetic Radiation Produced During Rocket-Triggered Lightning," *Science* **299**, 694 (2003).

52. Egorov, A. I., and S. I. Stepanov, "Long-Lived Plasmoids Produced in Humid Air as Analogues of Ball Lightning," *Technical Physics* **47**, 1584 (2002).

53. Elitzur, Moshe, *Astronomical Masers*, Dordrecht: Kluwer, 1992.

54. Endean, V. G., "Ball Lightning as Electromagnetic Energy," *Nature* **263**, 753 (1976).

55. Espinoza, Augusto, and Andrew Chubykalo, "Mathematical Foundation of Kapitsa's Hypothesis about the Origin and Structure of Ball Lightning," *Foundations of Physics* **33**, 863 (2003).

56. Faraday, Michael, *Experimental Researches in Electricity* (Dover, Mineola, New York, 2004) (Previously published by J.M. Dent & Sons, London, 1914.).

57. Finzi, Jack, Floyd E. Hovis, Victor N. Panfilov, Peter Hess, and C. Bradley Moore, "Vibrational Relaxation of Water Vapor," *Journal of Chemical Physics*. **67**, 4053 (1977).

58. Foley, H. M., "The Pressure Broadening of Spectral Lines," *Physical Review* **69**, 616 (1946).

59. Fryberger, David, *A Model for Ball Lightning*, Stanford Linear Accelerator Center Report No. SLAC-PUB-6473. (Stanford University, Stanford, California, 1994). (Presented at First International Workshop on the Unidentified Atmospheric Light Phenomena in Hessdalen, Hessdalen, Norway, March 23-27, 1994.)

60. Fujii, Y., R. B. Lindsay, and K. Urushihara, "Ultrasonic Absorption and Relaxation Times in Nitrogen, Oxygen, and Water Vapor," *Journal of the Acoustical Society of America* **35**, 961 (1963).

61. Gamache, Robert R., Richard Lynch, and Steven P. Neshyba, "New Developments in the Theory of Pressure-Broadening and Pressure-Shifting of Spectral Lines of H_2O: The Complex Robert-Bonamy Formalism," *Journal of Quantitative Spectroscopy and Radiative Transfer* **59**, 319 (1998).

62. Garfield, Eugene, "When Citation Analysis Strikes Ball Lightning," *Essays of an Information Scientist* **2**, 479 (1976).

63. Gilman, J. J., "Cohesion in Ball Lightning," *Applied Physics Letters* **83**(11), 2283 (2003).

64. Gilman,, J. J., "Cohesion in Ball Lightning and Cook Plasmas," in *Shock Compression of Condensed Matter - 2003: Proceedings of the Conference of the American Physical Society Topical Group on Shock Compression of Condensed Matter, Portland, Oregon, 20-25 July 2003*, edited by M. D. Furnish, Y. M. Gupta,

and J. W. Forbes (American Institute of Physics, Melville, New York, 2004), pp. 1257-1260.

65. Goodlet, B. L., "Lightning," *I. E. E. Journal*, **81**, 31 (1937).

66. Gordon, Roy G., William Klemperer, and Jeffrey I. Steinfeld, "Vibrational and Rotational Relaxation," *Annual Review of Chemical Physics* 19, 215 (1968).

67. Granatstein, Victor L., and Gregory S. Nusinovich, "Detecting Excess Ionizing Radiation by Electromagnetic Breakdown of Air," *Journal of Applied Physics* **108**, 063304 (2010).

68. Griffiths, David J., *Introduction to Electrodynamics*, 3rd Edition. Upper Saddle River: Prentice-Hall, 1999.

69. Gurevich, A. V., N. D. Borisov, and G. M. Milikh, *Physics of Microwave Discharges: Artifically Ionized Regions in the Atmosphere*. Amsterdam: Gordon and Breach, 1997.

70. Handel, Peter H., "Polarization Catastrophe Theory of Cloud Electricity - Speculation on a New Mechanism for Thunderstorm Electrification," *Journal of Geophysical Research* **90**, 5857 (1985).

71. Handel, Peter H., and Richard T. Schneider, "Nature of Resonances Leading to High-Pressure Cavitons," *Fusion Technology* **7**, 320 (1985).

72. Handel, Peter H., "New Approach to Ball Lightning," in *Science of Ball Lightning (Fire Ball): First International Symposium on Ball Lightning (Fire Ball); 4-6 July 1988; Waseda University, Tokyo, Japan*, edited by Yoshi-Hiko Ohtsuki (World Scientific, Teaneck, New Jersey, 1989), pp. 254-259.

73. Handel, Peter H., and Jean-François Leitner, "Development of the Maser-Caviton Ball Lightning Theory,"*Journal of Geophysical Research* **99**, 10689 (1994).

74. Handel, P. H., G. A. Carlson, M. Grace, J.-F. Leitner, "Electric Ponderomotive Forces Cause Explosive Ball Lightning Damages," *Proceedings Eighth International Symposium on Ball Lightning*, ISBL-04, 3-6 August 2004, National Central University, Chung-Li, Taiwan.

75. Handel, P. H., G. A. Carlson, and J.-F. Leitner, "Phase Shifts Considered as the Cause of the Motion of Ball Lightning," *Proceedings Second International Symposium on Unconventional Plasmas*, ISUP-06, 14-16 August 2006, Eindhoven, The Netherlands, Eds. G. C. Dijkhuis and H. Kikuchi.

76. Handel, Peter H., and Glenn A. Carlson, "Rise Time of Maser-Caviton Ball Lightning Energy Spikes," *Proceedings Ninth International Symposium on Ball*

Lightning, ISBL-06, 16-19 August 2006, Eindhoven, The Netherlands, Ed. G. C. Dijkhuis.

77. Handel, Peter H., Glenn A. Carlson, and Jean-François Leitner, "Maser-Caviton Ball Lightning Interaction Spiking with Cold Emission," *Proceedings Ninth International Symposium on Ball Lightning*, ISBL-06, 16-19 August 2006, Eindhoven, The Netherlands, Ed. G. C. Dijkhuis.

78. Hartmann, B., and B. Kleman, "On the Origin of the Water-Vapor Laser Lines," *Applied Physics Letters* **12**(5), 168 (1968).

79. Herlin, Melvin A., and Sanborn C. Brown, "Microwave Breakdown of a Gas in a Cylindrical Cavity of Arbitrary Length," *Physical Review* **74**, 1650 (1948).

80. Herlin, Melvin A., and Sanborn C. Brown, "Breakdown of a Gas at Microwave Frequencies," *Physical Review* **74**, 291 (1948).

81. Hill, E. L., Ball Lightning as a Physical Phenomenon," *Journal of Geophysical Research* **65**, 1947 (1960).

82. Jennings, S. G., "The Mean Free Path in Air," *Journal of Aerosol Science* **19**(2), 159 (1988).

83. Jennison, R. C., "Ball Lightning," *Nature* **224**, 895 (1969).

84. Jennison, R. C., "Ball Lightning and After-Images," *Nature* **230**, 576 (1971).

85. Jennison, R. C., "Can Ball Lightning Exist in a Vacuum?," *Nature* **245**, 95 (1973).

86. Kapitsa, P. L. (Капица, П. Л.), "О природе шаровой молнии" ("O prerode sharovoi molnii"), Dok. Akad. Nauk SSSR **101**, 245 (1955) (in Russian). (An English language translation of this article appears as P. L. Kapitsa, "The Nature of Ball Lightning," in Donald J. Ritchie, *Ball Lightning: A Collection of Soviet Research in English Translation* (Consultants Bureau, New York, 1961), pp. 11-16.)

87. Kapitza [Kapitsa], P. L., "Free Plasma Filament in a High Frequency Field at High Pressure," *Soviet Physics JETP* **30**, 973 (1970).

88. Kaw, P., G. Schmidt, and T. Wilcox. "Filamentation and trapping of electromagnetic radiation in plasmas," *Phys. Fluids* **16**, 1522-1525 (1973).

89. Keeton, Roy G., and H. E. Bass, "Vibrational and Rotational Relaxation of Water Vapor by Water Vapor, Nitrogen, and Argon at 500 K," *Journal of the Acoustical Society of America* **60**, 78 (1976).

90. Kim, J., S. P. Kuo, and Paul Kossey, “Modelling and Numerical Simulationof Microwave Pulse Propagation in an Air-Breakdown Environment,” *Journal of Plasma Physics* **53**, 253 (1995).

91. Kleinman, D. A., "The Maser Rate Equations and Spiking," *Bell System Technical Journal* **43** (4), 1505 (1964).

92. Knowles, S. H., C. H. Mayer, A. C. Cheung, D. M. Rank, and C. H. Townes, “Spectra, Variability, Size, and Polarization of H_2O Microwave Emission Sources in the Galaxy,” *Science* **163**, 1055 (1969).

93. Kogan-Beletskii, G. I., (Коган-Белечкий, Г. И.), “К вопросу о природе шаровой молнии” (“K voprosu o prirode sharovoi molnii”), *Priroda* **4**, 71 (1957) (in Russian). (An English translation of this article appears as G. I. Kogan-Beletskii, “The nature of ball lightning” in Donald J. Ritchie, *Ball Lightning: A Collection of Soviet Research in English Translation* (Consultants Bureau, New York, 1961).)

94. Kogelnik, H., and T. Li, “Laser Beams and Resonators,” *Applied Optics* **5**, 1550 (1966).

95. Kroll, Norman, and Kenneth M. Watson, “Theoretical Study of Ionization of Air by Intense Laser Pulses,” *Physical Review A* **5**, 1883 (1972).

96. Kung, R. T. V, and R. E. Center, “High Temperature Vibrational Relaxation of H_2O by H_2O, He, Ar, and N_2,” *Journal of Chemical Physics* **62**, 2187 (1975).

97. Laedke, E. W., and K. H. Spatschek, "Stable Three-Dimensional Envelope Solitons," *Physical Review Letters* **52**, 279 (1984).

98. Laedke, E. W., and K. H. Spatschek, “Stability Properties of Multidimensional Finite-Amplitude Solitons,” *Physical Review A* **30**, 3279 (1984).

99. Lambert, J. D., *Vibrational and Rotational Relaxatin in* Gases, Oxford: Clarendon Press, 1977.

100. Li, Tingye, “Diffraction Loss and Selection of Modes in Maser Resonators with Circular Mirrors,” *Bell System Technical Journal* **44**, 917 (1965).

101. Lorentz, H. A., “The Absorption and Emission Lines of Gaseous Bodies,” *Proceedings of the Royal Academy of Amsterdam* **8**, 591 (1906).

102. MacDonald, A. D., “High-Frequency Breakdown in Air at High Altitudes,” *Proceedings of the* IRE **47**, 436 (1959)

103. MacDonald, A. D., *Microwave Breakdown in Gases,* New York: Wiley & Sons, 1966.

104. Maitland, A., and M. H. Dunn, *Laser Physics*. Amsterdam: North-Holland, 1969.

105. Marchant, E. W., "Globular Lightning," *Nature* **125**, 128 (1930).

106. Marshall, Thomas C., Michael P. McCarthy, and W. David Rust, "Electric field magnitudes and lightning initiation in thunderstorms," *Journal of Geophysical Research* **100**, 7097 (1995).

107. Mayhan, Joseph T., Ronald L. Fante, Robert O'Keefe, Richard Elkin, Jack Klugerman, and J. Yos, "Comparison of Various Microwave Breakdown Prediction Models," *Journal of Applied Physics* **42**, 5362 (1971).

108. Messer, J. K., and Frank C. De Lucia, "The Pure Rotational Spectrum of Water Vapor – A Millimeter, Submillimeter, and Far Infrared Analysis," Int. J. Infrared and Millimeter Waves **4**, 505 (1983).

109. Meyerand, Jr., R. G., and A. F. Haught, "Gas Breakdown at Optical Frequencies," *Physical Review Letters* **11**, 401 (1963).

110. Miki, Megumu, Vladimire A. Rakov, Keith J. Rambo, George H. Schnetzer, and Martin A. Uman, "Electric Fields Near Triggered Lightning Channels Measured with Pockels Sensors," *Journal of Geophysical Research* **107**, 4227 (2002).

111. Miyazoe, Y., and M. Maeda, "On the Spiking Phenomenon in Organic Dye Lasers," *IEEE Journal of Quantum Electronics* **7**, 36 (1971).

112. Moore, C. B., K. B. Eack, G. D. Aulich, and W. Rison, "Energetic Radiation Associated with Lightning Stepped-Leaders," *Geophysical Research Letters* **28**, 2141 (2001).

113. Morris, E. C., "Microwave Absorption by Gas Mixtures at Pressures up to Several Hundred Bars," *Australian Journal of Physics* **24**, 157 (1971).

114. Muldrew, D. B., "The Physical Nature of Ball Lightning," *Geophysical Research Letters* **17**, 2277 (1990).

115. Muller, W., and H. Weber, "Decay Time of Optical Resonators," *Optics Communications* **23**, 440 (1977).

116. Mumma, Michael J., David Buhl, Gordon Chin, Drake Deming, Fred Espenak, Theodor Kostiuk, David Zipoy, "Discovery of Natural Gain Amplification in the 10-micrometer Carbon Dioxide Laser Bands on Mars: A Natural Laser," *Science* **212**, 45 (1981).

117. Nam, Sang Ki, and John P. Verboncoeur, “Global Model for High Power Microwave Breakdown at High Pressure in Air,” *Computer Physics Communications* **180**, 628 (2009).

118. Ohtsuki, Y. H., and H. Ofuruton, "Plasma fireballs formed by microwave interference in air," Nature **350**, 139 (1991). (See also, Y. H. Ohtsuki and H. Ofuruton, "Plasma fireballs formed by microwave interference in air (Corrections)," Nature **353**, 868 (1991).)

119. Oka, Takeshi, "Collision-Induced Transitions Between Rotational Levels," in Advances in Atomic and Molecular Physics, 9, edited by D. R. Bates (Elsevier, Burlington, 1974).

120. Payne, Vivienne H., Eli J. Mlawer, Karen E. Cady-Pereira, and Jean-Luc Moncet, “Water Vapor Continuum Absorption in the Microwave,” *IEEE Transactinos on Geoscience and Remote Sensing* **49**, 2194 (2011).

121. Pershing, Dean, and W. Michael Bollen, *Microwave Interaction with Air*, Report No. MRC/WDC-R-097 (Mission Research Corporation, Alexandria, Virginia, 1985). (Report to Naval Research Laboratory, Washington, DC. Available at http://handle.dtic.mil/100.2/ADA158447.)

122. Persico, M., and P. Van Leuven, “Short-Time Quantum Dynamics of a Driven Rigid Rotor,” *Zeitschrift für Physik D*, **41**, 139 (1997).

123. Pollack, M. A., and W. J. Tomlinson, "Molecular Level Parameters and Proposed Identifications for the CW Water-Vapor Laser," *Applied Physics Letters* **12**(5), 173 (1968).

124. Porteanu, H. E., S. Kühn, and R. Gesche, “Ignition Delay for Atmospheric Pressure Microplasmas,” *Contributions in Plasma Physics* **49**, 21 (2009).

125. Powell, J. R., and D. Finkelstein, "Ball Lightning," *American Scientist* **58**, 262 (1970).

126. Rabinowitz,, Mario, “Ball Lightning: Manifestations of Cosmic Little Black Holes,” *Astrophysics and Space Science* **277**, 409-426 (2001).

127. Raĭzer, I. U. P., Shneider, M. N., and Yatsenko, N. A. (1995). *Radio-Frequency Capacitive Discharges*. Boca Raton: CRC Press.

128. Raizer, Yuri P., *Gas Discharge Physics*, Berlin: Springer-Verlag, (1997).

129. Rakov, Vladimir A., and Martin A. Uman, *Lightning: Physics and Effects*, Cambridge: Cambridge University Press, 2003.

130. Ramsden, S. A., and W. E. R. Davies, “Radiation Scattered from the Plasma Produced by a Focused Ruby Laser Beam,” *Physical Review Letters* **13**, 227 (1964).

131. Rañada, Antonio F., "Knotted Solutions of the Maxwell Equations in Vacuum," *Journal of Physics A* **23**, L815 (1990).

132. Rañada, Antonio F., and José L. Trueba, "Ball Lightning an Electromagnetic Knot?," *Nature* **383**, 32 (1996).

133. Rañada, Antonio F., Mario Soler, and José L. Trueba, "Ball Lightning as a Force-Free Magnetic Knot," *Physical Review E* **62**, 7181 (2000).

134. Rayle, Warren D., *Ball Lightning Characteristics*, NASA Technical Note D-3188 (National Aeronautics and Space Administration, Washington, D.C., 1966).

135. Reardon, A. C., "Exact Solutions of Laser Rate Equations," *Journal of Modern Optics* **38** (5), 857 (1991).

136. Roesler, H., and K.-F. Sahm, “Vibrational and Rotational Relaxation in Water Vapor,” *Journal of the Acoustical Society of America* **37**, 386 (1965).

137. Rosenkranz, P. W., “Water Vapor Microwave Continuum Absorption: A Comparison of Measurements and Models,” *Radio Science* **33**, 919 (1998).

138. Rothman, L. S., C. P. Rinsland, A. Goldman, S. T. Massie, D. P. Edwards, J. M. Flaud, A. Perrin, C. Camy-Peyret, V. Dana, J. Y. Mandin, J. Schroeder, A. McCann, R. R. Gamache, R. B. Wattson, K. Yoshino, K. V. Chance, K. W. Jucks, “L. R. Brown, V. Nemchinov, P. Varanasi,, "The HITRAN Molecular Spectroscopic Database and HAWKS (HITRAN Atmospheric Workstation): 1996 Edition," *Journal of Quantitative Spectroscopy and Radiative Transfer* **60**, 665 (1998).

139. Rothman, L. S., I. E. Gordon, A. Barbe, D. Chris Benner, P. F. Bernath, M. Birk, V. Boudon, L. R. Brown, A. Campargue, J.-P. Champion, K. Chance, L. H. Coudert, V. Dana, V. M. Devi, S. Fally, J.-M. Flaud, R. R. Gamache, A. Goldman, D. Jacquemart, I. Kleiner, N. Lacome, W. J. Lafferty, J.-Y. Mandin, S. T. Massie, S. N. Mikhailenko, C. E. Miller, N. Moazzen-Ahmadi, O. V. Naumenko, A. V. Nikitin, J. Orphal, V. I. Perevalov, A. Perrin, A. Predoi-Cross, C. P. Rinsland, M. Rotger, M. Šimečková, M. A. H. Smith, K. Sung, S. A. Tashkun, J. Tennyson, R. A. Toth, A. C. Vandaele, J. Vander Auwera, “The HITRAN 2008 Molecular Spectroscopic Database,” *Journal of Quantitative Spectroscopy and Radiative Transfer* **110**, 533 (2009).

140. Saunders, C. P. R., “Thunderstorm Electrification,” in *Handbook of Atmospheric Electrodynamics*, H. Volland (Ed.), Boca Raton: CRC Press, 1995.

141. Schawlow, A. L., and C. H. Townes, "Infrared and Optical Masers," *Physical Review* **112** (6), 1940 (1958).

142. Schwartz, R. N., Z. I. Slawsky, and K. F. Herzfeld, "Calculation of Vibrational Relaxation times," *Journal of Chemical Physics* **20**, 1591 (1952).

143. Secrest, Don, "Theory of Rotational and Vibrational Energy Transfer in Molecules," *Annual Review of Physical Chemistry* 24, 379 (1973).

144. Sedov, L., I., *Similarity and Dimensional Methods in Mechanics*, Trans. Ed. Maurice Holt, Trans. Morris Friedman, New York: Academic Press, 1959.

145. Shambayati, S., "Atmosphere Attenuation and Noise Temperature at Microwave Frequencies," in *Low-Noise Systems in the Deep Space Network*, M. S. Reid (Ed.), Jet Propulsion Laboratory, California Institute of Technology, (2008). Available at http://descanso.jpl.nasa.gov/Monograph/series10_chapter.cfm.

146. Shimoda, Koichi, *Introduction to Laser Physics*, Second Edition, Berlin: Springer-Verlag, 1991.

147. Shved, G. M., and V. P. Ogibalov, "Natural Population Inversion for the CO_2 Vibrational States in Earth's Atmosphere," *Journal of Atmospheric and Solar-Terrestrial Physics* **62**, 993 (2000).

148. Siegman, A. E., "Unstable Optical Resonators for Laser Applications," *Proceedings of the IEEE* **53**, 277 (1965).

149. Siegman, A. E., *An Introduction to Lasers and Masers*, New York: McGraw-Hill, 1971.

150. Siegman, A. E., *Lasers*, Sausalito: University Science, 1986.

151. Silfvast, William T., *Laser Fundamentals*, 2nd Edition, Cambridge: Cambridge University Press, 2004.

152. Šimečková, Marie, David Jacquemart, Laurence S. Rothman, Robert R. Gamache, and Aaron Godman, "Einstein *A*-coefficients and Statistical Weights for Molecular Absorption Transitions in the HITRAN Database," *Journal of Quantitative Spectroscopy and Radiative Transfer* **98**, 130 (2006).

153. Singer, Stanley, *The Nature of Ball Lightning*, New York: Plenum Press, 1971.

154. Statz, H., and G. deMars, "Transients and Oscillation Pulses in Masers," in *Quantum Electronics, Proceedings of the First International Quantum Electronics*

Conference, Highview, NY, 1959, edited by Charles H. Townes, New York: Columbia University, 1960, p. 530.

155. Stenhoff, Mark, *Ball Lightning: An Unsolved Problem in Atmospheric Physics,* New York: Kluwer Academic, 1999.

156. Svelto, O., *Principles of Lasers*, 4th Edition (D. C. Hanna, Trans.), New York: Plenum Press, 1998.

157. Taylor, F. W., "Natural Lasers on Venus and Mars," *Nature* **306**, 640 (1983).

158. Tennyson, Jonathan, Nikolai F. Zobov, Ross Williamson, Oleg L. Polyansky, Peter F. Bernath, "Experimental Energy Levels of the Water Molecule," *Journal of Chemical Reference Data* **30**, 735 (2001).

159. Thomson, W., "Discussion on Lightning Conductors," *British Association for the Advancement of Science* **58**, 604 (1888).

160. Thornton, W. M., "On Thunderbolts," *Philosophical Magazine Series 6* **21**, 630 (1911).

161. Tiwari, Surendra N., "Radiative energy transfer in molecular gases," NASA-CR-190057, National Aeronautics and Space Administration, Washington, DC, (1992).

162. Townes, C. H., and A. L. Schawlow, *Microwave Spectroscopy*, New York: Dover Publications, 1975.

163. Ulaby, F. T., R. K. Moore, and A. K. Fung, *Microwave Remote Sensing: Active and Passive. Volume I, Microwave Remote Sensing Fundamentals and Radiometry*, Norwood: Artech House, 1986.

164. Uman, M. A., *Lightning*, New York: McGraw-Hill, 1969.

165. Uman, M. A., *The Lightning Discharge*, Orlando: Academic Press, 1987.

166. Uman, M. A., J. Schoene, V. A. Rakov, K. J. Rambo, and G. H. Schnetzer, "Correlated Time Derivatives of Current, Electric Field Intensity, and Magnetic Flux Density for Triggered Lightning at 15 m," *Journal of Geophysical Research.* **107**, 4160 (2002).

167. Van Vleck, J. H., and V. F. Weisskopf, "On the Shape of Collision-Broadened Lines," *Reviews of Modern Physics* **17**, 227 (1945).

168. Van Vleck, J. H., "The Absorption of Microwaves by Oxygen," *Physical Review* **71**, 413 (1947).

169. Vincenti, Walter G. and Charles H. Kruger, Jr., *Introduction to Physical Gas Dynamics*. New York: Wiley and Sons, 1965.

170. Watson, W. K. R, "A Theory of Ball Lightning Formation," *Nature* **185**, 449 (1960).

171. Weinstein, Lev Albertovich, *Open Resonators and Open Waveguides* (Golem Press, Boulder, Colorado, 1969). (Translation of original Russian edition, L. A. Vaynshteyn (Л. А. Вайнштейн), *Откртые резонаторы и открытые волноводе волноводы* (*Otkrytye rezonatory i otkrytye volnovody*), Sovetskoe Radio, Moskva, 1966.)

172. Weitz, E., and G. Flynn, "Laser Studies of Vibrational and Rotational Relaxation in Small Molecules," *Annual Review of Physical Chemistry* **25**, 275 (1974).

173. Winn, William P., G. W. Schwede, and C. B. Moore, "Measurements of Electric Fields in Thunderclouds," *Journal of Geophysical Research* **79**, 1761 (1974).

174. Wong, A. Y., "Cavitons," *Journal de Physique* **C6**, 27 (1977).

175. Woo, Wee, and J. S. DeGroot, *Analysis and Computations of Microwave-Atmospheric Interactions*, Report No. PRG-R-98, Final Report for the Period September 1, 1982 to August 31, 1983. (Plasma Research Group, University of California-Davis, Davis, California, 1984). (Available from http://handle.dtic.mil/100.2/ADA149666).

176. Woo, Wee, and J. S. DeGroot, "Microwave Absorption and Plasma Heating due to Microwave Breakdown in the Atmosphere," *Physics of Fluids* **27**, 475 (1984).

177. Wooding, E. R.,"Ball Lightning," *Nature* **199**, 272 (1963).

178. Zakharov, V. E., "Collapse of Langmuir Waves," *Soviet Physics JETP* **35**, 908 (1972).

179. Zeleznik, Frank J., "A Comparison of Rotational Collision Numbers Obtained from Different Definitions," NASA TN D-5321, National Aeronautics and Space Administration, Cleveland, Ohio (1969).

180. Zheng, X. H., "Quantitative Analysis for Ball Lightning," *Physics Letters A* **148**, 463 (1990).

181. Zhil'tsov, V. A., É. A. Manykin, E. A. Petrenko, A. A. Skovoroda, J. F. Leitner, and P. H. Handel, "Spatially Localized Microwave Discharge in the Atmosphere," *JETP* **81**, 1072 (1995).

182. Zittel, P. F., and D. E. Matsurzo, "Vibrational Relaxation of H_2O from 295 to 1020 K," *Journal of Chemical Physics* **90**, 977 (1989).

VITA

Glenn Andrew Carlson earned a Bachelor of Science in Nuclear Engineering and two Master of Science in Mechanical Engineering and Nuclear Engineering from the University of Illinois at Urbana-Champaign. He earned a *Juris Doctor* in Law from Saint Louis University and a Master of Science in Physics from the University of Missouri – St. Louis. He earned a Doctor of Philosophy in Physics through a cooperative program of the Missouri University of Science and Technology and the University of Missouri – St. Louis. He is a licensed Professional Engineer in ten states.